DISS. ETH No. 15376

STUDY OF ASPECTS OF DEEP HYDRODESULFURIZATION BY MEANS OF MODEL REACTIONS

A dissertation submitted to the
SWISS FEDERAL INSTITUTE OF TECHNOLOGY ZURICH

for the degree of
Doctor of Technical Sciences

presented by
MARINA EGOROVA
Master of Science in Chemistry, Novosibirsk State University
born 05.05.1976
citizen of Russia

accepted on the recommendation of
Prof. Dr. R. Prins, examiner
Prof. Dr. A. Wokaun, co-examiner

Zurich, 2003

To my husband Valeri
and
my parents

Contents

Abstract

Research on the cleaning of fuels, including hydrodesulfurization (HDS), hydrodenitrogenation (HDN) and dearomatization, has become an important subject of environmental catalysis studies worldwide. Legislative regulations in many countries call for the production and use of more environmentally friendly transportation fuels with the lower contents of sulfur, nitrogen and aromatics. Under deep HDS conditions, when most of sulfur has already been removed, the amounts of sulfur and nitrogen compounds are comparable. Thus, HDS and HDN reactions can influence each other by competitive adsorption. Aromatic compounds are always present in refinery streams. For these reasons, the present study focused on competitive HDS and HDN reactions and the influence of aromatics on HDS in order to gain insight into the nature of the inhibitory influence of nitrogen-containing and aromatic molecules on HDS.

Catalytic experiments were carried out under typical industrial conditions, i.e. between 300 and 340°C and a total pressure of 5 MPa in a continuous microflow reactor over sulfided NiMo, CoMo and Mo catalysts supported on alumina. 2-Methylpyridine and 2-methylpiperidine were chosen as nitrogen-containing model compounds. The HDN network of 2-methylpyridine was studied in detail over NiMo catalyst. 2-Methylpiperidine was the primary product, since the cleavage of the C-N bond in a heterocyclic aromatic ring can only take place after ring hydrogenation. The methyl group represented a steric hindrance for the C-N bond scission reaction. Therefore, the C-N bond breaking occurred predominantly on the free side of the molecule, between the nitrogen atom and the methylene group. H_2S had mainly a negative influence on the hydrogenation reaction of 2-methylpyridine to 2-methylpiperidine but a positive effect on the C-N bond cleavage.

The HDS networks of the sulfur-containing model compounds, dibenzothiophene and 4,6-dimethyldibenzothiophene, were studied over the NiMo catalyst. Both sulfur-containing molecules converted via two reaction pathways: i) direct desulfurization, or hydrogenolysis leading to the formation of biphenyls, and ii) hydrogenation followed by desulfurization giving first tetrahydro- and hexahydrodibenzothiophenes, which are further desulfurized to cyclohexylbenzenes or hydrogenated to perhydrodibenzothiophenes and then desulfurized to bicyclohexyls. Under our reaction conditions, dibenzothiophene underwent HDS with 90%

selectivity via the direct desulfurization pathway, whereas 75% of 4,6-dimethyldibenzothiophene was converted via the hydrogenation pathway. Moreover, the reactivity of dibenzothiophene was one order of magnitude higher than that of 4,6-dimethyldibenzothiophene in the absence of H_2S. It is suggested that the direct desulfurization pathway occurs via σ (perpendicular) adsorption of the molecule on the catalyst surface and the hydrogenation pathway via π (flat) adsorption of the reactant. The methyl groups in the vicinity of the sulfur atom constitute a strong steric hindrance for the σ adsorption of 4,6-dimethyldibenzothiophene. Thus, the HDS occurs mainly via flat adsorption in the hydrogenation pathway. H_2S inhibited the direct desulfurization pathway to a greater extent than the hydrogenation pathway. Therefore, the influence of H_2S on the overall HDS was much more pronounced in the case of dibenzothiophene than in the case of 4,6-dimethyldibenzothiophene.

2-Methylpyridine and 2-methylpiperidine had a strong inhibitory effect on the hydrogenation pathway of the HDS of dibenzothiophene and 4,6-dimethyldibenzothiophene. The retarding influence of 2-methylpiperidine was somewhat stronger than that of 2-methylpyridine. The same inhibitory behaviour was observed for the direct desulfurization of 4,6-dimethyldibenzothiophene. The direct desulfurization of dibenzothiophene, however, was suppressed in the presence of 2-methylpyridine but promoted at low partial pressures of 2-methylpiperidine. The promoting effect of 2-methylpiperidine decreased with increasing partial pressure up to 1 kPa. At higher partial pressures, 2-methylpiperidine had only a negative influence on the HDS of dibenzothiophene. Several reasons are suggested to explain the enhancement of the direct desulfurization pathway at low partial pressures of 2-methylpiperidine: a) transformation of hydrogenation sites into direct desulfurization sites, because the hydrogenation site consists of several metal centres and is not completely covered after adsorption of 2-methylpiperidine in the one-point mode; b) an electronic modification of the catalyst surface, resulting in an increase of the electron density on the metal centres due to interaction with the 2-methylpiperidine molecules, which leads to a greater number of sulfur vacancies or to higher intrinsic activity of the active site. The effect of sulfur-containing molecules on the HDN was also studied. 4,6-Dimethyldibenzothiophene and dibenzothiophene suppressed the hydrogenation of 2-methylpyridine but did not affect the C-N bond cleavage in the HDN of 2-methylpiperidine. Therefore, we assume that adsorption of 2-methylpiperidine on both direct desulfurization and hydrogenation sites is much stronger than that of 4,6-dimethyldibenzothiophene or dibenzothiophene.

The effect of naphthalene on the HDS of dibenzothiophene and 4,6-dimethyldibenzothiophene and the influence of the sulfur-containing molecules on the hydrogenation of naphthalene were studied. Naphthalene inhibited the direct desulfurization and hydrogenation pathways in the HDS of dibenzothiophene and 4,6-dimethyldibenzothiophene to the same extent. Thus, the hydrogenation of naphthalene takes place at both the direct desulfurization and the hydrogenation sites. Dibenzothiophene and 4,6-dimethyldibenzothiophene suppressed the hydrogenation of naphthalene to the same extent. Therefore, it is suggested that the adsorption of naphthalene was much weaker than that of sulfur-containing molecules on the active sites of the catalyst.

The role of the Ni and Co promoters on the activity and selectivity of the Mo catalyst in the HDS of dibenzothiophene and 4,6-dimethyldibenzothiophene was studied. Ni and Co clearly improved the direct desulfurization activity of the Mo catalyst in the HDS of dibenzothiophene and, to a lesser extent, in the HDS of 4,6-dimethyldibenzothiophene. The enhancement of the desulfurization via the hydrogenation pathway in the presence of promoted catalysts was similar in the HDS of dibenzothiophene and 4,6-dimethyldibenzothiophene. Since direct desulfurization is the main reaction pathway in the HDS of dibenzothiophene, the overall activity of the Mo catalyst improved remarkably in the transformation of dibenzothiophene. The NiMo catalyt tended to be somewhat more active than the CoMo catalyst. The CoMo catalyst, however, was more resistant to the negative influence of H_2S in the HDS of 4,6-dimethyldibenzothiophene. Thus, at a partial pressure of H_2S higher than 29 kPa, the CoMo catalyst performed better in the HDS of 4,6-dimethyldibenzothiophene than the NiMo catalyst.

Zusammenfassung

Forschung über die Reinigung von Treibstoff, u.a. Hydrodesulfurierung (HDS), Hydrodenitrifizierung (HDN) und Dearomatisierung, ist weltweit ein wichtiges Thema in der Katalyseforschung geworden. Gesetzliche Regelungen in verschiedenen Ländern haben zur Herstellung und Benutzung von umweltfreundlicheren Treibstoffen für Verkehrsmittel mit niedrigeren Gehalt von Schwefel, Stickstoff und aromatische Verbindungen geführt. Unter Bedingungen von tiefer HDS, wenn der Hauptanteil von Schwefel schon entfernt ist, sind die Mengen von schwefel- und stickstoffhaltigen Verbindungen vergleichbar. HDS und HDN Reaktionen sind also durch konkurrierende Adsorption voneinander abhängig. Die Produkte der Erdölverarbeitung enthalten zudem auch aromatische Verbindungen. Aus diesem Grund wurden während dieser Arbeit konkurrierende HDS und HDN Reaktionen, sowie die Auswirkung von aromatischen Verbindungen auf HDS untersucht, um damit einen Einblick in die Natur der inhibitorischen Auswirkung von stickstoffhaltigen und aromatischen Verbindungen auf HDS zu bekommen.

Katalytische Versuche wurden unter typischen industriellen Bedingungen durchgeführt, d.h. bei Temperaturen zwischen 300 und 340°C und unter 5 MPa Gesamtdruck in einem kontinuierlichen Mikroflow-Reaktor über sulfidierten NiMo, CoMo und Mo Katalysatoren auf Aluminiumoxid. Wir haben 2-Methylpyridin und 2-Methylpiperidin als stickstoffhaltige Modelverbindungen ausgewählt. Die HDN Reaktion von 2-Methylpyridin wurde in allen Einzelheiten über dem NiMo-Katalysator untersucht. 2-Methylpiperidin wurde als Primärprodukt beobachtet, da die C-N-Bindung in einem heterozyklischen aromatischen Ring nur nach einer Ringhydrogenierung gebrochen werden kann. Die Methylgruppe stellt eine sterische Hinderung für die Spaltung der C-N Bindung dar. Als Konsequenz wird die C-N-Bindung bevorzugt auf der freien Seite des Moleküls, zwischen Stickstoffatom und Methylengruppe, gebrochen. H_2S hat die Umwandlung von 2-Methylpyridin in 2-Methylpiperidin meistens negativ beeinflusst, hat aber eine positive Auswirkung auf die C-N-Bindungsspaltung.

Die HDS Reaktionen der schwefelhaltigen Modelverbindungen Dibenzothiophen und 4,6-Dimethyldibenzothiophen wurden über dem NiMo-Katalysator untersucht. Die beiden schwefelhaltigen Moleküle haben auf zwei Reaktionsrouten reagiert: i) direkte

Desulfurierung, oder Hydrogenolyse mit Biphenyl-Bildung, und ii) Hydrogenierung mit nachfolgender Desulfurierung, die zuerst Tetrahydro- und Hexahydrodibenzothiophen lieferte, die danach entweder in Cyklohexylbenzol weiter desulfuriert oder in die Perhydrodibenzothiophene hydrogeniert und in Bicyclohexyl desulfuriert wurden. Unter unseren Reaktionsbedingungen unterliegen Dibenzothiophen der HDS durch eine direkte Desulfurierungsroute mit 90% Selektivität, wobei 75% des 4,6-Dimethyldibenzothiophens über einen Hydrogenierungsroute reagiert haben. Die Reaktivität von Dibenzothiophen war zudem um eine Grössenordnung höher als diejenige von 4,6-Dimethyldibenzothiophen in Abwesenheit von H_2S. Es ist anzunehmen, dass die direkte Desulfurierungsroute durch eine σ (perpendikulare) Adsorption des Moleküls auf die Katalysatoroberfläche ablaüft und die Hydrogenierung durch π (flache) Adsorption des Edukts. Die Methylgruppen in der Nähe eines Schwefelatoms stellen eine starke sterische Hinderung für die σ-Adsorption des 4,6-Dimethyldibenzothiophens dar, d. h., die HDS geschieht hauptsachlich durch die flache Adsorption in der Hydrogenierungsroute. H_2S hat die direkte Desulfurierungsroute stärker inhibiert als die Hydrogenierungsroute. Die Auswirkung von H_2S auf die gesamte HDS war also viel stärker im Fall von Dibenzothiophen als für 4,6-Dimethyldibenzothiophen.

2-Methylpyridin und 2-Methylpiperidin haben einen starken inhibitorischen Effekt auf die Hydrogenierungsroute der HDS von Dibenzothiophen und 4,6-Dimethyldibenzothiophen. Die verlangsamende Wirkung war etwas stärker für 2-Methylpiperidin im Vergleich mit 2-Methylpyridin. Das gleiche inhibitorische Verhalten wurde für die direkte Desulfurierung von 4,6-Dimethyldibenzothiophen beobachtet. Die direkte Desulfurierung von Dibenzothiophen wurde allerdings in Gegenwart von 2-Methylpyridin verlangsamt, bei niedrigem Partialdruck von 2-Methylpiperidin hingegen beschleunigt. Die beschleunigende Wirkung von 2-Methylpiperidin ist bei der Zunahme dessen Partialdrucks auf 1 kPa gesunken. Bei höherem Partialdruck hat 2-Methylpiperidin auf die HDS von Dibenzothiophen nur eine negative Auswirkung. Man kann die Verbesserung der direkten Desulfurierung bei niedrigem Partialdruck von 2-Methylpiperidin aus verschiedenen Gründen erklären: a) die Umwandlung von Hydrogenierungszentren zu direkten Desulfurierungszentren, weil ein Hydrogenierungszentrum aus mehreren Metallzentren zusammengesetzt ist und nach Adsorption von 2-Methylpiperidin durch Stickstoffsatome nicht vollständig bedeckt ist; b) eine elektronische Modifizierung der Katalysatoroberfläche, die durch die Wechselwirkung mit 2-Methylpiperidin-Moleküle zur Zunahme der Elektronendichte in den Metallzentren führt, was die Zahl der Schwefel-Fehlstellen oder die Reaktivität der aktiven Zentren erhöht.

Es wurde auch der Einfluss von schwefelhaltigen Verbindungen auf die HDN untersucht. 4,6-Dimethyldibenzothiophen und Dibenzothiophen haben die Hydrogenierung von 2-Methylpyridin verlangsamt, haben aber die C-N-Bindungsspaltung in der HDN von 2-Methylpiperidin nicht beeinflusst. Wir vermuten also, dass die Adsorption von 2-Methylpiperidin sowohl an Direktdesulfurierungs- als auch an Hydrogenierungszentren viel stärker ist als die von 4,6-Dimethyldibenzothiophen oder Dibenzothiophen.

Der Effekt von Naphthalin auf die HDS von Dibenzothiophen und 4,6-Dimethyldibenzothiophen, sowie die Auswirkung von schwefelhaltigen Verbindungen auf die Hydrogenierung von Naphthalin wurden untersucht. Naphthalin hat die Direktdesulfurierungs- und Hydrogenierungsrouten in der HDS von 4,6-Dimethyldibenzothiophen und Dibenzothiophen gleichermassen inhibiert. Die Hydrogenierung von Naphthalin findet also sowohl an Direktdesulfurierungs-, als auch an Hydrogenierungszentren statt. Dibenzothiophen und 4,6-Dimethyldibenzothiophen haben die Hydrogenierung von Naphthalin in gleichem Grad verlangsamt. Wir vermuten, dass die Adsorption von Naphthalin auf die Aktivzentren des Katalysators viel schwächer ist als diejenige von schwefelhaltigen Molekülen.

Der Effekt von Ni und Co als Promoter auf die Aktivität und Selektivität des Mo-Katalysators wurde in der HDS von Dibenzothiophen und 4,6-Dimethyldibenzothiophen untersucht. Ni und Co haben die Direktdesulfurierungsaktivität des Mo-Katalysators in der HDS von Dibenzothiophene markant verbessert, sowie in gewissem Ausmass auch in der HDS von 4,6-Dimethyldibenzothiophen. Die Verbesserung der Desulfurierung durch die Hydrogenierungsroute in Gegenwart des dotierten Katalysators war in der HDS von Dibenzothiophen und 4,6-Dimethyldibenzothiophen ähnlich. Da die direkte Desulfurierung die Hauptreaktionsroute in der HDS von Dibenzothiophen ist, wurde die Gesamtaktivität des Mo-Katalysators in der Umwandlung von Dibenzothiophen markant verbessert. Grundsätzlich war der NiMo-Katalysator etwas aktiver als der CoMo-Katalysator. Letzterer war allerdings resistenter gegen die negative Auswirkung von H_2S in der HDS von 4,6-Dimethyldibenzothiophen. Ingesamt hat sich der CoMo-Katalysator für die HDS von 4,6-Dimethyldibenzothiophen bei Partialdrücken von H_2S über 29 kPa als besser erwiesen als der NiMo-Katalysator.

Chapter 1

Deep Desulfurization of Oil Refinery Streams

1.1 Hydrotreating in refining

A modern refinery is a highly integrated industrial enterprise, the main task of which is to efficiently produce a high yield of valuable products from a crude oil feed of variable composition. Employing different physical and chemical processes such as distillation, extraction, reforming, hydrogenation, cracking and blending the refinery converts crude oil to higher value products. The main products are liquid petroleum gas, gasoline, jet fuel, diesel fuel, wax, lubricants, bitumen and petrochemicals. Energy and hydrogen for internal and external use are also produced in a refinery [1].

Because of their high energy densities and convenient physical form, petroleum products are presently consumed in vast quantities and this consumption continues to grow at alarming rates. Transportation fuels, the major petroleum products, are receiving the highest scrutiny because of the pollution from exhaust gas. Environmental restrictions regarding the quality of transportation fuels and the emissions from the refinery itself are currently the most important and most costly issues. Pollutants of major concern include SO_x, CO, NO_x, particulates, olefins and aromatic hydrocarbons.

Hydrotreating or hydroprocessing refers to a variety of hydrogenation processes which saturate unsaturated hydrocarbons and remove S [by hydrodesulfurization (HDS)], N [by hydrodenitrogenation (HDN)], O [by hydrodeoxygenation (HDO)] and metals [by hydrodemetallization (HDM)] from different petroleum streams in a refinery. The main aim of hydrotreating is to diminish air pollution emissions, to avoid poisoning of noble metals and acid catalysts used in catalytic reforming and cracking and to improve the fuel quality [2].

Scheme 1.1 of a hypothetical refinery illustrates some basic refinery features. Typically, the desalted crude oil is initially separated into different fractions by distillation. The resulting straight-run fractions are characterized by their boiling point range (Table 1.1). Atmospheric distillation usually ends around 360 °C. The remaining fraction (atmospheric residue) is often separated by further vacuum distillation into vacuum gas oil (VGO) and vacuum residue. The atmospheric residue fraction may be the dominant fraction for some heavy crudes, in such cases conversion into lighter products becomes especially important. The type and concentration of heteroatom compounds vary significantly between the fractions as do the demands for hydrotreating. Different reactions are used for treating different refinery streams depending on the main purpose and the properties of the feed. For instance HDS is used before catalytic reforming, HDN before hydrocracking to avoid catalyst poisoning and HDM is used before fluid catalytic cracking (FCC) to avoid metal deposition. Thus, most of the straight-run fractions are hydrotreated (Scheme 1.1).

The structures containing the heteroatoms are distributed over the whole range of the straight-run distillate fractions of the crude, but they generally increase in concentration in the higher boiling point fractions and in the non-volatile residuum (Table 1.1). The role of hydrotreating grew in importance recently because of the use of heavier feedstocks, including synfuels derived from coal, shale oil and tar sands.

The S-containing molecules present in petroleum or synthetic oils are generally classified into two types: nonheterocycles and heterocycles. The former comprises thiols, sulfides and disulfides. Heterocycles are mainly composed of thiophenes with one to several aromatic rings and their alkyl or aryl substituents. Examples of S compounds are shown in Fig. 1.1.

The N-containing molecules in the feedstocks are divided to two types: nonheterocycles and heterocycles. Some examples are shown in Fig. 1.2. Among the nonheterocyclic compounds, aniline derivatives do not appear in oil fractions but do appear as intermediates in the reaction network of most heterocycles. Heterocyclic N compounds are present in the feedstocks and they are difficult to remove. Heterocyclic N-containing molecules are further divided into basic and nonbasic compounds. Basic compounds include six-membered ring heterocycles such as pyridine, quinoline and acridine. Nonbasic N compounds include five-membered ring heterocycles such as pyrrole, indole and carbazole [3] (Fig. 1.2).

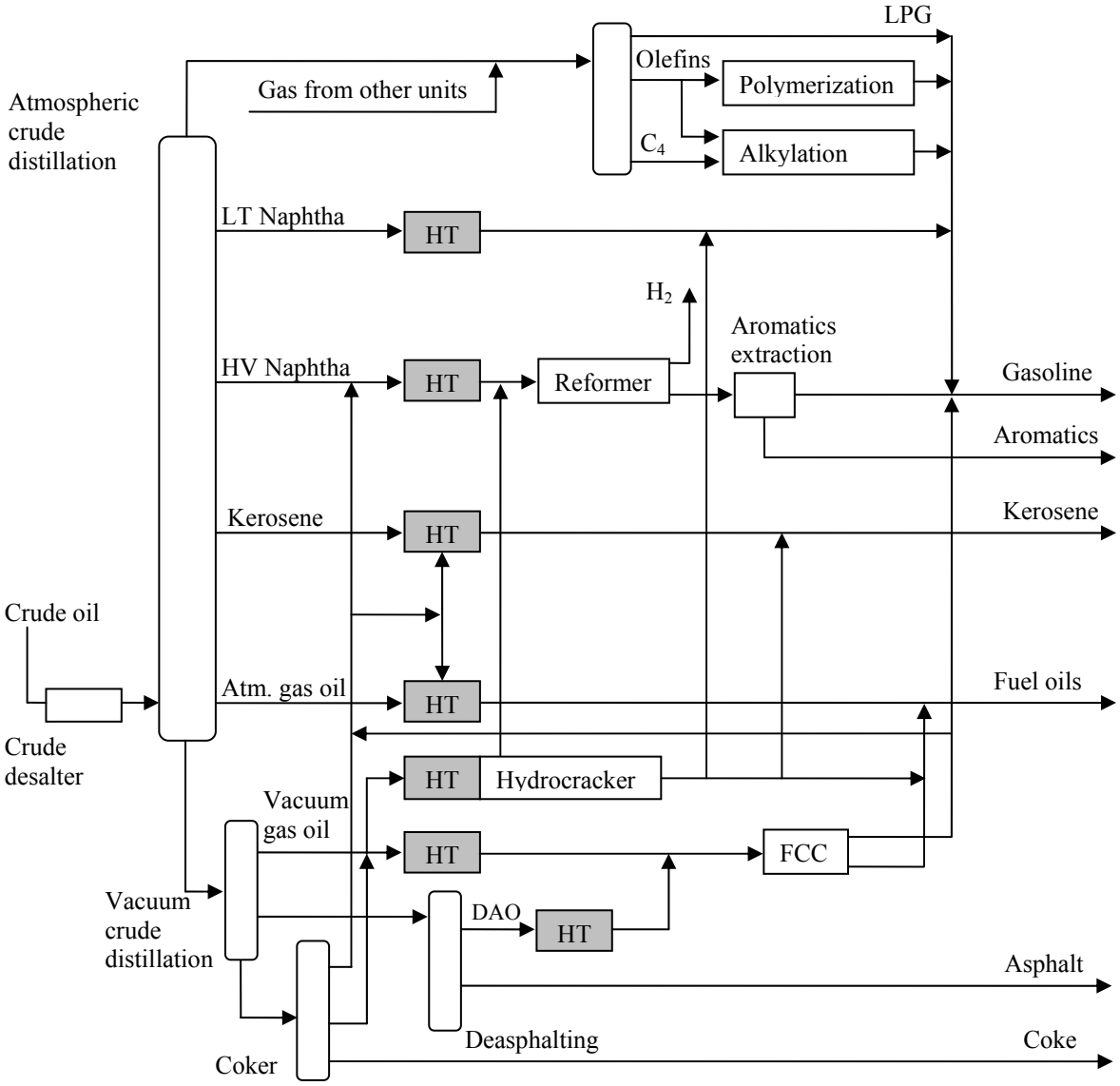

Scheme 1.1. Application of hydrotreatment (HT) in a hypothetical refinery.

Table 1.1. Properties of various straight-run refinery fractions [2].

	Naphtha	Kerosene	Gas oil	Atm. resid.	Vacuum GO	Vacuum resid
Boiling point (°C)	40-180	180-230	230-360	343+	343-500/550	500+
% of crude oil	~ 20	~ 10	~ 20	~ 50	~ 30	~ 20
S (%)	0.01-0.05	0.1-0.3	0.5-1.5	2.5-5	1.5-3	3-6
N (%)	0.001	0.01	0.01-0.05	0.2-0.5	0.05-0.3	0.3-0.6

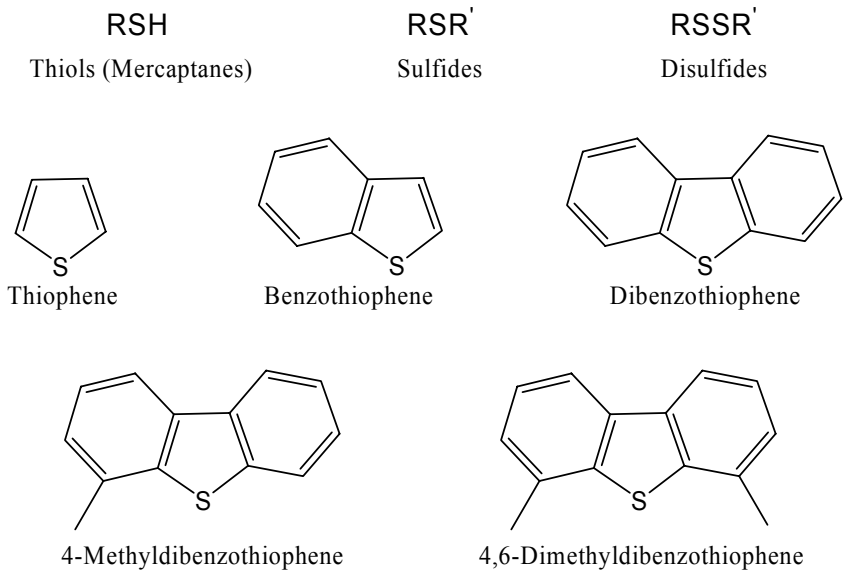

Fig. 1.1. Sulfur-containing molecules in petroleum.

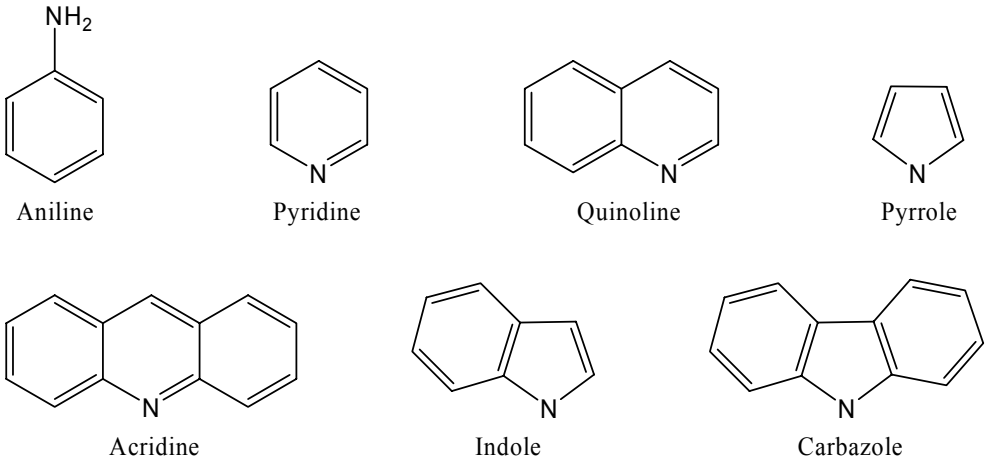

Fig. 1.2. Nitrogen-containing molecules in petroleum.

1.2 Deep hydrodesulfurization

The primary goal of recently proposed legislation is to reduce the sulfur content of transportation fuels [1,4]. Sulfur present in fuels leads to SO_x air pollution generated by vehicle engines. Diesel is presently used as the primary energy source for ship, trains, trucks and some automobiles. It is in principle a more attractive fuel than gasoline since the higher compression ratios used give higher fuel efficiencies. However, the further use of diesel will require solutions to some major environmental pollution problems (soot, smog and particulate formation). In particular, the deep HDS of diesel is presently a key goal. Currently, the fuel specifications in the USA, Japan and Western Europe limit the sulfur content of diesel fuels to less than 0.05 wt.% (500 ppm). New sulfur limits of 30 – 50 ppm for gasoline and diesel marketed in the European community and the USA will be introduced starting from January 1, 2005 [1,4,5].

The problem of the deep removal of sulfur has become more serious due to the lower and lower limit of sulfur content in finished fuel products by legislatorial specifications, and the higher and higher sulfur contents in crude oil. The increased interest in ultra-clean fuels is also due to the need for new emission control technologies for IC engines (especially those for diesel fuels) and for using on-board or on-site reforming of hydrocarbon fuels for new fuel cell vehicles.

Hydrotreater feedstocks are highly complex mixtures. In contrast to a model feed of one or a few organo-sulfur compounds in a solvent of choice, a real fuel consists of a cocktail of hundreds of paraffins, naphthenes, polycyclic aromatics, organo-sulfur and nitrogen compounds. Deep HDS is known to be affected by components in the reaction mixture such as organic heterocompounds and polyaromatic hydrocarbons [2,6,7]. Organic nitrogen compounds in petroleum are generally less reactive than the sulfur compounds. They are converted mainly under more severe conditions than the sulfur compounds and the reaction mechanisms are principally different because of the stronger C-N bond as compared with analogous C-S bonds (in heterocyclic ring systems) [8]. The HDS and HDN mechanisms of different heterocyclic molecules will be discussed in Chapter 3. In general, the following order of inhibition has been noticed for HDS. Saturated and mono-aromatic hydrocarbons < condensed aromatics ≈ oxygen compounds ≈ H_2S < organic sulfur compounds < basic nitrogen compounds [7]. Ammonia and basic nitrogen compounds have been identified as the

strongest inhibitors in HDS [6]. But even within the group of N-containing compounds, adsorption constants differ over nearly two orders of magnitude (e.g. from ammonia to 5,6,7,8-tetrahydroquinoline) [9].

Shifting from petroleum to coal-derived oils the nitrogen content in the fuel also increases. The oils from tar sand and shale are rich in nitrogen. Generally, the heavier the fuel the more stringent will be the need for the removal of nitrogen in order to reduce NO_x emissions, to avoid interference with acidic catalysts and to meet the specifications for marketable products [10]. The amount of N-containing molecules in different crude fractions is normally lower than that of S-compounds (Table 1.1). Therefore, in normal HDS the influence of nitrogen compounds is negligible. In deep HDS, however, when the amounts of S- and N-compounds are comparable, HDS and HDN influence each other by competitive adsorption of reacting molecules.

1.3 Catalytic HDS technologies

Catalytic HDS technologies are more developed and commercialized than other hydrotreating technologies. They include conventional hydrotreating, hydrotreating with advanced catalysts and/or reactor design and a combination of hydrotreating with some additional chemical processes to maintain the fuel specification. HDS of crude oil and refinery streams carried out at elevated temperature and hydrogen partial pressure in the presence of a catalyst converts organo-sulfur compounds to hydrogen sulfide and hydrocarbons [2,3,11].

1.3.1 Conventional HDS

The conventional HDS process is usually conducted over sulfided $CoMo/Al_2O_3$ or $NiMo/Al_2O_3$ catalyst [4,6,7,10,12-18]. Its performance in terms of desulfurization level, activity and selectivity depends on the properties of the specific catalyst used (active species concentration, support properties, synthesis route), the reaction conditions (sulfiding procedure, temperature, partial pressure of hydrogen and H_2S), nature and concentration of the sulfur compounds present in the feed stream, as well as reactor and process design.

The reactivity of organosulfur compounds varies widely depending on their structure and local sulfur atom environment. The low-boiling crude oil fraction contains mainly the aliphatic organosulfur compounds: mercaptans, sulfides and disulfides. They are very reactive in a conventional hydrotreating process and can easily be completely removed from the fuel. For higher boiling crude oil fractions such as heavy straight run naphtha, straight run diesel and light FCC naphtha, the organosulfur compounds predominantly contain thiophenic rings. These compounds include thiophenes and benzothiophenes and their alkylated derivatives. Thiophene-containing compounds are more difficult to convert via hydrotreating than mercaptans and sulfides. The heaviest fractions blended to the gasoline and diesel pools – bottom FCC naphtha, coker naphtha, FCC and coker diesel – contain mainly alkylated benzothiophenes, dibenzothiophenes and alkyldibenzothiophenes, as well as polynuclear organic sulfur compounds, i.e. the least reactive S-containing molecules in the HDS reaction.

The reactivity of sulfur compounds in HDS follows this order (from most to least reactive): thiophene > alkylated thiophene > benzothiophene > alkylated benzothiophene > dibenzothiophene and alkylated dibenzothiophene without substituents at the 4 and 6 positions > alkylated dibenzothiophene with alkyl substituents at the 4 and 6 positions [18-22]. Deep desulfurization of the fuels implies that more and more of the least reactive sulfur compounds must be converted.

1.3.2 Advanced HDS

Deep HDS of refinery streams becomes possible when the severity of the HDS process conditions is increased. This, however, leads to undesired side reactions. When FCC gasoline is desulfurized at a higher hydrogen pressure, many olefins are saturated and the octane number decreases. Higher temperature processing leads to increased coke formation and subsequent catalyst deactivation. The severity of the operating conditions is also limited by the design of the HDS unit [1]. Instead of applying more severe conditions, one could use new HDS catalysts with improved activity and selectivity. Ideal hydrotreating catalysts should be able to remove sulfur, nitrogen and, in specific cases, metal atoms from the refinery streams. At the same time they must also improve other fuel specifications, such as octane/cetane number or aromatics content, which are essential for high fuel quality and meeting environmental legislation standards. Hydrotreating efficiency can also be increased by

employing an advanced reactor design such as multiple bed systems within one reactor, new internals in the catalytic reactor or new types of catalysts and catalyst support. The best results can be achieved by a combination of the latter approaches, namely, using an appropriate catalyst with improved activity in a reactor of advanced design [1].

1.3.2.1 Advanced HDS catalysts

To improve the performance of the HDS catalyst, all steps in the preparation procedure should be considered. The key parameters are the choice of a precursor of the active species, support, synthesis and post-treatment of the synthesized catalyst.

The nature of the active phase can be modified by changing the amount of active component [23], introduction of additives and by changing the active component. Numerous additives have been studied, phosphorus [24-28] and fluorine [29-41] have received special attention. In some studies the sulfides of transition metals were replaced by nitrides [42,43] or carbides [44-47]. Noble metals are also used as active phase in hydrotreating catalysts for second stage HDS [48,49].

Various supports have been used to enhance the catalytic activity in HDS: carbon [50-55], silica [56-59], zeolites [60-71], titania and zirconia [72-77] and silica-alumina [56,78,79]. Combining new types of catalytic species with advanced catalyst supports such as ASA (amorphous silica-alumina) can result in an extremely high desulfurization performance [1]. The application of ASA-supported noble metal-based catalysts for the second-stage deep desulfurization of gas oil is an example [48,49]. The Pt and PtPd catalysts are very active in the deep HDS of pre-hydrotreated straight run gas oil under industrial conditions. These catalysts are able to reduce the sulfur content to 6 ppm, while simultaneously reducing the aromatics to 75% of their initial amount [80]. At high sulfur levels, the ASA supported noble metal catalysts are poisoned by sulfur and NiW/ASA catalysts become preferable for deep HDS and dearomatization.

The application of noble metal catalysts for deep HDS is limited by their sulfur resistance. Therefore, those catalysts are normally used when most of the sulfur compounds and H_2S have been removed from the process stream. A new concept of bifunctional catalysts has been proposed to increase the sulfur resistance of noble metal hydrotreating catalysts [81]. It combines catalysts supports with bimodal pore size distribution (e.g. zeolites) and two types of active sites. The first type of sites, placed in large pores, is accessible for organosulfur compounds and is sensitive to sulfur inhibition. The second type of active sites, placed in

small pores, is not accessible for large S-containing molecules and is resistant to poisoning by H_2S. Since hydrogen can easily access the sites located in small pores, it can be adsorbed dissociatively and transported within the pore system to regenerate the poisoned metal sites in the large pores. The practical applications of this concept have not been demonstrated yet.

1.3.2.2 New reactor systems

Besides improving the catalysts, the hydrotreating equipment can also be upgraded. Conventionally used hydrotreating reactors are fixed beds with a co-current supply of oil stream and hydrogen. These systems have an unfavorable H_2S profile concentration over the reactor. Due to a high H_2S concentration at the reactor outlet, the removal of the last ppm's of sulfur is inhibited. Counter-current operation can provide a more preferable concentration profile, since in this operation mode the oil feed is introduced at the top and hydrogen at the bottom of the reactor. H_2S is removed from the reactor at the top, avoiding a possible recombination with olefins at the reactor outlet. One commercial example of this approach is the hydrotreating process based on SynSat Technology [1]. The process is shown in Scheme 1.2.

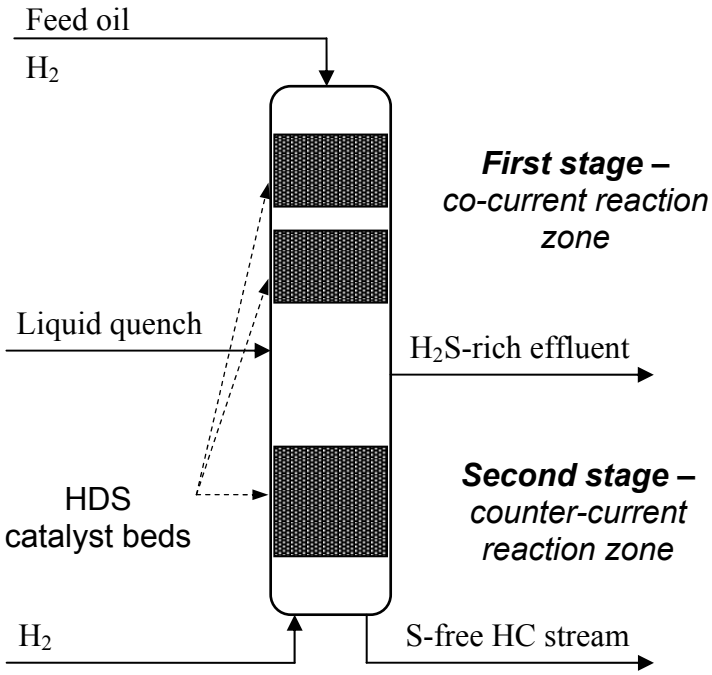

Scheme 1.2. Co-current/counter-current Syn Technology process.

In the first stage the feed and hydrogen co-currently contact the catalyst bed and organosulfur compounds are converted. The formed H_2S is then removed from the reactant flow. In the second stage the reactor system operates in the counter-current mode providing more favorable concentration profiles of H_2S and H_2 over the length of the reactor. Such a configuration allows application of catalysts sensitive to sulfur poisoning, i.e. noble metal containing catalysts, in the second stage of the process. Moreover, nitrogen and aromatics can be removed as well.

An ebullated bed reactor is an example of other types of reactors aimed at HDS of heavy refinery streams, processing of which results in fast catalyst deactivation due to coke formation. In this unit, the catalyst particles are fluidized by the feed and hydrogen and are therefore well mixed with the feed stream. The catalyst activity can be controlled by adding and withdrawing catalyst particles. The requirements to the catalysts used in this process are mechanical stability and resistance to the attrition.

1.3.2.3 Combination of hydrotreating with other reactions

Sulfur removal by an HDS process is usually accompanied by other hydrogenation reactions, which are particularly undesirable for FCC gasoline streams where olefins are present. Saturation of olefins during HDS results in a loss of octane number. To compensate for the loss of octane different options of FCC gasoline treatment before or after desulfurization can be considered.

By a combination of pre-aromatization of the FCC gasoline streams with conventional HDS, the sulfur content can be decreased to 10 ppm and the octane number increased from 89 to 100. Despite almost complete olefin saturation, the octane number is boosted by increasing the aromatics amount in the end product up to 68 wt%. However, the high level of aromatics in the final product makes the application of the proposed technology less attractive since new environmental rules require a limited amount of aromatics in gasoline.

Another possibility is the combination of conventional HDS with post treatment of the products to minimize the decrease in octane number. The key process here is the catalyst formulation. Due to improved desulfurization activity and sulfur and nitrogen tolerance of the catalyst, the process employs one fixed-bed reactor unit with the catalyst system divided in a multiple bed configuration. For instance, typically a combination of $CoMoP/Al_2O_3$ and GaCr/H-ZSM-5 catalysts is applied. This system is very efficient at reducing sulfur from 1450

ppm in a naphtha feed to 10 ppm in the final product with almost no decrease in octane number [1].

1.3.2.4 Catalytic distillation

To avoid octane loss in deep HDS, the FCC gasoline stream can be fractionated by distillation before desulfurization and each fraction can be desulfurized at appropriately severe conditions. This method is efficient since the olefins are mainly concentrated in the low-boiling fraction of the FCC naphtha whereas sulfur compounds are mainly present in the high-boiling fraction. Moreover, the HDS can be performed at different selective conditions depending on the nature of S-containing molecules. Thus, olefins are preserved in the final product. However, realizing this approach requires multiple hydrotreating reactors – one reactor per fraction. Combining distillation and HDS in a single vessel is a breakthrough. The process is based on simultaneous desulfurization and splitting FCC naphtha stream into fractions with different boiling points. The simplified outline of this process is shown in Scheme 1.3.

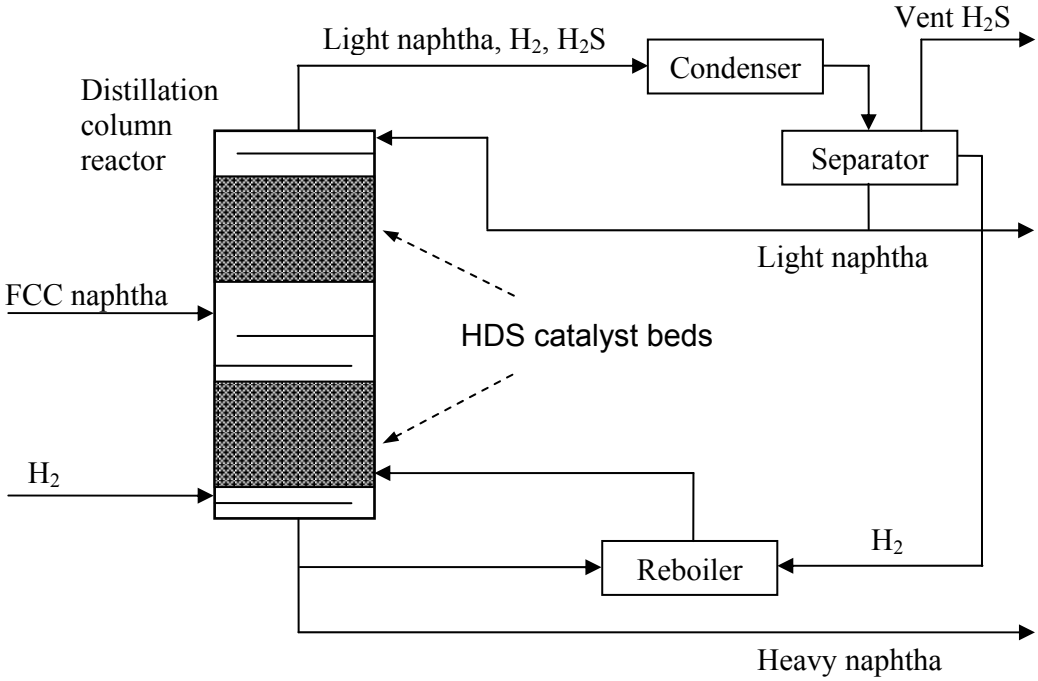

Scheme 1.3. Simplified flow scheme of the CDHDS based technology.

The main feature of the process is that, depending on the FCC naphtha properties and desired product specification, a distillation column is loaded with a hydrotreating catalyst at different levels of the column or through the whole column. Desulfurization conditions are different for light and heavy fractions, their severity being nicely controlled by the boiling temperature of the naphtha fraction. The lighter fractions, which contain most of the olefins and easily removable sulfur compounds, are subjected to desulfurization at lower temperatures at the top of the column. This leads to higher HDS selectivity and less hydrocracking or saturation of olefinic compounds. The higher boiling portions, containing resistant S-compounds, are subjected to desulfurization at higher temperatures at the bottom of the distillation column reactor. The reaction zone can not overheat since the heat released during the HDS reaction is used to boil the hydrocarbon stream. This leads to nearly perfect heat integration. Moreover, it was claimed that this technology is 25% less expensive than the conventional HDS process, making it very attractive for refineries.

There are also many technologies that do not use hydrogen for catalytic decomposition of S-containing compounds, so-called „Non-HDS“ based desulfurization technologies. These approaches allow high desulfurization levels by shifting the boiling point of S-compounds to higher values, separating those compounds by extraction or adsorption and decomposition via selective oxidation. Those technologies are not discussed here in detail since they are beyond the scope of this thesis.

1.4 Monolith reactor/catalysts for HDS of refinery streams

A fascinating option for highly efficient and innovative technologies arises from a combination of different functions in single units, performing more functions simultaneously [82]. Structured monolith reactors may play a key role in the design of novel processes based on multifunctional reactors. Depending on the point of view, a monolith can be considered to be a reactor or a catalyst: the border between catalyst and reactor vanishes [83]. The application of monolith-based catalysts/reactors was tried for different chemical processes. Examples of very high activity and selectivity have been reported [84-86].

Monolithic catalysts can be prepared in different ways. They can be produced by direct extrusion of support material (often cordierite is used, but different types of clays or typical catalyst carrier materials such as alumina are also used) or of a paste also containing

catalyst particles (e.g. zeolites, V-based catalysts) or a precursor of catalyst active species (e.g. polymers for carbon monoliths). The catalyst loading of the reactor in this case can be high [87]. Alternatively, catalysts, supports, or their precursors can be coated into a monolith structure by washcoating [84]. Different types of monolith catalysts are shown in Fig. 1.3.

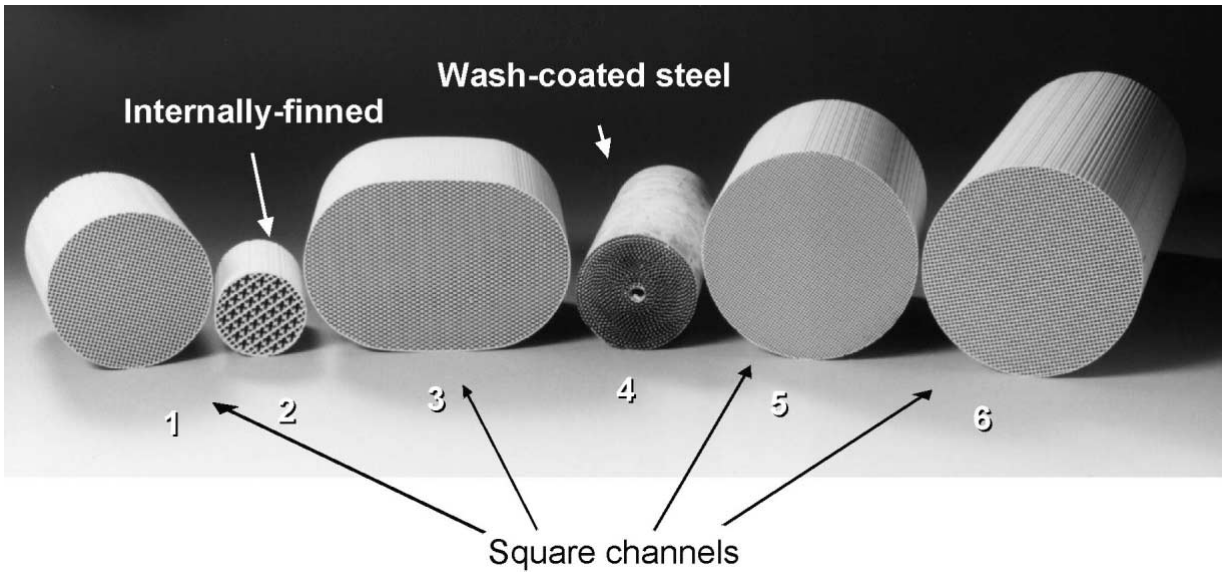

Fig. 1.3. Monolith structures of various shapes. Square channel cordierite structures (1,3,5,6), internally finned channels (2), washcoated steel monolith (4).

Monoliths are dominant catalyst structures for three-way catalysts in cars, selective reduction catalysts in power stations and for ozone destruction in airplanes. The application of structured catalysts for the desulfurization process can also be highly advantageous in comparison with common catalysts and reactors. Monoliths are not only applicable for single-phase processes, but are often preferable for multiphase processes [85,88-94]. If Taylor flow through a single tube is ensured, the diffusion limitations for gas-liquid processes can be reduced due to internal liquid recirculation during their transport through a channel (Fig. 1.4). This results in one order of magnitude faster mass transfer than in conventional reactors.

Monoliths can be used both for co- and counter-current operation in gas-liquid reactions. They can combine the advantages of the slurry and trickle bed reactors and eliminate their disadvantages [87]:

- The catalyst can be coated as a thin layer on the channel walls, and can be described as a “frozen slurry reactor”.

- Larger channel geometries (e.g. in the internally finned monolith channels) allow counter-current operation of gas and liquid.
- The catalyst inventory can be increased by using thicker coatings or using a monolith extruded from the catalyst support, e.g. an all-silica-monolith.
- The high cell density of the monoliths creates a high geometric surface area. Using a packed bed, unrealistically small particles would be needed to achieve this.
- The monolith reactor has a negligible pressure drop.
- Monolith reactors are intrinsically safer.

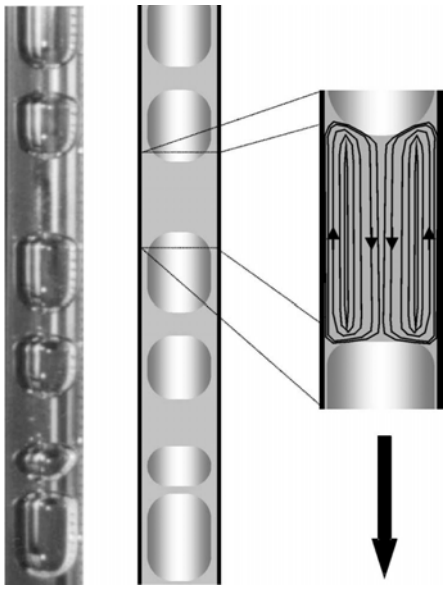

Fig. 1.4. Taylor flow through a single tube. Left: picture of air-water flow, middle: schematic representation of the gas and liquid slugs, right: CFD velocity pattern in a liquid slug showing the liquid recirculation.

The advantages of monolith reactors listed above result in larger reactor productivity, better selectivity control and higher efficiency, thus better catalyst utilization and low energy consumption. Monoliths exhibit a large flexibility in the operation conditions. They are well suited for optimal semi-batch, batch, continuous and transient processing. Different catalytic reactions can be combined, catalytic conversions can be joined with in situ separation, and heat integration is possible, all leading to process intensification.

Of course, monoliths have disadvantages. They are at this moment more expensive than particle catalysts. In fixed bed operation they will have to exhibit a sufficiently long

lifetime. In quickly (irreversibly) deactivating reactions, they can not be used. Of extreme importance is that the inlet distribution should be secured. In co-current flow, both gas and liquid have to be contacted evenly with the catalyst at the monolith walls.

Several options exist for application of monoliths in oil refineries. They include, but are not limited to, gas phase processes for removal of the last ppm S from gasoline and effluent gases, gas-liquid processes aimed at deep HDS, HDN, dearomatization and hydrocracking (co- and counter-current) employing catalytic distillation, reactive stripping and reactive adsorption; and gas-liquid-solid processes like moving bed application for hydrodemetallization and sulfur removal by reactive adsorption.

Catalyst preparation and extrusion should be developed further for specific applications, optimizing the structure and active phase distribution. Hydrodynamics and transport processes have to be described better to design reliable processes.

1.5 Conclusion

To improve the air quality in densely populated areas, the reduction of emissions from motorized vehicles undoubtedly plays a key role. Especially the relatively high emission of particulates, SO_x and NO_x by diesel engines is of great concern because of the suspected health risk and environmental impact. The reduction of diesel engine emissions is a rather complex issue with a number of possible solutions. One of these solutions is the improvement of diesel fuel quality, especially by lowering the sulfur and aromatics content and increasing the cetane number. Extreme reductions in the sulfur content will have an enormous impact on the costs and technology for diesel fuel production. Whereas the current sulfur content in automotive gas oil could still be achieved with conventional technology, newly proposed sulfur maximum levels will require more drastic changes in hydrotreating processes since the large scale production of ultra clean diesel fuel will be simply impossible with the current technology. Moreover, because of the increasing demand for diesel fuel, low quality blending streams have to be used to produce required volume.

In the HDS based technologies, less room for breakthroughs exists. Noble metal based catalysts with high sulfur tolerance and sufficient kinetics in sulfur removal seem to be the most challenging option for improvement of HDS based technologies. Application of catalytic distillation in combination with HDS is also attractive.

Reactive adsorption, in which the sulfur atom is removed from the molecule by the sorbent and the hydrocarbon part of the molecule is returned to the final product without any structural changes, is applicable at almost all points of the refinery where desulfurization is required. Due to the very high flexibility in the reactor design and process conditions, reactive adsorption can be easily adapted to streams with different properties and compositions.

Selective oxidation of sulfur compounds into hydrocarbons and volatile sulfur products might also be attractive for desulfurization. Substitution of expensive hydrogen, which is normally used in desulfurization, by air will bring high economical benefits. Thermodynamic feasibility of this process in the presence of different catalytic systems should be evaluated.

In all processes discussed, adequate chemical reaction engineering has a lot to offer. In particular, structured catalytic reactors have a high potential. In many respects, both for gas and for gas – liquid systems, structured reactors outperform the conventional reactors such as slurry and trickle bed reactors. Monolith are promising structured reactors. In gas – liquid applications they exhibit high production rates, high selectivity (for serial kinetics) and close to plug flow behavior. They allow counter-current operation for common industrial conditions. They can also be used in multifunctional reactors for processes such as catalytic distillation. Their usefulness in counter-current operation also makes them a potential candidate in catalytic distillation. In transient adsorption processes, structured reactors can be designed that exhibit a low pressure drop and a fast response.

1.6 References

[1] I.V. Babich, J.A. Moulijn, Fuel 82 (2003) 607.

[2] H. Topsøe, B.S. Clausen, F.E. Massoth, in, Catalysis: Science and Technology, 1996.

[3] T. Kabe, A. Ishihara, W. Qian, Hydrodesulfurization and hydrodenitrogenation, Kodansha Ltd., Tokyo, WILEY-VCH Verlag GmbH, Weinheim, 1999.

[4] C. Song, X.L. Ma, Appl. Catal. B 41 (2003) 207.

[5] S.F. Venner, Hydrocarb. Process. 79 (2000) 51.

[6] M.J. Girgis, B.C. Gates, Ind. Eng. Chem. Res. 30 (1991) 2021.

[7] H. Schulz, W. Bohringer, P. Waller, F. Ousmanov, Catal. Today 49 (1999) 87.

[8] H. Schulz, N.M. Rahman, M. Breysse, P. Tetenyi, D. Kallo, H.J. Lovink, M.R. Deagudelo, Stud. Surf. Sci. Catal. 75 (1993) 585.

[9] V. La Vopa, C.N. Satterfield, J. Catal. 110 (1988) 375.

[10] H. Schulz, M. Schon, N.M. Rahman, Stud. Surf. Sci. Catal. 27 (1986) 201.

[11] D.D. Whitehurst, T. Isoda, I. Mochida, Adv. Catal. 42 (1998) 345.

[12] M. Houalla, N.K. Nag, A.V. Sapre, D.H. Broderick, B.C. Gates, AIChE J. 24 (1978) 1015.

[13] M. Houalla, D.H. Broderick, A.V. Sapre, N.K. Nag, V.H.J. de Beer, B.C. Gates, H. Kwart, J. Catal. 61 (1980) 523.

[14] R. Prins, V.H.J. de Beer, G.A. Somorjai, Catal. Rev.-Sci. Eng. 31 (1989) 1.

[15] R.R. Chianelli, M. Daage, M.J. Ledoux, Adv. Catal. 40 (1994) 177.

[16] M. Daage, R.R. Chianelli, J. Catal. 149 (1994) 414.

[17] P. Grange, X. Vanhaeren, Catal. Today 36 (1997) 375.

[18] R. Shafi, G.J. Hutchings, Catal. Today 59 (2000) 423.

[19] T. Kabe, A. Ishihara, H. Tajima, Ind. Eng. Chem. Res. 31 (1992) 1577.

[20] T. Kabe, A. Ishihara, Q. Zhang, Appl. Catal. A 97 (1993) L1.

[21] X.L. Ma, K. Sakanishi, I. Mochida, Ind. Eng. Chem. Res. 35 (1996) 2487.

[22] B.C. Gates, H. Topsøe, Polyhedron 16 (1997) 3213.

[23] H. Qabazard, F. Abuseedo, A. Stanislaus, M. Andari, M. Absihalabi, Fuel Sci. Technol. Int. 13 (1995) 1135.

[24] R.E. Tischer, N.K. Narain, G.J. Stiegel, D.L. Cillo, Ind. Eng. Chem. Res. 26 (1987) 422.

[25] S. Eijsbouts, J.N.M. van Gestel, J.A.R. vanVeen, V.H.J. de Beer, R. Prins, J. Catal. 131 (1991) 412.

[26] J.A.R. van Veen, H.A. Colijn, P. Hendriks, A.J. van Welsenes, Fuel Process. Technol. 35 (1993) 137.

[27] C. Papadopoulou, H. Matralis, A. Lycourghiotis, P. Grange, B. Delmon, J. Chem. Soc.-Faraday Trans. 89 (1993) 3157.

[28] V. Zuzaniuk, R. Prins, J. Catal. 219 (2003) 85.

[29] V.C.F. Holm, A. Clark, Ind. Eng. Chem. Prod. Res. Dev. 2 (1963) 38.

[30] H.R. Gerberic, F.E. Lutinski, W.K. Hall, J. Catal. 6 (1966) 209.

[31] R. Covini, V. Fattore, N. Giordano, J. Catal. 7 (1967) 126.

[32] P.M. Boorman, R.A. Kydd, Z. Sarbak, A. Somogyvari, J. Catal. 96 (1985) 115.

[33] P.M. Boorman, R.A. Kydd, Z. Sarbak, A. Somogyvari, J. Catal. 100 (1986) 287.

[34] K. Jiratova, M. Kraus, Appl. Catal. 27 (1986) 21.

[35] P.M. Boorman, R.A. Kydd, Z. Sarbak, A. Somogyvari, J. Catal. 106 (1987) 544.

[36] H.K. Matralis, A. Lycourghiotis, P. Grange, B. Delmon, Appl. Catal. 38 (1988) 273.

[37] C. Papadopoulou, A. Lycourghiotis, P. Grange, B. Delmon, Appl. Catal. 38 (1988) 255.

[38] C. Kwak, J.J. Lee, J.S. Bae, K. Choi, S.H. Moon, Appl. Catal. A 200 (2000) 233.

[39] H. Kim, J.J. Lee, S.H. Moon, Appl. Catal. B 44 (2003) 287.

[40] W.P. Zhang, M.Y. Sun, R. Prins, J. Phys. Chem. B 107 (2003) 10977.

[41] V. Schwartz, M.Y. Sun, R. Prins, J. Phys. Chem. B 106 (2002) 2597.

[42] D.W. Kim, D.K. Lee, S.K. Ihm, Catal. Lett. 43 (1997) 91.

[43] M. Nagai, Y. Goto, H. Ishii, S. Omi, Appl. Catal. A 192 (2000) 189.

[44] D.J. Sajkowski, S.T. Oyama, Appl. Catal. A 134 (1996) 339.

[45] V. Schwartz, S.T. Oyama, J.G.G. Chen, J. Phys. Chem. B 104 (2000) 8800.

[46] P. Da Costa, C. Potvin, J.M. Manoli, J.L. Lemberton, G. Perot, G. Djega-Mariadassou, J. Mol. Catal. A 184 (2002) 323.

[47] P. Da Costa, C. Potvin, J.M. Manoli, M. Breysse, G. Djega-Mariadassou, Catal. Lett. 86 (2003) 133.

[48] H.R. Reinhoudt, M. van Gorsel, A.D. van Langeveld, J.A.R. van Veen, S.T. Sie, J.A. Moulijn, Hydrotreatment and Hydrocracking of Oil Fractions 127 (1999) 211.

[49] H.R. Reinhoudt, R. Troost, A.D. van Langeveld, S.T. Sie, J.A.R. van Veen, J.A. Moulijn, Fuel Process. Technol. 61 (1999) 133.

[50] M. Breysse, B.A. Bennett, D. Chadwick, J. Catal. 71 (1981) 430.

[51] A.J. Bridgewater, R. Burch, P.C.H. Mitchell, Appl. Catal. 4 (1982) 267.

[52] J.C. Duchet, E.M. van Oers, V.H.J. de Beer, R. Prins, J. Catal. 80 (1983) 386.

[53] H. Topsøe, R. Candia, N.Y. Topsøe, B.S. Clausen, Bull. Soc. Chim. Belg. 93 (1984) 783.

[54] H. Topsøe, B.S. Clausen, N.Y. Topsøe, E. Pedersen, Ind. Eng. Chem. Fundam. 25 (1986) 25.

[55] H. Farag, D.D. Whitehurst, K. Sakanishi, I. Mochida, Catal. Today 50 (1999) 9.

[56] G. Muralidhar, F.E. Massoth, J. Shabtai, J. Catal. 85 (1984) 44.

[57] Y.I. Yermakov, A.N. Startsev, V.A. Burmistrov, Appl. Catal. 11 (1984) 1.

[58] A.A. Spozhakina, N.G. Kostova, I.N. Yuchnovski, D.M. Shopov, T.M. Yurieva, T.K. Shochireva, Appl. Catal. 39 (1988) 333.

[59] R. Cattaneo, T. Shido, R. Prins, in, Hydrotreatment and Hydrocracking of Oil Fractions, Amsterdam, 1999, p. 421.

[60] M. Breysse, E. Furimsky, S. Kasztelan, M. Lacroix, G. Perot, Catal. Rev.-Sci. Eng. 44 (2002) 651.

[61] F. Bataille, J.L. Lemberton, G. Perot, P. Leyrit, T. Cseri, N. Marchal, S. Kasztelan, Appl. Catal. A 220 (2001) 191.

[62] V. Fornes, M.I. Vazquez, A. Corma, Zeolites 6 (1986) 125.

[63] R. Cid, F. Orellana, A.L. Agudo, Appl. Catal. 32 (1987) 327.

[64] P.W. de Bont, M.J. Vissenberg, V.H.J. de Beer, J.A.R. van Veen, R.A. van Santen, A.M. van der Kraan, Appl. Catal. A 202 (2000) 99.

[65] Y. Okamoto, H. Katsuyama, Ind. Eng. Chem. Res. 35 (1996) 1834.

[66] P. Michaud, J.L. Lemberton, G. Perot, Appl. Catal. A 169 (1998) 343.

[67] T. Kubota, H. Okamoto, Y. Okamoto, Catal. Lett. 67 (2000) 171.

[68] F. Bataille, J.L. Lemberton, G. Perot, P. Leyrit, T. Cseri, N. Marchal, S. Kasztelan, Appl. Catal. A 220 (2001) 191.

[69] M.J. Vissenberg, P.W. de Bont, W. Gruijters, V.H.J. de Beer, A.M. van der Kraan, R.A. van Santen, J.A.R. van Veen, J. Catal. 189 (2000) 209.

[70] R. Mariscal, R.M. Navarro, B. Pawelec, J.L.G. Fierro, Microporous Mesoporous Mater. 34 (2000) 181.

[71] G. Plazenet, E. Payen, J. Lynch, Phys. Chem. Chem. Phys. 4 (2002) 3924.

[72] K. Tanabe, H. Sasaki, H. Hattori, K. Ouchi, K. Makino, H. Itoh, G. Takeya, Fuel Process. Technol. 2 (1979) 253.

[73] J.G. Weissman, E.I. Ko, S. Kaytal, Appl. Catal. A 94 (1993) 45.

[74] M.J. Vissenberg, Y. van der Meer, E.J.M. Hensen, V.H.J. de Beer, A.M. van der Kraan, R.A. van Santen, J.A.R. van Veen, J. Catal. 198 (2001) 151.

[75] L. Coulier, J.A.R. van Veen, J.W. Niemantsverdriet, Catal. Lett. 79 (2002) 149.

[76] S.K. Maity, M.S. Rana, S.K. Bej, J. Ancheyta-Juarez, G.M. Dhar, T. Rao, Catal. Lett. 72 (2001) 115.

[77] P. Afanasiev, M. Cattenot, C. Geantet, N. Matsubayashi, K. Sato, S. Shimada, Appl. Catal. A 237 (2002) 227.

[78] L. Qu, W. Zhang, P.J. Kooyman, R. Prins, J. Catal. 215 (2003) 7.

[79] L.D. Sharma, M. Kumar, J.K. Gupta, M.S. Rana, V.S. Dangwal, G.M. Dhar, Indian J. Chem. Technol. 8 (2001) 169.

[80] H.R. Reinhoudt, PhD Thesis, Delft University of Technology, 1999.

[81] C. Song, CHEMTECH 3 (1999) 26.

[82] A.I. Stankiewicz, J.A. Moulijn, Chem. Eng. Prog. 96 (2000) 22.

[83] A. Cybulski, J.A. Moulijn, Catal. Rev.-Sci. Eng. 36 (1994) 179.

[84] A.E.W. Beers, I. Hoek, T.A. Nijhuis, R.S. Downing, F. Kapteijn, J.A. Moulijn, Top. Catal. 13 (2000) 275.

[85] T.A. Nijhuis, M.T. Kreutzer, A.C.J. Romijn, F. Kapteijn, J.A. Moulijn, Catal. Today 66 (2001) 157.

[86] A.E.W. Beers, R.A. Spruijt, T.A. Nijhuis, F. Kapteijn, J.A. Moulijn, Catal. Today 66 (2001) 175.

[87] F. Kapteijn, T.A. Nijhuis, J.J. Heiszwolf, J.A. Moulijn, Catal. Today 66 (2001) 133.

[88] C.N. Satterfield, F. Ozel, Ind. Eng. Chem. Fundam. 16 (1977) 61.

[89] V. Hatziantoniou, B. Andersson, Ind. Eng. Chem. Fundam. 23 (1984) 82.

[90] S. Irandoust, B. Andersson, Chem. Eng. Sci. 43 (1988) 1983.

[91] S. Irandoust, B. Andersson, E. Bengtsson, M. Siverstrom, Ind. Eng. Chem. Res. 28 (1989) 1489.

[92] H.A. Smits, A. Stankiewicz, W.C. Glasz, T.H.A. Fogl, J.A. Moulijn, Chem. Eng. Sci. 51 (1996) 3019.

[93] J.G. Weissman, Fuel Process. Technol. 50 (1997) 199.

[94] B.W. van Hasselt, P.J.M. Lebens, H.P.A. Calis, F. Kapteijn, S.T. Sie, J.A. Moulijn, C.M. van den Bleek, Chem. Eng. Sci. 54 (1999) 4791.

Chapter 2

Structure of Sulfide Catalysts

2.1 Introduction

Industrial hydrotreating catalysts contain molybdenum and cobalt or nickel, supported on γ-Al_2O_3 [1-4]. Since oil fractions always contain sulfur, a metal or metal oxide that would be introduced as a catalyst would quickly become sulfided by the H_2S that is produced during hydrotreating. In practice, one therefore sulfides supported metal oxides under controlled conditions before starting the hydrotreating process. When supported alone on alumina, molybdenum sulfide has a much higher activity for the removal of S, N and O atoms than cobalt or nickel sulfide. Therefore, molybdenum sulfide is traditionally considered to be the actual catalyst. Sulfided $CoMo/Al_2O_3$ and $NiMo/Al_2O_3$ catalysts, on the other hand, have substantially higher catalytic activities than Mo/Al_2O_3. Consequently, cobalt and nickel are referred to as promoters [1-4]. Cobalt is used mainly as a promoter for sulfided Mo/Al_2O_3 in HDS, whereas nickel is the choice for HDN.

Hydrotreating catalysts originated in the 1920s when German researchers developed unsupported metal sulfide catalysts to liquefy coal. However, it was not until the 1970s that the structures of these catalysts and the mechanisms of their catalytic action began to be understood. It was established that under catalytic reaction conditions, most of the molybdenum in industrial hydrotreating catalysts is present as small MoS_2 particles in the pores of the γ-Al_2O_3 support. It was not until the 1980s that the location of the cobalt and the nickel promoter ions in the hydrotreating catalysts was more or less determined.

2.2 Structure of the catalyst

2.2.1 Structure of the oxidic catalyst precursor

Hydrotreating catalysts are usually prepared by a sequential pore volume impregnation procedure or by co-impregnation [2-5]. In the former method, the γ-Al_2O_3 support is first impregnated with an aqueous solution of ammonium heptamolybdate $(NH_4)_6Mo_7O_{24}$, followed by drying and calcination in air. In a second step, the resulting material is further impregnated with an aqueous solution of nickel nitrate $Ni(NO_3)_2$ or cobalt nitrate $Co(NO_3)_2$ and then dried and calcined. Alternatively (and preferentially in the industry), all inorganic materials are co-impregnated in order to shorten the preparation procedure and lower the operation cost, and the resulting catalyst precursor is then dried and calcined.

The detailed nature and structure of the molybdenum species in the oxide precursor state of the catalyst are still under debate. The strong interaction between molybdenum with the hydroxyl groups on the Al_2O_3 surface has been assumed to result in a MoO_3 monolayer structure [6,7]. This has been later proved by a thermodynamic study [8]. Massoth has suggested that the molybdenum is present in small patches or chains rather than a well defined two-dimensional monolayer [9]. A similar conclusion was reached in a combined ^{1}H-NMR and low temperature chemisorption study [10], and in several EXAFS studies [11-14]. The latter studies show that Mo is present in structures without a significant order outside the first coordination shell. Even for relatively high-loading Mo/Al_2O_3 catalysts (15 wt% MoO_3), infrared emission spectroscopy could not detect bands due to a MoO_3 phase [15], indicating that the molybdenum is present in a highly dispersed phase.

Investigations on Ni- and Co-promoted catalysts confirmed an interaction between molybdenum and nickel or cobalt in the catalyst in the oxidic state. Thus, the order of impregnation and calcination - first molybdenum and then nickel or cobalt or vice versa - plays an important role in the activity of the final sulfided catalyst. Catalysts in which the support is impregnated first with a solution containing molybdenum invariably have a higher activity. It has been suggested that the nickel or cobalt cations interact with the polymolybdate phase by forming a metal heteropolymolybdate [16,17]. Several publications deal with this subject: For instance, the infrared absorption bands of NO adsorbed on $CoMo/Al_2O_3$ are shifted from those of NO on Co/Al_2O_3 [18], and Raman bands due to polymeric molybdenum

oxide species decrease in intensity with increasing cobalt loading in an oxidic $CoMo/Al_2O_3$ catalyst [19]. The results suggest that nickel or cobalt cations interact especially with the most highly polymerized molybdenum oxide species to form species in which nickel or cobalt and molybdenum interact. In this way the promoter cations stay at the surface and close to the molybdenum cations and are well positioned to form the active Ni-Mo-S structure during sulfidation (see below). Furthermore, the promoter ions interact to a lesser extent with the support and thus can be used more efficiently after sulfidation. The reason for the interaction of Co or Ni cations with the Mo oxyanions or polymeric Mo species is that the isoelectric point (IEP) of the Mo-containing compounds is much lower than that of the alumina surface. The IEP is the pH value at which the surface is not charged when in contact with an electrolyte solution. Surfaces are positively charged by proton uptake at a pH value below the IEP and negatively charged at a pH greater than the IEP. Under the usual impregnation conditions (pH around 5), the oxidic Mo-containing species are negatively charged, and the alumina surface is positively charged. As a result, the nickel and cobalt cations adsorb on the oxidic Mo-containing species.

2.2.2 Structure of the sulfidic catalyst

The oxidic catalyst precursors, which are formed during the impregnation, drying and calcination steps, are transformed into the actual hydrotreating catalyst by sulfidation in a mixture of H_2 and one or more compounds containing sulfur. H_2S, thiophene, CS_2, dimethyl disulfide or the oil fraction to be hydrotreated can be used for the sulfidation. The properties of the final sulfidic catalyst depend to a great extent on the calcination and sulfidation steps. Calcination at high temperature induces a strong interaction between molybdenum and cobalt or nickel cations and the Al_2O_3 support. Consequently, it is difficult to transform the oxidic species into sulfides. Mössbauer spectroscopy of $CoMo/Al_2O_3$ catalysts showed that, at increasingly high calcination temperatures, increasingly more Co^{2+} ions are incorporated into the bulk of the alumina [20]. The higher the calcination temperature, the higher the sulfidation temperature needed to bring these cations back to the surface to provide a high catalytic activity for hydrotreating. At temperatures that are too high, however, the metal sulfides particles sinter or do not form the catalytically active Co-Mo-S structure. Optimum

calcination and sulfidation temperatures are in the range 673-773 K for Al_2O_3-supported catalysts [21].

The sulfidation mechanism was investigated by temperature-programmed sulfidation, in which the oxidic catalyst is heated in a flow of H_2S and H_2, and the consumption of H_2S and H_2 and the evolution of H_2O are measured continuously [22]. It was found that H_2S is taken up and H_2O given off, even at room temperature, indicating a sulfur-oxygen exchange reaction. This conclusion was confirmed by Cattaneo et al. with quick extended X-ray absorption fine structure (QEXAFS) studies (Fig. 2.1, phase 2), which also demonstrated that the Mo (VI) species containing both oxygen and sulfur transform into intermediate MoS_3-type species at temperatures between 520 and 570 K (Fig. 2.1, phase 3) [23]. At higher temperatures, the MoS_3 is reduced to MoS_2 (Fig. 2.1, Phase 4) with concomitant H_2 consumption and H_2S evolution [22].

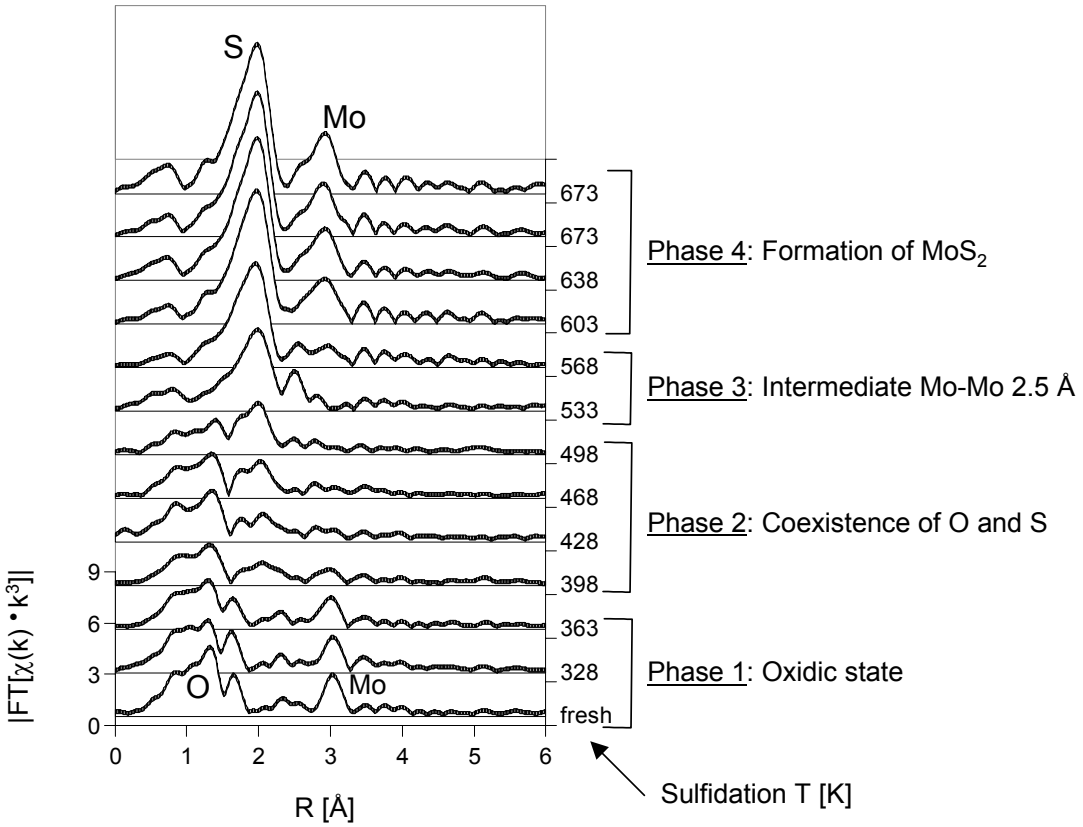

Fig. 2.1. Quick EXAFS spectra of the sulfidation of a Mo/Al_2O_3 catalyst, measured during continuous heating of the catalyst in 5% H_2S in H_2 from room temperature to 673 K at 5 K/min and holding at 673 K for 30 min [23].

MoS_2 has a layer lattice, and the sulfur-sulfur interaction between successive MoS_2 layers is weak (van der Waals force). Crystals grow as platelets with relatively large dimensions parallel to the basal sulfur planes and small dimensions perpendicular to the basal planes. High-resolution transmission electron microscopy of model HDS catalysts consisting of MoS_2 crystallites on planar Al_2O_3 showed that the MoS_2 crystallites occurred as platelets with a height-to-width ratio between 0.4 and 0.7 (Fig. 2.2).

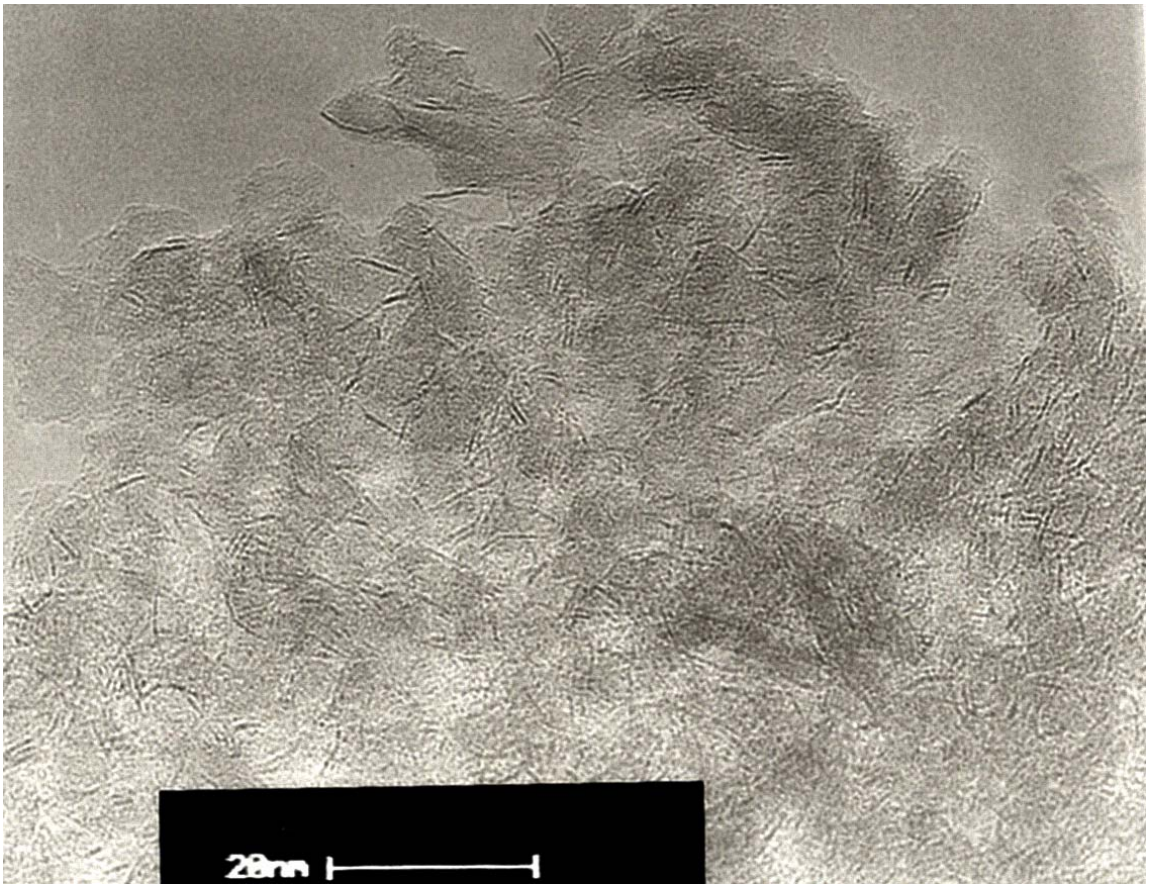

Fig. 2.2. TEM imagine of a sulfided $NiMo/Al_2O_3$ catalyst.

Investigations of model catalysts consisting of MoS_2 grown on γ-Al_2O_3 films on the surfaces of $MgAl_2O_4$ supports have shown that MoS_2 grows with its basal plane parallel to the (111) surface of γ-Al_2O_3 and perpendicular to the (100) γ-Al_2O_3 surface [24]. This observation suggests that the edges of the MoS_2 platelets are bonded to the (100) surface of γ-Al_2O_3 by Mo-O-Al bonds (Fig. 2.3).

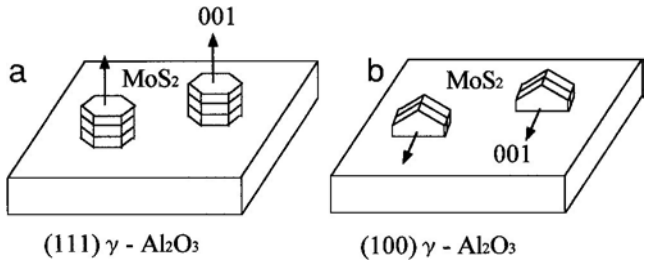

Fig. 2.3. Orientation of small MoS_2 particles on (111) – (a) and (100) – (b) γ-Al_2O_3 surface.

Nickel may be present in three forms after sulfidation: as Ni_3S_2 crystallites on the support, as nickel atoms adsorbed on the edges of the MoS_2 crystallites (the so-called Ni-Mo-S phase) and as nickel cations at octahedral or tetrahedral sites in the γ-Al_2O_3 lattice (Fig. 2.4). Analogously, cobalt can be present as segregated Co_9S_8, as Co-Mo-S and as cobalt cations in the support. Depending on the relative concentrations of nickel (or cobalt) and molybdenum and on the pretreatment conditions, a sulfided catalyst may contain a relatively large amount of either Ni_3S_2 (or Co_9S_8) or the Ni-Mo-S (or Co-Mo-S) phase.

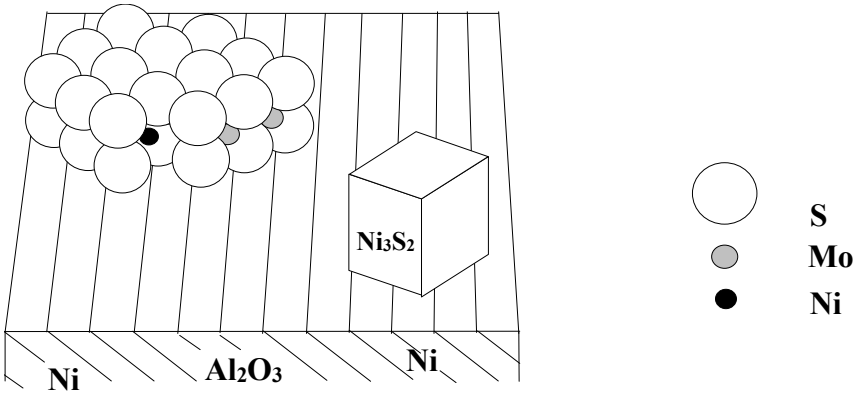

Fig. 2.4. Three forms of nickel present in a sulfided $NiMo/Al_2O_3$ catalyst: as active sites on the MoS_2 edges (the so-called Ni-Mo-S phase), as segregated Ni_3S_2, and as Ni^{2+} ions in the support lattice.

Several *in-situ* characterization techniques such as Mössbauer [20], infrared, and EXAFS confirmed the Ni-Mo-S (or Co-Mo-S) edge decoration model. The infrared spectra of NO molecules adsorbed on sulfided $CoMo/Al_2O_3$ catalysts indicated that as the cobalt content increased at a fixed molybdenum content, the number of NO molecules adsorbed on cobalt

sites increased and the number of NO molecules adsorbed on molybdenum sites decreased [25]. Cobalt atoms at edge-decoration sites cover molybdenum atoms and block adsorption of NO on these molybdenum atoms. The observed behavior is therefore in accordance with the edge-decoration location. EXAFS studies showed that a nickel atom in a sulfided NiMo catalyst supported on γ-Al_2O_3 or on carbon is surrounded by four or five sulfur atoms at a distance of 2.2 Å, by one or two molybdenum atoms at a distance of 2.8 Å, and by one nickel atom at a distance of 3.2 Å [26]. These data are consistent with a model in which the nickel atoms are located at the MoS_2 edges in the molybdenum plane in a square pyramidal coordination. The nickel atoms are connected to the MoS_2 by four sulfur atoms, and depending on the H_2S partial pressure a fifth sulfur atom may be present in the apical position in front of the nickel atom (Fig. 2.5). Recent density functional theory (DFT) calculations suggested a different edge-decoration model [27]. Instead of substituting molybdenum atoms at the $(10\bar{1}0)$ molybdenum edge, cobalt atoms were claimed to prefer to substitute molybdenum atoms at the $(\bar{1}010)$ sulfur edge. Other DFT calculations [28], however, indicated that these particular edge positions are an artifact of the too small MoS_2 clusters used to model MoS_2 in the calculations [27]. DFT calculations with larger MoS_2 clusters showed that the most favorable location of the promoter atoms is the substitutional position at the molybdenum edge. The nickel and cobalt atoms extend, as it were, the MoS_2 lattice by taking up molybdenum positions [28]. This conclusion is in good agreement with the EXAFS results (Fig. 2.5) [26].

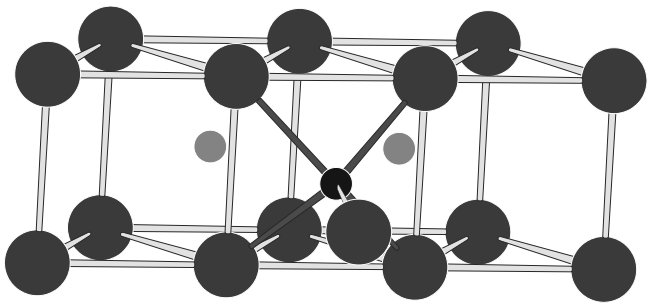

Fig. 2.5. Structure involving the nickel atoms in the Ni-Mo-S phase as determined by EXAFS [26]. The big balls are sulfur atoms; the small black is a nickel atom; and the small greyballs are molybdenum atoms.

Mössbauer data of Crajé et al. showed that the cobalt quadrupole splitting in $CoMo/Al_2O_3$ varies continuously with the cobalt loading and sulfiding temperature, which was suggested to be a consequence of the increasing size and ordering of the cobalt sulfide particles at the MoS_2 edges [29]. At very low cobalt loadings and after sulfiding at relatively low temperatures, all the cobalt atoms can be positioned around the MoS_2 edges and the catalytic activity initially increases with increasing Co/Mo ratio. If all the edge positions are occupied, then additional cobalt atoms must be located on top of the cobalt atoms that are already present or must be present separately as Co_9S_8 crystallites. Since the Co_9S_8 particles have a low catalytic activity and cover the MoS_2 particles, the HDS activity of CoMo catalysts decreases at increasingly high Co/Mo ratios. Maximum activity is usually observed at a Co/Mo ratio of 0.3 to 0.5. This result implies that the MoS_2 particles present on the Al_2O_3 support must be so small that the ratio of the number of molybdenum edge atoms to the total number of molybdenum atoms is the same (i.e. 0.3-0.5) [30]. Commercial catalysts usually have Co/Mo or Ni/Mo ratios slightly higher than 0.5, with molybdenum loadings of about 10 to 15 wt%.

2.2.3 Nature of active sites

As will be seen in Section 3.1, different types of reactions are involved in HDS and HDN. Then the question is what are the active sites for these reactions. Are molybdenum sites the catalytically active sites, and if so, how are they promoted by nickel and cobalt, or do the nickel and cobalt atoms constitute new sites which are supported on and influenced by MoS_2?

It was commonly assumed that the catalytically active sites in hydrotreating catalyst are the molybdenum atoms at the surfaces of the MoS_2 crystallites, with at least one sulfur vacancy at a site to allow the reacting molecule to bind chemically to the molybdenum atom [1-4]. Since sulfur atoms in the basal planes of MoS_2 are much more difficult to remove than sulfur atoms at edges and corners, exposed molybdenum atoms are predominantly present at edges and corners. Catalysis therefore occurs at MoS_2 edges and corners rather than on basal planes, as verified in a surface-science study in which a MoS_2 single crystal, with high basal plane to edge surface area ratio, was found to have a low HDS activity. Its activity increased after sulfur atoms were sputtered away from the basal plane and the molybdenum atoms became exposed [31]. Scanning tunnelling microscopy was used recently to image MoS_2

nanoparticles on a gold surface [32]. Most MoS_2 nanoparticles had triangular shapes rather than the hexagonal shapes observed by electron microscopy for MoS_2 crystallites on Al_2O_3. Exposure of the MoS_2 nanoparticles to hydrogen led to the creation of sulfur vacancies. Such vacancies at the MoS_2 edge are supposed to be the catalytically active sites for HDS.

Because the HDN and HDS activities of a MoS_2/Al_2O_3 catalyst both increase substantially with addition of nickel or cobalt, several explanations have been proposed for the promoting function of nickel and cobalt [1-4]. One of the proposed models was based on the observations that unsupported CoMo catalysts have only two phases: Co_9S_8 and MoS_2 that interact with each other [33,34]. Even a mechanical mixture of Co_9S_8 and MoS_2, when in close contact, can be rather active [35,36]. Delmon and co-workers therefore believed that segregated cobalt sulfide is the promoter and that it supplies MoS_2 with hydrogen atoms. These "spilled-over" hydrogen atoms were inferred to create reduced centers on the MoS_2 surface, which are the catalytically active sites [33,34]. The Co_9S_8 would then have "remote control" over the MoS_2 surface. Combined Mössbauer spectroscopy and HDS activity studies demonstrated, however, that the promoter effect of cobalt is related to the cobalt atoms in the Co-Mo-S phase and not to the separate Co_9S_8 [37,38]. Small amounts of cobalt strongly increased the thiophene HDS activity and led preferentially to the Co-Mo-S phase. Co_9S_8 formed only at higher cobalt loadings at which the activity had already levelled off. The catalytic activity actually decreased when Co_9S_8 became the dominant phase at high cobalt loadings.

Topsøe and coworkers attributed the promotion effect to the cobalt present in the Co-Mo-S phase, based mainly on *in-situ* emission Mössbauer spectroscopy [37]. Cobalt atoms are located at the edges of the MoS_2 crystallites [38,39]. A significant contribution of separate Co_9S_8 was excluded [37,38]. This so-called Co-Mo-S model (or Ni-Mo-S model for NiMo catalysts) is currently the most accepted one.

However, the Co-Mo-S model does not indicate whether the catalytic activity arises from molybdenum promoted by the presence of cobalt or from the cobalt sites themselves. Both cobalt and nickel sulfides, when supported on carbon, have higher HDS activities than MoS_2/C [40]. Therefore, it has been suggested that the cobalt atoms in the Co-Mo-S phase and nickel atoms in the Ni-Mo-S phase might be the actual catalysts and not the promoters. In the past, the idea that cobalt and nickel might be the catalysts in sulfided CoMo and NiMo systems was rejected because sulfided Co/Al_2O_3 and Ni/Al_2O_3 had very low HDS activities. However, during the usual pretreatment of Co/Al_2O_3 and Ni/Al_2O_3 (without molybdenum)

catalysts, cobalt and nickel cations interact strongly with the Al_2O_3 support. Therefore, during subsequent sulfidation, the metal cations are not sulfided at all and do not contribute to the HDS activity. Alternatively, severe sulfidation brings the metal cations back to the surface but lowers their dispersions (by sintering), and thus lowers their activities.

Carbon-supported cobalt and nickel sulfide catalysts, when carefully prepared, are indeed highly active. The activity of a sulfided CoMo/C catalyst, per cobalt atom, correlated much better with the estimated number of surface cobalt atoms in a sulfided Co/C catalyst than with the estimated number of edge molybdenum atoms in a MoS_2/C catalyst [41]. The observation that the hydrogenation activity of CoMo (or NiMo) catalysts resembles that of sulfided cobalt or nickel catalysts and is different from that of supported MoS_2 is further evidence that cobalt and nickel are the catalytic sites rather than molybdenum. As previously mentioned, infrared [25] and Mo-edge EXAFS data [26,42] showed that molybdenum in CoMo and NiMo catalysts is fully coordinated and not accessible to reactant molecules. The molybdenum therefore can not be catalytically active. Although attempts to show direct proof of nickel or cobalt as the actual catalytically active sites gave both positive and negative results by EXAFS data of catalysts adsorbed with selenophene (analog of thiophene) [43-45], it seems clear that the first reaction takes place on cobalt but not on molybdenum.

Recent theoretical calculations have concentrated on a combined action of nickel (or cobalt) and molybdenum [27,28,46-48]. In HDS, a sulfur-containing molecule is supposed to adsorb on a site with a sulfur vacancy and react to give a hydrocarbon molecule and a sulfur atom. This sulfur atom occupies the vacancy and must be removed by hydrogen before the catalytic cycle can start again. It has been pointed out that a sulfur atom between a nickel (or cobalt) and a molybdenum atom is less strongly bonded than a sulfur atom between two molybdenum atoms. Therefore, it can be more easily removed. This would explain the promoter effect of nickel and cobalt on molybdenum in HDS. If HDN were to occur analogously to HDS, a nitrogen atom should be taken up by the metal sulfide catalyst particles and later be removed by hydrogen in the same way. This seems less likely than the equivalent sulfur uptake and removal in HDS, and it is suggested that the sites used in HDN are different from those used in HDS. As will be shown in Chapter 3, C-S bond breaking is kinetically important in HDS, whereas the hydrogenation of N-containing aromatic rings is kinetically the most important step in HDN.

Now the question is how the metal atoms are situated at the catalyst surface and what is the structure of the catalytic sites. Therefore, we first consider the edges of pure and

promoted MoS_2. Raybaud *et al.* reported DFT calculations representing the edge surface of unpromoted [28] and promoted MoS_2 [48]. Two types of edges are present in stoichiometric, hexagonal MoS_2 particles (Fig. 2.6). The $(10\bar{1}0)$ edge is terminated by molybdenum atoms, and is therefore called the molybdenum edge; in contrast, sulfur atoms terminate the $(\bar{1}010)$ edge (sulfur edge).

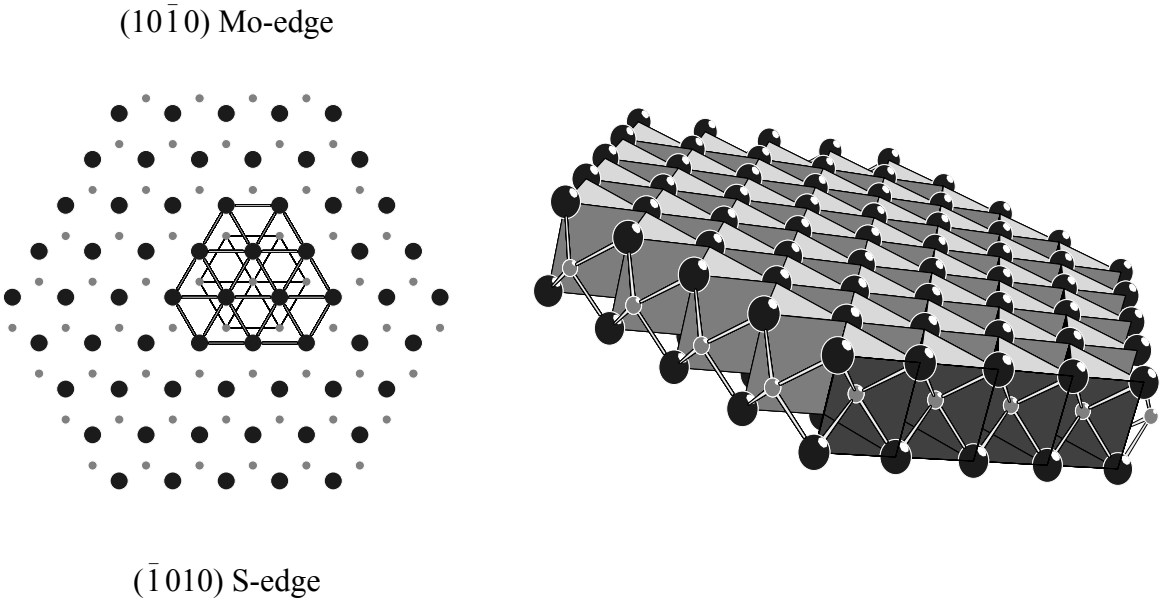

Fig. 2.6. Stoichiometric, hexagonally shaped MoS_2 particle with 25 Å diameter and 40% molybdenum edge atoms. Large balls are sulfur atoms, small balls are molybdenum atoms.

The local density functional calculations showed that addition of sulfur atoms to the molybdenum edge is an exothermic process for sulfur coverages up to 50% [28]. Sulfur removal from the sulfur edge is endothermic. At low H_2S pressures in the gas phase, and thus at low H_2S/H_2 partial pressure ratios, the molybdenum atoms at the Mo edge have four sulfur nearest neighbors (Fig. 2.6). At a high H_2S/H_2 ratio ($\geq$0.01), the molybdenum atoms have six sulfur nearest neighbors (Fig. 2.7), where the extra sulfur atoms are in bridging positions between molybdenum edge atoms.

The most stable position for the cobalt promoter atoms was calculated to be at the edge, substituting as it were for the molybdenum atoms [48]. The promoter decreased the equilibrium sulfur coverage of the edge from 50 to 0-17% for the Mo edge with Co/Mo = 1,

and it weakened the sulfur-metal bond. In a naive ionic model of the bonding in metal sulfides, this result makes sense because the charge on Co^{2+} is lower than that on Mo^{4+}. The coordination of cobalt at the edge is almost identical to that of the molybdenum edge atoms in Figs. 2.6 and 2.7, apart from shorter Co-S than Mo-S distances (Fig. 2.8).

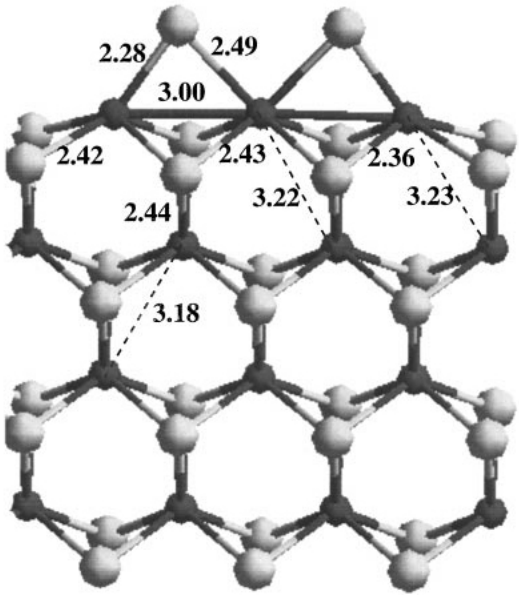

Fig. 2.7. Energy-optimized structure representing the molybdenum atoms at the Mo-terminated edge of MoS_2 particles at 33% sulfur coverage [28]. Black balls are molybdenum atoms, grey balls are sulfur atoms; the distances are in Angstrøms.

The DFT calculations showed that the edge structure of MoS_2 and promoted MoS_2 can be substantially different from that of ideally cleaved MoS_2 slabs. The surface can relax and take up sulfur atoms, as was predicted years ago by Farragher [49]. The molybdenum (or CoMo) structures presented in Figs. 2.7 and 2.8 may represent the actual sites during catalysis. It is more likely, however, that some reorganization occurs before catalysis takes place. For instance, one could envisage that the bridging edge sulfur atoms in Figs. 2.7 and 2.8 shifts to non-bridging on-top positions, thus creating a vacancy at the cobalt, nickel, or molybdenum atoms at the edge. A reacting molecule can then adsorb with its sulfur atom (in HDS) or nitrogen atom (in HDN) on this vacancy. Such a reorganized site may be the site where elimination of NH_3 from a nitrogen-containing molecule takes place. Probably the more open sites, with two or more vacancies, are the sites where aromatic molecules are

hydrogenated. At such sites, the aromatic ring can be π bonded to the exposed molybdenum, cobalt, or nickel atoms at the molybdenum edge, as in Fig. 2.6.

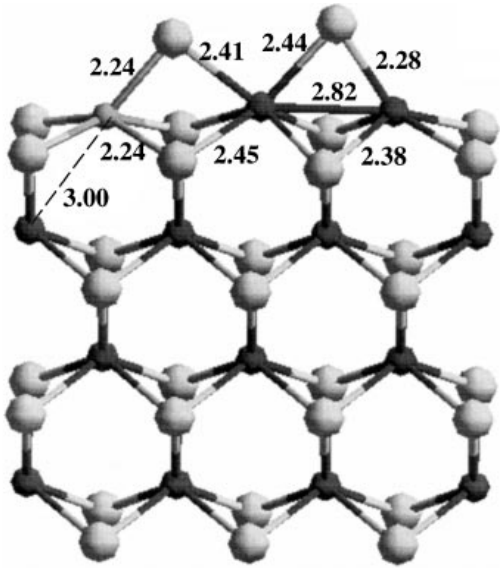

Fig. 2.8. Fully optimized structures of the promoted Mo edge with Co/Mo = 0.33 and 33% S, where the big balls are S, the dark ones are Mo and the small one is Co [48].

In most publications, no distinction is made between the structures of nickel and cobalt. It is commonly assumed that both are situated at identical positions at the MoS_2 edge, in the Ni-Mo-S and Co-Mo-S structures. The DFT calculations of Raybaud *et al.* [48] suggest that the sulfur coverage on the Mo edge is lower in the nickel case than in the cobalt case. Future theoretical studies may indicate whether this difference is sufficient to explain why NiMo is the better hydrogenation, thus HDN catalyst and CoMo the better HDS catalyst.

2.3 References

[1] T.C. Ho, Catal. Rev.-Sci. Eng. 30 (1988) 117.

[2] R. Prins, V.H.J. de Beer, G.A. Somorjai, Catal. Rev.-Sci. Eng. 31 (1989) 1.

[3] H. Topsøe, B.S. Clausen, F.E. Massoth, in, Catalysis: Science and Technology, 1996,

[4] R. Prins, Adv. Catal. 46 (2002) 399.

[5] R.R. Chianelli, M. Daage, M.J. Ledoux, Adv. Catal. 40 (1994) 177.

[6] G.C.A. Schuit, B.C. Gates, AIChE J. 19 (1973) 417.

[7] F.E. Massoth, Adv. Catal. 27 (1978) 265.

[8] T. Lim, S.W. Weller, J. Catal. 108 (1987) 175.

[9] F.E. Massoth, J. Catal. 36 (1975) 164.

[10] H. Kraus, R. Prins, J. Catal. 164 (1996) 260.

[11] N.S. Chiu, S.H. Bauer, M.F.L. Johnson, J. Catal. 89 (1984) 226.

[12] T.G. Parham, R.P. Merrill, J. Catal. 85 (1984) 295.

[13] G. Sankar, P.R. Sarode, A. Srinivasan, C.N.R. Rao, S. Vasudevan, J.M. Thomas, Proc. Indian Acad. Sci.-Chem. Sci. 93 (1984) 321.

[14] B.S. Clausen, B. Lengeler, H. Topsøe, Polyhedron 5 (1986) 199.

[15] C. Li, Q. Xin, K.L. Wang, X.X. Guo, Appl. Spectrosc. 45 (1991) 874.

[16] S. Kasztelan, J. Grimblot, J.P. Bonnelle, J. Phys. Chem. 91 (1987) 1503.

[17] M. Adachi, C. Contescu, J.A. Schwarz, J. Catal. 162 (1996) 66.

[18] N. Topsøe, H. Topsøe, J. Catal. 75 (1982) 354.

[19] X. Gao, Q. Xin, Catal. Lett. 18 (1993) 409.

[20] C. Wivel, B.S. Clausen, R. Candia, S. Mørup, H. Topsøe, J. Catal. 87 (1984) 497.

[21] R. Prada Silvy, P. Grange, B. Delmon, Stud. Surf. Sci. Catal. 52 (1990).

[22] P. Arnoldy, J.A.M. van den Heijkant, G.D. de Bok, J.A. Moulijn, J. Catal. 92 (1985) 35.

[23] R. Cattaneo, T. Weber, T. Shido, R. Prins, J. Catal. 191 (2000) 225.

[24] Y. Sakashita, T. Yoneda, J. Catal. 185 (1999) 487.

[25] N. Topsøe, H. Topsøe, J. Catal. 84 (1983) 386.

[26] S.P.A. Louwers, R. Prins, J. Catal. 133 (1992) 94.

[27] L.S. Byskov, J.K. Nørskov, B.S. Clausen, H. Topsøe, J. Catal. 187 (1999) 109.

[28] P. Raybaud, J. Hafner, G. Kresse, S. Kasztelan, H. Toulhoat, J. Catal. 189 (2000) 129.

[29] M.W.J. Crajé, S.P.A. Louwers, V.H.J. de Beer, R. Prins, A.M. van der Kraan, J. Phys. Chem. 96 (1992) 5445.

[30] A.L. Farragher, P. Cossee, *in* "Proceedings of the 5th International Congress on Catalysis", (J. W. Hightower, Ed.), North-Holland, Amsterdam, 1973; Vol. 2. p. 1301.

[31] M.H. Farias, A.J. Gellman, G.A. Somorjai, R.R. Chianelli, K.S. Liang, Surf. Sci. 140 (1984) 181.

[32] S. Helveg, J.V. Lauritsen, E. Laegsgaard, I. Stensgaard, J.K. Nørskov, B.S. Clausen, H. Topsøe, F. Besenbacher, Phys. Rev. Lett. 84 (2000) 951.

[33] B. Delmon, Bull. Soc. Chim. Belg. (1979) 979.

[34] P. Grange, X. Vanhaeren, Catal. Today 36 (1997) 375.

[35] G, Hagenbac, P. Courty, B. Delmon, J. Catal. 23 (1971) 295.

[36] G, Hagenbac, P. Courty, B. Delmon, J. Catal. 31 (1973) 264.

[37] H. Topsøe, B.S. Clausen, R. Candia, C. Wivel, S. Mørup, J. Catal. 68 (1981) 433.

[38] C. Wivel, R. Candia, B.S. Clausen, S. Mørup, H. Topsøe, J. Catal. 68 (1981) 453.

[39] P. Ratnasamy, S. Sivasanker, Catal. Rev.-Sci. Eng. 22 (1980) 401.

[40] J.C. Duchet, E.M. van Oers, V.H.J. de Beer, R. Prins, J. Catal. 80 (1983) 386.

[41] J.P.R. Vissers, V.H.J. de Beer, R. Prins, J. Chem. Soc. Faraday Trans. I 83 (1987) 2145.

[42] S. Bouwens, R. Prins, V.H.J. de Beer, D.C. Koningsberger, J. Phys. Chem. 94 (1990) 3711.

[43] L. Medici, M. Harada, R. Prins, Mendeleev Commun. (1996) 121.

[44] B.R.G. Leliveld, J.A.J. van Dillen, J.W. Geus, D.C. Koningsberger, M. de Boer, J. Phys. Chem. B 101 (1997) 11160.

[45] R.G. Leliveld, A.J. van Dillen, J.W. Geus, D.C. Koningsberger, J. Catal. 175 (1998) 108.

[46] J.K. Nørskov, B.S. Clausen, H. Topsøe, Catal. Lett. 13 (1992) 1.

[47] H. Toulhoat, P. Raybaud, S. Kasztelan, G. Kresse, J. Hafner, Catal. Today 50 (1999) 629.

[48] P. Raybaud, J. Hafner, G. Kresse, S. Kasztelan, H. Toulhoat, J. Catal. 190 (2000) 128.

[49] A.L. Farragher, Adv. Colloid Interface Sci. 11 (1979) 3.

Chapter 3

Experimental

3.1 Model compounds

Hydrodesulfurization (HDS) has for a long time been one of the most important processes in oil refineries. The HDS reactions of different model compounds have therefore been studied extensively. Because of the growing interest to hydroprocessing of high-boiling petroleum fractions and because of increasingly stringent air quality regulations, recent research has been focused on the HDS of thiophenic compounds, since they are the least reactive organosulfur compounds in petroleum and other fossil fuels. Numerous review papers were devoted to mechanisms of HDS [1-9]. Thiophene, benzothiophene, dibenzothiophene and their substituents are mainly used as the model sulfur-containing molecules.

The increased interest in processing heavy feeds led to an increase in studies of the hydrodenitrogenation (HDN) of model compounds. Different aspects of HDN have been discussed in the literature [8-16]. Nitrogen in different feedstocks is present predominantly in heterocyclic aromatic compounds. Pyridine and quinoline are the most frequently used model compounds that mimic the properties of the nitrogen-containing compounds found in oil distillates.

3.1.1 S-containing molecules

The HDS of organosulfur compounds is exothermic and essentially irreversible under the reaction conditions employed industrially (e.g. 340 – 425°C and 55 – 170 atm) [1,4]. As

will be discussed in the following, sulfur removal occurs either with or without hydrogenation of the heterocyclic ring. The pathways that involve the ring hydrogenation prior to the sulfur removal can be affected by thermodynamics, since hydrogenation of organosulfur compounds is equilibrium limited at practical HDS temperatures. Thus, sulfur removal via hydrogenation may be inhibited at low pressures and high temperatures because of the low equilibrium concentrations of hydrogenated intermediates [5].

The HDS networks were studied in detail for thiophene, benzothiophene and dibenzothiophene. The majority of experiments on the HDS of thiophene has been performed at atmospheric pressure [1,4]. It was suggested that the HDS of thiophene proceeds via two parallel pathways (Scheme 3.1). In one reaction route thiophene is hydrodesulfurized to butadiene that is further hydrogenated to give 1-butene and cis- and trans-2-butene. Butenes are then hydrogenated to n-butane. In the second pathway thiophene is first hydrogenated to tetrahydrothiophene that is desulfurized to butadiene. Tetrahydrothiophene and butadiene were observed in trace amounts in the reaction products. These intermediates were suggested to be very reactive and to transform rapidly to butenes and butane [5]. This makes the use of the thiophene as the S-containing model compound less interesting, since one cannot distinguish the different reaction pathways.

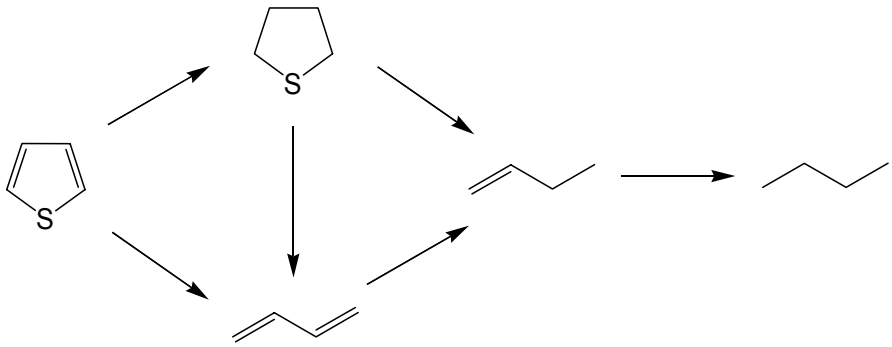

Scheme 3.1. Reaction network of the HDS of thiophene suggested by low-pressure studies [1].

The HDS of benzothiophene has also been reported to proceed via two reaction pathways: hydrogenolysis to ethylbenzene and hydrogenation to dihydrobenzothiophene followed by hydrogenolysis to ethylbenzene (Scheme 3.2) [4,17,18]. Therefore, both reaction pathways in the HDS of benzothiophene lead to the formation of the same final product,

ethylbenzene. This makes the use of benzothiophene as the model S-containing molecule less attractive.

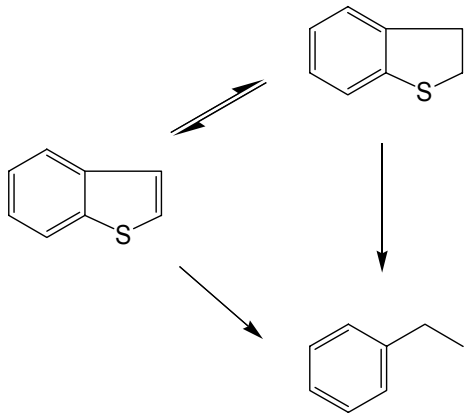

Scheme 3.2. Reaction network of the HDS of benzothiophene proposed by van Parijs et al. [18].

A detailed network of the HDS of dibenzothiophene was proposed by Houalla et al. in 1978 [19]. The reaction network and kinetic parameters are presented in Scheme 3.3. These data indicate that dibenzothiophene conversion occurs selectively via the path with the least hydrogen consumption and that hydrogenation of biphenyl and cyclohexylbenzene is comparatively slow. A similar network, desulfurization to biphenyl and hydrogenation to tetrahydro- and hexahydrodibenzothiophene followed by desulfurization to cyclohexylbenzene, was proposed in numerous studies [20-24].

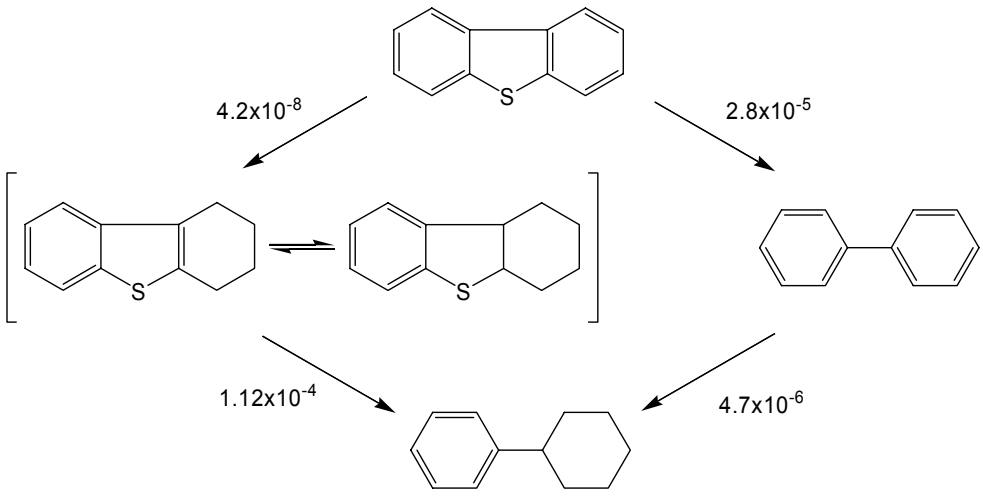

Scheme 3.3. Reaction network of the HDS of dibenzothiophene proposed by Houalla et al. [25].

Dibenzothiophene is less reactive than thiophene and benzothiophene [5,9]. Therefore, it is easier to follow the reaction intermediates in the HDS network. The two reaction products biphenyl and cyclohexylbenzene correspond to the desulfurization and hydrogenation pathways, respectively. Thus, dibenzothiophene would be a better model compound to study HDS than thiophene or benzothiophene and therefore we used dibenzothiophene in our studies. The results on the HDS network of dibenzothiophene will be described in detail in Chapters 5 and 8. The effect of N-containing molecules and H_2S on the HDS of dibenzothiophene will be presented in Chapters 5, 6 and 8.

The effects of substituents on the HDS of dibenzothiophene are well known [25-32]. Substituents groups at the carbon adjacent to the sulfur atom retard the HDS rate significantly while substituents groups at carbon atoms far from the sulfur atom increase or do not affect the HDS reactivity. 4,6-Dimethyldibenzothiophene is often used as refractory model S compound. The HDS mechanism of 4,6-dimethyldibenzothiophene is similar to that of dibenzothiophene shown in Scheme 3.3. However, the methyl groups hinder the direct sulfur removal so strongly that the HDS mainly occurs via the hydrogenation pathway, in contrast to the HDS of benzothiophene. Therefore, we decided to use also 4,6-dimethyldibenzothiophene as a model S-containing molecule. The reaction network of the HDS of 4,6-dimethyldibenzothiophene and the effect of N compounds and H_2S are described in Chapters 7 and 8.

3.1.2 N-containing molecules

As the smallest heterocyclic nitrogen compound pyridine was believed to be the simplest model molecule to study HDN. Pyridine was often used to test the HDN activities of catalysts [33-37]. The reactions taking place in the HDN of pyridine are well understood and are presented in Scheme 3.4.

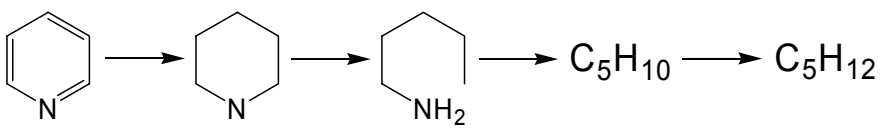

Scheme 3.4. Reaction network in the HDN of pyridine.

The C-N bond in aromatic rings is much stronger than that in aliphatic rings. Consequently, the C-N bond in pyridine can only be broken after hydrogenation of the ring to piperidine. The hydrogenation is catalyzed by sulfur-poor sites on the metal sulfide surface, since H_2S has a negative influence on this step. This reaction is also favored by hydrogen [11,34,38]. Thereafter, the nitrogen atom can be removed by Hofmann β-elimination or by nucleophilic substitution. In the Hofmann elimination, an acid helps to quaternize the nitrogen atom, thereby creating a better leaving group, whereas a base promotes elimination by removal of a β-hydrogen atom (Scheme 3.5).

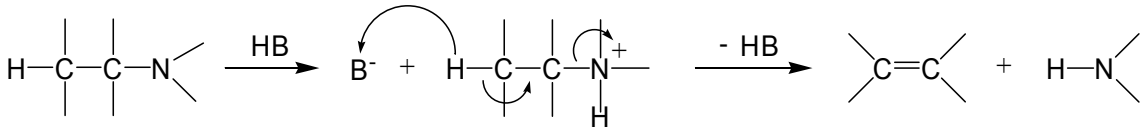

Scheme 3.5. C-N bond cleavage by Hofmann elimination.

Amines which have no β-hydrogen atoms can still be denitrogenated, although at higher temperatures. Thus, benzylamine (C_6H_5-CH_2-NH_2) was completely denitrogenated to give toluene at 350°C [39]. This result can be explained by nucleophilic substitution of the amine group by an SH group, followed by hydrogenolysis of the C-S bond, which is known to be very easy [40,41] (Scheme 3.6).

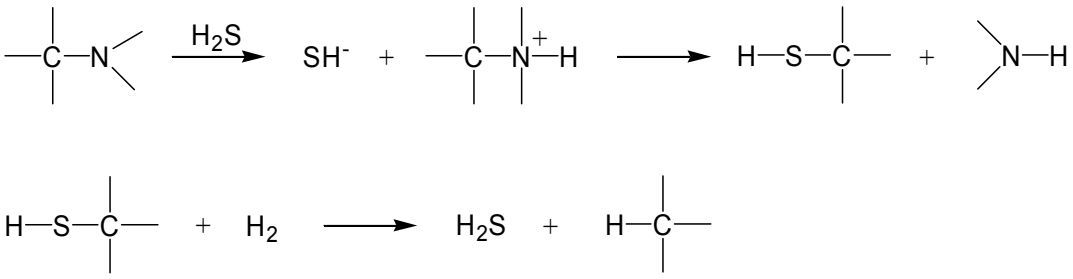

Scheme 3.6. C-N bond cleavage by S_N^2 nucleophilic substitution.

In the HDN of pyridine and piperidine, neither 5-aminopentene-1, the product of elimination of piperidine, nor 5-aminopentanethiol-1, the product of nucleophilic substitution, have ever been observed as intermediates probably because of their high reactivity and transformation to pentylamine before desorption from the catalyst surface. For non-cyclic amines the removal of the nitrogen atom by nucleophilic substitution was found to play an

important role in the HDN [42]. For cyclic amines like piperidine the HDN mechanism is still under investigation. It is known that H_2S has a positive influence on the C-N bond cleavage [11,34,38]. This could be evidence of both β-elimination and nucleophilic substitution as possible mechanisms of the C-N bond breaking that take place on relatively sulfur-rich sites on the surface of the metal sulfide catalyst.

In the HDN of pyridine and piperidine a side reaction of disproportionation is always taking place in parallel with HDN and it leads to the formation of products with high molecular weight. Namely, two piperidine molecules can disproportionate to N-pentylpiperidine and ammonia [11,16,38,43,44]. Mechanistically it is another example of a S_N^2 nucleophilic substitution of the NH_2 group of one amine molecule by the amine group of another amine molecule [45] (Scheme 3.7). Therefore, we decided to use in our studies 2-methylpyridine and 2-methylpiperidine as model N-containing molecules. It was shown that the disproportionation reaction is strongly suppressed by the presence of the methyl group on the α carbon atom. The HDN reaction network of 2-methylpyridine and 2-methylpiperidine will be described in Chapter 4 and the effect of H_2S on the HDN of 2-methylpyridine and 2-methylpiperidine will be discussed in Chapter 5.

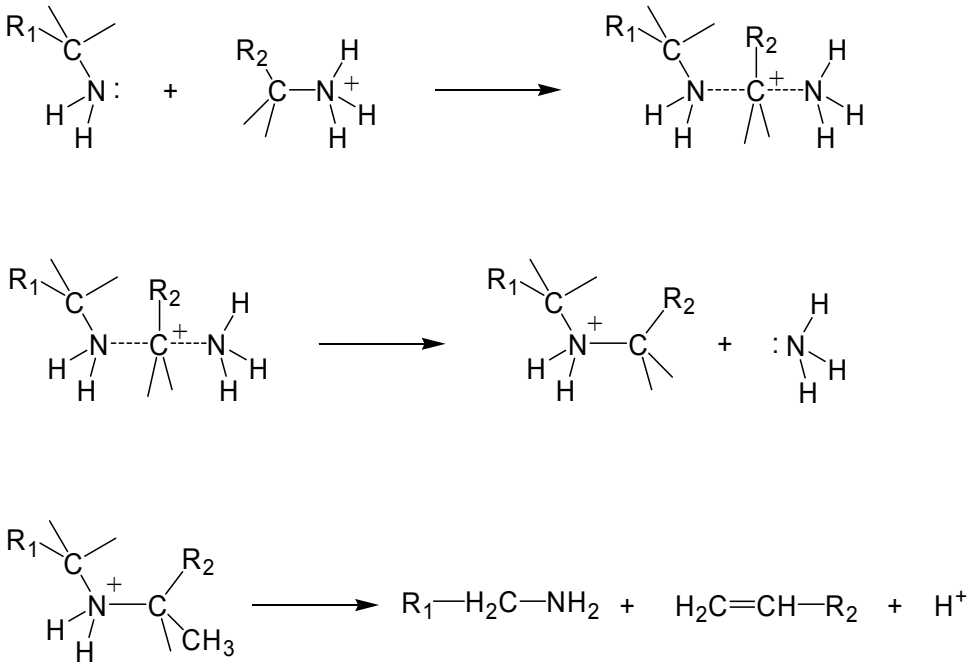

Scheme 3.7. Mechanism of the disproportionation of two amine molecules.

3.2 High-pressure set-up

A high pressure set-up was built in order to simulate the process that takes place in an industrial hydrotreater [Chapter 1]. The HDS and HDN experiments were carried out at 5 MPa total pressure and a temperature of 260 – 360°C in a continuous flow mode in a fixed-bed reactor. The catalyst was placed in the middle of a tube reactor made of inconel (12 mm internal diameter) that was heated with an oven. The main parts of the unit are shown in the simplified Scheme 3.8.

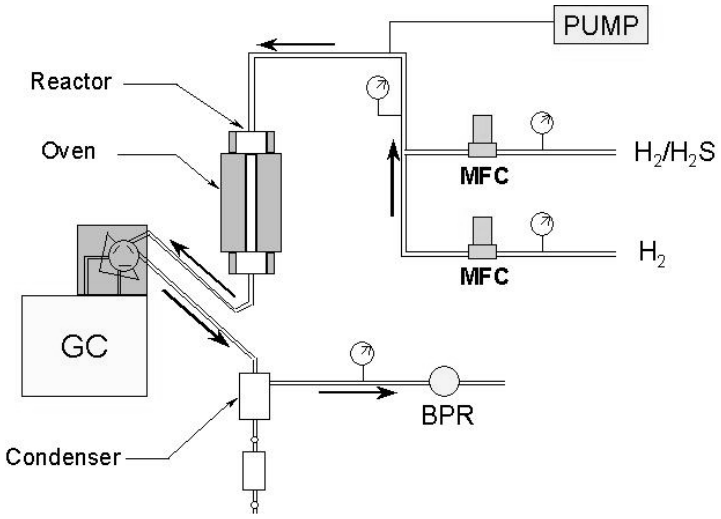

MFC – mass flow controller
BPR – back pressure regulator

Scheme 3.8. Simplified arrangement and the real appearance of the high-pressure set-up.

The reactants (S and N compounds and olefins) were mixed with dodecane and (or) heptane, which were used as references for the GC analysis in HDS and HDN experiments respectively. These mixtures were solved in decane or toluene, which were used as solvents, and simulated the presence of hydrocarbons during HDS and (or) HDN in real refinery operations. The obtained mixture was fed to the reactor by means of a Gilson 307 piston pump. H_2S was added to the feed in order to maintain the properties of the sulfided catalyst and to avoid the influence of H_2S released during HDS reaction. The gas flows of hydrogen and of the hydrogen – hydrogen sulfide mixture (90% H_2; 10% H_2S) were controlled by two

mass flow controllers (Brooks, Series 5850E). Gases and liquids were mixed before being heated in order to avoid plugs in the liquid inlet. The liquid reactants were fed co-current with the gases at the top of the reactor inlet (Scheme 3.8). The temperature of the reactor was controlled by an oven and also monitored inside the catalytic bed. The catalyst (0.05 g) was diluted with 8 g SiC to obtain good heat transfer. Another 8 g SiC were added above the catalyst bed to achieve plug-flow conditions. A more detailed description of the reactor is given in the dissertation of M. Flechsenhar [46]. After the reaction, the products (at the same pressure as in the reactor) flow through a 6-port valve heated at 300°C to maintain all products in the gas phase. This system allows sampling of all products to the chromatograph for analysis. It has a great advantage over the previous sampling system that was based on the splitting of the reaction products flow in two parts, one small flow to be analyzed in the gas chromatograph, and one big flow to be condensed [46]. The old system had several drawbacks: condensation, different flow rates producing different pressures, changing amounts analyzed in the gas chromatograph, leading to a bad mass balance. These problems were solved by using the 6-port-valve system that is shown in Scheme 3.9.

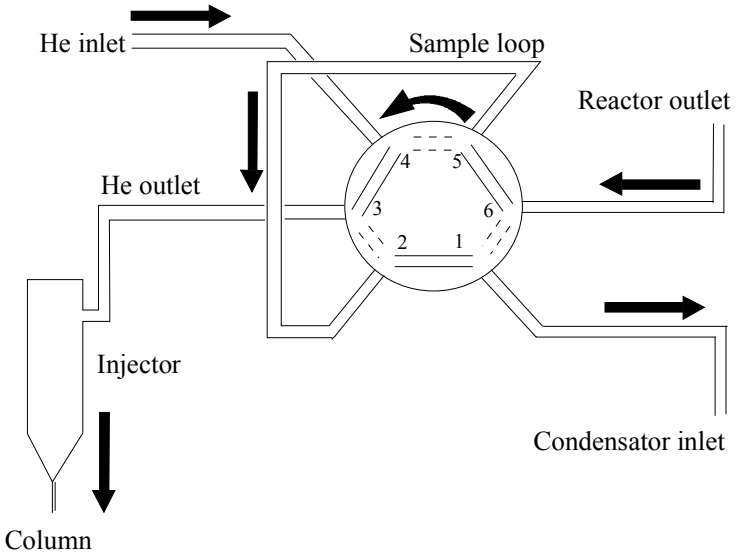

Scheme 3.9. Sampling system with the 6-port-valve.

Helium, the carrier gas for the GC column, was continuously flowing through the valve (inlet port 4, outlet port 3). Reaction products were continuously flowing through the sample loop (50 µl, ports 5-2) and then going to the condenser. When the sample was taken,

the valve turned 60° to connect the helium inlet to the sample loop, so that the content of the sample loop was purged into the injector. After 12 seconds the valve returned to the original position. During this period the reactor flow was led directly to the condenser (ports 6-1). This sampling system shows no mass balance problem if the operation temperature was above 280°C (this temperature depends on the boiling point of the reactants used). The reaction products were injected from the valve into the gas chromatograph equipped with a 50 m CP-Sil 8 CB fused silica capillary column (0.25 mm ID, 0.25 μm film thickness) for quantitative analysis. Detection was made with a flame ionization detector (FID) as well as with a pulsed flame photometric detector (PFPD), which is especially sensitive to nitrogen and sulfur-containing compounds. The detection method will be discussed more extensively in Section 3.4.1. After the 6-port-valve, the products were condensed in the condenser at room temperature. The heavy products were collected as a fluid in the condenser and the light gases (H_2, H_2S and NH_3) were purged from the back pressure regulator.

On-line analysis of the reaction products using the 6-port-valve system was performed in HDN experiments. In all HDS experiments, however, off-line analysis of the condensed fluid was used because of the high boiling points of the reactants and reaction products. The total pressure was maintained constant at 5 MPa using a back pressure regulator. A safety system was integrated in the unit. In case of over- and under-pressure (± 0.3 MPa) and in case of over- and under-heating (± 20°C) the inlet gases of H_2 and H_2/H_2S mixture and liquid were interrupted.

3.3 Catalysts preparation

The NiMo/γ-Al_2O_3, CoMo/γ-Al_2O_3 and Mo/γ-Al_2O_3 catalysts used in this work contained 8 wt% Mo and 3 wt% promoter (Ni or Co) and were prepared by successive incipient wetness impregnation of γ-Al_2O_3 (CONDEA, pore volume: 0.5 $cm^3 \cdot g^{-1}$, specific area 230 $m^2 \cdot g^{-1}$) with an aqueous solution of $(NH_4)_6Mo_7O_{24} \cdot 4H_2O$, followed (for the promoted catalysts) by an aqueous solution of $Ni(NO_3)_2 \cdot 6H_2O$ or $Co(NO_3)_2 \cdot 6H_2O$ (all Aldrich). The γ-Al_2O_3 support was milled and sieved prior being used to a particle size of 0.063 to 0.090 mm. After each impregnation step the catalyst was dried in air at ambient temperature for 4 h, then dried in an oven at 120 °C for 15 h, and finally calcined at 500 °C for 4 h.

A sample of 0.05 g of catalyst was diluted with 8 g SiC to achieve plug-flow conditions in the continuous flow fixed bed reactor. The oxidized form of the catalyst was sulfided *in situ* with a mixture of 10 % H_2S in H_2 (25 ml/min) at 400°C and 1.0 MPa for 4 hours. After sulfidation, the pressure was increased to 5.0 MPa, the temperature was decreased to reaction temperature, and the liquid reactant was fed to the reactor by means of a Gilson 307 piston pump. The reaction was stable after 3 to 4 h, and during two weeks of operation almost no catalyst deactivation was observed.

The gas-phase feed consisted of 130 kPa decane or toluene (as solvent for the dibenzothiophenes and amine), 8 kPa dodecane (as reference for dibenzothiophenes and their derivatives in the GC analysis), 11 kPa heptane (as reference for the N-compounds in the GC analysis), 1 kPa dibenzothiophene or 4,6-dimethyldibenzothiophene, 0.1 – 10 kPa amine reactant (2-methylpyridine or 2-methylpiperidine), 35 kPa H_2S (unless noted otherwise) and ~ 4.8 MPa H_2. Toluene was chosen as the solvent due to its good ability to dissolve aromatic heterocycles like dibenzothiophene. We checked that in the presence of S- or N-containing molecules toluene did not undergo hydrogenation to methylcyclohexane.

3.4 Product analysis

The product analysis was performed online with a Varian 3800 GC instrument equipped with a flame ionization detector (FID) and a pulsed flame photometric detector (PFPD). The FID detector was used to determine the concentration of the carbon-containing molecules. The signal of the FID is proportional to the number of carbon atoms present in the molecule. The N-containing molecules and their products were calibrated in the presence of heptane, while S compounds and their derivatives were calibrated in the presence of dodecane. Heptane and dodecane were used as internal standards to calculate the amount of different species in the HDN and HDS reactions respectively. The response factors (RF) of the compounds were determined by injecting a known amount of some molecule together with a known amount of internal standard. The quantitative analysis was performed using the correlation $\eta_i/\eta_{int.st.}=RF\cdot A_i/A_{int.st.}$.

Weight time was defined as $\tau=w_{cat}/n_{feed}$, where w_{cat} denotes the catalyst weight and n_{feed} the total molar flow to the reactor (1 g·min/mol = $1.8\cdot10^{-2}$ g·h/l). The weight time (τ) was

changed by varying the flow rates of the liquid and the gaseous reactants while keeping their ratio constant.

3.4.1 Pulsed flame photometric detector

The pulsed flame photometric detector is an improvement of the flame photometric detector (FPD). This improvement consists in a higher selectivity and sensitivity for several chemical elements. In a conventional FPD, a sample containing the heteroatoms of interest is burned in a hydrogen-rich flame to produce molecular products that emit light (chemiluminescent chemical reactions). The emitted light is isolated from background emissions by the use of wavelength-selective filters, detected by a photo-detector and amplified. The sensitivity of the conventional FPD is limited by the light emission of flame background combustion products, including CH*, C_2*, and OH*. The light emitted by such combustion products is referred to as the background emission. The narrow bandpass optical filters that attempt to isolate the emission wavelengths of the elements of interest (sulfur or nitrogen) from the emission bands of the flame background are limited. The novel solution to this problem was to set the fuel gas flow such that a continuous flame could not be sustained. By inserting a constant ignition source into the gas flow stream, the fuel gases would ignite, propagate back through a quartz combustor tube to a constriction in the flow path, extinguish, then refill the detector, ignite and repeat the cycle. The result was a PFPD detector shown in Scheme 3.10.

The combustion of hydrocarbons is highly exothermic, rapid and irreversible, thus the light emitted is concentrated in a pulse of duration approximately equal to the time required for the flame to propagate through the combustor (2-3 msec). The chemiluminescence reactions of S, P, N are less energetic and more reversible and they need more time to decay, so the emission of S_2*, HPO*, and HNO* occurs some time after the hydrocarbons [47,48]. By measuring after the hydrocarbon combustion and their emission, it is possible to amplify the heteroatom emissions. This selective amplification of the element-specific emissions is the basis of the PFPD's unique sensitivity and selectivity.

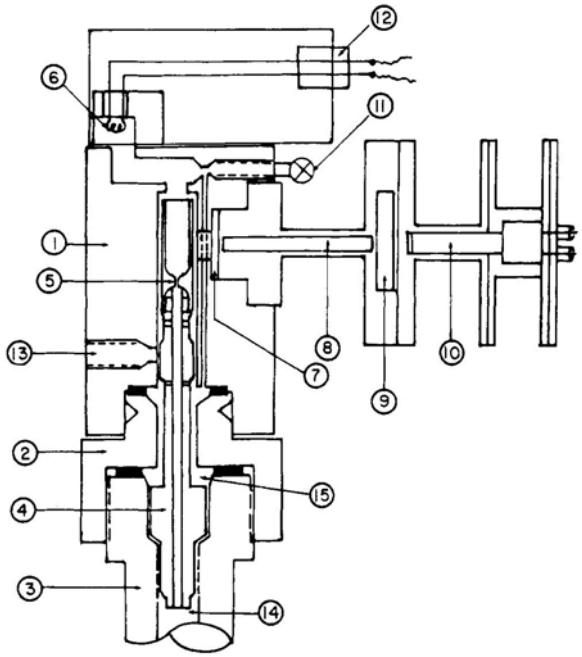

Scheme 3.10. Schematic diagram of the PFPD. (1) – main structure, (2) – GC adapter, (3) – GC – FID mount, (4) – combustion cell holder, (5) – quartz combustor, (6) – igniter, (7) – window, (8) – quartz rod light guide, (9) – color glass filter, (10) – photomultiplier, (11) – auxiliary screw valve, (12) – igniter and heater electrical feedthroughs, (13) – external material sampling inlet, (14) – hydrogen inlet, (15) – air inlet.

3.5 References

[1] B.C. Gates, J.R. Katzer, G.C.A. Schuit, in, Chemistry of Catalytic Processes, McGraw-Hill, New-York, 1979,

[2] O. Weisser, S. Landa, in, Sulphide Catalysts , Their Properties and Applications, Pergamon Press, Oxford, 1973.

[3] G.C.A. Schuit, B.C. Gates, AIChE J. 19 (1973) 417.

[4] P. Afanasiev, M. Cattenot, C. Geantet, N. Matsubayashi, K. Sato, S. Shimada, Appl. Catal. A 237 (2002) 227.

[5] M.J. Girgis, B.C. Gates, Ind. Eng. Chem. Res. 30 (1991) 2021.

[6] A.N. Startsev, Catal. Rev.-Sci. Eng. 37 (1995) 353.

[7] B. Delmon, Bull. Soc. Chim. Belg. 104 (1995) 173.

[8] H. Topsøe, B.S. Clausen, F.E. Massoth, in, Catalysis: Science and Technology, 1996,

[9] T. Kabe, A. Ishihara, W. Qian, Hydrodesulfurization and hydrodenitrogenation, Kodansha Ltd., Tokyo, WILEY-VCH Verlag GmbH, Weinheim, 1999.

[10] J.R. Katzer, R. Sivasubramanian, Catal. Rev.-Sci. Eng. 20 (1979) 155.

[11] H. Schulz, M. Schon, N.M. Rahman, Stud. Surf. Sci. Catal. 27 (1986) 201.

[12] T.C. Ho, Catal. Rev.-Sci. Eng. 30 (1988) 117.

[13] G. Perot, Catal. Today 10 (1991) 447.

[14] S. Kasztelan, T. des Courieres, M. Breysse, Catal. Today 10 (1991) 433.

[15] J.K. Minderhoud, J.A.R. van Veen, Fuel Process. Technol. 35 (1993) 87.

[16] R. Prins, Adv. Catal. 46 (2002) 399.

[17] F.P. Daly, J. Catal. 51 (1978) 221.

[18] I.A. van Parijs, L.H. Hosten, G.F. Froment, Ind. Eng. Chem. Prod. Res. Dev. 25 (1986) 437.

[19] M. Houalla, N.K. Nag, A.V. Sapre, D.H. Broderick, B.C. Gates, AIChE J. 24 (1978) 1015.

[20] M. Nagai, T. Kabe, J. Jpn. Petrol. Inst. 23 (1980) 82.

[21] D.H. Broderick, B.C. Gates, AIChE J. 27 (1981) 663.

[22] G.H. Singhal, R.L. Espino, J.E. Sobel, J. Catal. 67 (1981) 446.

[23] G.H. Singhal, R.L. Espino, J.E. Sobel, G.A. Huff, J. Catal. 67 (1981) 457.

[24] M.L. Vrinat, L. Demourgues, J. Chim. Phys.-Chim. Biol. 79 (1982) 45.

[25] M. Houalla, D.H. Broderick, A.V. Sapre, N.K. Nag, V.H.J. de Beer, B.C. Gates, H. Kwart, J. Catal. 61 (1980) 523.

[26] D.R. Kilanowski, H. Teeuwen, V.H.J. de Beer, B.C. Gates, G.C.A. Schuit, H. Kwart, J. Catal. 55 (1978) 129.

[27] A. Ishihara, H. Tajima, T. Kabe, Chem. Lett. (1992) 669.

[28] T. Kabe, A. Ishihara, H. Tajima, Ind. Eng. Chem. Res. 31 (1992) 1577.

[29] T. Kabe, A. Ishihara, Q. Zhang, Appl. Catal. A 97 (1993) L1.

[30] X.L. Ma, K. Sakanishi, I. Mochida, Ind. Eng. Chem. Res. 35 (1996) 2487.

[31] V. Lamure-Meille, E. Schulz, M. Lemaire, M. Vrinat, Appl. Catal. A 131 (1995) 143.

[32] F. Bataille, J.L. Lemberton, P. Michaud, G. Perot, M. Vrinat, M. Lemaire, E. Schulz, M. Breysse, S. Kasztelan, J. Catal. 191 (2000) 409.

[33] M.J. Ledoux, A. Bouassida, R. Benazouz, Appl. Catal. 9 (1984) 41.

[34] M. Jian, J.L.R. Cerda, R. Prins, Bull. Soc. Chim. Belg. 104 (1995) 225.

[35] R. Pille, G. Froment, in, Hydrotreatment and Hydrocracking of Oil Fractions, ELSEVIER, Amsterdam, 1997, p. 403.
[36] Y. Chu, Z. Wei, S. Yang, C. Li, Q. Xin, E. Min, Appl. Catal. A 176 (1999) 17.
[37] J. Cinibulk, Z. Vit, Appl. Catal. A 204 (2000) 107.
[38] R.T. Hanlon, Energy & Fuels 1 (1987) 424.
[39] L. Vivier, V. Dominguez, G. Perot, S. Kasztelan, J. Mol. Catal. 67 (1991) 267.
[40] R.L. Wilson, C. Kemball, J. Catal. 3 (1964) 426.
[41] P. Kieran, C. Kemball, J. Catal. 4 (1965) 380.
[42] Y. Zhao, P. Kukula, R. Prins, accepted for publication in J. Catal. (2003).
[43] J, Sonnemans, W.J. Neyens, P. Mars, J. Catal. 34 (1974) 230.
[44] G.C. Hadjiloizou, J.B. Butt, J.S. Dranoff, Ind. Eng. Chem. Res. 31 (1992) 2503.
[45] M. Cattenot, J.L. Portefaix, J. Afonso, M. Breysse, M. Lacroix, G. Perot, J. Catal. 173 (1998) 366.
[46] M. Flechsenbar, Dissertation 12471, ETH, Zurich, 1997.
[47] E. Atar, S. Cheskis, A. Amirav, Anal. Chem. 63 (1991) 2061.
[48] S. Cheskis, E. Atar, A. Amirav, Anal. Chem. 65 (1993) 539.

Chapter 4

On the Role of β Hydrogen Atoms in the Hydrodenitrogenation of 2-Methylpyridine and 2-Methylpiperidine

4.1 Introduction

Heterocyclic compounds like pyridine, quinoline, and acridine are the main nitrogen-containing compounds in oil. They are removed by hydrodenitrogenation (HDN) in a hydrotreating process in which gasoline or gasoil is treated with hydrogen over a metal sulfide catalyst like nickel-promoted molybdenum sulfide (Ni-MoS_2) supported on alumina [1]. Several groups have studied the HDN of pyridine [2-7], because, as the smallest nitrogen-containing heterocyclic molecule, pyridine was believed to be the simplest model molecule to study HDN. Although the network of reactions taking place in the HDN of pyridine is now well understood, the study of the kinetics of the HDN of pyridine proved to be extremely difficult. The reason for this difficulty is the occurrence of a side reaction of piperidine, the first intermediate in the HDN of pyridine. Two piperidine molecules disproportionate to *N*-pentylpiperidine and ammonia [1-5]. Opening of the piperidine ring and removal of ammonia can take place from piperidine as well as from *N*-pentylpiperidine. Consequently the network of the HDN becomes very complicated and a trustworthy kinetic analysis of the separate reactions is almost impossible.

The disproportionation of piperidine to *N*-pentylpiperidine takes place by nucleophilic substitution at the carbon atom in the α position to the nitrogen atom in the piperidine ring (Scheme 4.1) [3,8]. It is well known that a nucleophilic attack is hindered by substitution on the α carbon atom [9]. Substitution of a hydrogen atom by a methyl group on the α carbon

atom might therefore hinder the disproportionation so much, that it is strongly suppressed and that it hardly interferes with the other reactions taking place during the HDN of pyridine and piperidine. Therefore we decided to study the HDN of 2-methylpyridine (2-MPy) and 2-methylpiperidine (2-MPiper).

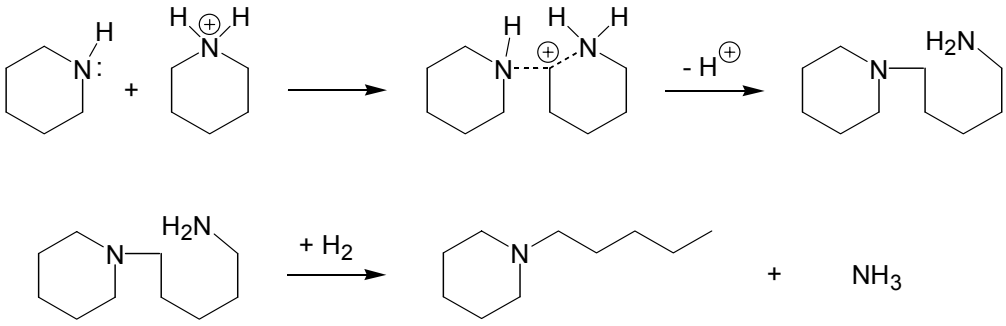

Scheme 4.1. Mechanism of the disproportionation of piperidine.

2-Methylpyridine and 2-methylpiperidine were studied before by Cerny and Trka [10,11] and Ren et al. [12]. Ren et al. studied the Langmuir-Hinshelwood-Hougen-Watson kinetics of the HDN of 2-methylpyridine in a continuous flow reactor at 4.9 MPa and 240-280°C [12]. They observed 2-methylpiperidine as primary product and hexane and cyclohexane as final products. No intermediates between 2-methylpiperidine and hexane were reported. Cerny and Trka performed their investigations in an autoclave at 15.5 MPa and 250°C. Because of the high H_2 pressure, low temperature, and absence of H_2S in their experiments, mainly ring hydrogenation, and only a small amount of products due to nitrogen removal was observed. They concluded that the 2-methylpiperidine ring opens preferentially on the side that does not contain the methyl group and that the HDN reaction of more substituted pyridine derivatives is slower [10]. This is in disagreement with results of Portefaix et al. who observed that the HDN reaction of 2,6-dimethylpiperidine was faster than that of piperidine [13]. Their result suggests that the presence of a methyl group leads to a faster ring opening. Portefaix et al. performed their HDN work at the much lower H_2 pressure of 2 MPa and relatively high H_2S pressure of 33.3 kPa, this may explain the different results. Further study is clearly called for.

Another reason for studying the HDN of 2-methylpiperidine is the presence of three additional hydrogen atoms on the methyl carbon atom in β position relative to the nitrogen

atom. HDN occurs (partly) via Hofmann elimination in which on the one hand the bond between the α carbon atom and the nitrogen atom is broken and on the other hand the bond between a hydrogen atom and the β carbon atom is broken. Portefaix et al. compared the HDN of piperidine, 3,5-dimethylpiperidine, and 2,6-dimethylpiperidine and concluded that Hofmann elimination is quicker when more β hydrogen atoms are present [13]. This implicates that elimination of a β H atom from the methyl groups in 2,6-dimethylpiperidine is an important step in the HDN of this molecule. Portefaix et al. only reported the conversion of the reactant and nothing about the resulting products. Therefore, it seemed of interest to investigate if the elimination reaction of 2-methylpiperidine takes place by removal of a hydrogen atom from the methyl group and leads preferentially to 1-aminohexane.

4.2 Experimental

The NiMo/γ-Al_2O_3 catalyst used in this work contained 8 wt% Mo and 3 wt% Ni and was prepared by successive incipient wetness impregnation of γ-Al_2O_3 as described in Chapter 3. The catalyst was sulfided *in situ* with a mixture of 10% H_2S in H_2 at 400°C and 1.0 MPa for 4 h. After sulfidation, the pressure was increased to 5.0 MPa (unless indicated otherwise), and the liquid reactant was fed to the reactor by means of a high-pressure syringe pump (ISCO 500D). Blank experiments with and without SiC were carried out at 573 and 623 K. The composition of the gas-phase feed in most experiments consisted of 5 kPa amine reactant, 140 kPa decane (as solvent for the amine), 20 kPa heptane (as reference for GC analysis), 20 kPa H_2S and 4.8 MPa H_2 (unless indicated otherwise).

The reaction products were analyzed by on-line gas chromatography as described in Chapter 3. Mass spectrometry and NMR spectroscopy were used for the identification of the reaction products. The MS analysis was performed with an Agilent 6890 gas chromatograph equipped with a HP-5MS capillary column (crosslinked 5% PH ME siloxane, 30 m × 0.25 mm × 0.25 μm) and with an Agilent 5973 mass selective detector. The temperature of the injector was 270°C, the initial temperature of the column oven was 80°C, and heating to 300°C started after two min with 20°C/min. ^1H and ^{13}C NMR spectra of isolated compounds were recorded on a BRUKER DPX-300 instrument at 300 and 75 MHz, respectively, at room temperature using $CDCl_3$ as a solvent.

4.3 Results

4.3.1 HDN of 2-methylpyridine

The results of the HDN of 2-methylpyridine at 340°C, 4.8 MPa H_2, and 20 kPa H_2S are shown in Fig. 4.1. No products with mass higher than that of the reactant (such as condensation products) were observed and the mass balance was always better than 95%. The product selectivities show (Fig. 4.1b) that 2-methylpiperidine is the only primary product, as expected, since the HDN of heterocyclic N-containing aromatic molecules can only occur after ring hydrogenation [1,3,14,15]. The maximum yield of 34% of 2-methylpiperidine and its selectivity against 2-methylpyridine conversion indicate that the ratio of the effective rate constants of formation and further reaction of 2-methylpiperidine is about 0.8 [16].

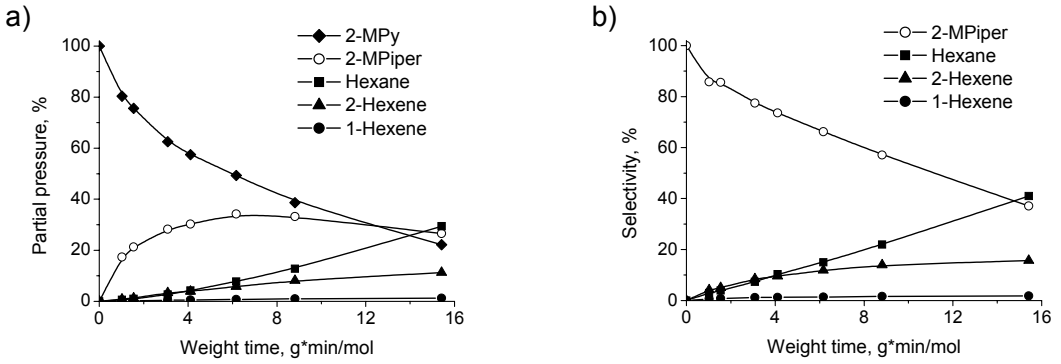

Fig. 4.1. Relative concentrations (a) and selectivities (b) of the products of the HDN of 2-methylpyridine as a function of weight time.

2-Hexene (*cis* and *trans*), 1-hexene, and hexane were observed as the main secondary products (Fig. 4.1b). These products are actually expected to be tertiary products, because HDN of aliphatic amines is generally considered to occur by Hofmann elimination or by nucleophilic substitution of the NH_2 group by an SH group followed by elimination or hydrogenolysis [1,14]. In either case, the nitrogen atom of 2-methylpiperidine is removed in

two steps. The first step is a ring opening by C-N bond breaking and the second step is the removal of the nitrogen atom in the form of ammonia by breaking the other C-N bond. Of the products that are possible after the first C-N bond breaking, only traces of 1-aminohexane and 2-aminohexane were observed. The reason is that their rates of further reaction are much higher than their rates of formation, as will be shown below in sections 4.3.4 and 4.3.5. These amines have a high basicity and thus larger equilibrium adsorption constants than 2-methylpyridine. Even at low concentration they may therefore have an important (inhibiting) influence on the HDN kinetics [15]. For that reason, the HDN of 2-methylpiperidine, the primary product of the HDN of 2-methylpyridine, and of 1-aminohexane and 2-aminohexane, the expected secondary (or tertiary, see below) products, were studied in detail as well.

4.3.2 HDN of 2-methylpiperidine

The HDN of 2-methylpiperidine was carried out at 340°C, 4.8 MPa H_2, and 20 kPa H_2S. Fig. 4.2 shows that at least four compounds have non-zero selectivity at zero conversion of 2-methylpiperidine and thus might be considered to be primary products. Three of these products were identified by their GC retention times and MS spectra as 1-aminohexane, 2-aminohexane, and 2-methylpyridine. The yield of 2-aminohexane was much higher than that of 1-aminohexane. This confirms the results of Cerny [10], although they were obtained under quite different conditions, and suggests that the bond between the N atom and the methylene group is more easily broken than that between the N atom and the $CH(CH_3)$ group. This is also perfectly in line with previous results of Cattenot et al. [8] and Vivier et al. [17] indicating that the amino group bonded to a methylene group cleavages very easily by nucleophilic substitution (S_N2).

GC-MS showed that the fourth compound had a molecular weight of 97, but no commercially available compound could be found that had the same retention time and a matching MS spectrum. Therefore, the product of the HDN reaction was collected and a fraction that contained the basic nitrogen-containing molecules was separated from a hydrocarbon fraction. Since the pulsed flame photometric detector had shown that the fourth compound contains a nitrogen atom, it was extracted from the HDN product by an aqueous HCl solution. Neutralization of this aqueous extract and subsequent extraction with chloroform gave a chloroform solution of all primary products as well as the remaining 2-

methylpiperidine. After evaporation of the chloroform, the mixture of nitrogen-containing compounds was separated by column chromatography using silicagel and a 50:50:1 solution of CH_3OH : $CHCl_3$: NH_4OH (25% aqua solution of NH_3) as a mobile phase. The fraction containing the fourth unknown product was evaporated and the obtained raw material with a purity of 90% was analyzed by NMR spectroscopy. The ^1H NMR spectrum of the fourth compound in $CDCl_3$ showed peaks at δ 3.46–3.52 (m, 2H, CH_2N), 2.13 (t of t, ^3J=6.5Hz, ^5J=1.8 Hz, 2H, CH_2C=), 1.91 (t, ^5J=1.8 Hz, 3H, CH_3), 1.62–1.71 (m, 2H, $C\underline{H}_2CH_2C$=), and 1.51–1.59 ppm (m, 2H, $C\underline{H}_2CH_2N$), while its ^{13}C NMR spectrum in $CDCl_3$ showed peaks at δ 168.45 (s, CN), 48.98 (t, CN), 30.26 (t, $\underline{C}H_2C$=), 27.33 (q, CH_3), 21.57 (t, $\underline{C}H_2CH_2N$), and 19.52 ppm (t, $\underline{C}H_2CH_2C$=). The NMR spectra together with the obtained MS spectrum (MS (EI, 70 eV) m/z 97 (M^+, 63), 96 (11), 69 (61), 68 (21), 56 (26), 55 (17), 54 (15), 42 (100), 41 (65), 39 (33), 28 (41), 27 (26)) enabled us to identify the fourth primary product as 2-methyl-3,4,5,6-tetrahydropyridine. Both the NMR and MS spectra were in good accordance with the spectra assigned to this molecule in the literature [18,19].

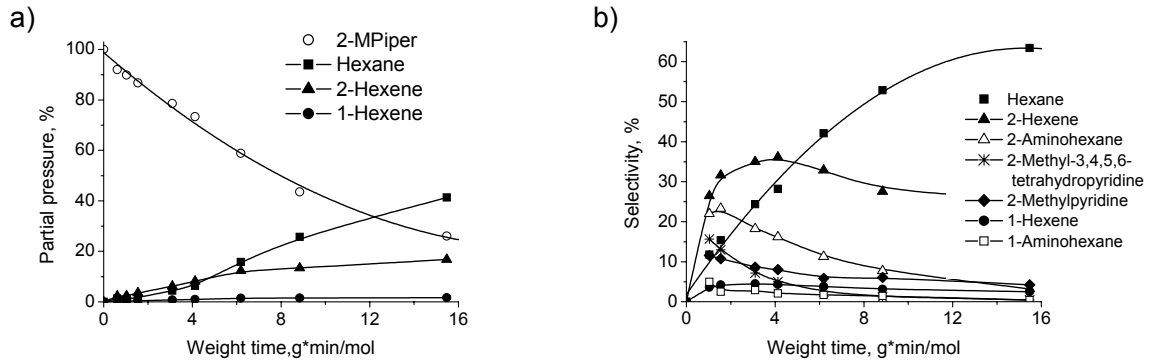

Fig. 4.2. Relative concentrations (a) and selectivities (b) of the products of the HDN of 2-methylpiperidine as a function of weight time.

HDN experiments with 2-methylpiperidine at other conditions than 340°C and 5 MPa suggested that 2-methyl-3,4,5,6-tetrahydropyridine is formed by a catalytic as well as a thermal reaction. Experiments in the empty steel reactor and in the reactor filled with SiC only, without catalyst, showed that the 2-methyl-3,4,5,6-tetrahydropyridine yield increased by increasing the temperature from 300 to 350°C, as to be expected for a simple dehydrogenation reaction. Over the $NiMo/Al_2O_3$ catalyst diluted with SiC, however, the yield decreased substantially from 300 to 350°C. The 2-methyl-3,4,5,6-tetrahydropyridine yield was also

lower over the catalyst than over the SiC or in the empty reactor. This suggests that in the presence of the catalyst not only dehydrogenation occurs, but also reactions to other products, which lower the yield of 2-methyl-3,4,5,6-tetrahydropyridine. As to be expected, in the presence of the catalyst, decreasing the H_2 pressure from 5 to 3 MPa raised the 2-methyl-3,4,5,6-tetrahydropyridine yield.

4.3.3 Comparison of piperidine, 2-methylpiperidine, and 2,6-dimethylpiperidine

As indicated in the Introduction [Section 4.1], Portefaix et al. reported that the amount of HDN product was larger for 2,6-dimethylpiperidine than for piperidine at the following reaction conditions: 275°C, 2 MPa H_2, and 33.3 kPa H_2S [13]. They related this to the presence of more β H atoms in 2,6-dimethylpiperidine, which would facilitate the Hofmann elimination. These results seem in contradiction with those of Cerny [10] and with our results for 2-methylpiperidine described in the previous section, which suggested that the ring opening occurs preferentially between the nitrogen atom and the methylene group and not between the nitrogen atom and the carbon atom bearing the methyl group. We therefore decided to repeat the measurements of Portefaix et al. under their conditions.

From the results presented in Fig. 4.3 it is clear that the conversion of piperidine is very slow and hardly reaches 2% at a weight time of 10 g·min/mol, whereas the conversion of 2-methylpiperidine is almost 20%, and that of *cis*-2,6-dimethylpiperidine is more than 50% at the same weight time. The conversions at a weight time of 2.4 g·min/mol are in good agreement with those of Portefaix et al. [13]. Analyzing the resulting products, we found, however, that for piperidine the main product was not that of HDN but pyridine. For 2-methylpiperidine the main products were 2-methylpyridine (17%) and 2-methyl-3,4,5,6-tetrahydropyridine (64%), and for *cis*-2,6-dimethylpiperidine the main products were 2,6-dimethylpyridine (2%), 2,6-dimethyl-3,4,5,6-tetrahydropyridine (66%), and *trans*-2,6-dimethylpiperidine (32%), with the selectivities in parentheses.

The observed high selectivities to fully dehydrogenated pyridine molecules at low conversions are not in contradiction with thermodynamics, which indicates that the pyridine/piperidine ratio cannot be higher than 0.01 at 275°C and 2 MPa H_2 [20]. The tetrahydropyridine/piperidine ratio can be much higher, however. Portefaix et al. apparently

underestimated the latter ratio and the isomerization of *cis*-2,6-dimethylpiperidine to *trans*-2,6-dimethylpiperidine, when assuming, without any product analysis, that most of the piperidine-type molecules would convert to HDN products. At high weight time and high conversion, thermodynamics controls and HDN products will indeed dominate. At low conversion, however, kinetics may dominate the product distribution and it is in this regime that mechanistic results should be obtained.

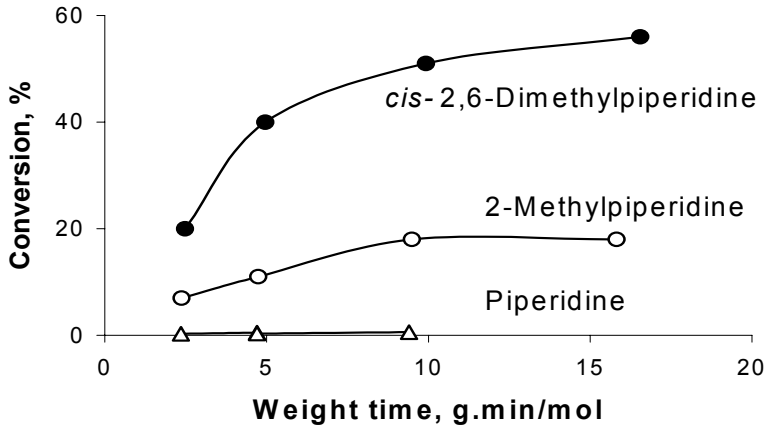

Fig. 4.3. Total conversions in the HDN of piperidine, 2-methylpiperidine, and *cis*-2,6-dimethylpiperidine as a function of weight time at 275°C, 2 MPa, and 33.3 kPa H_2S.

All the compounds mentioned above are products of dehydrogenation and isomerization, and not of HDN or C-N bond cleavage. The selectivities for ring opening and HDN were calculated from the sum of the observed amines and saturated and unsaturated hydrocarbons and amounted to 9% for piperidine, 5% for 2-methylpiperidine, and 0.7% for *cis*-2,6-dimethylpiperidine at 2.4 g·min/mol. These selectivities are small, dehydrogenation and isomerization (for *cis*-2,6-dimethylpiperidine) dominate at the low H_2 pressure of 1.8 MPa. The yield (selectivity times conversion) of these ring opening and HDN products was indeed higher for *cis*-2,6-dimethylpiperidine than for piperidine, as reported by Portefaix et al. [13].

We studied these three piperidine molecules also under conditions in which elimination is really the dominating reaction, so that a fair comparison of the HDN rates of the three molecules can be made. At 340°C, 5 MPa, and 20 kPa H_2S the 2-methylpiperidine

conversion was 20% lower than that of piperidine, while the conversion of *cis*-2,6-dimethylpiperidine was higher than that of piperidine below a weight time of τ=5.5 g·min/mol and lower above this value. The reason for the high initial reaction rate of *cis*-2,6-dimethylpiperidine is a fast isomerization of *cis*- to *trans*-2,6-dimethylpiperidine. For τ>5.5 g·min/mol, the equilibrium between *cis*- and *trans*-2,6-dimethylpiperidine is established, and other, slower reactions determine the reaction rate of both isomers of 2,6-dimethylpiperidine. Even at 340°C, 5 MPa, and 20 kPa H_2S, conversion to products other than obtained by HDN is not negligible for these three molecules. For piperidine the total selectivity for dehydrogenation to pyridine and disproportionation to *N*-pentylpiperidine was always below 10%. For 2-methylpiperidine and *cis*-2,6-dimethylpiperidine the selectivities to the dehydrogenation products (substituted pyridine and tetrahydropyridine) were 22 and 24% respectively, at the lowest weight time measured (1.4 g·min/mol). Taking into account only the products of hydrodenitrogenation, we found that piperidine undergoes HDN 30% faster than 2-methylpiperidine and 50% faster than 2,6-dimethylpiperidine (Fig. 4.4).

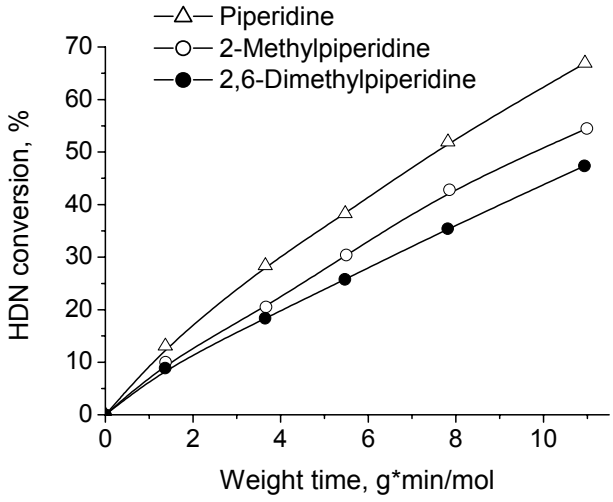

Fig. 4.4. HDN conversion of piperidine, 2-methylpiperidine, and *cis*-2,6-dimethylpiperidine as a function of weight time at 340°C, 5 MPa, and 20 kPa H_2S.

4.3.4 HDN of 1-aminohexane

The HDN of 1-aminohexane becomes fast above 300°C (Fig. 4.5) and 2-hexene and hexane are the main products. A plot of the product selectivities versus weight time (Fig. 4.6) shows that 1-hexene, and *trans*- and *cis*-2-hexene are primary products. According to the Hofmann elimination mechanism only 1-hexene can be formed from 1-aminohexane. However, the isomerization of 1-hexene to 2-hexene is so fast above 300°C that it is difficult to distinguish if 2-hexene is a primary or secondary product. Addition of 1-pentene to the feed indeed showed that the isomerization to *cis*- and *trans*-2-pentene was fast. This means that the ratio of 1-hexene and 2-hexene above 300°C is mainly determined by thermodynamics and hardly by the kinetics of the formation of these alkenes. Consequently, the ratio of 1-hexene to 2-hexene cannot be used to distinguish between the two ways of C-N bond breaking in 2-methylpiperidine either. At 260°C the conversion of 1-aminohexane is less than 5%, even at high weight time (20 g·min/mol), against 50% at 300°C. The comparison of the selectivity plots at 300°C (Fig. 4.6) and 260°C (Fig. 4.7) confirms that *trans*- and *cis*-2-hexene are secondary products, because the selectivities decrease at decreasing temperature and conversion.

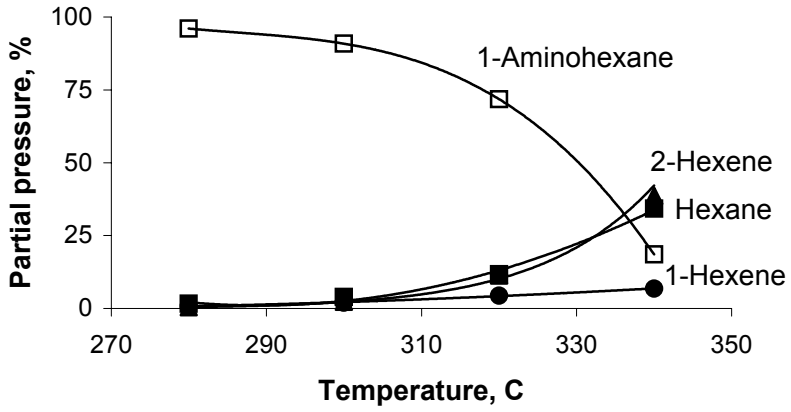

Fig. 4.5. Conversion and relative product concentrations in the HDN of 1-aminohexane between 280 and 340°C and at τ=5 g·min/mol.

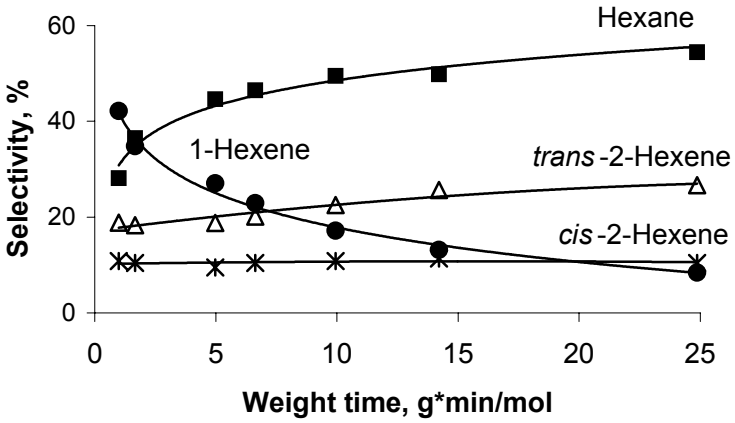

Fig. 4.6. Product selectivities of the HDN of 1-aminohexane at 300°C.

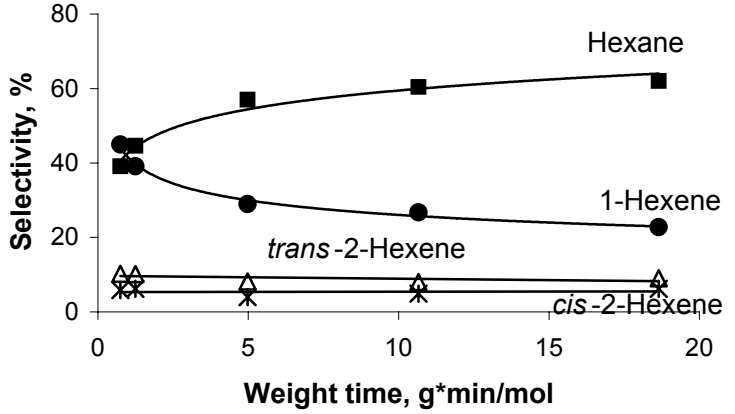

Fig. 4.7. Product selectivities of the HDN of 1-aminohexane at 260°C.

At the higher H_2S pressure of 80 kPa, the selectivity to hexane was higher than at 16 kPa. The HDN activity was hardly influenced by this change in H_2S partial pressure (at a constant H_2 pressure of 3.8 MPa), but the selectivity had changed. Not only the hexane selectivity was higher, but the 2-hexene selectivity was substantially lower and that of 1-hexene higher at 80 kPa H_2S. Apparently, isomerization of 1-hexene to *cis* and *trans*-2-hexene needs vacancies at the metal sulfide surface. The higher selectivity towards hexane formation

indicates that nucleophilic attack of H_2S on 1-aminohexane must have led to hexanethiol, which very quickly reacted to hexane by hydrogenolysis and 1-hexene by elimination [1].

4.3.5 HDN of 2-aminohexane

The HDN of 2-aminohexane was complicated by the formation of di-2-hexylamine, a disproportionation product of the reaction of two 2-aminohexane molecules (Fig. 4.8). As to be expected for this molecule with two chiral atoms (2-aminohexane itself has one chiral atom), the gas chromatogram showed two peaks with equal intensities, equal MS spectra, and only a small difference in retention time. One peak belongs to the (*R,R*)- and (*S,S*)-isomers, the other to the meso (*R,S*)-isomer.

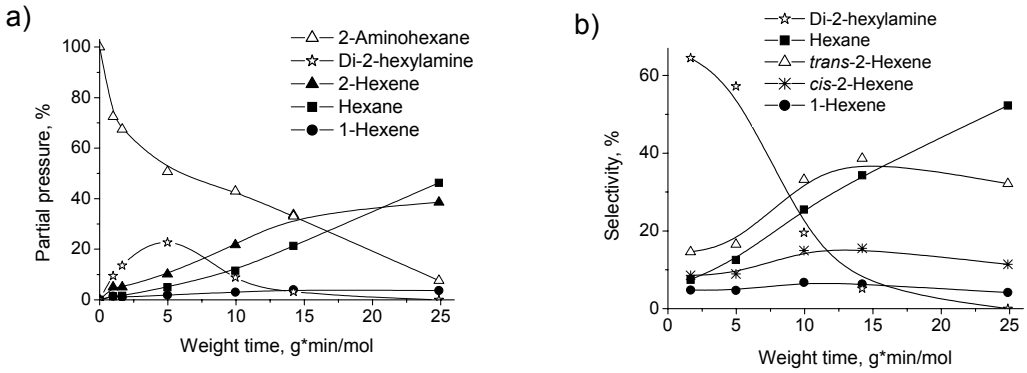

Fig. 4.8. Relative concentrations (a) and selectivities (b) of the products of the HDN of 2-aminohexane as a function of weight time at 20 kPa H_2S.

Experiments between 220 and 350°C showed that not only di-2-hexylamine behaves as a primary product, but 1-hexene, and *cis*- and *trans*-2-hexene as well (Fig. 4.8b). Hofmann elimination explains why 1-hexene as well as 2-hexene is formed. The activation energy for elimination is higher than that of nucleophilic substitution because the hexene selectivity increased with temperature. The selectivity of di-2-hexylamine is very high at low temperature. At the lowest temperature studied (220°C), it was higher than 90% when extrapolated to zero 2-aminohexane conversion. In this case, the only other product was hexane. The formation of hexane is explained by nucleophilic substitution of the NH_2 group by an SH group, followed by hydrogenolysis of the C-S bond.

Increasing the H_2S pressure from 16 to 80 kPa, at the same H_2 pressure of 3.8 MPa, led to a faster conversion of 2-aminohexane to hydrocarbons while the production of the disproportionation product di-2-hexylamine decreased (Fig. 4.9). Whereas at 16 kPa H_2S it reached a maximum yield of 25%, at 80 kPa H_2S the maximum yield was only 10%. At the higher H_2S partial pressure, a new intermediate was observed. It behaved as a primary product and was analyzed to be 2-hexanethiol. This intermediate is formed by an S_N2 reaction between 2-aminohexane and H_2S. At higher H_2S partial pressure, it will be formed faster and will hydrogenolyze less fast to hexane because of less vacancies on the metal sulfide surface. Therefore, it is easier to observe 2-hexanethiol at higher H_2S pressure.

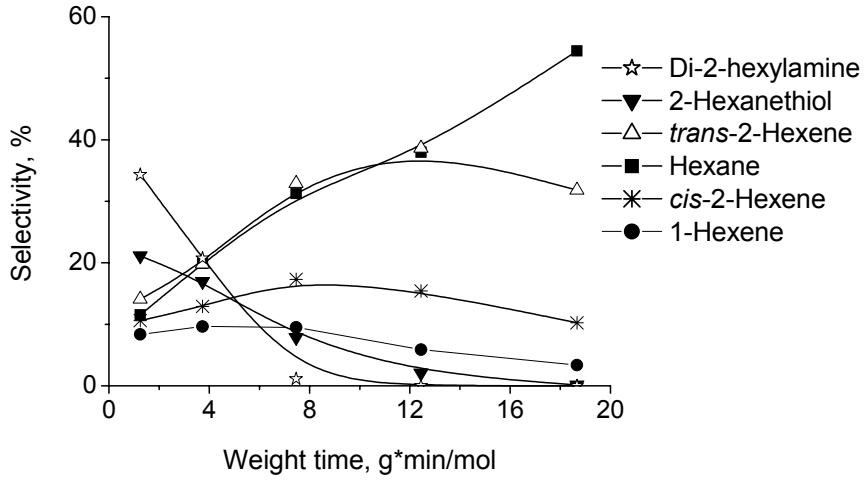

Fig. 4.9. Product selectivities of the HDN of 2-aminohexane as a function of weight time at 80 kPa H_2S.

4.4 Discussion

Combining the results of the HDN of 2-methylpyridine, 2-methylpiperidine, 1-aminohexane, and 2-aminohexane, we arrive at the reaction Scheme 4.2. For all intermediates, except two, direct relationships between parent and daughter molecules could be established by measuring the product selectivities as a function of weight time and extrapolating to zero weight time. Thus, 2-methylpiperidine proved to be the primary product of 2-methylpyridine,

while 2-methylpyridine as well as 2-methyl-3,4,5,6-tetrahydropyridine behaved as primary products of 2-methylpiperidine.

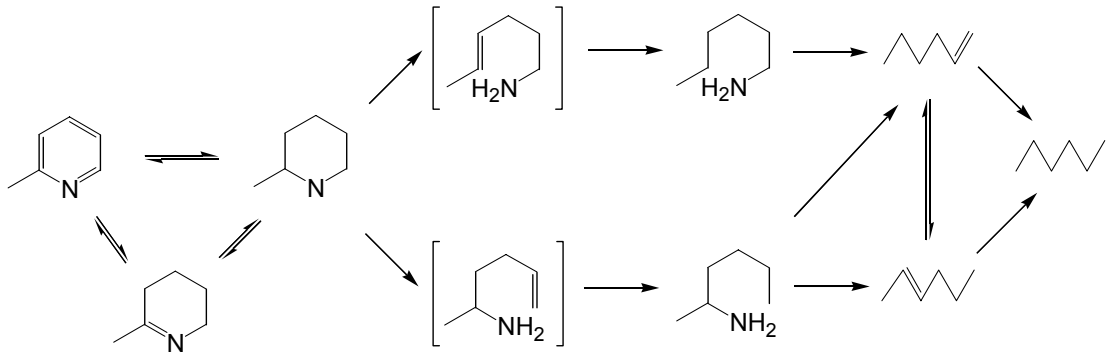

Scheme 4.2. Reaction network of the HDN of 2-methylpyridine and 2-methylpiperidine.

The other two apparent primary products in the HDN of 2-methylpiperidine, 1-aminohexane and 2-aminohexane should actually be secondary rather than primary products. If opening of the piperidine ring would occur by Hofmann elimination, it would lead to 5-amino-1-hexene when the C-N bond with the methylene group is broken, and to 6-amino-1-hexene and 6-amino-2-hexene when the C-N bond with the $CH(CH_3)$ group is broken (Scheme 4.2). These products were not detected in the HDN of 2-methylpiperidine. The equivalent of 5-amino-1-hexene has never been observed in the HDN of pyridine either [6]. The reason is most probably that these amino-alkenes adsorb strongly on the catalyst surface because of the presence of a nitrogen atom in the molecule and are very quickly hydrogenated to the corresponding saturated amines before they desorb from the catalytic site. Alternatively, if opening of the pyridine ring would occur by nucleophilic attack by H_2S, then 5-aminohexanethiol, 6-aminohexanethiol, and 6-amino-2-hexanethiol would be primary products. Thiols react very quickly by elimination to alkenes and by hydrogenolysis to alkanes. In the first and most important case, amino-alkenes should be formed, in the latter case amines. Again, because of strong adsorption and fast hydrogenation, the amino-alkenes have not been detected. As a result, only 1-aminohexane and 2-aminohexane occur in the product, their selectivities do not go to zero at low conversion, they behave as (quasi) primary products in the HDN of 2-methylpiperidine.

2-Methylpyridine and 2-methyl-3,4,5,6-tetrahydropyridine both behaved as primary products in the HDN of 2-methylpiperidine. One might expect 2-methyl-3,4,5,6-

tetrahydropyridine to be the dehydrogenation intermediate between 2-methylpiperidine and 2-methylpyridine, in which case it is surprising that 2-methylpyridine behaves as a primary product too. If the rate of dehydrogenation of 2-methyl-3,4,5,6-tetrahydropyridine to 2-methylpyridine is of the same order of magnitude as its rate of desorption from the catalytic site, both molecules might have non-zero selectivities at zero 2-methylpiperidine conversion. Another explanation could be that 2-methyl-3,4,5,6-tetrahydropyridine is (partially) produced by a thermal dehydrogenation reaction, while 2-methylpyridine is directly, without desorption of intermediates, produced by a catalytic reaction. We have not studied this question any further, because it is only a side effect in our study of the HDN of 2-methylpyridine and 2-methylpiperidine.

An investigation of the HDN of 1-aminohexane and 2-aminohexane is not only important for a better understanding of the kinetics of the HDN of 2-methylpyridine and 2-methylpiperidine, but also for an understanding of how the ring opening of the piperidine ring takes place. Because of the methyl group in α position to the nitrogen atom, C-N bond breaking in 2-methylpiperidine can take place in two ways: between the nitrogen atom and the carbon atom of the methylene group, or between the nitrogen atom and the carbon atom carrying the methyl group. The latter possibility should prevail if, as suggested by Portefaix et al. [13,21] and Cattenot et al. [8], the number of β H atoms determines the course of the Hofmann elimination reaction. Unfortunately, the ratio of the concentrations of 1-aminohexane and 2-aminohexane cannot be used as a direct measure for the ratio of the N-CH_2 and N-$CH(CH_3)$ bond breakings. The reason is that the concentrations of these amines not only depend on their rates of formation, but also on their rates of reaction to hexenes and hexane. Thus, the very low amount of 1-aminohexane that is produced in the HDN of 2-methylpiperidine (Fig. 4.2b) can be either due to a slow breaking of the N-$CH(CH_3)$ bond, or to a fast disappearance of 1-aminohexane by HDN, or to both. For that reason, it was necessary to investigate the HDN of 1-aminohexane and 2-aminohexane separately.

Comparison of the conversion of 2-aminohexane (Fig. 4.8a) and 1-aminohexane (not shown) showed that the reactivity of 2-aminohexane is higher than that of 1-aminohexane. Despite a higher reactivity, much more 2-aminohexane than 1-aminohexane was detected in the HDN of 2-methylpiperidine (Fig. 4.2b). This proves that the first C-N bond breaking in 2-methylpiperidine occurs predominantly between the nitrogen atom and the carbon atom of the methylene group. If only the number of β H atoms plays a role, as suggested by Portefaix et al. [13], then 2.5 times more 1-aminohexane than 2-aminohexane should have been formed.

Actually, 3 to 4 times more 2-aminohexane was formed! It is clear that the number of β H atoms is not the most important factor in the Hofmann elimination. The same conclusion was reached in the HDN of 2-methylcyclohexylamine, in which the type of β H atom proved to be the most important factor [22]. Thus, the β H atom at the tertiary carbon atom was removed much faster than the β H atom at the secondary carbon atom, leading to more 1-methylcyclohexene than 3-methylcyclohexene. Analogously, the results of the HDN of 2-aminohexane described in Section 4.3.5 demonstrated that 3 to 4 times more 2-hexene was produced than 1-hexene, although there are 1.5 times less H atoms on the CH_2 group in β position to the nitrogen atom than on the CH_3 group in 2-aminohexane. It is clear that the ease of breaking of the C-H bond plays an important role in the elimination. A hydrogen atom on a tertiary carbon atom is more easily abstracted by a base than β H atoms on secondary or primary carbon atoms. This is the basis of the Zaytzev rule that states that elimination preferentially leads to more substituted alkenes [9].

The fact that much more 2-aminohexane than 1-aminohexane is formed in the HDN of 2-methylpiperidine further indicates that the methyl group actually has a negative rather than a positive influence on the elimination. All β H atoms on the two carbon atoms in β position to the nitrogen atom belong to methylene groups. Thus, they should have the same tendency to be eliminated. If the methyl group played no role in elimination, neither positive nor negative, then, on the basis of the number and type (methylene) of the H atoms, equal amounts of 2-aminohexane and 1-aminohexane should have been formed. The fact that the rate of breaking of the N-$CH(CH_3)$ bond is lower than that of the N-CH_2 bond indicates that the methyl group hinders the adsorption of 2-methylpiperidine in a conformation in which the nitrogen atom and the β H atom of the methylene group next to the $CH(CH_3)$ group approach the metal sulfide surface. Such a steric hindrance does not exist for the adsorption of the other side of the 2-methylpiperidine molecule on the metal sulfide surface.

Our results are in good agreement with the rule that nucleophilic substitution is favored at low temperature, while elimination is favored at high temperature. The H_2S pressure may also steer the reaction in different directions. At low H_2S pressure, nucleophilic substitution is dominated by the reaction of an amine reactant with another amine molecule, leading to disproportionation products such as di-2-hexylamine (Fig. 4.8). In this sense, the metal sulfide surface that is depleted of sulfur behaves similar as a metal surface, on which disproportionation of amines is important as well [23]. At high H_2S pressure, H_2S becomes

the dominant nucleophile that reacts with the amine, transforming the amine into a thiol molecule that relatively quickly reacts to an alkene by elimination and to an alkane by hydrogenolysis. Hydrogenolysis needs sulfur vacancies at the metal sulfide surface. Consequently, an increase in H_2S pressure has a positive effect on hexane formation at lower H_2S pressures, because more thiol is formed. At higher H_2S pressures, however, hardly any vacancies are available anymore and the thiol can only undergo elimination to an alkene.

From the higher rate of HDN conversion of *cis*-2,6-dimethylpiperidine than of piperidine, Portefaix et al. concluded that the rate of elimination of ammonia from an amine is larger when more β H atoms are present [13]. Our analysis of all the products of the HDN reactions of piperidine, 2-methylpiperidine, and *cis*-2,6-dimethylpiperidine shows that this conclusion is not correct. Indeed, the rate of disappearance of *cis*-2,6-dimethylpiperidine is higher than that of piperidine (Fig. 4.3) at 275ºC, 2 MPa H_2 and 33.3 kPa H_2S. However, the majority of the product at 2 MPa H_2 is not formed by elimination, but rather by dehydrogenation and isomerization. On the other hand, at 340°C and 5 MPa, dehydrogenation is much less important and the main products were formed by ring opening and HDN. Under such conditions, the rate of elimination decreases from piperidine to 2-methylpiperidine to *cis*-2,6-dimethylpiperidine (Fig. 4.4). This is then in agreement with our observation that the 2-methylpiperidine ring is preferentially opened between the N atom and the methylene group. Thus, it is clear that, contrary to the proposal of Portefaix et al. [13], the addition of a methyl group in α position to the nitrogen atom in piperidine does not increase the HDN rate. On the contrary, the methyl group constitutes a strong steric hindrance for the right adsorption conformation of the nitrogen atom and the β H atom.

4.5 Conclusion

The hydrodenitrogenation (HDN) of 2-methylpyridine and its intermediate products 2-methylpiperidine, 1-aminohexane, and 2-aminohexane were studied. The presence of most intermediates could be explained by a combination of pyridine ring hydrogenation, piperidine ring opening by elimination, and nitrogen removal by elimination as well as by nucleophilic substitution of the amino group by a sulfhydryl group, followed by elimination of H_2S or hydrogenolysis of the C-S bond. Amino-alkenes, which are expected to be the primary products of the ring opening of alkylpiperidine, were not observed, probably because of fast

hydrogenation to the corresponding amines. The ring opening of 2-methylpiperidine occurred preferentially between the nitrogen atom and the methylene group, rather than between the nitrogen atom and the carbon atom bearing the methyl group. This was confirmed by comparative HDN experiments of piperidine, 2-methylpiperidine, and 2,6-dimethylpiperidine. Although the methyl groups offer extra β hydrogen atoms, these primary hydrogen atoms are not used for elimination. Instead, the methyl groups hinder the adsorption leading to the elimination of the β hydrogen atoms on the side of the molecule bearing the methyl group.

4.6 References

[1] R. Prins, Adv. Catal. 46 (2002) 399.

[2] J. Sonnemans, W. J. Neyens, P. Mars, J. Catal. 34 (1974) 230.

[3] H. Schulz, M. Schon, N. M. Rahman, Stud. Surf. Sci. Catal. 27 (1986) 201.

[4] R. T. Hanlon, Energy & Fuels 1 (1987) 424.

[5] G. C. Hadjiloizou, J.B. Butt, J. S. Dranoff, Ind. Eng. Chem. Res. 31 (1992) 2503.

[6] M. Jian, R. Prins, Catal. Lett. 35 (1995) 193.

[7] R. Pille, G. Froment, Stud. Surf. Sci. Catal. 106 (1997) 403.

[8] M. Cattenot, J. L. Portefaix, A. Afonso, M. Breysse, M. Lacroix, G. Perot, J. Catal. 173 (1998) 366.

[9] J. March, in, Advanced Organic Chemistry, 3rd. Ed., Chap. 10. Wiley, New York, 1985.

[10] M. Cerny, Coll. Czech. Chem. Commun. 44 (1979) 85.

[11] M. Cerny, A. Trka, Czech. Chem. Commun. 48 (1983) 3413.

[12] S. Ren, Z. Wang, Y. Hu, Ranliao Huaxue Xuebo 15 (1987) 255.

[13] J. L. Portefaix, M. Cattenot, M. Gerriche, J. Thivolle-Cazat, M. Breysse, Catal. Today 10 (1991) 473.

[14] N. Nelson, R. B. Levy, J. Catal. 58 (1979) 485.

[15] G. Perot, Catal. Today 10 (1991) 447.

[16] O. Levenspiel, in, Chemical Reaction Engineering, 3rd. Ed., Chap. 8. Wiley, New York, 1999.

[17] L. Vivier, V. Dominguez, G. Perot, S. Kasztelan, J. Mol. Catal. 67 (1991) 267.

[18] G. Asensio, M. E. Gonzales-Nunez, C. B. Bernardini, R. Mello, W. Adam, J. Am. Chem. Soc. 105 (1983) 6877.

[19] D. H. Hua, Shou Wu Miao, S. Narasimha Bharathi, T. Katsuhira, A. A. Bravo, J. Org. Chem. 55 (1990) 3682.

[20] J. F. Cocchetto, C. N. Satterfield, Ind. Eng. Chem., Process Des. Dev., 15 (1976) 272.

[21] J. L. Portefaix, M. Cattenot, M. Guerriche, M. Breysse, Catal. Lett. 9 (1991) 127.

[22] F. Rota, V. Ranade, R. Prins, J. Catal. 201 (2001) 389.

[23] G. Meitzner, W. J. Mykytka, J. H. Sinfelt, J. Catal. 98 (1986) 513.

Chapter 5

Mutual Influence of the HDS of Dibenzothiophene and HDN of 2-Methylpyridine

5.1 Introduction

New environmental legislation has put the oil industry under increased pressure to limit the level of sulfur in gasoline and diesel fuel with a view to reducing exhaust emissions. A sulfur specification of 350 ppm is currently practiced in the EEC and a sulfur content as low as 50 or even 10 ppm is foreseen for the year 2005. Basic nitrogen compounds inhibit the hydrodesulfurization (HDS) of sulfur compounds through competitive adsorption, but in normal HDS this influence is negligible because the amount of N-containing molecules in gasoil is much smaller than that of S-containing molecules. Nitrogen compounds will be harmful in deep HDS, however, because then the amounts of N- and S-containing molecules are comparable.

The significance of competitive adsorption in hydrotreating reactions has been recognized for a long time [1] and several research groups investigated the effect of N-compounds on HDS [2-8] and of S-compounds on hydrodenitrogenation (HDN) [2,3,9,10]. Studies of the mutual influence of S- and N-containing molecules during hydrotreating showed that N-compounds have an inhibitory effect on HDS reactions, whereas the presence of S-containing molecules in some cases promotes HDN [10,11]. In the simulation of the kinetics, it is usually assumed that one active site is present on which HDS and HDN reactions take place [7,12], although the presence of two different sites (desulfurization and hydrogenation) was already reported in 1964 for the HDS of thiophene [13].

A systematic study of the interaction between catalytic hydrodesulfurization and hydrodenitrogenation was made by Satterfield et al. [2]. They studied the mutual influences of

the HDS of thiophene and HDN of pyridine in the presence of sulfided $CoMo/Al_2O_3$, $NiMo/Al_2O_3$, NiW/Al_2O_3 and NiW/SiO_2-Al_2O_3 catalysts. Over all four catalysts pyridine inhibited the HDS reaction, whereas thiophene had a dual effect on HDN. At low temperature thiophene inhibited the HDN reaction by competing with pyridine for hydrogenation sites and at high temperature the dominant effect was an improvement of C-N bond cleavage by H_2S, the product of the HDS reaction. The enhancement of the HDN by H_2S was ascribed to the conservation of the catalyst in a completely sulfided state, in which it has a better HDN activity. The HDS sites were classified into two types: i) active sites that are responsible for the majority of the HDS activity, but that are extremely sensitive to basic nitrogen compounds, and ii) active sites that are less active in HDS, but also less susceptible to poisoning. Furthermore it was shown [3] that the first type of sites was responsible for the hydrogenation of S-containing molecules, because tetrahydrothiophene was not observed when pyridine was present in the feed.

Two reaction pathways were found for the HDS of dibenzothiophene (DBT), which take place on different sites. The first type of sites is responsible for the hydrogenation pathway, and the second type of sites is facilitating the direct sulfur removal or hydrogenolysis [4-6,14-18]. N-containing molecules were found to be strong inhibitors for the minor, hydrogenation pathway of the HDS of DBT. The overall conversion of DBT decreased only slightly, suggesting that the amount of product formed via the hydrogenolysis pathway increased. Some authors have even claimed an enhancement of this route in the presence of N-compounds [4-6].

We have studied the mutual influences of the HDS of DBT and the HDN of 2-methylpyridine (2-MPy) and 2-methylpiperidine (2-MPiper) over a sulfided $NiMo/Al_2O_3$ catalyst. DBT was chosen because it allows to study the removal of sulfur by the direct desulfurization pathway (hydrogenolysis) as well as by the hydrogenation pathway (hydrogenation followed by desulfurization). Pyridine is the smallest model molecule for studying HDN, but, although the reactions taking place in its HDN are now well understood, the study of its HDN kinetics proved to be extremely difficult. The reason for this difficulty is that two molecules of piperidine, the first intermediate in the HDN of pyridine, disproportionate to *N*-pentylpiperidine and ammonia [19]. However, the introduction of a methyl group on the α carbon atom of piperidine strongly suppresses the disproportionation, so that it hardly interferes with the other reactions taking place during the HDN of 2-MPy and

2-MPiper [Chapter 4]. Therefore, we decided to use 2-MPy and 2-MPiper in our study of the influence of N-containing molecules on the HDS of DBT.

5.2 Experimental

The NiMo/γ-Al_2O_3 catalyst used in this work contained 8 wt% Mo and 3 wt% Ni and was prepared by successive incipient wetness impregnation of γ-Al_2O_3 as described in Chapter 3. Reactions were carried out in a continuous mode in a fixed-bed inconel reactor. The details are given in Chapter 3. The experiments were carried out at 300 and 340°C. The composition of the gas-phase feed consisted of 130 kPa toluene (as solvent for the DBT and amine), 8 kPa dodecane (as reference for DBT and its derivatives in the GC analysis), 11 kPa heptane (as reference for the N-compounds in the GC analysis), 1 kPa dibenzothiophene, 2-10 kPa amine reactant, 35 kPa H_2S (unless noted otherwise) and 4.8 MPa H_2. Toluene was chosen as the solvent due to its good ability to dissolve aromatic heterocycles like dibenzothiophene. We checked that in the presence of S- or N-containing molecules toluene did not undergo hydrogenation to methylcyclohexane. The partial pressure of H_2S was kept sufficiently higher than that of DBT to avoid the influence of H_2S formed during the HDS reaction.

The reaction products were analyzed by on- and off-line gas chromatography as described in Chapter 3. Off-line analysis was used for the HDS of DBT because of the high boiling points of the reactant and reaction products. Detection was performed with a flame ionization detector as well as with a pulsed flame photometric detector.

5.3 Results

5.3.1 HDS of dibenzothiophene

The results of the experiments of the HDS of DBT carried out at 300 and 340°C (Figs. 5.1 and 5.2) show that the reaction goes via two parallel pathways (Scheme 5.1): direct desulfurization (DDS), which yields biphenyl (BP), and hydrogenation (HYD) followed by

desulfurization, which gives first tetrahydrodibenzothiophene (TH-DBT) and then cyclohexylbenzene (CHB). The two final products are biphenyl and cyclohexylbenzene. At 300°C the selectivity of the biphenyl formation is about 85% at low and 80% at high weight time (Fig. 5.1b), whereas at the higher temperature of 340°C those values are 90 and 70% respectively (Fig. 5.2b). These results indicate that the DDS route is much easier than the HYD route, since the amount of biphenyl is six to nine times higher than the sum of tetrahydrodibenzothiophene and cyclohexylbenzene. Slow hydrogenation of biphenyl to cyclohexylbenzene took place at both reaction temperatures, since the biphenyl selectivity decreased with weight time and the increase of the cyclohexylbenzene selectivity with weight time was higher than the decrease of the tetrahydrodibenzothiophene selectivity. The resulting overall mechanism of the HDS of DBT is represented in Scheme 5.1.

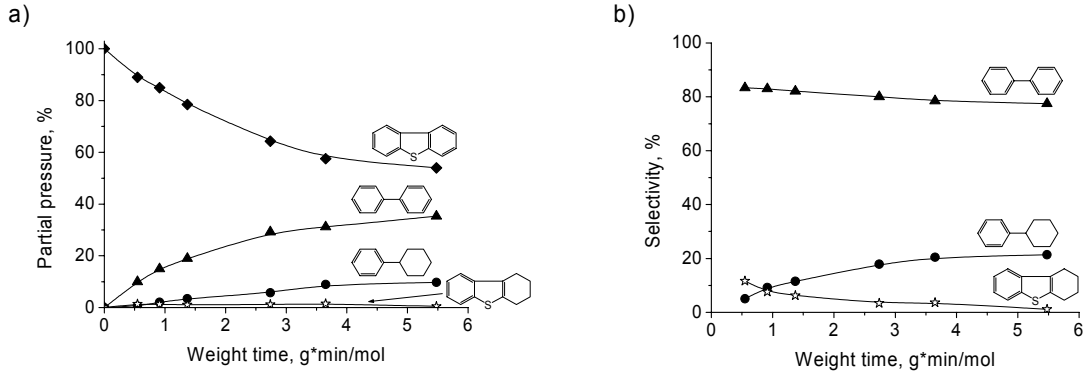

Fig. 5.1. Relative partial pressures (a) and selectivities (b) of the products of the HDS of dibenzothiophene at 300°C as a function of weight time.

The DDS pathway is slightly enhanced at higher temperatures, since the selectivity towards biphenyl formation at low weight time is higher at 340 than at 300°C. Thus, an increase of the temperature has a positive effect on the desulfurization reaction. At high weight time, the biphenyl selectivity was lower at 340 than at 300°C, due to increased hydrogenation of biphenyl. At 340°C and τ=5.5 g·min/mol the DBT conversion was about 90%, but at 300°C it was only 45%. As a consequence, the hydrogenation of biphenyl is not only intrinsically faster but also less inhibited by DBT at 340°C.

The HDS of DBT is generally assumed to be a first order reaction with respect to DBT [11]. Our DBT conversions at 300°C confirm this, since we obtained a linear dependency

when plotting $\ln[(C_{DBT})/(C_{DBT})^0]$ versus weight time and a high R^2 value. Also in the presence of the N-containing molecules the HDS of DBT could be approximated with first order kinetics. Therefore, all the rate constants of the HDS of DBT with and without N-compounds at 300°C were evaluated assuming the HDS of DBT to be a first order reaction.

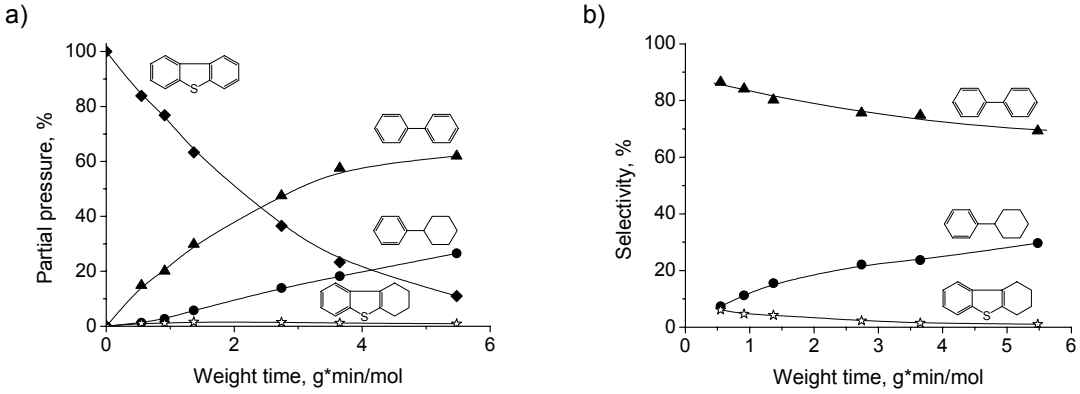

Fig. 5.2. Relative partial pressures (a) and selectivities (b) of the products of the HDS of dibenzothiophene at 340°C as a function of weight time.

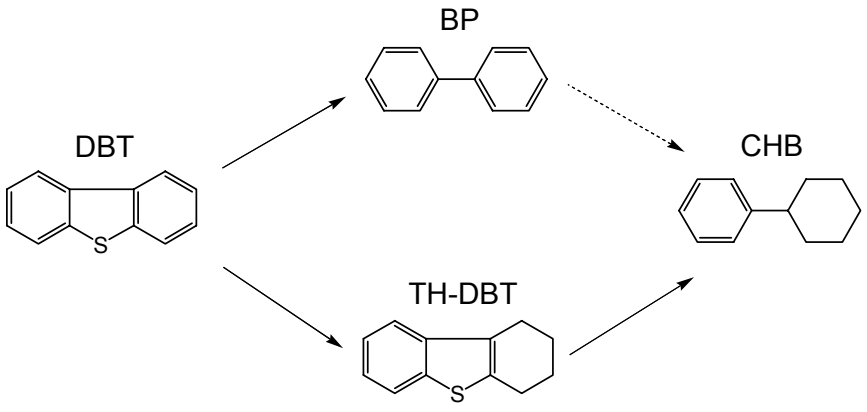

Scheme 5.1. Reaction network of the HDS of dibenzothiophene.

5.3.2 Inhibition of the HDS by N-containing molecules

The HDS of DBT was studied in the presence of 2-MPy and 2-MPiper at 300 and 340°C at different conversion levels of the N-compounds. The HDN network of 2-MPy and 2-MPiper was determined earlier [Chapter 4] and is presented in Scheme 5.2. As expected, 2-MPiper is the only primary product in the HDN of 2-MPy, since the HDN of heterocyclic N-containing aromatic molecules can only occur after ring hydrogenation [20]. The HDN of 2-MPiper showed that four compounds, 1-aminohexane, 2-aminohexane, 2-methylpyridine and 2-methyl-3,4,5,6-tetrahydropyridine, have non-zero selectivity at zero conversion of 2-MPiper and thus might be considered to be primary products. Actually, aminoalkenes and amino-alkanethiols are expected to be primary products. Aminoalkenes, which are the primary products of the ring opening via elimination of alkylpiperidine, were not observed, probably because of their fast hydrogenation to the corresponding amines. Amino-alkanethiols can be formed by nucleophilic substitution of the alkylpiperidine by H_2S. They are probably not observed because of a fast H_2S elimination or C-S hydrogenolysis. Comparison of the conversion of 2-aminohexane and 1-aminohexane showed that the reactivity of 2-aminohexane is higher than that of 1-aminohexane. Despite this higher reactivity, much more 2-aminohexane than 1-aminohexane was detected in the HDN of 2-MPiper [Chapter 4]. Therefore, it can be concluded that the first C-N bond breaking in 2-MPiper occurs predominantly between the nitrogen atom and the carbon atom of the methylene group and that the methyl group actually has a negative rather than a positive influence on the C-N bond breaking. This suggests that the HDN of 2-MPiper occurs by nucleophilic substitution to 5-amino-hexanethiol rather than via elimination to 5-amino-hexene-1.

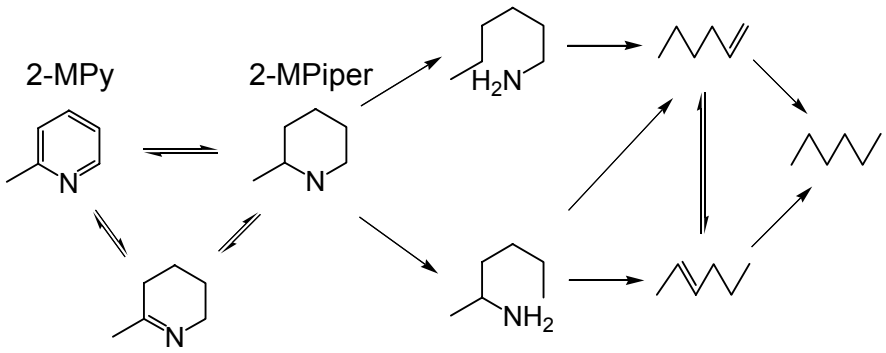

Scheme 5.2. Reaction network of the HDN of 2-methylpyridine and 2-methylpiperidine.

We first studied the HDS of 1 kPa DBT at 300°C in the presence of 2, 6 and 10 kPa of 2-MPy and 2-MPiper. At this temperature 2-MPy only converts to 2-MPiper and, because of thermodynamics [21,22], this reaction is irreversible. In the presence of the N-containing molecules the HYD pathway of the HDS of DBT is strongly suppressed, since the selectivity towards biphenyl formation is increased from 85 to 96-98%. The conversion of DBT decreased with increasing partial pressure of the N-compounds, indicating that 2-MPy and 2-MPiper not only suppress the hydrogenation route, but inhibit the hydrogenolysis (DDS) pathway as well. Since the transformation of DBT is still well described by first order kinetics, we calculated k'_{DBT} (the rate constant of the HDS of DBT in the presence of the N-compound) and plotted the ratio k'_{DBT}/k_{DBT}, where k_{DBT} is the rate constant of the HDS of DBT alone, versus the partial pressure of the N-containing molecule in the gas phase (Fig. 5.3). One can see that the inhibition effect of 2-MPy is much stronger than that of 2-MPiper. While no conversion of 2-MPiper was observed in the competitive experiments, the conversion of 2-MPy varied from 50 to 20% when increasing its partial pressure in the feed.

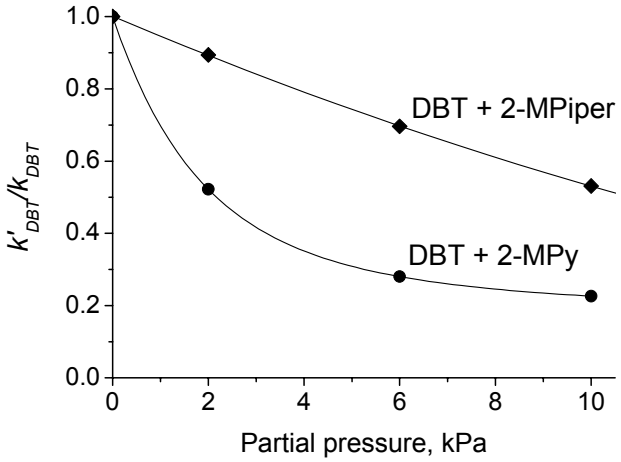

Fig. 5.3. Inhibition of the HDS of 1 kPa DBT in the presence of 2-MPy (●) and 2-MPiper (♦) at 300°C.

At 340°C, DBT could be fully converted and 2-MPy and 2-MPiper underwent hydrodenitrogenation in the simultaneous HDS and HDN reactions. Different partial pressures of 2-MPy and 2-MPiper (2, 6 and 10 kPa) were used. Again, just trace amounts of

products formed via the HYD pathway of the HDS of DBT were observed; this route is strongly suppressed at 340°C as well. The inhibition of the direct desulfurization pathway is clearly seen at high partial pressures of 2-MPy and 2-MPiper (Fig. 5.4). The decrease of the DBT conversion is almost the same in the presence of 10 kPa of both N-compounds. However, at 2 and 6 kPa the inhibitory influence of 2-MPy is stronger, as was observed at 300°C. For the lowest concentration of 2-MPy and 2-MPiper studied (2 kPa) one can hardly see any influence on the DBT conversion and in these experiments we observed an enhancement of the biphenyl formation (Fig. 5.5). This can be explained by the blocking of the HYD pathway, so that a higher amount of DBT is available for DDS. We verified this by kinetic calculations, assuming the DDS and HYD reactions of the DBT HDS to be first order irreversible reactions running in parallel. The rate constants were obtained using the selectivity data (90% for DDS and 10% for HYD). Then excluding the HYD pathway from the HDS network of DBT we obtained 72% conversion towards biphenyl at τ=3.5 g·min/mol. In Fig. 5.5 the theoretical conversion of DBT to biphenyl in the absence of the HYD pathway is presented by dashed line. Therefore, we conclude that the enhancement of the biphenyl formation is due to the absence of the HYD route. At low concentrations of 2-MPy and 2-MPiper, the inhibition of the DDS pathway is minor and the DDS pathway profits fully from the blocking of the HYD pathway. At higher concentrations of 2-MPy and 2-MPiper, the DDS pathway is slowed down as well and the biphenyl curves lie under the curve obtained in the absence of the N-containing molecules (Fig. 5.5).

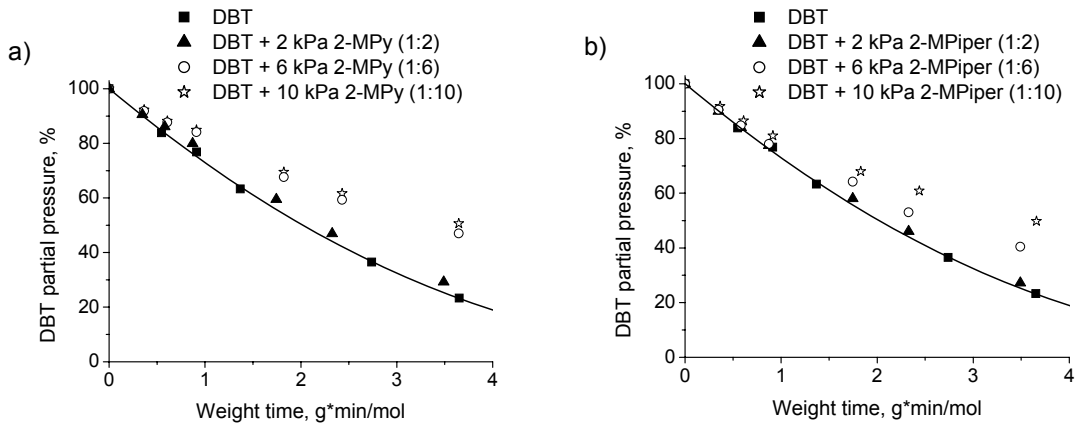

Fig. 5.4. Inhibition of the HDS of DBT in the presence of 2-MPy (a) and 2-MPiper (b) at 340°C.

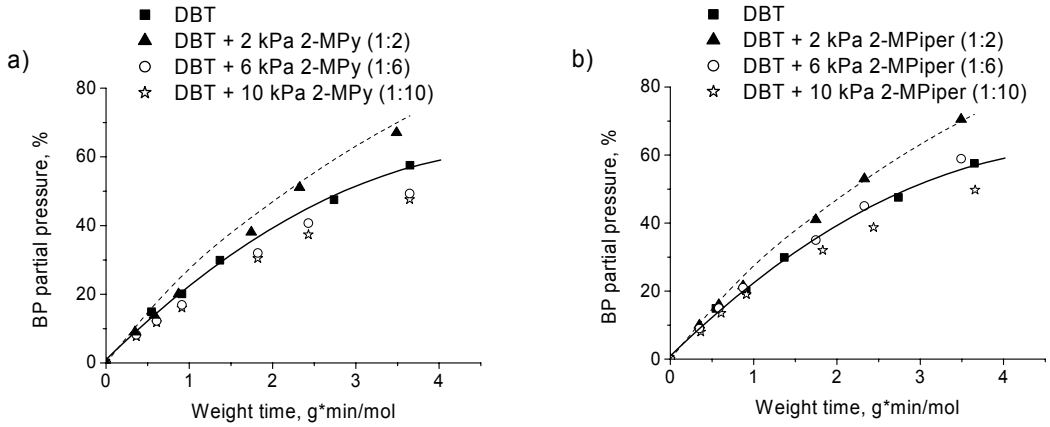

Fig. 5.5. Relative partial pressures of biphenyl in the HDS of DBT in the presence of 2-MPy (a) and 2-MPiper (b) at 340°C.

5.3.3 Effect of H_2S on the HDN of 2-methylpyridine

Before studying the influence of DBT on the HDN of 2-MPy, we investigated the effect of H_2S on the two reactions that take place in the HDN of 2-MPy: the hydrogenation of 2-MPy and the removal of nitrogen from 2-MPiper. Experiments on the hydrogenation of 2-MPy were performed at 300°C, because at this temperature only hydrogenation to 2-MPiper occurred; 2-MPiper, in turn, did not react further. The removal of nitrogen from 2-MPy was studied at 340°C.

The cleavage of the C(sp^3)-N bond is known to be promoted by H_2S [23-25]. In agreement with these results, our experiments of the HDN of 2-MPiper showed an enhancement of the HDN conversion with increasing H_2S partial pressure from 30 to 160 kPa (Fig. 5.6).

The conversion of 2-MPy at a fixed weight time of 3 g·min/mol and a temperature of 300°C is presented in Fig. 5.7 as a function of the H_2S pressure. The 2-MPy conversion increased up to 10 kPa H_2S and decreased at higher H_2S partial pressure. In the literature only inhibition of the hydrogenation of N-containing aromatic molecules by H_2S has been reported [26,27]. The occurrence of an optimum H_2S concentration may be caused by the fact that at high concentration H_2S adsorbs on the active sites and poisons the hydrogenation reaction,

whereas at very low H_2S concentration the catalyst surface reconstructs and the number of hydrogenation sites increases.

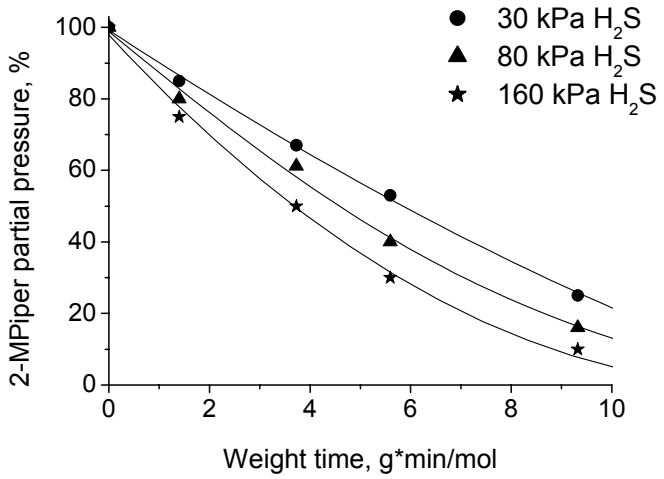

Fig. 5.6. HDN of 2-MPiper at 340°C and different H_2S partial pressures.

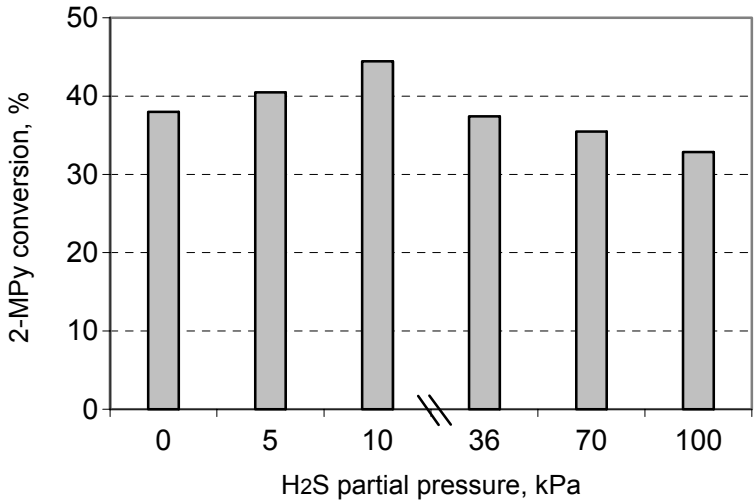

Fig. 5.7. Conversion of 2-MPy at 300°C and different H_2S partial pressures and a weight time of 3 g·min/mol.

The hydrogenation of 2-MPy at 300°C starts quite fast and levels off with weight time (Fig. 5.8). To determine if poisoning by the product was responsible for this levelling off, the reaction was repeated in the presence of 1 kPa 2-MPiper at a ratio of 2-MPy/2-MPiper = 6. The results show that such a small amount of 2-MPiper indeed strongly inhibits the hydrogenation reaction (Fig. 5.8). It indicates that 2-MPiper strongly adsorbs on the hydrogenation sites.

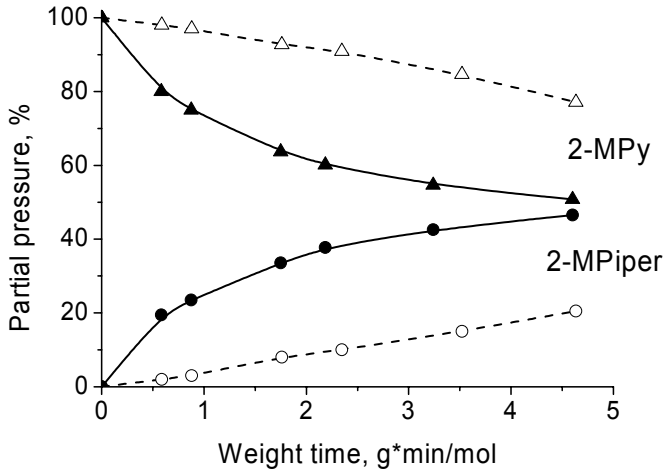

Fig. 5.8. Hydrogenation of 6 kPa 2-MPy at 300°C in the presence (----) and absence (—) of 1 kPa 2-MPiper.

Studying the effect of H_2S on the HDN of 2-MPy at 340°C, we observed a decrease of 2-MPy conversion with increase of H_2S partial pressure from 0 to 10 kPa. The loss in the conversion was mainly due to the decrease of 2-MPiper formation, whereas the HDN conversion of 2-MPy to nitrogen-free C_6 products was enhanced almost by a factor of four (Fig. 5.9). A successive increase of the H_2S partial pressure up to 100 kPa (30, 70 and 100) led to a further decrease of the 2-MPy conversion and 2-MPiper formation and to the increase of the HDN conversion of 2-MPy. However, these changes were not that significant as for the increase in H_2S partial pressure from 0 to 10 kPa (Fig. 5.9). Therefore, we can conclude that at 340°C H_2S has a negative effect on the hydrogenation of 2-MPy and a positive influence on the HDN conversion of 2-MPy as well as 2-MPiper. These results are in good agreement with those reported in [23,24].

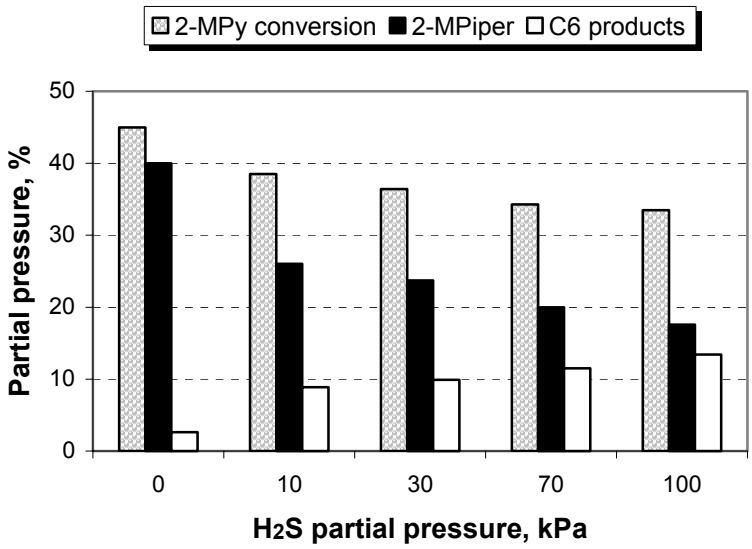

Fig. 5.9. Total conversion and product distribution in the HDN of 2-MPy at 340°C and different H_2S partial pressures.

5.3.4 Influence of DBT on the HDN of N-compounds

The N-containing molecules had a negative influence on both pathways of the HDS of DBT. They almost blocked the HYD pathway and inhibited the DDS pathway. In turn, DBT has a negative effect on the hydrogenation of 2-MPy at 300°C. The conversion of 6 kPa 2-MPy to 2-MPiper decreased almost by a factor of two in the presence of 1 kPa DBT (Fig. 5.10). This cannot be caused by the H_2S released in the HDS reaction since the partial pressure of H_2S in the feed was 35 kPa, 35 times higher than that of DBT. The observed inhibition effect must therefore be due to the presence of DBT.

The influence of DBT on the HDN of the N-containing molecules was also studied at 340°C, when C-N bond cleavage took place as well. The results of the HDN of 2-MPy, carried out in parallel with the HDS of DBT, and of the HDN of 2-MPy alone are presented in Fig. 5.11. In the presence of DBT, the conversion of 2-MPy and the yield of 2-MPiper decreased, while the amount of C_6 products (hexane, hexenes and hexylamines) hardly changed. The conversion of 2-MPy was lower at 340 than at 300°C, since the hydrogenation

of 2-MPy to 2-MPiper becomes reversible. The inhibitory influence of DBT on the hydrogenation of 2-MPy was less strong at 340 than at 300°C. The influence of DBT on the C-N bond cleavage of 2-MPiper to hexane, hexenes and hexylamines was studied at 340°C. Figure 5.12 shows that DBT does not have any influence on the HDN of 2-MPiper.

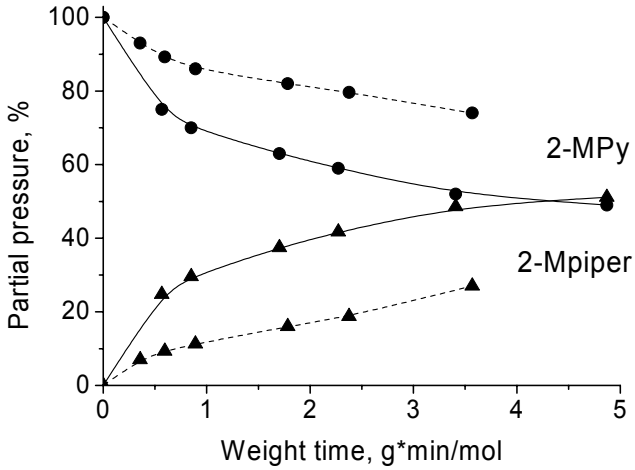

Fig. 5.10. Hydrogenation of 6 kPa 2-MPy at 300°C in the presence (----) and absence (—) of 1 kPa DBT.

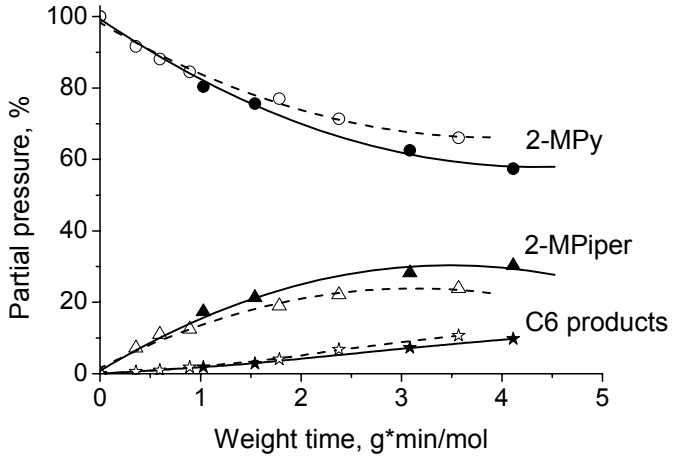

Fig. 5.11. HDN of 6 kPa 2-MPy at 340°C in the presence (----) and absence (—) of 1kPa DBT.

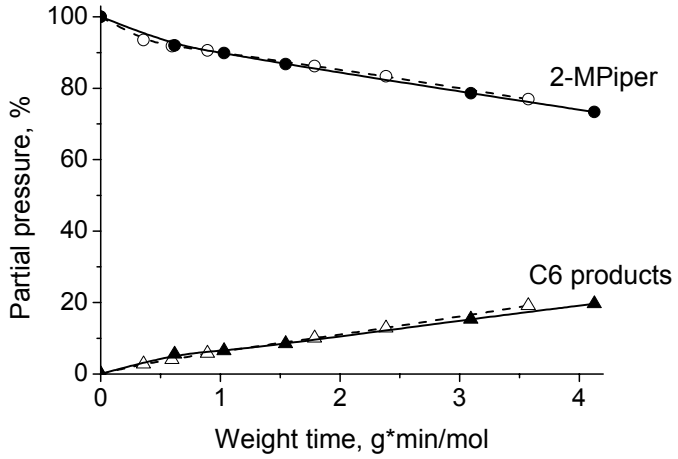

Fig. 5.12. HDN of 6 kPa 2-MPiper at 340°C in the presence (----) and absence (──) of 1kPa DBT.

5.4 Discussion

As originally proposed by Houalla et al. [28], the reaction pathways for the HDS of DBT are i) direct desulfurization to form biphenyl and ii) hydrogenation to give 1,2,3,4-tetrahydrodibenzothiophene or 1,2,3,4,10,11-hexahydrodibenzothiophene, which are further desulfurized to cyclohexylbenzene. Our results show that over NiMo the desulfurization pathway is six times faster than the hydrogenation pathway at 300°C and nine times faster at 340°C (Figs. 5.1b and 5.2b). Desulfurization of the hydrogenated intermediate tetrahydrodibenzothiophene is also much faster than hydrogenation, since only amounts of tetrahydrodibenzothiophene as small as 1-2% were observed during the HDS reaction.

The biphenyl formed in the DDS pathway was slowly hydrogenated to cyclohexylbenzene at 300°C and somewhat faster at 340°C (Figs. 5.1b and 5.2b). The hydrogenation of biphenyl to cyclohexylbenzene during the HDS of DBT has also been observed in other studies [15,16,18]. It is more evident over NiMo catalysts than over CoMo catalysts [29], because NiMo is a better hydrogenation catalyst in comparison with CoMo. The higher activity of a nickel-containing catalyst has been ascribed to the structure of the catalyst. NiMo catalysts are more sensitive to the inhibiting effect of H_2S than CoMo catalysts

in HDS reactions [30-32]. This indicates that the state of sulfidation of a NiMo catalyst changes more strongly with the H_2S partial pressure than that of a CoMo catalyst. At lower H_2S partial pressure, the NiMo catalyst may be more easily depleted of sulfur and thus have a better hydrogenation activity. No further hydrogenation of cyclohexylbenzene to bicyclohexyl was observed under our reaction conditions. Therefore, Scheme 5.1 describes our results of the HDS of DBT best.

The hydrogenation of biphenyl, in the absence of S- or N-containing molecules, was about ten times slower over our $NiMo/Al_2O_3$ catalyst than the hydrogenation of the biphenyl formed during the HDS reaction, however. Similarly low hydrogenation rates of biphenyl were obtained by Nagai et al. [5]. In their study of the HDS of DBT, they changed a feed, that contained 5 wt% DBT, to a feed containing 5 wt% DBT and 1 wt% biphenyl, and later switched back to the initial feed. No noticeable changes in the concentration of the cyclohexylbenzene formed were observed after the changes in the feed composition. We ascribe the difference between the hydrogenation of added biphenyl and of biphenyl formed in situ to hidden kinetics. When biphenyl is formed in situ, by the DDS of DBT, it is still adsorbed on the catalyst surface. In this flat, adsorbed state it can directly be hydrogenated, before desorbing from the catalytic site. When added to the gas phase, biphenyl has to diffuse to the catalytic sites and adsorb. In the gas phase, the two phenyl rings of biphenyl are not co-planar and some activation energy has to be brought up to adsorb biphenyl in a flat conformation. This may explain the difference in the rate of hydrogenation between added and in situ formed biphenyl.

H_2S inhibits the DDS pathway of the HDS of DBT strongly, but the HYD pathway only slightly [33]. This suggests that the hydrogenolysis and hydrogenation of DBT proceed on different catalytic sites. The sites active for the hydrogenation of DBT are very sensitive to poisoning by nitrogen bases, whereas the sites responsible for direct C-S bond cleavage are less susceptible to poisoning [4,5]. It was even reported that acridine has a promotion effect on the direct desulfurization of DBT over sulfided NiMo and NiW supported catalysts [34,35]. However, it has never been confirmed by systematic studies.

In the competitive HDS and HDN experiments at 300°C, with feeds containing 1 kPa DBT and different partial pressures (2, 6 and 10 kPa) of 2-MPy or 2-MPiper, a decrease of the total conversion of DBT was observed in all reactions. The inhibition was stronger in the presence of 2-MPy than in that of 2-MPiper (Fig. 5.3). The HDS rate constant (k'_{DBT}) changed slightly in the presence of 2 kPa 2-MPiper, whereas in the presence of 2 kPa 2-MPy it

decreased by 50%. The products of the HYD pathway of the HDS of DBT, such as tetrahydrodibenzothiophene and cyclohexylbenzene, were observed in very small amounts (2-4% of the total conversion). This shows that even small amounts of N-compounds significantly inhibit the hydrogenation of DBT and means that the slight inhibition of the HDS of DBT at 2 kPa of 2-MPiper is mainly due to the small contribution of the HYD route. At higher concentrations of 2-MPiper the inhibition of the DDS route becomes obvious. In the presence of 2-MPy, the DDS pathway is inhibited already at low 2-MPy partial pressures.

At the higher temperature of 340°C, the DDS pathway was enhanced (Fig. 5.2b) and less sensitive to the low concentrations of N-compounds (Fig. 5.4). An amount of 2 kPa 2-MPy decreased the DBT conversion slightly, while 2 kPa 2-MPiper hardly changed the DBT conversion. The formation of biphenyl was enhanced (Fig. 5.5). Similar increases in one product, induced by inhibition of another product, were reported by others [4,5]. However, this increase in the concentration of biphenyl is not the result of a promoting effect of the N-containing molecules on the HDS of DBT, but the result of an increase of the DBT concentration, due to the absence of the HYD pathway. As a result, the ultimate yield of biphenyl can be 100 instead of 90% (dashed line in Fig. 5.5). Moreover, in the presence of N-containing molecules biphenyl is not further hydrogenated to cyclohexylbenzene. At higher 2-MPy and 2-MPiper concentrations, the inhibition of DDS became noticeable. Like at 300°C, also at 340°C the inhibitory effect of 2-MPy is larger than that of 2-MPiper. Hence, the N-containing molecules have a negative influence on both HYD and DDS pathways at both reaction temperatures, but, whereas the HYD route is strongly inhibited, the DDS route is less affected.

The less basic 2-MPy was found to be a stronger inhibitor than the more basic 2-MPiper for the DDS of DBT. This is in agreement with report that pyridine is a stronger poison than piperidine in the HDS of DBT [5]. Although the aqueous basicity (pK_a) of aliphatic heterocyclic compounds is almost two times higher than that of heterocyclic aromatic compounds, their adsorption constants are lower [5,36]. Apparently, the aqueous basicity is a poor predictor of adsorption strength. A more appropriate parameter is the gas-phase proton affinity, which has a good correlation with the adsorption constant [7]. Indeed, the proton affinity and the adsorption constant of piperidine on sulfided NiMo catalyst are lower than those of pyridine [5]. This suggests that the stronger inhibitory effect of 2-MPy than of 2-MPiper is due to a higher adsorption constant on the catalyst surface. All observations are basically related to the major DDS pathway of the HDS of DBT. The picture

for the HYD site can be different, because of the different nature of the site. Indeed, our results show that the more basic 2-MPiper inhibits the HYD pathway somewhat stronger than 2-MPy. This is in accordance with results reported by Zeuthen et al. [37], who showed that basic N-compounds influenced the HDS of diesel strongly. Since most sulfur compounds in their diesel were of the 4,6-dialkylDBT-type that undergo HDS mainly via the HYD pathway, these results are in good agreement with ours.

The adsorption constants of 2-MPy and 2-MPiper on the HDS sites were determined by analyzing our experimental results with the Langmuir-Hinshelwood model, by assuming that the HDS of DBT proceeds on a site that can be poisoned by 2-MPy and 2-MPiper:

$$\frac{\partial P_{DBT}}{\partial \tau} = \frac{k \cdot K_{DBT} \cdot P_{DBT}}{1 + K_{DBT} \cdot P_{DBT} + K_N \cdot P_N}$$

In the analysis we used the data of the HDS of DBT itself and of the HDS of DBT in the presence of 2, 6 and 10 kPa 2-MPy and 2-MPiper obtained at 300°C. The adsorption constants of DBT, 2-MPy and 2-MPiper on the HDS sites of the NiMo/γ-Al_2O_3 catalyst were found to be equal to 0.029, 0.53 and 0.076 kPa^{-1} respectively. This shows that the adsorption constant of DBT is about twenty times smaller than that of 2-MPy and two times smaller than that of 2-MPiper and that the adsorption constant of 2-MPy is seven times higher than that of 2-MPiper.

Two reactions take part in the HDN of 2-MPy (Scheme 5.2), hydrogenation-dehydrogenation and C-N bond cleavage. This suggests the presence of two active sites: sites responsible for the hydrogenation-dehydrogenation and sites promoting the C-N bond breaking. H_2S has a dual effect on the HDN reactions of pyridine and quinoline [24,38,39]. It slightly inhibits the hydrogenation and dehydrogenation, but markedly accelerates the overall HDN rate because it promotes C(sp^3)-N bond cleavage. Our results show that there is an optimum H_2S concentration for the hydrogenation of 2-MPy at 300°C (Fig. 5.7). On the one hand, H_2S creates acidic sites on the catalyst surface, thereby increasing the adsorption of a basic aromatic molecule. On the other hand, at higher concentrations H_2S covers the vacancies on the catalyst surface and hinders the adsorption of N-containing molecules. 2-MPiper at 340°C undergoes mainly HDN and H_2S has a positive influence on the C-N bond cleavage (Fig. 5.6). Therefore, the effect of H_2S on the overall conversion of 2-MPy could be promoting at lower and retarding at higher H_2S partial pressures. However, our experiments

showed that H_2S has a small negative influence on the overall conversion of 2-MPy at 340°C but a positive effect on the HDN conversion (Fig. 5.9). At first sight, it looks as if these results contradict the promotion effect of low amounts of H_2S on both hydrogenation and C-N bond cleavage. However, at the higher temperature of 340°C one more reaction takes part in the HDN of 2-MPy and that is the reverse reaction of dehydrogenation of 2-MPiper to 2-MPy. This reaction can be also promoted by a small amount of H_2S, just as the hydrogenation reaction, therefore, the overall conversion of 2-MPy would decrease with increase of H_2S partial pressure. These results are in good agreement with those evidencing the dual effect of H_2S on HDN [24,38,39].

A detailed study of the interaction between catalytic hydrodesulfurization and hydrodenitrogenation was first performed by Satterfield et al. [2,3] with thiophene and pyridine as model compounds. Thiophene had a dual effect on the HDN of pyridine. At low temperatures, the competitive adsorption of thiophene on hydrogenation sites retarded the hydrogenation of pyridine to piperidine, and thus reduced the overall reaction rate. At higher temperatures, H_2S produced in the HDS of thiophene increased the rate of piperidine hydrogenolysis and enhanced the overall HDN reaction rate. Since these results were obtained in the absence of hydrogen sulfide, it is not clear if the inhibitory effect of the S-containing compound was due to H_2S released in the HDS reaction or due to the S-containing molecule itself. Therefore, we performed our experiments at an H_2S partial pressure, which was 35 times higher than that of DBT. The results show that DBT adsorbs much stronger on the hydrogenation sites than H_2S, since the conversion of 2-MPy to 2-MPiper in the presence of DBT decreased by factor of two at 300ºC (Fig. 5.10). At the higher temperature of 340°C, the inhibitory effect of DBT on the hydrogenation of 2-MPy was less drastic as at 300°C, but still obvious (Fig. 5.11).

Satterfield et al. showed that sulfur compounds as well as H_2S promote the rupture of C-N bonds [2]. They also demonstrated that H_2S released in the HDS of thiophene, and not thiophene itself, was responsible for the enhancement effect on HDN. This was confirmed by our results, which showed that, in the HDN of 2-MPy and of 2-MPiper, there was no change in the formation of C_6 products when DBT was added to the feed (Figs. 5.11 and 5.12). This proves that the active sites that facilitate C-N bond cleavage are different from those responsible for the HYD and DDS of S-containing molecules. At the same time, as mentioned above, N-containing compounds retard both DDS and HYD pathways, but to a different extent. The HYD pathway of the HDS of DBT was strongly suppressed in the presence of 2-

MPy and 2-MPiper at 300°C as well as at 340°C, whereas the DDS pathway was inhibited to a smaller extent. At high temperature and low partial pressures of 2-MPy and 2-MPiper it was almost not affected. Thus, while C-N bond cleavage needs another site than the HYD and DDS of S-containing molecules (see above), the hydrogenation of S- and N-containing molecules may take place at the same active sites.

The enhancement of the C-N bond rupture and better HDN activity of the catalyst in the presence of higher amounts of H_2S was previously associated with the maintenance of the catalyst in a completely sulfided state [3], since the active S-containing species will be unstable on the catalyst surface and will rapidly decompose in the absence of sufficient sulfur in the feed. However, we observed an increase in the HDN conversion of 2-MPiper at much higher H_2S partial pressures than needed to keep the catalyst in a completely sulfided state. 2-MPiper undergoes HDN via elimination or via nucleophilic substitution of the amine group by an SH group followed by hydrogenolysis of the C-S bond. In the latter case, H_2S should be of importance in the HDN of 2-MPiper. It was recently shown that aliphatic amines undergo HDN mainly via nucleophilic substitution [40]. Therefore, the enhancement of the HDN of 2-MPiper with increasing H_2S partial pressure may be ascribed to the reaction mechanism and not only to the sulfided state of the catalyst.

5.5 Conclusion

The influence of 2-MPy and 2-MPiper on the hydrodesulfurization of DBT and the effect of DBT on the hydrodenitrogenation of 2-MPy and 2-MPiper was studied over a sulfided $NiMo/Al_2O_3$ catalyst at 5 MPa, 35 kPa H_2S and 300 and 340°C. Both N-containing molecules strongly suppressed the hydrogenation pathway of the hydrodesulfurization of DBT and inhibited the direct desulfurization route at both reaction temperatures. The inhibitory effect on the direct desulfurization was stronger for 2-MPy than for 2-methylpiperidine. H_2S promoted the hydrogenation of 2-MPy up to 10 kPa and inhibited it at higher partial pressures. H_2S had a positive influence on the hydrodenitrogenation conversions of 2-MPiper and 2-MPy. DBT had a negative effect on the hydrogenation of 2-MPy, but did not influence the C-N bond cleavage of 2-MPiper. Therefore, C-N and C-S bond breaking take place at different active sites, whereas the hydrogenation sites for N- and S-containing molecules may be the same.

5.6 References

[1] F.W. Kirsch, H. Shalit, H. Heinemann, Ind. Eng. Chem. 51 (1959) 1379.

[2] C.N. Satterfield, M. Modell, J.F. Mayer, AIChE J. 21 (1975) 1100.

[3] C.N. Satterfield, M. Modell, J.A. Wilkens, Ind. Eng. Chem. Proc. Des. Dev. 19 (1980) 154.

[4] M. Nagai, T. Kabe, J. Catal. 81 (1983) 440.

[5] M. Nagai, T. Sato, A. Aiba, J. Catal. 97 (1986) 52.

[6] V. La Vopa, C.N. Satterfield, Chem. Eng. Commun. 70 (1988) 171.

[7] V. La Vopa, C.N. Satterfield, J. Catal. 110 (1988) 375.

[8] G.C. Laredo, J.A. De los Reyes, J.L. Cano, J.J. Castillo, Appl. Catal. A 207 (2001) 103.

[9] M. Cerny, Collect. Czech. Chem. Commun. 47 (1982) 1465.

[10] U.S. Ozkan, S.G. Ni, L.P. Zhang, E. Moctezuma, Energy & Fuels 8 (1994) 249.

[11] M.J. Girgis, B.C. Gates, Ind. Eng. Chem. Res. 30 (1991) 2021.

[12] P. Zeuthen, P. Stolze, U.B. Pedersen, Bull. Soc. Chim. Belg. 96 (1987) 985.

[13] P. Desikan, C.H. Amberg, Can. J. Chem. 42 (1964) 843.

[14] G.H. Singhal, R.L. Espino, J.E. Sobel, G.A. Huff, J. Catal. 67 (1981) 457.

[15] T.C. Ho, J.E. Sobel, J. Catal. 128 (1991) 581.

[16] B.C. Gates, H. Topsøe, Polyhedron 16 (1997) 3213.

[17] T. Kabe, K. Akamatsu, A. Ishihara, S. Otsuki, M. Godo, Q. Zhang, W.H. Qian, Ind. Eng. Chem. Res. 36 (1997) 5146.

[18] V. Meille, E. Schulz, M. Lemaire, M. Vrinat, J. Catal. 170 (1997) 29.

[19] R. Prins, Adv. Catal. 46 (2002) 399.

[20] N. Nelson, R.B. Levy, J. Catal. 58 (1979) 485.

[21] C.N. Satterfield, J.F. Cocchetto, AICHE J. 21 (1975) 1107.

[22] J.F. Cocchetto, C.N. Satterfield, Ind. Eng. Chem. Proc. Des. Dev. 15 (1976) 272.

[23] R.T. Hanlon, Energy & Fuels 1 (1987) 424.

[24] M. Jian, J.L.R. Cerda, R. Prins, Bull. Soc. Chim. Belg. 104 (1995) 225.

[25] F. Rota, R. Prins, J. Mol. Catal. A 162 (2000) 359.

[26] S.H. Yang, C.N. Satterfield, J. Catal. 81 (1983) 168.

[27] A. Olalde, G. Perot, Appl. Catal. 13 (1985) 373.

[28] M. Houalla, N.K. Nag, A.V. Sapre, D.H. Broderick, B.C. Gates, AIChE J. 24 (1978) 1015.

[29] T. Kabe, A. Ishihara, Q. Zhang, Appl. Catal. A 97 (1993) L1.

[30] S. Kasahara, T. Shimizu, M. Yamada, Catal. Today 35 (1997) 59.

[31] W. Robinson, J.A.R. van Veen, V.H.J. de Beer, R.A. van Santen, Fuel Proc. Tech. 61 (1999) 89.

[32] E.J.M. Hensen, V.H.J. de Beer, J.A.R. van Veen, R.A. van Santen, J. Catal. 215 (2003) 353.

[33] F. Bataille, J.L. Lemberton, P. Michaud, G. Perot, M. Vrinat, M. Lemaire, E. Schulz, M. Breysse, S. Kasztelan, J. Catal. 191 (2000) 409.

[34] M. Nagai, Ind. Eng Chem Prod. Res. Dev. 24 (1985) 489.

[35] M. Nagai, Chem. Lett. 6 (1987) 1023.

[36] A. Albert, Heterocyclic chemistry, The Athlone Press, London, 1959.

[37] P. Zeuthen, K.G. Knudsen, D.D. Whitehurst, Catal. Today 65 (2001) 307.

[38] C.N. Satterfield, S. Gultekin, Ind. Eng. Chem. Proc. Des. Dev. 20 (1981) 62.

[39] S.H. Yang, C.N. Satterfield, Ind. Eng. Chem. Proc. Des. Dev. 23 (1984) 20.

[40] Y. Zhao, P. Kukula, R. Prins, J. Catal. 221 (2004) 441.

Chapter 6

Promotion Effect of 2-Methylpiperidine on the Direct Desulfurization of Dibenzothiophene over NiMo/γ-Al_2O_3

6.1 Introduction

The long term trend in the petroleum industry is to process heavier feedstocks that contain a high percentage of sulfur and nitrogen. Therefore, knowledge of the mutual influence of hydrodesulfurization (HDS) and hydrodenitrogenation (HDN) is becoming more important. Studies on competitive HDS and HDN have shown that N-containing molecules strongly inhibit HDS reactions [1-12], because of their high adsorption constants on the catalyst surface. Moreover, the inhibitory effect of N-compounds depends on the nature of the molecule. In some cases, molecules with a different number or location of substituents have a different inhibitory influence. Thus, 2,6-dimethylpyridine was a weaker inhibitor in the HDS of thiophene than 4-methylpyridine and 3,5-dimethylpyridine [6,13]. This led to the conclusion that the inhibiting effect of pyridines on HDS occurs when these molecules are adsorbed perpendicular to the catalyst surface, since in this conformation the adsorption of 2,6-dimethylpyridine would be the weakest because of the steric hindrance of the methyl groups [13]. However, pyridines may undergo hydrogenation under HDS reaction conditions. As a consequence, if 2,6-dimethylpyridine were hydrogenated faster than the other substituted pyridines, its inhibitory influence would be the weakest, because of the weaker adsorption of 2,6-dimethylpiperidine in a one-point mode with steric hindrance due to the two methyl groups on the α and α' carbon atoms. The inhibition of HDS has also been correlated with the basicity of N-containing molecules [6], and it was observed that the more basic molecules have the strongest inhibitory influence. Nagai et al. found a correlation with gas phase proton affinities rather than with solution basicities [4].

Dibenzothiophene (DBT) is often used as a model compound for HDS, since it is a good representative of the S-containing molecules in middle and heavy distillates. The HDS of DBT consists of two reaction pathways: i) direct desulfurization (DDS) leading to the formation of biphenyl, and ii) hydrogenation (HYD) of DBT to tetrahydrodibenzothiophene followed by desulfurization to cyclohexylbenzene. Several research groups reported that N-containing molecules inhibit the DDS and the HYD pathways of the HDS of DBT to different extents: the HYD route was strongly suppressed, whereas the DDS route was less affected [4,14-17]. In some cases even a promotion of the DDS pathway was observed, whereas the total conversion of S-compound decreased [4,14,15]. Nagai reported a real promotion of the DDS of DBT over NiMo/Al_2O_3 and NiW/Al_2O_3 catalysts, i.e. the enhancement of the overall conversion of DBT in the presence of acridine, but gave no explanation [16,17].

At 340°C, 4.8 MPa H_2 and 35 kPa H_2S we observed a strong inhibition of the HYD pathway of the HDS of DBT at different partial pressures of 2-MPy and 2-MPiper and an enhancement of the biphenyl formation in the presence of 2 kPa 2-MPy and 2-MPiper [Chapter 5]. This promotion was explained by the higher amount of DBT available for the DDS, because of suppression of the HYD pathway. We proved this with calculations in which it was assumed that the rate constant of the DDS route was not affected at low concentration of N-compounds and that the HYD pathway was totally blocked. In our previous study [Chapter 5] we found that 2-MPiper has a somewhat stronger inhibitory influence on the HYD route than 2-MPy. The DDS pathway was hardly affected at 2 kPa and only slightly retarded at 6 and 10 kPa 2-MPy and 2-MPiper. Moreover, the inhibitory effect of 2-MPy on the DDS was stronger than that of 2-MPiper. Since the HDS of DBT goes mainly via the DDS pathway, 2-MPy was also the stronger poison for the overall HDS of DBT.

In the present work we studied the effect of 2-MPy and 2-MPiper on the HDS of DBT in more detail. We extended the partial pressure range of the N-containing molecules in the feed to clarify the mechanism of the poisoning influence and also decreased the temperature to 300°C. At the lower temperature the inhibitory effect of N-containing molecules should be more pronounced and can therefore be studied better. While at 340°C 2-MPy reacts to 2-MPiper and 2-MPiper reacts further to acyclic amines and hydrocarbons, at 300°C 2-MPy is only hydrogenated to 2-MPiper and the reaction is irreversible because of thermodynamics. The cleavage of the C-N bond does not take place at 300°C under our conditions.

6.2 Experimental

The NiMo/γ-Al_2O_3 catalyst used in this work contained 8 wt% Mo and 3 wt% Ni and was prepared by successive incipient wetness impregnation of γ-Al_2O_3 as described in Chapter 3. Reactions were carried out in a continuous mode in a fixed-bed inconel reactor [Chapter 3]. The experiments were carried out at 300°C. The feed consisted of 130 kPa toluene (as solvent for the DBT and amine), 8 kPa dodecane (as reference for DBT and its derivatives in the GC analysis), 11 kPa heptane (as reference for the N-compounds in the GC analysis), 1 kPa dibenzothiophene, 0.1-6 kPa amine reactant (2-MPy or 2-MPiper), 35 kPa H_2S and 4.8 MPa H_2.

The reaction products were analyzed by on- and off-line gas chromatography, as described in Chapter 3. Weight time was defined as $\tau = w_{cat}/n_{feed}$, where w_{cat} denotes the catalyst weight and n_{feed} the total molar flow to the reactor. The HDS of DBT alone and in the presence of the N-containing molecules could be well described with a first-order kinetic model with respect to DBT. This fact is in good agreement with literature [8].

6.3 Results

2-MPy and 2-MPiper were chosen as N-containing molecules because the methyl group on the α-carbon atom of pyridine strongly suppresses the disproportionation reaction of two molecules of piperidine, the first intermediate in the HDN of pyridine, to N-pentylpiperidine and ammonia [Chapter 4]. Thus, the overall reaction network of 2-MPy and 2-MPiper is less complicated than that of pyridine and piperidine, and is schematically presented in Scheme 6.1.

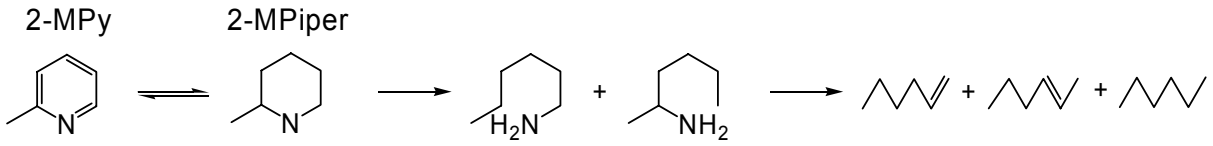

Scheme 6.1. Reaction network of the HDN of 2-methylpyridine and 2-methylpiperidine.

As mentioned in the introduction, DBT undergoes HDS via two reaction pathways: DDS and HYD. At 300°C the selectivity towards biphenyl formation is about 85% at low and 80% at high weight time [Chapter 5]. These results indicate that the DDS route is much easier than the HYD one and that slow hydrogenation of biphenyl to cyclohexylbenzene takes place in the presence of a NiMo/γ-Al_2O_3 catalyst. Therefore, the overall reaction network of the HDS of DBT is as shown in Scheme 6.2.

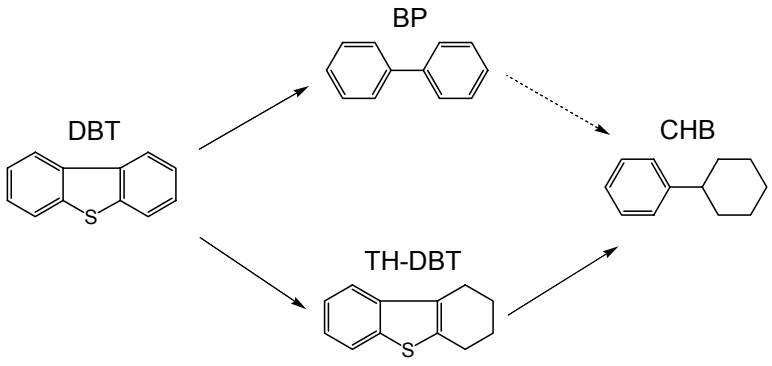

Scheme 6.2. Reaction network of the HDS of dibenzothiophene.

The results of the HDS of 1 kPa DBT in the presence of 0.1, 0.5, 1, 2 and 6 kPa of 2-MPy are presented in Fig. 6.1. The overall conversion of DBT was slightly decreased at the lowest partial pressure of 0.1 kPa 2-MPy and it decreased further with increasing 2-MPy partial pressure. The HYD pathway of the HDS of DBT was already strongly suppressed at 0.1 kPa 2-MPy. Its selectivity had decreased from 15% in the absence of 2-MPy to only 4% at 0.1 kPa 2-MPy and 2% at 6 kPa 2-MPy. Thus, the HYD route is greatly inhibited at all 2-MPy concentrations. The selectivity towards biphenyl formation stayed constant in the course of one single competitive experiment, showing that the hydrogenation of biphenyl to cyclohexylbenzene is also inhibited in the presence of 2-MPy.

The conversion to biphenyl in the presence and absence of 2-MPy is shown in Fig. 6.2. It is clear that the biphenyl production was higher in the presence of 0.1, 0.5 and 1 kPa 2-MPy than in its absence. A direct comparison of the conversion to biphenyl in the presence of 2-MPy with the conversion to biphenyl in the absence of 2-MPy is not meaningful, however, since in the first case biphenyl is the final product, whereas in the second case it is partly converted further to cyclohexylbenzene. Furthermore, a higher conversion to biphenyl (eventually 96-98%) is possible in the presence of 2-MPy, because the HYD route is almost

completely suppressed in the presence of 2-MPy. We calculated the theoretical conversion to biphenyl, assuming that the rate constant of the DDS pathway is not affected by the presence of 2-MPy and that the HYD pathway is fully suppressed (dashed bold line in Fig. 6.2). If we now compare the observed conversions to biphenyl with this theoretical estimate, we see that the DDS activity is hardly affected at 0.1 kPa 2-MPy and decreases at higher 2-MPy partial pressures. Therefore, after correction for these ″trivial″ effects, it is clear that 2-MPy does not promote the formation of biphenyl. 2-MPy suppresses not only the HYD pathway, but also the DDS pathway, be it to a smaller extent. The inhibitory influence of 2-MPy on the DDS of DBT could not be described with a Langmuir-Hinshelwood model with one adsorption constant. The inhibiting effect increased with the partial pressure of 2-MPy, as if its adsorption constant depended on its partial pressure. We will return to this problem in the following.

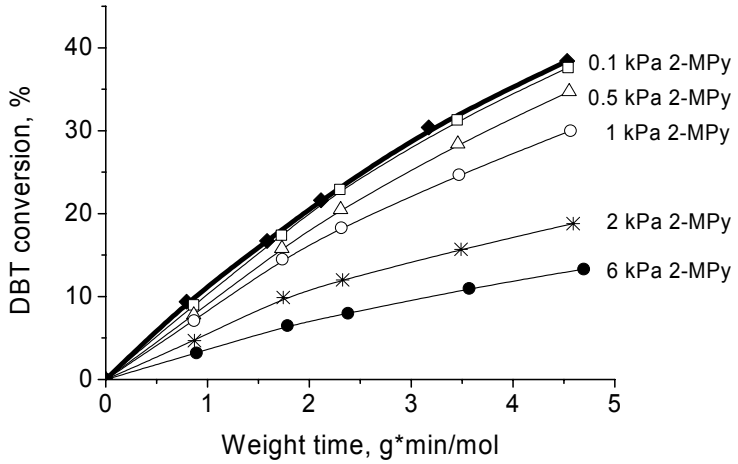

Fig. 6.1. Total conversion of 1 kPa DBT at 300°C and different 2-methylpyridine partial pressures. The heavy line represents the results for DBT alone.

Also in the HDS of 1 kPa DBT in the presence of 0.1, 0.5, 1, 2 and 6 kPa 2-MPiper the HYD pathway was strongly suppressed. The selectivity to HYD products decreased from 15% in the absence of 2-MPiper to 3% at 0.1 kPa and to 1% at 6 kPa 2-MPiper. These values show that 2-MPiper has a somewhat stronger inhibitory influence on the HYD pathway than 2-MPy. As was observed in case of 2-MPy, 2-MPiper also inhibited the hydrogenation of biphenyl to cyclohexylbenzene.

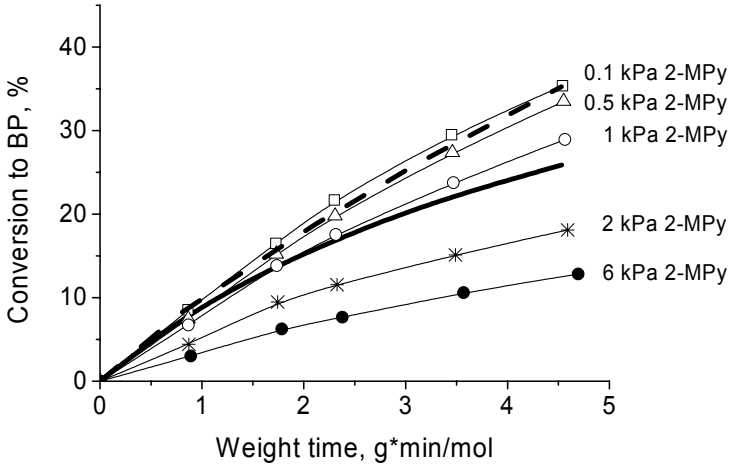

Fig. 6.2. Conversion to biphenyl in the HDS of DBT at 300°C and different 2-methylpyridine partial pressures. The heavy line represents the conversion to biphenyl in the absence of 2-MPy. The heavy dashed line represents the conversion to biphenyl in the absence of 2-MPy corrected for further hydrogenation of biphenyl and for the absence of the HYD pathway.

The conversion of DBT was enhanced in the presence of 0.1, 0.5 and 1 kPa 2-MPiper and decreased in the presence of 2 and 6 kPa 2-MPiper (Fig. 6.3). The formation of biphenyl was higher at all partial pressures of 2-MPiper than in the absence of 2-MPiper (Fig. 6.4). After correcting for the further hydrogenation of biphenyl and for the suppression of the HYD pathway (see above) the DDS conversion was still enhanced at 0.1, 0.5 and 1 kPa of 2-MPiper (Fig. 6.4). These results show that below 2 kPa 2-MPiper the DDS route of the HDS of DBT is promoted, since the total conversion of DBT is enhanced and the yield of biphenyl is higher than theoretically possible. Therefore, the influence of 2-MPiper on the HDS of DBT can not be described with a Langmuir-Hinshelwood model either, since we deal with a promotion at low and inhibition at high partial pressures of 2-MPiper.

2-MPiper is not converted under our reaction conditions (300°C, 4.8 MPa H_2 and 35 kPa H_2S), whereas the conversion of 2-MPy to 2-MPiper varied from 85 to 30% at the highest weight time (τ = 4.5 g·min/mol) when increasing the 2-MPy partial pressure in the feed from 0.1 to 6 kPa. This may explain the non-linear inhibitory influence of 2-MPy on the DDS pathway, since we actually deal with inhibition and promotion at the same time. At the lowest partial pressure of 0.1 kPa 2-MPy the inhibitory effect of 2-MPy is compensated by the promotion due to the 2-MPiper formed. Above 1 kPa, not only 2-MPy but also 2-MPiper acts

as a poison for the DDS of DBT. Thus, 2-MPy would have almost no inhibitory effect at low partial pressure and a strong inhibitory effect at high partial pressure.

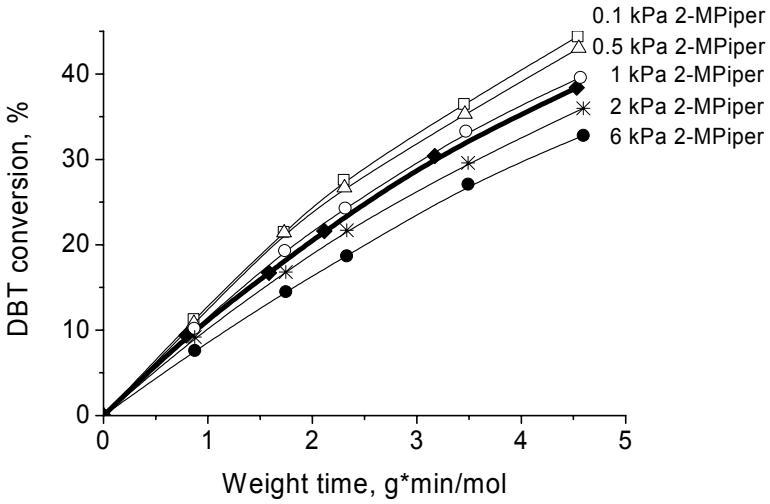

Fig. 6.3. Total conversion of 1 kPa DBT at 300°C and different 2-methylpiperidine partial pressures. The heavy line represents the results for DBT alone.

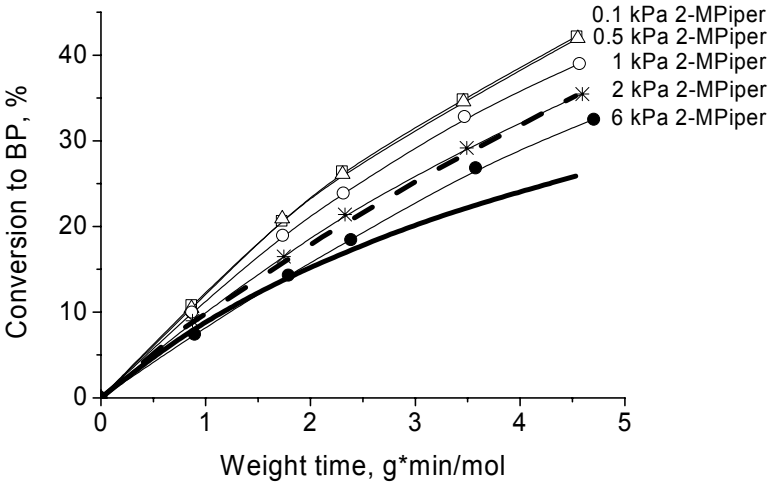

Fig. 6.4. Conversion to biphenyl in the HDS of DBT at 300°C and different 2-methylpiperidine partial pressures. The heavy line represents the conversion to biphenyl in the absence of 2-MPiper. The heavy dashed line represents the conversion to biphenyl in the absence of 2-MPiper corrected for further hydrogenation of biphenyl and for the absence of the HYD pathway.

6.4 Discussion

The enhancement of the DDS pathway in the HDS of DBT at low partial pressures of 2-MPiper can only be explained if we assume that the catalyst surface is changed and that an increased number of active sites is created. This means that either the active catalyst surface becomes rougher due to the adsorption of small amounts of 2-MPiper, or that the number of DDS sites is increased by a transformation of HYD sites to DDS sites. How can such a transformation take place and what are the active sites for the DDS and HYD pathways?

It is generally assumed that the catalytically active sites in Mo/γ-Al_2O_3 hydrotreating catalysts are the molybdenum atoms at the edges and corners of the MoS_2 crystallites, which have at least one sulfur vacancy to allow chemical adsorption of the reacting molecule on the molybdenum atom [18-20]. Upon addition of nickel and cobalt the HDS and HDN activities of a MoS_2/γ-Al_2O_3 catalyst increase substantially. Density functional theory (DFT) calculations showed that the most stable position for the promoter atom (Co or Ni) is at the edge, substituting the molybdenum atom [21], forming the so-called Co-Mo-S phase (Ni-Mo-S phase for Ni-Mo catalysts) [20]. DFT calculations suggest that a combined action of the promoter (Ni or Co) and molybdenum atom is responsible for the catalysis [21-23]. It was shown that a sulfur atom between a nickel (or cobalt) and a molybdenum atom is less strongly bonded than a sulfur atom between two molybdenum atoms and can be more easily removed, creating a vacancy.

Therefore, the catalytically active sites in our system are the nickel or molybdenum atoms present at the molybdenum edge. One vacancy at a metal atom could be enough to perform the DDS of DBT, in which case the molecule is adsorbed in a one-point way perpendicular to the catalyst surface. However, when DBT is π-adsorbed and follows the HYD pathway, it needs more space and at least two neighbouring vacancies must be available.

Most likely 2-MPy is adsorbed in a flat conformation through its aromatic π-system and is coordinated by two metal atoms as shown in Scheme 6.3. 2-MPiper has no π electrons and can, therefore, only adsorb through the nitrogen atom in a one-point manner (Scheme 6.4). When 2-MPiper is adsorbed on a HYD site, consisting of several S-free metal atoms, it leaves the neighbouring metal atom free. This metal atom is not available for hydrogenation

of DBT, because hydrogenation needs at least two neighbouring free sites, but it is available for one-point adsorption of DBT, and thus, for the DDS pathway of the HDS of DBT. In this way a HYD active site can transform into a DDS site at low partial pressures of 2-MPiper. This would explain the promotion of the direct sulfur removal route in the HDS of DBT. At higher concentration, 2-MPiper blocks both metal centres on the HYD active site, thereby decreasing also the DDS rate of the HDS of DBT.

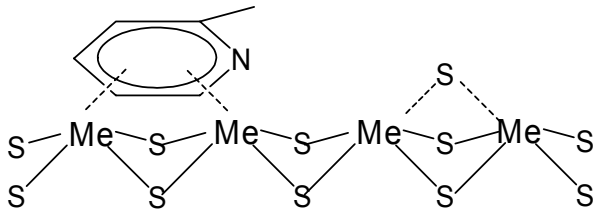

Scheme 6.3. Flat adsorption of 2-methylpyridine on the HYD active site.

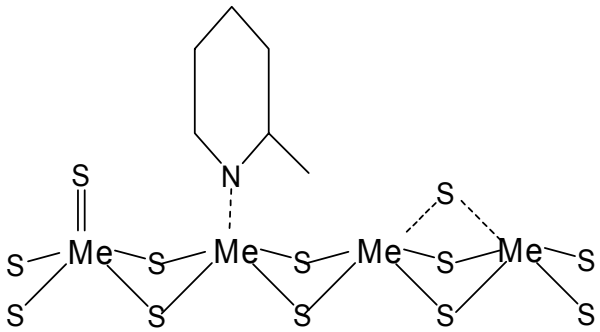

Scheme 6.4. One-point adsorption of 2-methylpiperidine on the DDS active site.

A similar explanation can be given in terms of edge and corner active sites. Let us assume that edge centres are responsible for the DDS pathway or for the perpendicular adsorption of reactant, whereas the corner sites situated between two edges have more room for adsorption and can therefore coordinate the molecule in a flat mode and perform the HYD pathway. When 2-MPy is present in the feed, both DDS and HYD sites are poisoned. On the other hand, when 2-MPiper adsorbs on an HYD site, it leaves room available for the DDS.

Another explanation for the DDS improvement could be an electronic modification of the catalyst surface. The adsorption of 2-MPiper may lead to an increase of the electron

density on the metal atoms, which, in turn, can cause an increase in the number of sulfur vacancies on the Ni-Mo-S surface or an increase in the intrinsic catalytic activity of the site. In other words, low partial pressures of 2-MPiper result in an increased number of DDS sites or in an increase in their activity. At higher concentrations of 2-MPiper, the N-compound adsorbs on more and more sites, inhibiting the total conversion of DBT.

Two other explanations seem less likely. One is that the improvement of the DDS of DBT in the presence of 2-MPiper could result from an acid-base interaction between 2-MPiper and DBT. This seems not likely, because the lone pair of the 2-MPiper is bonded to the catalyst surface and not available for an interaction with DBT. Another explanation could have been that the N-containing molecule acts a mediator, as in electrocatalytic promotion [24]. Whereas such a type of promotion would have been possible for a positive influence of 2-MPy on the HYD pathway of the HDS of DBT, it is not possible for 2-MPiper in the DDS pathway.

6.5 Conclusion

Both 2-MPy and 2M-Piper poisoned the HYD pathway of the HDS of DBT greatly, but the inhibitory influence of 2-MPiper was somewhat stronger than that of 2-MPy. The DDS route of the HDS of DBT was suppressed in the presence of 2-MPy and promoted at low partial pressures of 2-MPiper. The total conversion of DBT was also enhanced in the presence of 0.1, 0.5 and 1 kPa 2-MPiper.

The enhancement of the DDS pathway at low partial pressures of 2-MPiper can be explained in three ways: a) transformation of HYD sites into DDS sites, because the HYD site consists of several metal centres and is not completely covered after adsorption of 2-MPiper in the one-point mode; b) electronic modification of the catalyst surface, resulting in an increase of the electron density on the metal centres due to interaction with the 2-MPiper molecules that leads to an increased number of sulfur vacancies or to an increased intrinsic activity of the active site; c) interaction between 2-MPiper and DBT (acid – base interaction) when they are both adsorbed perpendicular to the catalyst surface.

6.6 References

[1] F.W. Kirsch, H. Shalit and H. Heinemann, Ind. Eng. Chem. 51 (1959) 1379.

[2] C.N. Satterfield, M. Modell and J.F. Mayer, AIChE J. 21 (1975) 1100.

[3] C.N. Satterfield, M. Modell and J.A. Wilkens, Ind. Eng. Chem. Proc. Des. Dev. 19 (1980) 154.

[4] M. Nagai, T. Sato, A and Aiba, J. Catal. 97 (1986) 52.

[5] J. Yang and F.E. Massoth, Appl. Catal. 34 (1987) 215.

[6] V. La Vopa and C.N. Satterfield, J. Catal. 110 (1988) 375.

[7] F. Gioia and F. Murena, J. Hazard. Mater. 57 (1998) 177.

[8] G.C. Laredo, J.A. De los Reyes, J.L. Cano and J.J. Castillo, Appl. Catal. A 207 (2001) 103.

[9] C. Kwak, J.J. Lee, J.S. Bae and S.H. Moon, Appl. Catal. B 35 (2001) 59.

[10] P. Zeuthen, K.G. Knudsen and D.D. Whitehurst, Catal. Today 65 (2001) 307.

[11] T. Koltai, M. Macaud, A. Guevara, E. Schulz, M. Lemaire, R. Bacaud and M. Vrinat, Appl. Catal. A 231 (2002) 253.

[12] G.C. Laredo, E. Altamirano and J.A. De los Reyes, Appl. Catal. A 243 (2003) 207.

[13] H. Kwart, J. Katzer and J. Horgan, J. Phys. Chem. 86 (1982) 2641.

[14] M. Nagai and T. Kabe, J. Catal. 81 (1983) 440.

[15] V. La Vopa and C.N. Satterfield, Chem. Eng. Commun. 70 (1988) 171.

[16] M. Nagai, Ind. Eng. Chem. Prod. Res. Dev. 24 (1985) 489.

[17] M. Nagai, Chem. Lett. 6 (1987) 1023.

[18] R. Prins, V.H.J. de Beer and G.A. Somorjai, Catal. Rev.-Sci. Eng. 31 (1989) 1.

[19] R.R. Chianelli, M. Daage and M.J. Ledoux, Adv. Catal. 40 (1994) 177.

[20] H. Topsøe, B.S. Clausen and F.E. Massoth, in ‚Catalysis: Science and Technology, Vol 11, Springer, Berlin, 1996.

[21] P. Raybaud, J. Hafner, G. Kresse, S. Kasztelan and H. Toulhoat, J. Catal. 190 (2000) 128.

[22] L.S. Byskov, J.K. Nørskov, B.S. Clausen and H. Topsøe, J. Catal. 187 (1999) 109.

[23] P. Raybaud, J. Hafner, G. Kresse, S. Kasztelan and H. Toulhoat, J. Catal. 189 (2000) 129.

[24] M.M. Baizer, H. Lund, in, Organic Electrochemistry, Marcel Dekker Journals, New York, 1983.

Chapter 7

Competitive HDS of 4,6-Dimethyldibenzothiophene, HDN of 2-Methylpyridine and Hydrogenation of Naphthalene over sulfided NiMo/γ-Al_2O_3

7.1 Introduction

Research on the purification of fuels, including desulfurization, denitrogenation and dearomatization, has become an important subject of environmental catalysis studies worldwide. The three major types of transportation fuels, gasoline, jet and diesel fuel, differ in composition and properties [1]. Diesel fuel contains the most refractory sulfur-compounds, alkylated benzothiophenes and alkylated and non-alkylated dibenzothiophenes. The sulfur content in diesel fuel is of environmental concern because, upon combustion, sulfur-containing molecules are converted to hydrocarbons and SO_x; the latter compounds not only contribute to acid rain, but also poison the catalytic converter for the treatment of exhaust emission. Reducing the contents of aromatics as well as sulfur is generally desirable with respect to the quality of diesel fuel; the reduction of aromatics increases the cetane number and generally improves combustion characteristics [2,3]. Organic nitrogen compounds are constituents of liquid fuels that contribute to harmful NO_x emissions and poison acidic catalysts. They are among the strongest inhibitors of hydrodesulfurization (HDS) [4-10]. This inhibitory effect becomes more pronounced under conditions of deep HDS when the amounts of S and N compounds are comparable.

Dibenzothiophene (DBT) and its substituted derivatives undergo HDS via two parallel pathways: i) direct desulfurization (DDS) or hydrogenolysis leading to the formation of biphenyls and ii) hydrogenation (HYD) followed by desulfurization giving first tetrahydro- and hexahydrodibenzothiophenes, which are further desulfurized to cyclohexylbenzenes and

bicyclohexyls [11-14]. DBT and 4,6-dimethyldibenzothiophene (4,6-DMDBT) are used as model S compounds in our studies, because they represent the family of the most refractory S-containing molecules in oil distillates. It is well known that, over a $NiMo/Al_2O_3$ catalyst, DBT reacts preferentially via the DDS pathway [Chapter 5], whereas 4,6-DMDBT converts mainly via the HYD pathway [15]. This is due to the strong steric hindrance of the two methyl groups in the 4 and 6 positions adjacent to the sulfur atom of DBT. The methyl substituents hinder the perpendicular one-point adsorption of the molecule on the catalyst surface that is needed for the DDS pathway of the HDS. The overall reactivity of DBT over Ni- or Co-promoted Mo/Al_2O_3 catalysts is one order of magnitude higher than that of 4,6-DMDBT [13,16,17].

The first systematic studies on simultaneous catalytic HDS and hydrodenitrogenation (HDN) were performed by Satterfield et al. [18,19]. They investigated the interaction in the HDS of thiophene and HDN of pyridine. However, when using thiophene as S-containing molecule, one cannot distinguish the DDS and HYD pathways in the HDS. In our previous work on the mutual influence of HDS and HDN we used DBT as a model S compound and 2-methylpyridine (2-MPy) and 2-methylpiperidine (2-MPiper) as N-containing molecules [Chapter 5]. Both N compounds had a strong inhibitory effect on the HYD pathway of the HDS of DBT, with 2-MPiper having a somewhat stronger effect than 2-MPy. Both N-containing molecules also inhibited the DDS pathway of the HDS of DBT, 2-MPy being a stronger inhibitor than 2-MPiper. In the work reported here we studied the influence of 2-MPy and 2-MPiper on the HDS of 4,6-DMDBT, which undergoes HDS predominantly via the HYD route, and compared the results with those obtained for the HDS of DBT. We investigated the effect of the solvent and of naphthalene on the HDS of DBT and 4,6-DMDBT. The reverse influence of S-containing molecules on the HDN of 2-MPy and 2-MPiper and on the hydrogenation of naphthalene was investigated as well.

7.2 Experimental

The $NiMo/\gamma\text{-}Al_2O_3$ catalyst contained 8 wt% Mo and 3 wt% Ni and was prepared by successive incipient wetness impregnation of $\gamma\text{-}Al_2O_3$ (Condea, pore volume 0.5 cm^3g^{-1}, specific surface area 230 m^2g^{-1}) with an aqueous solution of $(NH_4)_6Mo_7O_{24}\cdot 4H_2O$ followed by an aqueous solution of $Ni(NO_3)_2\cdot 6H_2O$ (both Aldrich). After each impregnation step the

catalyst was dried in air at ambient temperature for 4 h, then dried in an oven at 120°C for 15 h and finally calcined at 500°C for 4 h.

Reactions were carried out in continuous mode in a fixed-bed inconel reactor as described previously [Chapter 3]. The experiments were carried out at 300 and 340°C. The composition of the gas-phase feed consisted of 130 kPa toluene or decane (as solvent for the DBTs and amine), 8 kPa dodecane (as reference for DBT, 4,6-DMDBT and their derivatives in the GC analysis), 11 kPa heptane (as reference for the N-compounds in the GC analysis), 1 kPa DBT or 4,6-DMDBT, 2-10 kPa 2-MPy or 2-MPiper, 1-10 kPa naphthalene, 35 kPa H_2S and 4.8 MPa H_2. The partial pressure of H_2S in all the experiments was 35 times higher than that of DBT or 4,6-DMDBT to avoid an effect of the H_2S formed during the HDS reaction.

The reaction products were analyzed by on- and off-line gas chromatography as described earlier [Chapter 3]. Weight time was defined as $\tau = w_{cat}/n_{feed}$, where w_{cat} denotes the catalyst weight and n_{feed} the total molar flow to the reactor. The weight time (τ) was changed by varying the flow rates of the liquid and the gaseous reactants while keeping their ratio constant. The reaction was stable after 3 to 4 h; during two weeks of operation almost no deactivation of the catalyst was observed.

7.3 Results

7.3.1 HDS of 4,6-dimethyldibenzothiophene

The rate of the HDS of 4,6-DMDBT and the resulting product distribution were investigated at 300 and 340°C. 4,6-DMDBT undergoes HDS via the same reaction pathways as DBT: direct desulfurization and hydrogenation followed by desulfurization. The HYD pathway predominates at both reaction temperatures, since the amount of products obtained via this route is four to six times higher than that of 3,3'-dimethylbiphenyl formed via the DDS route (Figs. 7.1a and 7.2a).

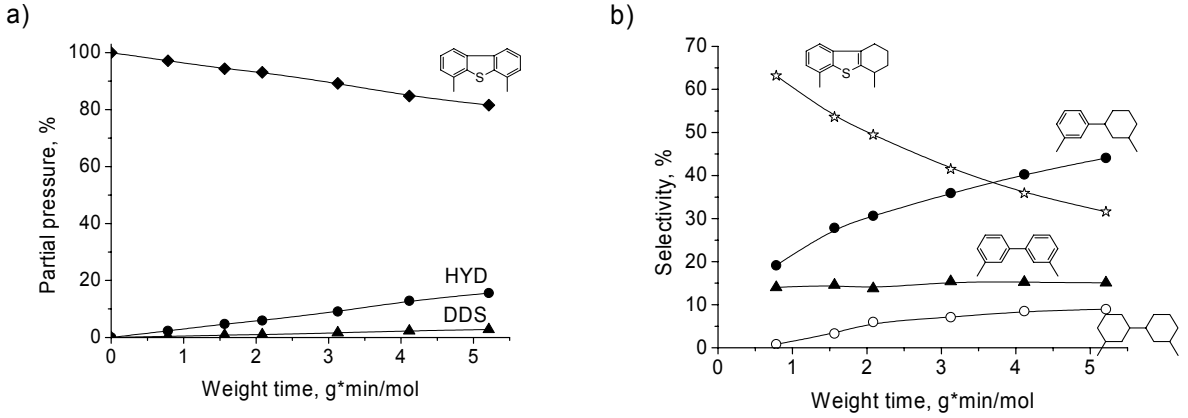

Fig. 7.1. Relative partial pressures (a) and selectivities (b) of the products of the HDS of 4,6-dimethyldibenzothiophene at 300°C as a function of weight time.

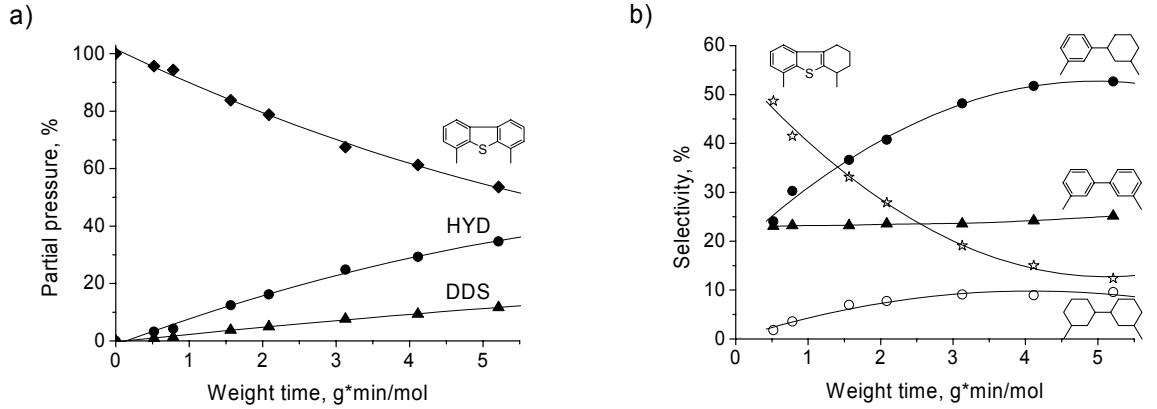

Fig. 7.2. Relative partial pressures (a) and selectivities (b) of the products of the HDS of 4,6-dimethyldibenzothiophene at 340°C as a function of weight time.

The selectivity towards 3,3'-dimethylbiphenyl formation or the DDS selectivity is 15% at 300°C and 25% at 340°C; the selectivity towards the HYD pathway is 85 and 75% respectively (Figs. 7.1b and 7.2b). The selectivity towards the formation of 3,3'-dimethylbiphenyl remains constant during the course of the reaction, showing that this product is not hydrogenated further. 4,6-Dimethyltetrahydrodibenzothiophene formed via hydrogenation of 4,6-DMDBT is desulfurized to methylcyclohexyltoluene. We consider that 3,3'-dimethylbicyclohexyl is the product of further hydrogenation of the tetrahydro-intermediate to the perhydro-intermediate and subsequent desulfurization and not the product

of the hydrogenation of methylcyclohexyltoluene; this is because the hydrogenation of the second ring in the biphenyl-like structures should be much more difficult than that of the first ring, and the latter does not occur. The perhydro-intermediate was not observed in the product, probably because of its fast conversion and thus low concentration. Therefore, the overall reaction network of the HDS of 4,6-DMDBT is as shown in Scheme 7.1.

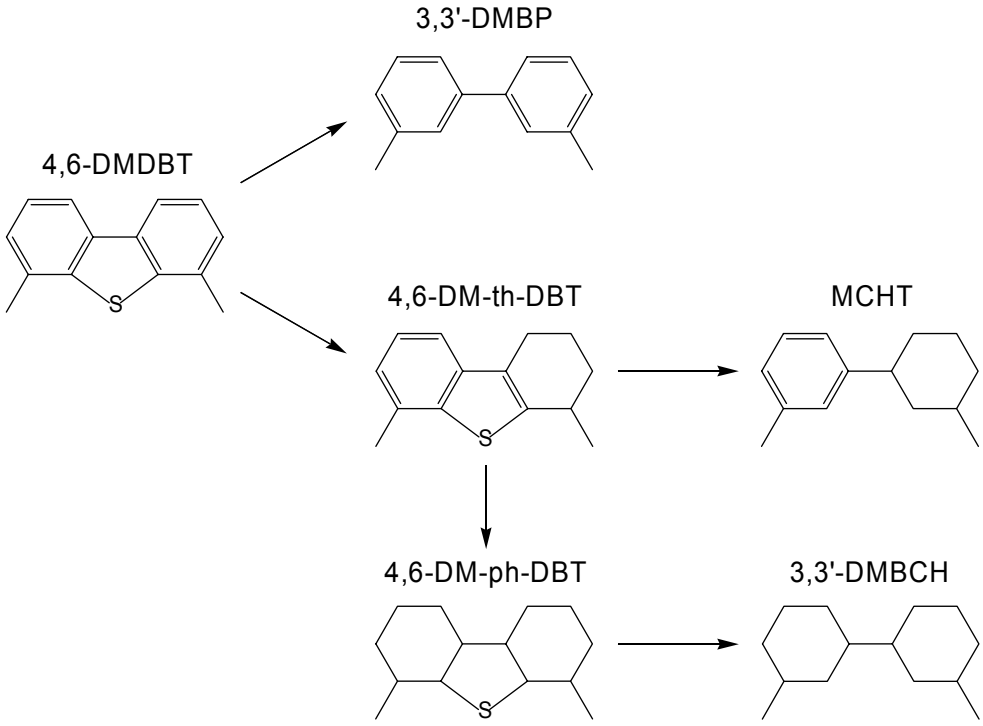

Scheme 7.1. Reaction network of the HDS of 4,6-dimethyldibenzothiophene.

7.3.2 Influence of N-containing molecules on HDS

The effect of the N compounds on the HDS of 4,6-DMDBT was studied at 340°C, where the conversion of 4,6-DMDBT was high enough to observe inhibitory effects. 2-MPy and 2-MPiper were used as model N-containing molecules since it was shown previously that the presence of the methyl group on the α-carbon atom of pyridine strongly suppresses the unwanted side reaction of disproportionation, which usually takes place in the HDN of pyridine and piperidine [Chapter 4].

The results of competitive experiments performed at 2 and 6 kPa 2-MPy and 2-MPiper are shown in Figs. 7.3a and 7.3b. Both N-containing molecules strongly inhibit the overall HDS of 4,6-DMDBT. Already at 2 kPa 2-MPy or 2-MPiper, the conversion of 4,6-DMDBT decreased by a factor of 5 to 6, and at 6 kPa 2-MPy or 2-MPiper, the conversion of 4,6-DMDBT hardly reached 4% at τ = 5 g·min/mol. The inhibitory effects of 2-MPy and 2-MPiper are almost the same (Figs. 7.3a and 7.3b).

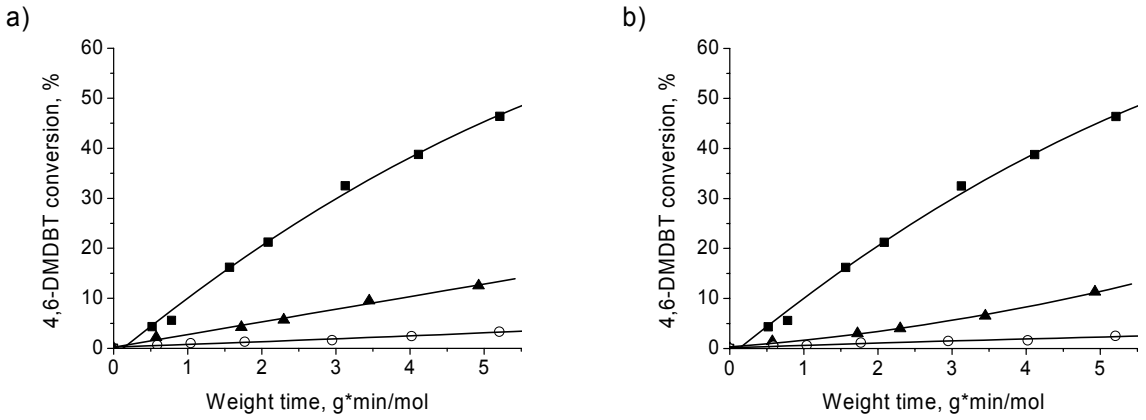

Fig. 7.3. Inhibition of the HDS of 4,6-DMDBT in the presence of 2-methylpyridine (a) and 2-methylpiperidine (b) at 340°C. HDS of 4,6-DMDBT alone(■), in the presence of 2 kPa (▲) and 6 kPa (○) N-compounds.

Also the product distribution was almost identical; therefore, only the results of 2-MPiper are presented in Figs. 7.4a and 7.4b. The selectivity of the DDS pathway in the HDS of 4,6-DMDBT increased in the presence of the N-containing molecules from 25 to 35% at 2 kPa 2-MPy or 2-MPiper and to 45% at 6 kPa 2-MPy or 2-MPiper, but the HYD route still remained the major pathway. However, at 6 kPa 2-MPy and 2-MPiper, the only product of the HYD route is the partially hydrogenated 4,6-dimethyltetrahydrodibenzothiophene. At 2 kPa of 2-MPy or 2-MPiper, this compound is the main HYD product. The character of the selectivity curve of 4,6-dimethyltetrahydrodibenzothiophene (Fig. 7.4a) shows that when the N compounds are converted this intermediate can react further. Sulfur removal is, thus, strongly suppressed in the presence of N-containing molecules.

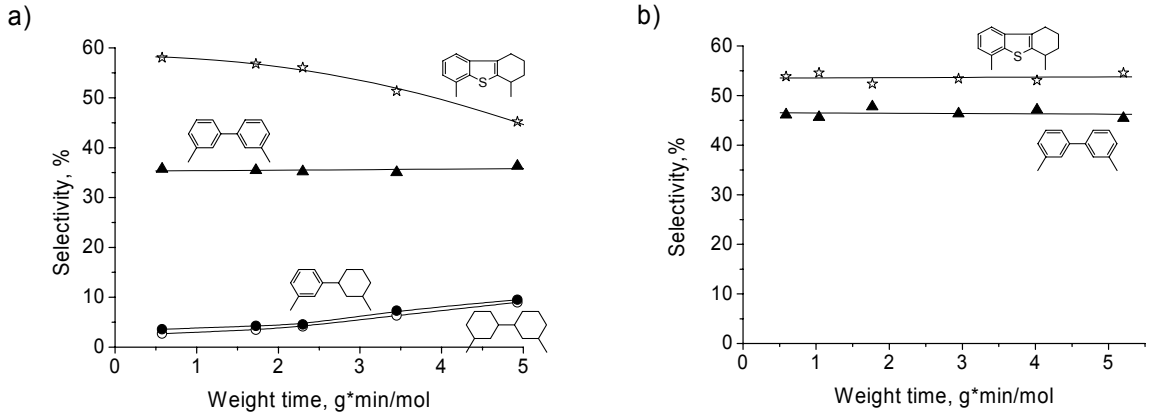

Fig. 7.4. Product distribution in the HDS of 4,6-DMDBT at 340°C in the presence of 2 kPa (a) and 6 kPa (b) of 2-MPiper.

7.3.3 Influence of S-containing molecules on HDN

The influence of DBT and 4,6-DMDBT on the HDN of 2-MPy and 2-MPiper was studied at 340°C. The HDN network of 2-MPy and 2-MPiper was determined earlier [Chapter 4] (Scheme 7.2). 2-MPiper is the primary product in the HDN of 2-MPy, since the cleavage of the C-N bond in heterocyclic N-containing aromatic molecules can only occur after ring hydrogenation [20]. We found previously that the first C-N bond breaking in 2-MPiper occurs predominantly between the nitrogen atom and the carbon atom of the methylene group and that the methyl group has a negative rather than a positive influence on the C-N bond breaking [Chapter 4].

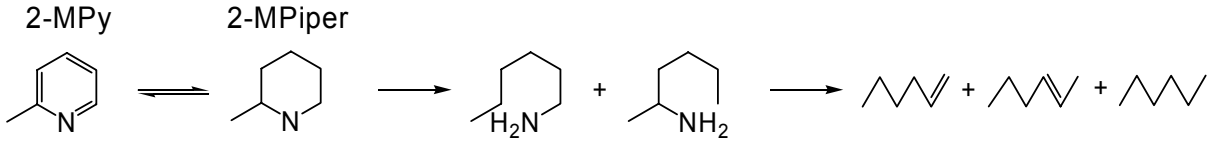

Scheme 7.2. Reaction network of the HDN of 2-methylpyridine and 2-methylpiperidine.

In the presence of 1 kPa 4,6-DMDBT, the conversion of 6 kPa 2-MPy and the yield of 2-MPiper decreased, while the amount of C_6 products (hexane, hexenes and hexylamines) increased slightly (Fig. 7.5). No changes were observed in the HDN of 2-MPiper in the

presence of 4,6-DMDBT, neither in the conversion of 2-MPiper, nor in the formation of C_6 products (Fig. 7.6). The effect of 4,6-DMDBT on the HDN of 2-MPy and 2-MPiper was, thus, identical to that of DBT [Chapter 5]. Hence, both S-containing molecules have an inhibitory effect on the hydrogenation of 2-MPy and no effect on the C-N bond cleavage in 2-MPiper.

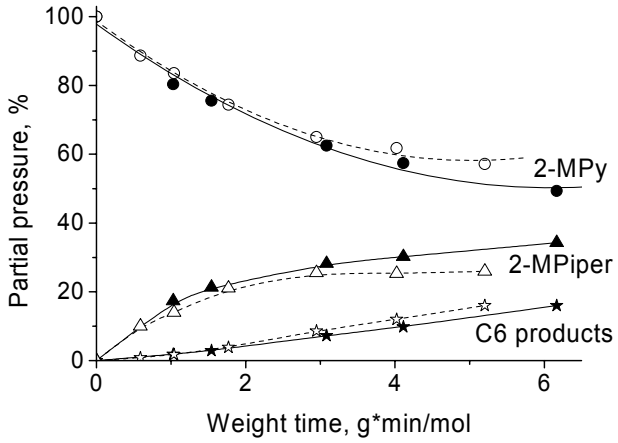

Fig. 7.5. HDN of 6 kPa 2-MPy at 340°C in the presence (----) and absence (——) of 1 kPa 4,6-DMDBT.

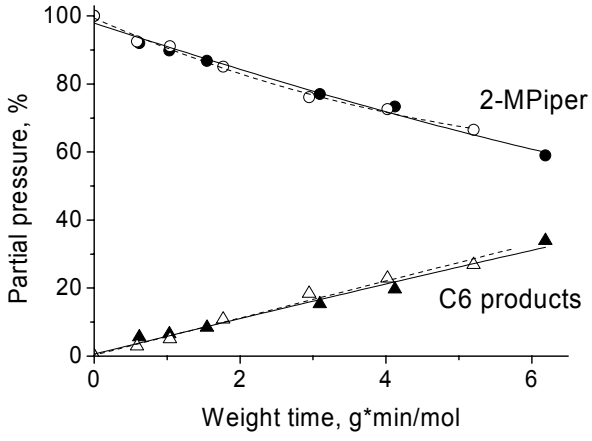

Fig. 7.6. HDN of 6 kPa 2-MPiper at 340°C in the presence (----) and absence (——) of 1 kPa 4,6-DMDBT.

7.3.4 Effect of solvent on HDS

Toluene was the solvent in most of our HDS reactions, since the solubility of DBT and 4,6-DMDBT is much better in an aromatic solvent. However, aromatic molecules may compete with the S-containing reactant for the active sites on the catalyst surface. In order to determine whether the solvent had any effect on the HDS conversion we also performed HDS experiments of DBT and 4,6-DMDBT in decane. The results show that the conversions of both DBT (Fig. 7.7a) and 4,6-DMDBT (Fig. 7.7b) are the same in toluene and decane at 340°C. The product distribution was also the same. Therefore, we conclude that the use of toluene as a solvent does not influence the HDS reactions of DBT and 4,6-DMDBT at 340°C. Toluene itself did not undergo hydrogenation when S- or N-containing molecules were present in the feed.

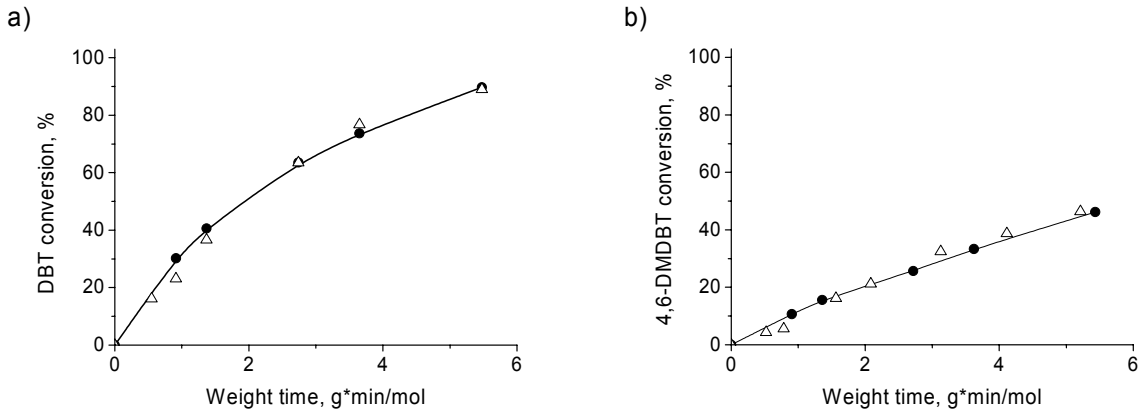

Fig. 7.7. Effect of the solvent on the HDS of DBT (a) and 4,6-DMDBT (b) at 340°C in decane (●) and toluene (Δ).

7.3.5 Effect of naphthalene on HDS

The effect of naphthalene on the HDS of DBT and 4,6-DMDBT was studied at 340°C. Naphthalene was used to study the effect of condensed aromatics on HDS. Already at 1 kPa naphthalene the conversion of DBT decreased slightly and at 10 kPa naphthalene by 10%

(Fig. 7.8a); the product distribution remained the same however. The inhibitory effect of 10 kPa naphthalene was stronger in the HDS of 4,6-DMDBT than in the HDS of DBT. The initial rate of the HDS of 4,6-DMDBT decreased by a factor of 1.8, whereas that of DBT was affected by a factor of 1.34 at 10 kPa naphthalene (cf. Figs. 7.8a and 7.8b). The selectivities in the HDS of 4,6-DMDBT were not influenced by the presence of naphthalene. Thus, naphthalene affected the DDS and the HYD pathways of the HDS of both S-containing molecules to the same extent. The inhibitory effect of naphthalene was much weaker than that of the N-containing molecules.

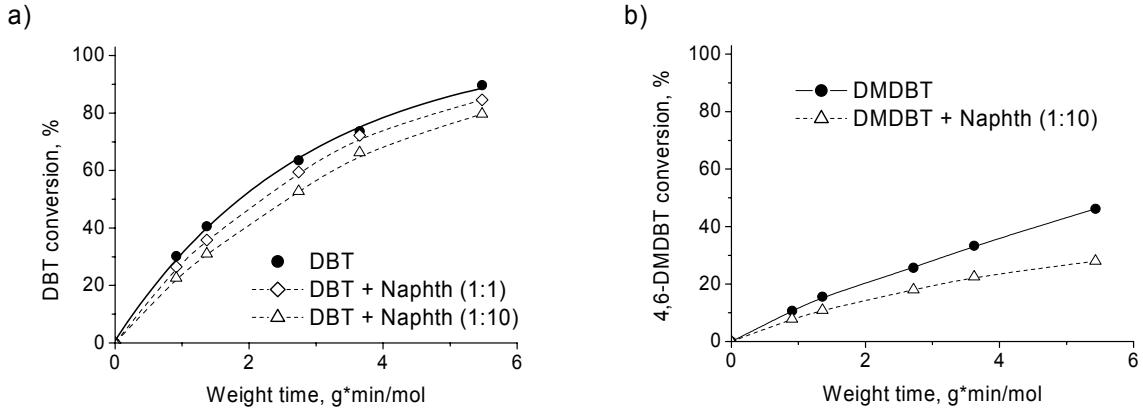

Fig. 7.8. Inhibition of the HDS of DBT (a) and 4,6-DMDBT (b) in the presence of naphthalene at 340°C.

7.3.6 Influence of S-containing molecules on hydrogenation

The effects of the S-containing molecules on the hydrogenation of naphthalene are presented in Fig. 7.9. At a partial pressure of 1 kPa, DBT and 4,6-DMDBT inhibited the hydrogenation of 10 kPa naphthalene equally strongly. The partial pressure of hydrogen sulfide in these experiments was kept high to avoid an effect of H_2S formed during the HDS reaction. Under the conditions of our study (5 MPa total pressure and 340°C) naphthalene is mainly converted to tetralin over $NiMo/Al_2O_3$. Further hydrogenation took place extremely slowly, as demonstrated by the negligible amounts of decalin: at 75% conversion of naphthalene the sum of *cis*-decalin and *trans*-decalin was only 1%.

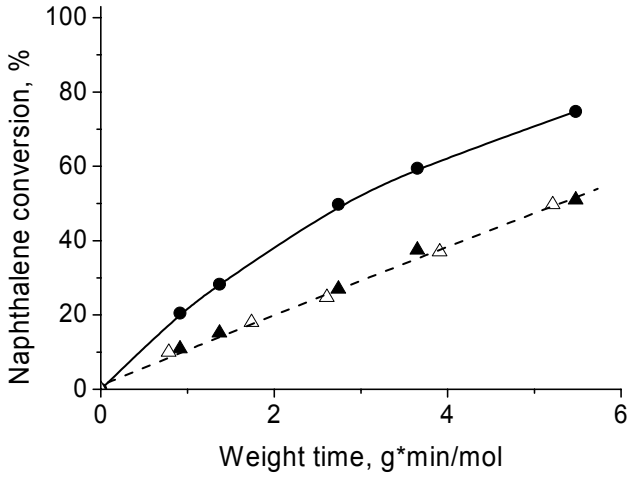

Fig. 7.9. Hydrogenation of 10 kPa naphthalene to tetralin at 340°C and in the presence (----) and absence (——) of 1 kPa DBT (▲) or 4,6-DMDBT (Δ).

7.4 Discussion

The aim of the present study was to compare the influence of N-containing molecules and aromatics on the HDS of DBT and 4,6-DMDBT in order to gain insight into the nature of the DDS and HYD active sites. The main difference between the HDS of DBT and 4,6-DMDBT is that DBT reacts predominantly via the DDS pathway and 4,6-DMDBT mainly via the HYD route. Thus, the selectivities for the DDS and HYD pathways in the HDS of DBT were 85 and 15% at 300°C and 90 and 10% at 340°C respectively [Chapter 5]. The product distribution showed that slow hydrogenation of biphenyl to cyclohexylbenzene took place, since the selectivity towards biphenyl formation decreased with weight time and the increase in the cyclohexylbenzene selectivity with weight time was higher than the decrease in the tetrahydrodibenzothiophene selectivity (Fig. 7.10). Therefore, the overall HDS network of DBT is as shown in Scheme 7.3.

In the HDS of 4,6-DMDBT, the selectivities towards the DDS and HYD are 15 and 85% at 300°C and 25 and 75% at 340°C respectively (Figs. 7.1b and 7.2b). Thus, the product distribution is the reverse as in the HDS of DBT, where the DDS prevails. The further hydrogenation of 3,3'-dimethylbiphenyl to methylcyclohexyltoluene in the HDS of 4,6-

DMDBT does not take place, since the selectivity towards the formation of 3,3'-dimethylbiphenyl remained constant during the reaction. Temperature has a stronger promotional effect on the direct sulfur removal from both DBT and 4,6-DMDBT, since the DDS pathway is enhanced at 340°C compared to 300°C. Furthermore, the removal of sulfur from the partially hydrogenated intermediate improved, because the amount of 4,6-dimethyltetrahydrodibenzothiophene decreased and the amount of methylcyclohexyltoluene increased more strongly in the course of the reaction at higher temperature (cf. Figs. 7.1b and 7.2b).

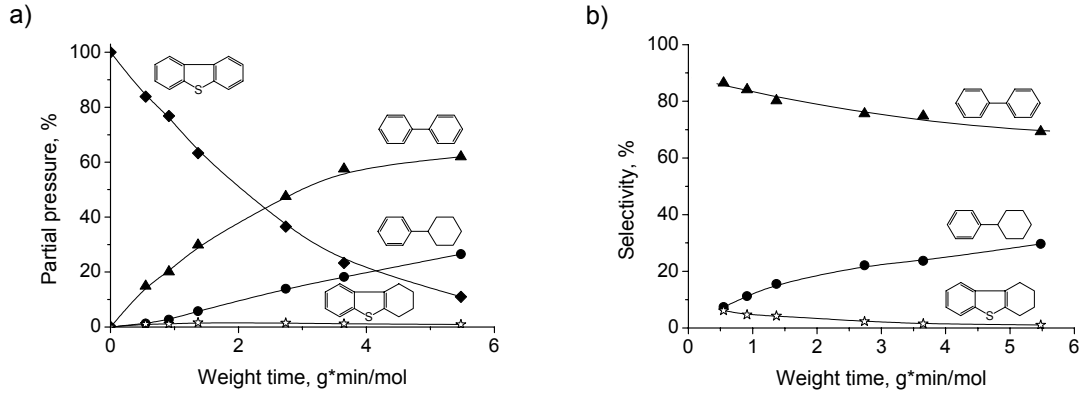

Fig. 7.10. Relative partial pressures (a) and selectivities (b) of the products of the HDS of dibenzothiophene at 340°C as a function of weight time.

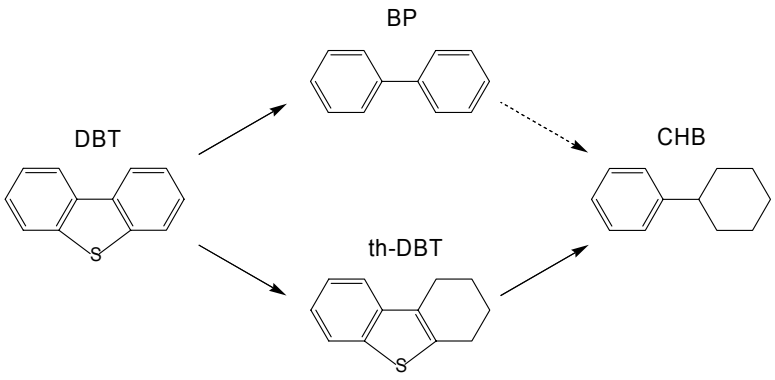

Scheme 7.3. Reaction network of the HDS of dibenzothiophene.

The HDS of DBT and 4,6-DMDBT can be well described as pseudo-first order reactions with respect to the reactant, in good agreement with the literature [21-24]. The kinetic results at 300 and 340°C show that the overall HDS of DBT is about three times faster than that of 4,6-DMDBT (Table 7.1). This value is somewhat smaller than the values of 5 to 6 [16,25,26] and 10 [13] reported in the literature. This can be explained by the high partial pressure of H_2S in our experiments to avoid the influence of H_2S released during HDS. Because hydrogen sulfide inhibits the HYD pathway to a lesser extent than the DDS pathway [17] and since HYD is the main route for the transformation of 4,6-DMDBT, the HDS of this molecule is less affected in the presence of H_2S. We also conclude from the data in Table 7.1 that the DDS of 4,6-DMDBT is 12 to 17 times slower than that of DBT. However, the HYD pathway of 4,6-DMDBT is two times faster than that of DBT. This must be due to the positive influence of the two methyl groups on the hydrogenation of an aromatic ring. Meille et al. observed a higher reactivity in the HDS of 2,8-DMDBT than in the HDS of DBT [16] and proposed an analogy with the hydrogenation of aromatics: toluene is more easily hydrogenated than benzene [27] and 3-methylbiphenyl more easily than biphenyl over metal sulfide catalysts [28]. In agreement with this explanation, we found that the hydrogenation of 3,3'-dimethylbiphenyl at 340°C was two times faster than that of biphenyl over the $NiMo/Al_2O_3$ catalyst.

Table 7.1. Rate constants of the DDS and HYD pathways in the HDS of DBT and 4,6-DMDBT at 300 and 340°C

	300°C		340°C	
	k_{DDS}	k_{HYD}	k_{DDS}	k_{HYD}
DBT	0.102	0.018	0.35	0.04
4,6-DMDBT	0.006	0.033	0.03	0.09

Although the HYD pathway is faster in the HDS of 4,6-DMDBT, the removal of sulfur from 4,6-dimethyltetrahydrodibenzothiophene takes place much slower than from tetrahydrodibenzothiophene, since the selectivity towards the formation of this intermediate is much higher in the HDS of 4,6-DMDBT than in that of DBT (cf. Figs. 7.2b and 7.10b). This means that the two methyl groups in the 4 and 6 positions not only sterically hinder the sulfur removal in the DDS but also in the HYD pathway. 4,6-DMDBT has a flat structure like DBT. The methyl groups adjacent to the sulfur atom are more spacious than the σ orbitals on the sulfur atom and hinder the molecule to approach the catalyst surface via the sulfur atom.

Therefore, the adsorption of 4,6-DMDBT in the σ mode is weaker than that of DBT. When two double bonds of one benzene ring are hydrogenated, the hydrogenated part of the molecule is not flat any more (Scheme 7.4). The methyl group of the hydrogenated ring does not have to affect the adsorption because it can be turned away from the catalyst surface. However, the partially hydrogenated ring is puckered and one methylene group is under and one above the plane of the molecule. As a consequence, one of the hydrogen atom, at the carbon atom below the plane, hinders the adsorption. When a methyl group is present in the partially hydrogenated ring the structure is more rigid and the hydrogen of the methylene group extends further towards the catalyst surface. Therefore, the molecule is tilted on the surface and the adsorption of 4,6-dimethyltetrahydrodibenzothiophene is weaker than that of tetrahydrodibenzothiophene. Because of the resulting longer lifetime of 4,6-dimethyltetrahydrodibenzothiophene than of tetrahydrodibenzothiophene, the hydrogenation of the second benzene ring attains importance and 3,3'-dimethylbicyclohexyl is formed.

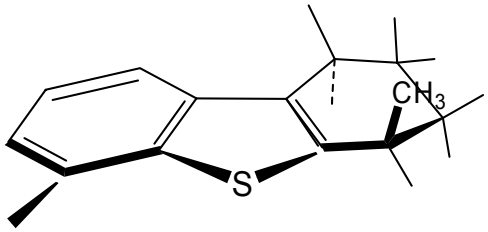

Scheme 7.4. Conformation structure of 4,6-dimethyltetrahydrodibenzothiophene.

Figure 7.11 shows that k_{HYD}, the rate constant for the HYD pathway in the HDS of DBT, strongly decreases in the presence of 2-MPy and 2-MPiper [Chapter 5]; 2-MPiper retards k_{HYD} to a somewhat greater extent than 2-MPy. The major product of the HYD pathway is tetrahydrodibenzothiophene, but even at the highest partial pressure of 6 kPa 2-MPy and 2-Mpiper the reaction of tetrahydrodibenzothiophene to cyclohexylbenzene was not totally inhibited. The DDS pathway was much less affected by 2-MPy and 2-MPiper; k_{DDS} was hardly affected at 2 kPa 2-MPiper and only slightly at 2 kPa 2-MPy (Fig. 7.11). Since the HYD pathway was strongly inhibited already at low partial pressures of the N compounds and the total conversion changed slightly, the formation of biphenyl was enhanced. This enhancement resulted from the larger amount of DBT available for DDS, because HYD hardly occurred. This was proven by calculations in which it was assumed that the rate

constant of the DDS pathway did not change in the presence of small amounts of 2-MPy and 2-MPiper and that the HYD pathway was completely blocked. At higher partial pressure of the N-containing molecules (6 kPa), the DDS pathway was more inhibited and 2-MPy had a stronger inhibitory effect than 2-MPiper (Fig. 7.11).

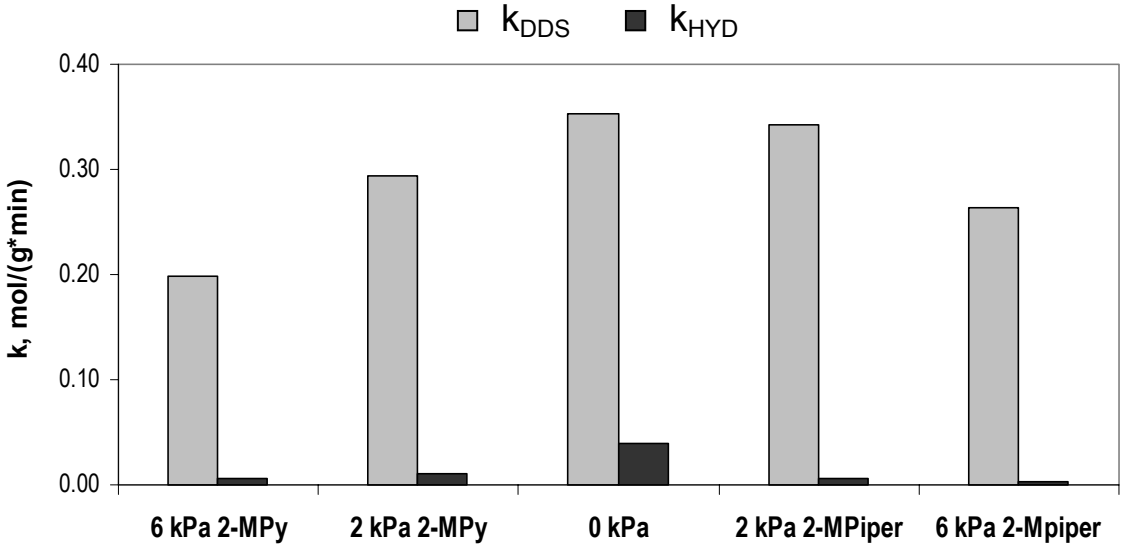

Fig. 7.11. Rate constants of the DDS and HYD pathways in the HDS of DBT at 340°C and in the presence of 2-MPy and 2-MPiper.

In the HDS of 4,6-DMDBT the difference between the effect of 2-MPy and 2-MPiper (Fig. 7.3) is less pronounced than in the case of DBT, as shown too by the rate constants of the DDS and HYD pathways (Fig. 7.12). For the HYD pathway the HDS of DBT and 4,6-DMDBT are similar: N-containing molecules have a strong inhibitory influence and the effect of 2-MPiper is slightly stronger than that of 2-MPy (cf. Figs. 7.11 and 7.12). The inhibition can be indicated by the factor k_{HYD}/k^*_{HYD}, where k_{HYD} is the rate constant of the HYD pathway in a single HDS reaction and k^*_{HYD} is the HYD rate constant in a competitive experiment. The inhibition factors for the HYD route in the presence of 2-MPy and 2-MPiper were very similar in the HDS of DBT and 4,6-DMDBT. However, in the HDS of DBT the final product of the HYD pathway, cyclohexylbenzene, was observed at all partial pressures of N-containing molecules, whereas in the HDS of 4,6-DMDBT, at 6 kPa 2-MPy and 2-MPiper, the only product of the HYD route was 4,6-dimethyltetrahydrodibenzothiophene (Fig. 7.4b). Therefore, the real desulfurization of 4,6-DMDBT in the presence of N-

compounds occurs predominantly via the DDS pathway. This indicates again the greater difficulty in the removal of sulfur from 4,6-dimethyltetrahydrodibenzothiophene than from tetrahydrodibenzothiophene. As indicated above, this difficulty may be due to the weaker adsorption of the tetrahydro-intermediate of 4,6-DMDBT than of DBT. Thus, this intermediate can hardly compete with the N-containing molecules for the active site. The DDS of 4,6-DMDBT was suppressed to a greater extent by the N compounds than that of DBT (cf. Figs. 7.11 and 7.12), which results from the weaker σ adsorption of 4,6-DMDBT than of DBT. Another difference in the HDS of DBT and 4,6-DMDBT is that the product of the DDS pathway is hydrogenated further in the case of DBT and does not react in the case of 4,6-DMDBT, despite the faster hydrogenation of 3,3'-dimethylbiphenyl as compared to biphenyl.

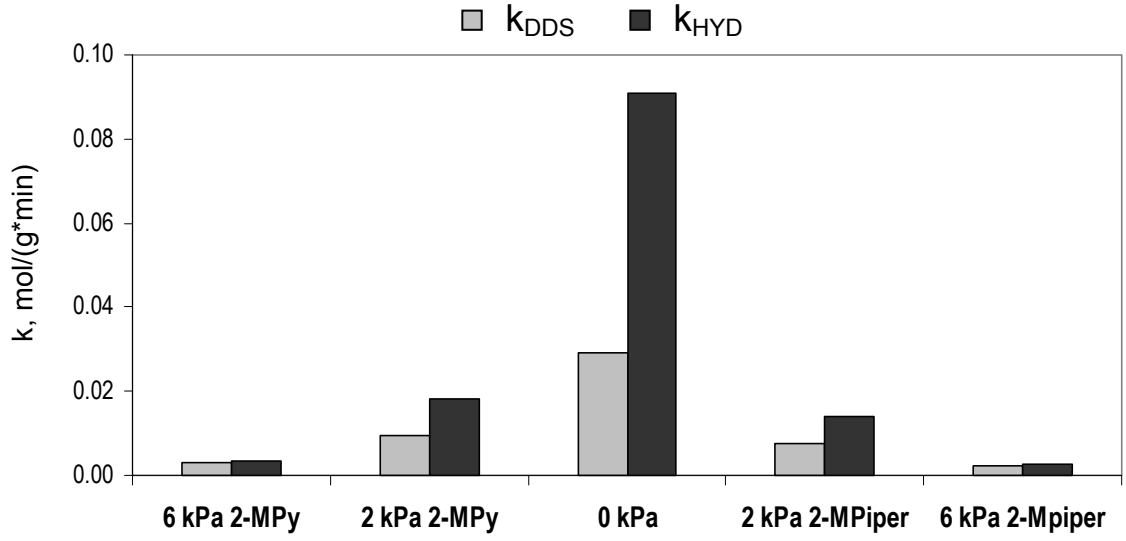

Fig. 7.12. Rate constants of the DDS and HYD pathways in the HDS of 4,6-DMDBT at 340°C and in the presence of 2-MPy and 2-MPiper.

To better understand the nature of the inhibitory influence we studied the effect of 4,6-DMDBT on the HDN reactions. 4,6-DMDBT decreases slightly the hydrogenation of 2-MPy to 2-MPiper but has no influence on the C-N bond scission, since the conversion of 2-MPiper did not change in the presence of 4,6-DMDBT (Fig. 7.6). The same results were obtained in the simultaneous HDN of 2-MPy and the HDS of DBT [Chapter 5]. Previously, we had concluded that C-N and C-S bond cleavage take place at different sites, since the DDS of

DBT and, correspondingly, the overall HDS was more strongly affected by 2-MPy, and DBT had an inhibitory effect on the hydrogenation of 2-MPy but not on the HDN of 2-MPiper. In the case of 4,6-DMDBT, however, 2-MPiper has a stronger retarding effect than 2-MPy on both DDS and HYD routes (Fig. 7.12). 4,6-DMDBT, in turn, had no influence on the C-N bond cleavage. DBT and 4,6-DMDBT can adsorb in the π mode and thus hinder the hydrogenation of 2-MPy. In the σ mode, however, the S-containing molecules adsorb apparently much weaker than 2-MPiper and therefore do not hinder the transformation of 2-MPiper.

A special case is the influence of 2-MPiper on the DDS of DBT [Chapter 6]. Up to 1 kPa 2-MPiper promotes the DDS of DBT, but does not promote the DDS of 4,6-DMDBT. This enhancement was suggested to be the result of a structural or electronic modification of the catalyst surface through the adsorption of 2-MPiper in the σ mode. Because 2-MPiper promotes the DDS of DBT at low concentrations, the overall HDS is affected only slightly [Chapter 5]. The DDS of 4,6-DMDBT is inhibited more strongly in the presence of 2 kPa 2-MPiper than that of DBT. This may be the result of the small adsorption constant of 4,6-DMDBT in the σ mode $K_{2-MPiper} \gg K^{\sigma}_{DBT} \gg K^{\sigma}_{4,6-DMDBT}$ because of the hindrance of the methyl groups. This is why the DDS of 4,6-DMDBT is not improved at low partial pressures of 2-MPiper, in contrast to the DDS of DBT. Because the adsorption of 2-MPiper is much stronger than that of the S-containing molecules, the HDN of 2-MPiper is not affected by DBT and 4,6-DMDBT.

The composition of the hydrocarbons in the feed may affect the catalytic activity and selectivity under deep HDS conditions. Aromatic hydrocarbons in fuels have a detrimental effect on the catalyst activity [29]. In a series of papers Kabe and Ishihara et al. discussed the influence of solvents on the activity and selectivity of a sulfided $CoMo/Al_2O_3$ catalyst in the HDS of benzothiophene (BT) and DBT [30-32]. They found that the catalytic activity decreased in the order toluene > decalin > n-pentadecane > 1-methylnaphthalene in the HDS of BT and in the order n-heptane > xylene > decalin > tetralin in the HDS of DBT. The activation energies were unaffected by the solvents, but the heats of adsorption of BT and DBT on the $CoMo/Al_2O_3$ catalyst depended on the solvent and correlated well with the catalytic activity. Solvents with the largest retarding effects decreased the heats of adsorption of BT and DBT to a greater extent. Furthermore, in the HDS of DBT the solvent mainly affected the conversion to biphenyl, whereas it hardly affected the formation of

cyclohexylbenzene [32]. According to a Langmuir-Hinshelwood model, with reactant and solvent molecules in the gas phase, the heat of adsorption of a reactant should not be affected by the presence of another molecule. However, if we assume that a solvent layer is present on the catalyst surface, then there will be an interaction between reactant and solvent molecules and the interaction energy will influence the apparent heat of adsorption. Ishihara et al. worked at rather low temperatures of 150 to 250°C, which favours the formation of a liquid layer on the catalyst surface.

We found no difference between decane and toluene in the HDS rates of DBT and 4,6-DMDBT (Fig. 7.7); the product distribution was also unaffected. Toluene did not undergo hydrogenation to methylcyclohexane when DBT or 4,6-DMDBT were present in the feed. This indicates that the adsorption of toluene is much weaker than that of the S-containing molecules. The results reported by Kabe et al. [30] indicate that the effects of the solvent are more pronounced below 300°C. At 300°C, there was hardly any difference between n-heptane and xylene, which are very similar to the solvents used in our study. Moreover, the effects of the solvent were more pronounced at 0.1 than at 1 wt% DBT in the feed [31]. Our experiments were performed at 340°C with 1.4 wt% DBT and 1.6 wt% 4,6-DMDBT. Therefore, our results do not contradict the results of Ishihara et al. At 340°C, toluene, as an aromatic molecule, does not compete with the S compounds for the active sites although there is a large excess amount of it in the feed.

Only limited information is available about the inhibition of the HDS of thiophene [5], DBT [33] and 4,6-DMDBT [9,34-37] by polycyclic aromatic compounds. Most studies indicate that the influence of aromatics on HDS is not negligible but that it is much weaker than that of basic organonitrogen compounds. Our results show that the rate constant of the HDS of DBT decreased by a factor of 1.34 and that of 4,6-DMDBT by a factor of 1.8 in the presence of 10 kPa naphthalene (Figs. 7.8a and 7.8b). Because naphthalene did not change the selectivities, the rate constants of the DDS and HYD pathways are affected to the same extent (Fig. 7.13). Farag et al. reported that a 100-fold excess of naphthalene relative to 4,6-DMDBT resulted in only slight decrease in the HYD selectivity [37]. They also mentioned, however, that the HYD/DDS ratio varied with the conversion of 4,6-DMDBT. These changes in the HYD/DDS ratios might be due to the fact that their study was carried out in an autoclave. In that case, the quantitative analysis can easily have an error of 10 to 15%. We believe that the HYD/DDS ratio stays constant within a single experiment on the HDS of 4,6-DMDBT, since the selectivity towards 3,3'-dimethylbiphenyl formation is constant in the course of the

reaction (Figs. 7.1b and 7.2b). The HYD/DDS ratio is also unaffected by the presence of naphthalene (Fig. 7.13). In the case of the HDS of DBT, biphenyl is hydrogenated further to cyclohexylbenzene. The presence of naphthalene does not change the product distribution in the HDS of DBT (Fig. 7.13).

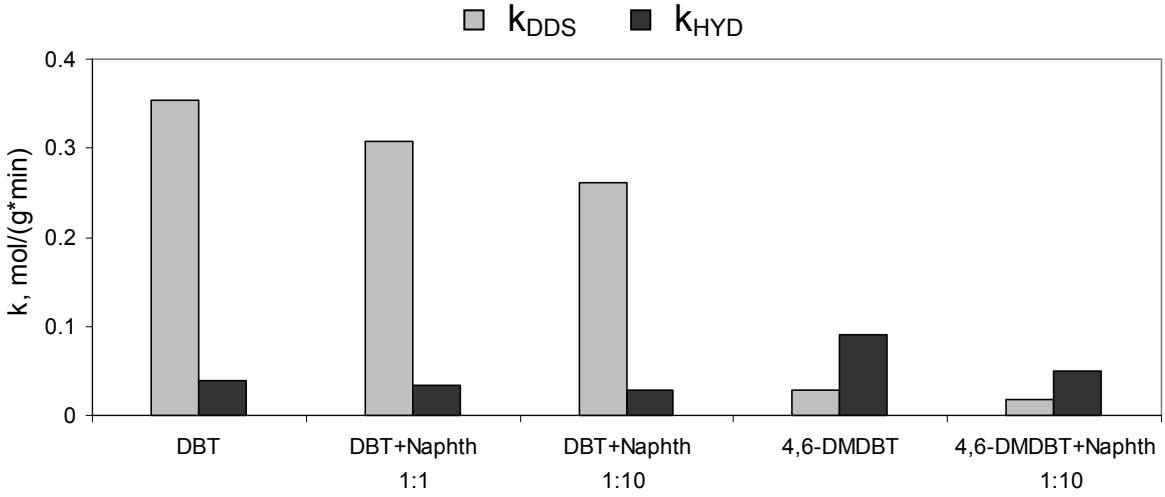

Fig. 7.13. Rate constants of the DDS and HYD pathways in the HDS of DBT and 4,6-DMDBT at 340°C and in the presence of naphthalene.

Under our reaction conditions naphthalene converts predominantly to tetralin; only small amounts of decalin were observed, in good agreement with results obtained by Isoda et al. [35,36]. The effect of S-containing molecules on the hydrogenation reaction has been studied mainly in terms of the influence of H_2S [38-40]. We investigated the effect of DBT and 4,6-DMDBT on the hydrogenation of naphthalene at a reasonably high partial pressure of H_2S in order to avoid the influence of the H_2S released during the HDS reaction. Our data indicate that hydrogenation is inhibited in the presence of S compounds and that DBT and 4,6-DMDBT have the same effect (Fig. 7.9). Both DDS and HYD pathways of the HDS of DBT and 4,6-DMDBT are affected to the same extent in the presence of naphthalene, and the hydrogenation of naphthalene is equally suppressed by DBT and 4,6-DMDBT. Thus, we conclude that the hydrogenation of naphthalene takes place at both the DDS and the HYD sites. Moreover, we assume that the DDS and the HYD sites are the same and that the only factor, which determines the HDS pathway, is the adsorption conformation of the S-

containing molecule. Kogan et al. also suggested that the HYD pathway of the HDS of thiophene takes place at the same catalytic sites as the DDS pathway [41].

7.5 Conclusion

In studying the mutual influence of the HDS of 4,6-DMDBT and HDN of 2-MPy and 2-MPiper, we found that both N-containing molecules are strong inhibitors of HDS. Moreover, the inhibitory effect of 2-MPiper was somewhat stronger than that of 2-MPy for the DDS and HYD pathways of the HDS of 4,6-DMDBT. 4,6-DMDBT and DBT suppressed the hydrogenation of 2-MPy but did not affect the C-N bond cleavage in the HDN of 2-MPiper. Therefore, we assume that adsorption of 2-MPiper on both DDS and HYD sites is much stronger than that of 4,6-DMDBT or DBT.

When toluene is used as a solvent, neither the rates of the HDS of DBT and 4,6-DMDBT nor the product distributions are affected. Toluene itself does not undergo hydrogenation in the presence of S or N compounds. Thus, the molecules of the solvent do not compete with reactant for the active sites.

Naphthalene inhibited the DDS and HYD pathways in the HDS of DBT and 4,6-DMDBT to the same extent. Thus, the hydrogenation of naphthalene takes place at both the DDS and the HYD sites. DBT and 4,6-DMDBT suppressed the hydrogenation of naphthalene to the same extent. We assume that the adsorption of naphthalene is much weaker than that of S-containing molecules.

7.6 References

[1] S. Mayo, E. Brevoord, L. Gerritsen, F. Plantenga, Hydrocarb. Process. 80 (2001) 84A.

[2] B.H. Cooper, B.B.L. Donnis, Appl. Catal. A 137 (1996) 203.

[3] C. Song, X.L. Ma, Appl. Catal. B 41 (2003) 207.

[4] M. Nagai, T. Sato, A. Aiba, J. Catal. 97 (1986) 52.

[5] V. La Vopa, C.N. Satterfield, J. Catal. 110 (1988) 375.

[6] S. Chand, Res. Ind. 39 (1994) 194.

[7] G.C. Laredo, J.A. De los Reyes, J.L. Cano, J.J. Castillo, Appl. Catal. A 207 (2001) 103.

[8] G.C. Laredo, E. Altamirano, J.A. De los Reyes, Appl. Catal. A 243 (2003) 207.

[9] T. Koltai, M. Macaud, A. Guevara, E. Schulz, M. Lemaire, R. Bacaud, M. Vrinat, Appl. Catal. A 231 (2002) 253.

[10] C. Kwak, J.J. Lee, J.S. Bae, S.H. Moon, Appl. Catal. B 35 (2001) 59.

[11] M. Houalla, N.K. Nag, A.V. Sapre, D.H. Broderick, B.C. Gates, AIChE J. 24 (1978) 1015.

[12] M.J. Girgis, B.C. Gates, Ind. Eng. Chem. Res. 30 (1991) 2021.

[13] B.C. Gates, H. Topsøe, Polyhedron 16 (1997) 3213.

[14] R. Shafi, G.J. Hutchings, Catal. Today 59 (2000) 423.

[15] D.D. Whitehurst, T. Isoda, I. Mochida, Adv. Catal. 42 (1998) 345.

[16] V. Meille, E. Schulz, M. Lemaire, M. Vrinat, J. Catal. 170 (1997) 29.

[17] F. Bataille, J.L. Lemberton, P. Michaud, G. Perot, M. Vrinat, M. Lemaire, E. Schulz, M. Breysse, S. Kasztelan, J. Catal. 191 (2000) 409.

[18] C.N. Satterfield, M. Modell, J.F. Mayer, AIChE J. 21 (1975) 1100.

[19] C.N. Satterfield, M. Modell, J.A. Wilkens, Ind. Eng. Chem. Proc. Des. Dev. 19 (1980) 154.

[20] N. Nelson, R.B. Levy, J. Catal. 58 (1979) 485.

[21] V. Vanrysselberghe, G.F. Froment, Ind. Eng. Chem. Res. 35 (1996) 3311.

[22] X.L. Ma, K. Sakanishi, I. Mochida, Ind. Eng. Chem. Res. 35 (1996) 2487.

[23] T. Kabe, K. Akamatsu, A. Ishihara, S. Otsuki, M. Godo, Q. Zhang, W.H. Qian, Ind. Eng. Chem. Res. 36 (1997) 5146.

[24] T.C. Ho, J. Catal. 219 (2003) 442.

[25] D.R. Kilanowski, H. Teeuwen, V.H.J. de Beer, B.C. Gates, G.C.A. Schuit, H. Kwart, J. Catal. 55 (1978) 129.

[26] M. Houalla, D.H. Broderick, A.V. Sapre, N.K. Nag, V.H.J. de Beer, B.C. Gates, H. Kwart, J. Catal. 61 (1980) 523.

[27] O. Weisser, S. Landa, Sulphide Catalysts , Their Properties and Applications, Pergamon Press, Oxford, 1973.

[28] V. Lamure-Meille, E. Schulz, M. Lemaire, M. Vrinat, Appl. Catal. A 131 (1995) 143.

[29] P.T. Vasudevan, J.L.G. Fierro, Catal. Rev.-Sci. Eng. 38 (1996) 161.

[30] T. Kabe, A. Ishihara, M. Nomura, T. Itoh, P.Y. Qi, Chem. Lett. (1991) 2233.

[31] A. Ishihara, T. Itoh, T. Hino, M. Nomura, P.Y. Qi, T. Kabe, J. Catal. 140 (1993) 184.

[32] A. Ishihara, T. Kabe, Ind. Eng. Chem. Res. 32 (1993) 753.

[33] M. Nagai, T. Kabe, J. Catal. 81 (1983) 440.

[34] X.L. Ma, K. Sakanishi, T. Isoda, I. Mochida, Ind. Eng. Chem. Res. 34 (1995) 748.

[35] T. Isoda, S. Nagao, X.L. Ma, Y. Korai, I. Mochida, Energy & Fuels 10 (1996) 482.

[36] T. Isoda, S. Nagao, X.L. Ma, Y. Korai, I. Mochida, Energy & Fuels 10 (1996) 487.

[37] H. Farag, K. Sakanishi, I. Mochida, D.D. Whitehurst, Energy & Fuels 13 (1999) 449.

[38] S. Gultekin, S.A. Ali, C.N. Satterfield, Ind. Eng. Chem. Proc. Des. Dev. 23 (1984) 179.

[39] D.H. Broderick, A.V. Sapre, B.C. Gates, H. Kwart, G.C.A. Schuit, J. Catal. 73 (1982) 45.

[40] A.V. Sapre, B.C. Gates, Ind. Eng. Chem. Proc. Des. Dev. 21 (1982) 86.

[41] V.M. Kogan, R.G. Gaziev, S.W. Lee, N.N. Rozhdestvenskaya, Appl. Catal. A 251 (2003) 187.

Chapter 8

Hydrodesulfurization of Dibenzothiophene and 4,6-Dimethyldibenzothiophene over Sulfided NiMo/γ-Al_2O_3, CoMo/γ-Al_2O_3 and Mo/γ-Al_2O_3 Catalysts

8.1 Introduction

To improve the hydrodesulfurization (HDS) process, it is necessary to gain a better understanding of the conversion mechanisms of various sulfur compounds. Dibenzothiophene (DBT) and 4,6-dimethyldibenzothiophenes (4,6-DMDBT) are present in gasoil and belong to the most refractory sulfur-containing molecules [1-12]. They are, therefore, often used as model sulfur compounds. DBT and alkyl-substituted DBT undergo HDS via two reaction pathways: i) direct desulfurization (DDS), which leads to the formation of biphenyls; ii) hydrogenation (HYD) yielding tetrahydro- and hexahydro-intermediates followed by desulfurization to cyclohexylbenzenes and bicyclohexyls. DBT is converted predominantly via the DDS pathway, whereas 4,6-DMDBT reacts mainly via the HYD pathway [5,8,12-14, Chapters 5 and 7]. The reactivity of 4,6-DMDBT over Co- or Ni-promoted catalysts is five to ten times smaller than that of DBT [10,12,15]. The difficulty in converting alkyl-substituted DBTs is due to the steric hindrance of alkyl groups, which are close to the sulfur atom and prevent the interaction of the sulfur atom with the active site. Kabe et al. reported that the adsorption constant of 4,6-DMDBT on the CoMo/Al_2O_3 catalyst was twice as high as that of DBT and suggested that DBTs adsorb by means of π bonding to the catalyst [6]. In this adsorption mode, the methyl groups do not hinder the adsorption of the molecule on the catalyst surface. Thus, they suggested that C-S bond scission occurs when DBT is adsorbed via the sulfur atom in the σ mode. In this case, the methyl groups hinder C-S bond scission [6]. They also reported that 4-methyltetrahydrodibenzothiophene, the hydrogenated

intermediate in the HYD pathway, is easier to desulfurize than 4-methyldibenzothiophene. In our previous work we observed that 4,6-DMDBT converts somewhat faster via the HYD route than DBT over $NiMo/Al_2O_3$ but that the desulfurization of 4,6-dimethyltetrahydrodibenzothiophene occurs much slower than that of tetrahydrodibenzothiophene [Chapter 7]. Thus, the two methyl substituents have a negative influence on the transformation of the partially hydrogenated intermediate. Further research is required to determine why the reactivity of 4,6-DMDBT is low.

A better knowledge of the catalytic sites involved in the transformation of sulfur-containing molecules may help us gain insight into the process of sulfur removal. Therefore, we studied the HDS of DBT and 4,6-DMDBT over different catalysts: sulfided $NiMo/\gamma$-Al_2O_3, $CoMo/\gamma$-Al_2O_3 and Mo/γ-Al_2O_3. Some researchers described the HDS of hindered sulfur-containing compounds over the CoMo or the NiMo catalysts [8,10,16,17], while others compared the catalysts [12,18-23]. Landau et al. found that a Co-promoted catalyst is more active in the HDS of substituted DBTs [20]. Mochida's group, on the other hand, reported that NiMo performs better than CoMo in the HDS of a gas oil [18] but is affected more strongly by aromatic compounds and H_2S [21]. Knudsen et al. studied catalysts for ultra deep HDS of diesel fuel and found that a NiMo catalyst performed well only when most of the heterocyclic compounds had been removed [23]. Thereafter, the NiMo catalyst was more active than the CoMo catalyst. At low H_2 pressures and high temperatures, a CoMo catalyst performs better than a NiMo catalyst [23]. To clarify the effect of the promoter, we carried out a detailed analysis of the HDS mechanisms of DBT and 4,6-DMDBT over sulfided CoMo, NiMo and Mo catalysts supported on alumina. The effect of H_2S was studied to gain a better understanding of the nature of the DDS and HYD sites that take part in the HDS.

8.2 Experimental

The Mo/γ-Al_2O_3, $NiMo/\gamma$-Al_2O_3 and $CoMo/\gamma$-Al_2O_3 catalysts used in this work contained 8 wt% Mo and 0 or 3 wt% promoter (Ni or Co). They were prepared by successive incipient wetness impregnation of γ-Al_2O_3 (Condea, pore volume 0.5 cm^3g^{-1}, specific surface area 230 m^2g^{-1}) with an aqueous solution of $(NH_4)_6Mo_7O_{24}\cdot 4H_2O$, followed (for the promoted catalysts) by an aqueous solution of $Ni(NO_3)_2\cdot 6H_2O$ or $Co(NO_3)_2\cdot 6H_2O$ (all Aldrich). After

each impregnation step the catalysts were dried in air at ambient temperature for 4 h and then in an oven at 120°C for 15 h and finally calcined at 500°C for 4 h.

Reactions were carried out in a continuous mode in a fixed-bed inconel reactor, as described in Chapter 3. All the experiments were performed at 340°C. The gas-phase feed consisted of 130 kPa toluene (the solvent for the DBTs), 8 kPa dodecane (the reference for DBTs and their derivatives in the GC analysis), 1 kPa DBT or 4,6-DMDBT, 0 – 100 kPa H_2S and 4.8 MPa H_2.

The reaction products were analyzed by off-line gas chromatography [Chapter 3]. Weight time was defined as $\tau = w_{cat}/n_{feed}$, where w_{cat} denotes the catalyst weight and n_{feed} the total molar flow to the reactor (1 g·min/mol = $1.8 \cdot 10^{-2}$ g·h/l). The weight time (τ) was changed by varying the flow rates of the liquid and the gaseous reactants while keeping their ratio constant. The reaction was stable after 3 to 4 h; during the two weeks of operation there was almost no deactivation of the catalyst.

8.3 Results

8.3.1 HDS of DBT over CoMo/γ-Al_2O_3

The HDS of DBT was studied at 340°C and 35 kPa H_2S over the CoMo/γ-Al_2O_3 catalyst. Fig. 8.1 shows the relative partial pressures of DBT and its products as well as the product selectivities. Four reaction products were observed: Biphenyl and cyclohexylbenzene were the final products of the DDS and HYD pathways respectively and tetrahydrodibenzothiophene and hexahydrodibenzothiophene were intermediates in the HYD pathway of the HDS (Fig. 8.1a). GC-MS showed that the tetrahydro-intermediate was 1,2,3,4-tetrahydrodibenzothiophene, with the double bond at the bridge between the partially hydrogenated 6-ring and the thiophene ring. Only trace amounts of hexahydrodibenzothiophene were detected; its relative partial pressure did not exceed 0.5% and its selectivity was 1.5% at the lowest weight time, decreasing to 0.14% at the highest weight time (values not plotted in Fig. 8.1).

The product distribution (Fig. 8.1b) shows that the selectivity of biphenyl formation, that is the selectivity for the DDS pathway, is 70% and remains constant during the reaction.

This indicates that hydrogenation of biphenyl to cyclohexylbenzene does not take place over the CoMo catalyst. The selectivity towards the formation of tetrahydrodibenzothiophene was rather low, 6% at the lowest and 0.45% at the highest weight time. This shows that this intermediate is quickly converted.

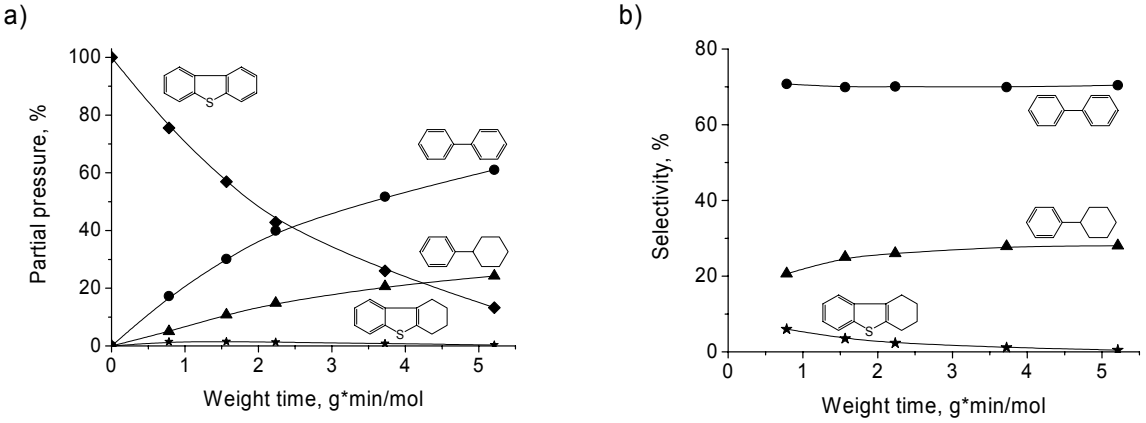

Fig. 8.1. Relative partial pressures (a) and selectivities (b) of the products in the HDS of dibenzothiophene at 340°C and 35 kPa H_2S over CoMo/γ-Al_2O_3 as a function of weight time.

8.3.2 HDS of DBT over Mo/γ-Al_2O_3

Fig. 8.2 shows the relative partial pressures and product selectivities in the HDS of DBT over Mo/γ-Al_2O_3 at 340°C and 35 kPa H_2S. The overall conversion was much lower over Mo than over CoMo and the product distribution was completely different. In contrast to the CoMo (Fig. 8.1a) and NiMo catalysts [Chapter 5], Mo/γ-Al_2O_3 mainly catalyzed the HYD pathway (Fig. 8.2a). Biphenyl, the product of the DDS pathway, was detected in much smaller amounts over the Mo catalyst than over the CoMo catalyst. The HYD curve represents the sum of all the hydrogenation products (1,2,3,4-tetrahydrodibenzothiophene, hexahydrodibenzothiophene, cyclohexylbenzene and bicyclohexyl) (Fig. 8.2a). The presence of bicyclohexyl is typical of Mo/γ-Al_2O_3 (Fig. 8.2b). This product was not observed at all over the NiMo and CoMo catalysts.

The selectivity towards biphenyl formation (DDS selectivity) approached 35 % at low weight time and decreased to 25 % at higher weight time (Fig. 8.2b). This indicates that biphenyl is hydrogenated to cyclohexylbenzene during the HDS reaction. Up to a weight time of 4 g·min/mol, the main reaction product is tetrahydrodibenzothiophene, the intermediate in the HYD pathway (Fig. 8.2b). The yield of hexahydrodibenzothiophene was about 3 to 22 times higher in the presence of the Mo catalyst than in the presence of the CoMo catalyst. Thus, the removal of sulfur from partially hydrogenated intermediates is more difficult over the Mo/γ-Al_2O_3 catalyst.

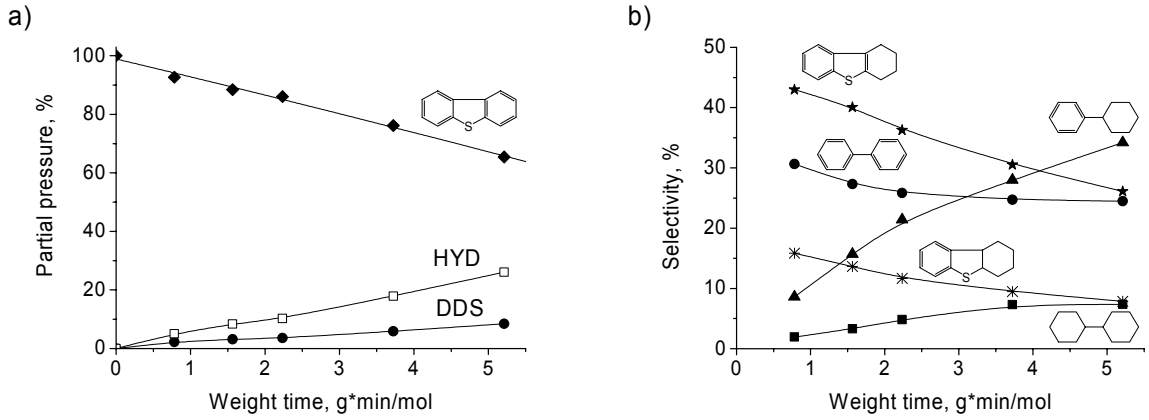

Fig. 8.2. Relative partial pressures (a) and selectivities (b) of the products in the HDS of dibenzothiophene at 340°C and 35 kPa H_2S over Mo/γ-Al_2O_3 as a function of weight time.

8.3.3 HDS of 4,6-DMDBT over CoMo/γ-Al_2O_3

Fig. 8.3 shows the results of the HDS of 4,6-DMDBT over the CoMo/γ-Al_2O_3 catalyst at 340°C and 35 kPa H_2S. 3,3'-Dimethylbiphenyl was the product of the DDS route and 4,6-dimethyltetrahydrodibenzothiophene, 1-methyl-3-(2-methylphenyl)cyclohexane (which we will refer to as methylcyclohexyl-toluene) and 3,3'-dimethylbicyclohexyl were the products of the HYD pathway. The results of the GC-MS analysis showed that the tetrahydro-intermediate was 4,6-dimethyl-1,2,3,4-tetrahydrodibenzothiophene. The conversion via the

HYD route was much higher than that via the DDS pathway (Fig. 8.3a), and the total conversion was much smaller than that of DBT (cf. Figs. 8.1a and 8.3a).

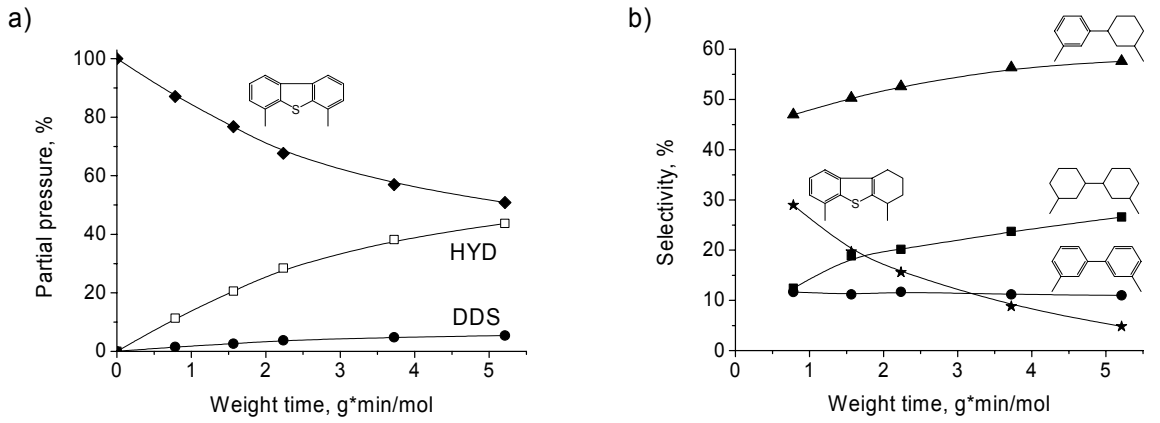

Fig. 8.3. Relative partial pressures (a) and selectivities (b) of the products in the HDS of 4,6-dimethyldibenzothiophene at 340°C and 35 kPa H_2S over CoMo/γ-Al_2O_3 as a function of weight time.

The selectivity towards the formation of 3,3'-dimethylbiphenyl (DDS selectivity) was only 12 % and remained constant during the reaction (Fig. 8.3b). Therefore, the product of the DDS pathway is not hydrogenated further. The main reaction product is methylcyclohexyl-toluene even at the lowest weight time, and 3,3'-dimethylbicyclohexyl is the second most abundant product at $\tau \geq 1.7$ g·min/mol (Fig. 8.3b). The yield of the partially hydrogenated intermediate, 4,6-dimethyltetrahydrodibenzothiophene, is higher than that of tetrahydrodibenzothiophene in the HDS of DBT. Therefore, the methyl groups at the carbon atoms adjacent to the sulfur atom suppress not only the DDS of 4,6-DMDBT, but also the desulfurization via the HYD pathway.

8.3.4 HDS of 4,6-DMDBT over Mo/γ-Al_2O_3

The Mo/γ-Al_2O_3 catalyst was only slightly less active in the HDS of 4,6-DMDBT than in the HDS of DBT under the same reaction conditions (340°C and 35 kPa H_2S) (cf. Figs. 8.2a and 8.4a). This behavior is different than that of CoMo, for which the transformation of 4,6-DMDBT was much more difficult than that of DBT. As for the CoMo catalyst, the

products observed over the Mo catalyst were 3,3'-dimethylbiphenyl, formed via the DDS pathway, and 4,6-dimethyl-1,2,3,4-tetrahydrodibenzothiophene, methylcyclohexyl-toluene and 3,3'-dimethylbicyclohexyl, obtained via the HYD pathway. On the Mo catalyst the HYD conversions of DBT and 4,6-DMDBT were almost the same, while the DDS conversion of 4,6-DMDBT was somewhat lower than that of DBT (cf. Figs. 8.2a and 8.4a).

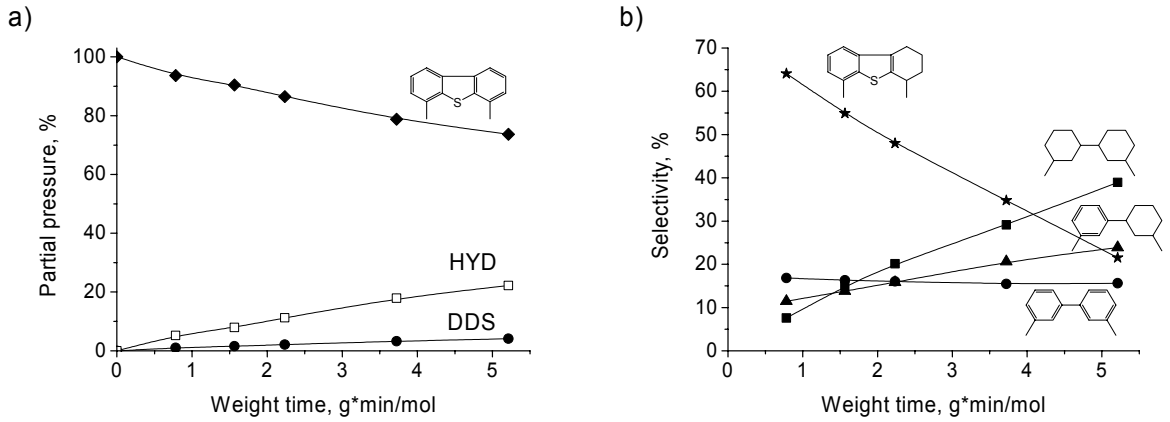

Fig. 8.4. Relative partial pressures (a) and selectivities (b) of the products in the HDS of 4,6-dimethyldibenzothiophene at 340°C and 35 kPa H_2S over Mo/γ-Al_2O_3 as a function of weight time.

The selectivity towards 3,3'-dimethylbiphenyl formation (DDS selectivity) is 16% during the whole reaction (Fig. 8.4b), somewhat higher than over the CoMo catalyst (12 %). However, the yield of 3,3'-dimethylbiphenyl was higher over the CoMo catalyst because of the higher conversion of the reactant. 4,6-Dimethyltetrahydrodibenzothiophene is the main reaction product up to τ = 4 g·min/mol (Fig. 8.4b). This indicates that, also in the case of the HDS of 4,6-DMDBT over Mo/γ-Al_2O_3, the sulfur removal from the partially hydrogenated molecule is quite difficult (cf. Figs. 8.2b and 8.4b) and is strongly suppressed compared to the Co-promoted catalyst (cf. Figs. 8.3b and 8.4b). The main desulfurized product of the HDS of 4,6-DMDBT over the Mo catalyst was 3,3'-dimethylbicyclohexyl.

8.3.5 Effect of H_2S on the HDS of DBT and 4,6-DMDBT

The effect of different partial pressures (0, 10, 35 and 100 kPa) of hydrogen sulfide on the HDS of DBT and 4,6-DMDBT was studied over all three catalysts: NiMo/γ-Al_2O_3, CoMo/γ-Al_2O_3 and Mo/γ-Al_2O_3. Over NiMo/γ-Al_2O_3 the HDS of DBT was extremely fast in the absence of H_2S and reached 100% conversion already at τ = 1.5 g·min/mol. Over CoMo/γ-Al_2O_3 the same conversion was reached at τ = 2.3 g·min/mol and over the Mo/γ-Al_2O_3 catalyst the conversion of DBT was only 55% at τ = 3.7 g·min/mol.

H_2S strongly inhibited the conversion of DBT over all three catalysts. At 100 kPa H_2S and τ = 3.7 min/mol the conversion of DBT reached 60% over NiMo, 53% over CoMo and 24% over the Mo catalyst. The conversion of DBT and 4,6-DMDBT is well described by first-order kinetics. Fig. 8.5 gives the rate constants of the total conversion of DBT (k_{tot}) for the three catalysts at different partial pressures of H_2S (grey bars in the diagram). In the absence of H_2S, the rate of total DBT conversion was almost ten times higher over the NiMo catalyst and six times higher over the CoMo catalyst than over the Mo catalyst. This is in good agreement with published results [10,15]. These k_{tot} ratios hardly changed in the presence of 10 kPa H_2S. However, at 35 kPa H_2S, the NiMo catalyst performed only five times faster and the CoMo catalyst four times faster than the Mo catalyst. On the other hand, at 100 kPa H_2S the NiMo catalyst was three times and the CoMo catalyst only two times more active than the Mo catalyst (Figs. 8.5a-c). The inhibition factor for the overall conversion of DBT in the presence of H_2S can be expressed as the ratio of the rate constants in the absence ($k_{tot}^{H_2}$) and presence of H_2S ($k_{tot}^{H_2S}$). The ratios $k_{tot}^{H_2}/k_{tot}^{H_2S}$ for the different catalysts and for different partial pressures of H_2S (Table 8.1) indicate that H_2S inhibits the HDS of DBT more strongly over the NiMo and CoMo catalysts than over Mo.

Table 8.1. Relative kinetic parameters in the HDS of DBT over NiMo/γ-Al_2O_3, CoMo/γ-Al_2O_3 and Mo/γ-Al_2O_3 at 340°C and different H_2S partial pressures.

H_2S, kPa	NiMo/γ-Al_2O_3		CoMo/γ-Al_2O_3		Mo/γ-Al_2O_3	
	$k_{tot}^{H_2}/k_{tot}^{H_2S}$	k_{DDS}/k_{DESULF}^{HYD}	$k_{tot}^{H_2}/k_{tot}^{H_2S}$	k_{DDS}/k_{DESULF}^{HYD}	$k_{tot}^{H_2}/k_{tot}^{H_2S}$	k_{DDS}/k_{DESULF}^{HYD}
0	1	0.06	1	0.05	1	0.04
10	2.2	0.06	3.4	0.04	2.9	0.04
35	6.0	0.06	3.9	0.05	3.0	0.04
100	9.3	0.06	7.1	0.04	3.2	0.05

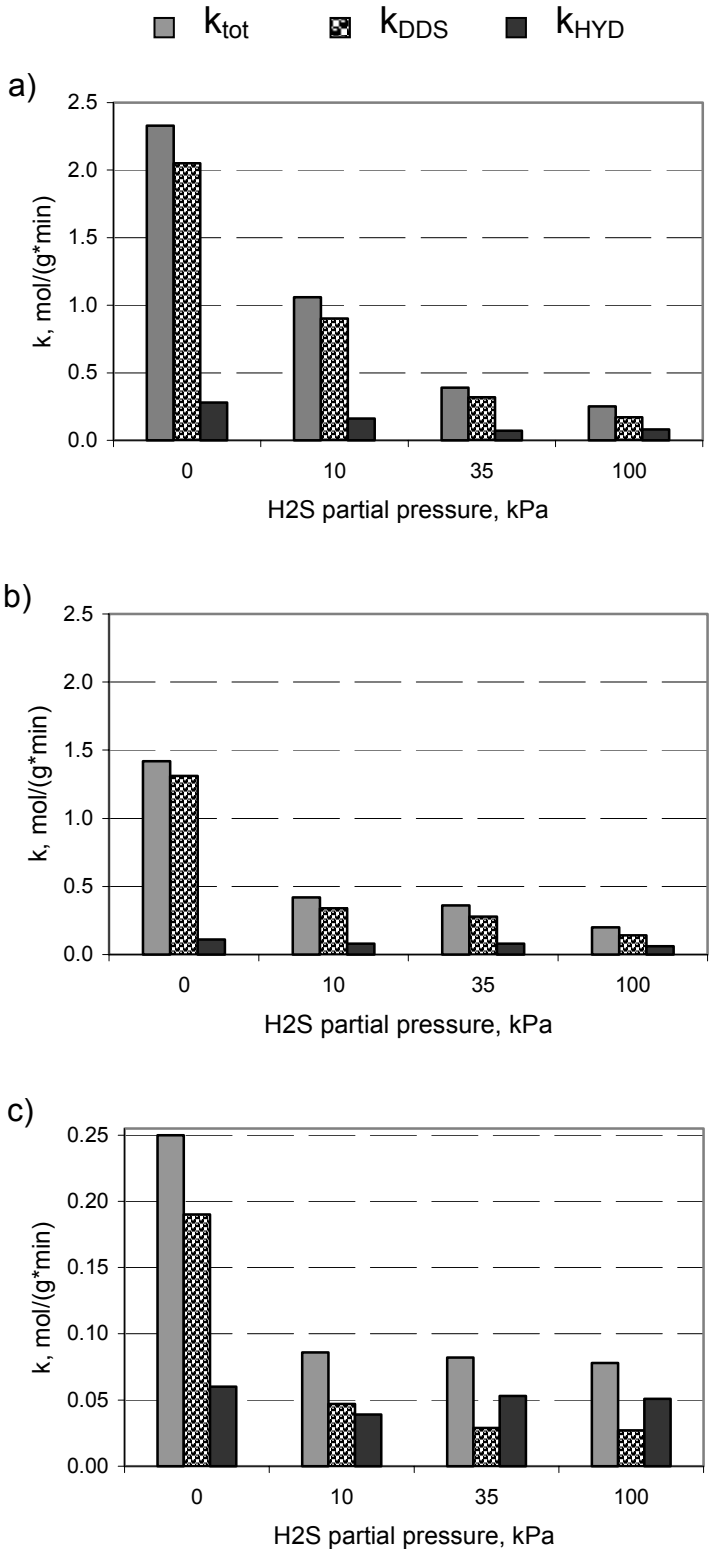

Fig. 8.5. Rate constants of the total, DDS and HYD conversions of DBT over NiMo/γ-Al_2O_3 (a), CoMo/γ-Al_2O_3 (b) and Mo/γ-Al_2O_3 (c) catalysts at different partial pressures of H_2S.

To analyze the product distributions at different partial pressures of H_2S, the rate constants of the DDS pathway (k_{DDS}) and of the HYD pathway (k_{HYD}) in the HDS of DBT were determined from k_{tot} and the selectivities at low weight time. The resulting k_{DDS} and k_{HYD} values are presented in Fig. 8.5. In the absence of H_2S, all three catalysts performed better via the DDS than via the HYD pathway. The Ni- and Co-promoters greatly improved the DDS as well as the HYD activity of the Mo catalyst. The yields of the partially hydrogenated intermediates were much lower over the NiMo and CoMo catalysts than over the Mo catalyst. Therefore, the desulfurization (the total sulfur removal) of DBT via the HYD pathway is also improved by the promoters. At 10 kPa H_2S the activity of all three catalysts decreased strongly (Fig. 8.5). At higher partial pressures of H_2S, however, the CoMo catalyst was less affected than the NiMo catalyst, and the activity of the Mo catalyst hardly changed. Over all the catalysts, the DDS pathway was suppressed to a greater extent than the HYD pathway. The rate constant of the HYD pathway, k_{HYD}, was almost the same at 0 and 100 kPa H_2S over the Mo catalyst. As a consequence, at 35 and 100 kPa H_2S the contribution of the HYD pathway was larger than that of the DDS pathway (Fig. 8.5c). The product analysis showed, however, that the relative yield of the partially hydrogenated intermediates increased with increasing partial pressure of H_2S. Therefore, we estimated the rate constant k_{DESULF}^{HYD} of the final desulfurization step in the HYD pathway. In the sequential first-order reactions A → B → C with rate constants k_{HYD} and k_{DESULF}^{HYD}, the concentration of the intermediate B is given by the expression [24]:

$$C_B = C_{A0} \cdot \frac{k_{HYD}}{k_{DESULF}^{HYD} - k_{HYD}} \cdot \left(e^{-k_{HYD} \cdot \tau} - e^{-k_{DESULF}^{HYD} \cdot \tau} \right)$$

The rate constant of the HYD pathway (k_{HYD}) is already known; thus, we can calculate k_{DESULF}^{HYD} from the concentration of the intermediate B, tetrahydrodibenzothiophene, at weight time τ. The rate constants k_{DESULF}^{HYD} for the different catalysts and at different H_2S partial pressures are plotted in Fig. 8.6. The activity of the CoMo and NiMo catalysts for the final sulfur removal via HYD is much higher than that of the Mo catalyst. H_2S suppresses k_{DESULF}^{HYD} much more strongly than k_{HYD}, the rate constant of the hydrogenation of DBT to tetrahydrodibenzothiophene. The ratio of the rate constants of sulfur removal via the DDS and HYD pathways (k_{DDS}/k_{DESULF}^{HYD}) remained constant at different partial pressures of H_2S over all

three catalysts (Table 8.1). This means that the desulfurizations of DBT to biphenyl and of tetrahydrodibenzothiophene to cyclohexylbenzene are inhibited to the same extent by H_2S. The k_{DDS}/k^{HYD}_{DESULF} ratios show that the desulfurization via the DDS pathway is 16 to 25 times slower than the desulfurization of the hydrogenated intermediate (Table 8.1).

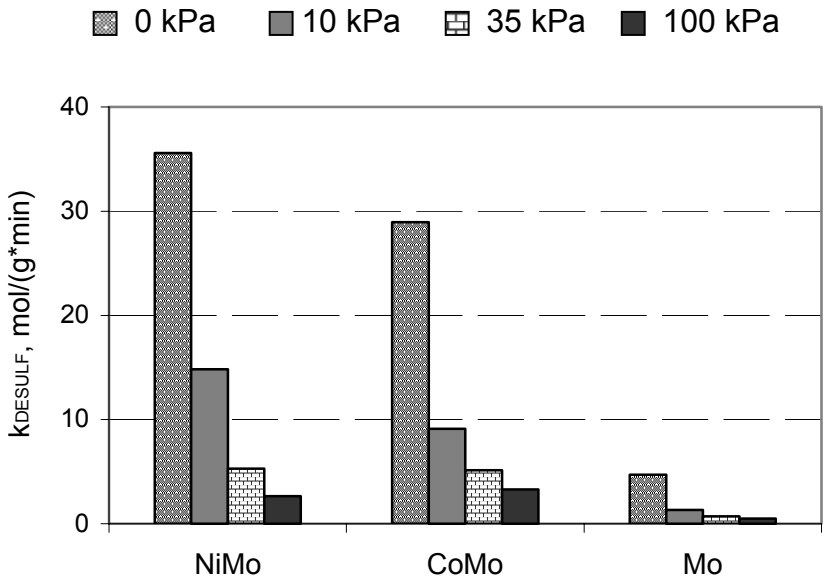

Fig. 8.6. Rate constants k^{HYD}_{DESULF} of the desulfurization of tetrahydrodibenzothiophene over NiMo/γ-Al_2O_3, CoMo/γ-Al_2O_3 and Mo/γ-Al_2O_3 catalysts at different partial pressures of H_2S.

The rate constants of the hydrogenation, k_{HYD}, and the rate constants of the desulfurizations via the DDS and HYD pathways, k_{DDS} and k^{HYD}_{DESULF}, for the HDS of 4,6-DMDBT in the presence of different catalysts and at different partial pressures of H_2S were calculated in the same way as for the HDS of DBT. The results are presented in Fig. 8.7. The differences in the performance of the Co- or Ni-promoted catalyst and the Mo catalyst were smaller in the HDS of 4,6-DMDBT than in the HDS of DBT (cf. Figs. 8.5 and 8.7). Thus, the rate constant k_{tot} of the overall conversion of 4,6-DMDBT was only 2.2 times higher over the NiMo catalyst than over the Mo catalyst and 1.9 times higher over the CoMo catalyst in the absence of H_2S (Fig. 8.8). Increasing the partial pressure of H_2S led to a decrease of k_{tot} for all catalysts, but most strongly for NiMo (Table 8.2). As a consequence, at 100 and 35 kPa H_2S, the CoMo catalyst was more active in the HDS of 4,6-DMDBT than the NiMo catalyst.

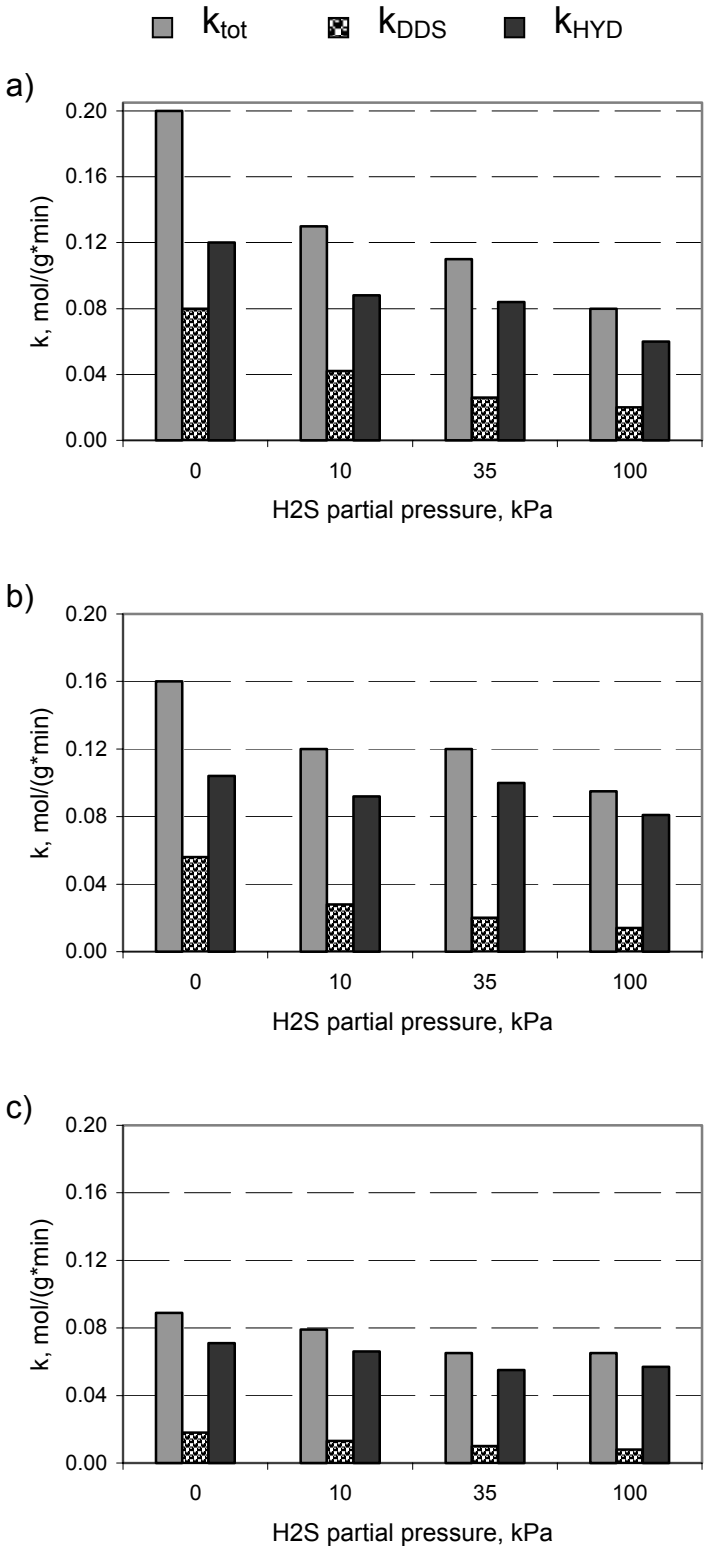

Fig. 8.7. Rate constants of the total, DDS and HYD conversions of 4,6-DMDBT over NiMo/γ-Al_2O_3 (a), CoMo/γ-Al_2O_3 (b) and Mo/γ-Al_2O_3 (c) catalysts at different partial pressures of H_2S.

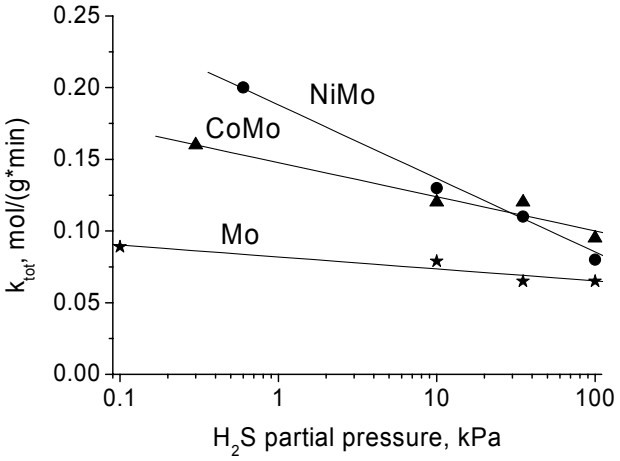

Fig. 8.8. Rate constants of the total conversion of 4,6-DMDBT over NiMo/γ-Al_2O_3, CoMo/γ-Al_2O_3 and Mo/γ-Al_2O_3 catalysts at different partial pressures of H_2S.

Table 8.2. Relative kinetic parameters in the HDS of 4,6-DMDBT over NiMo/γ-Al_2O_3, CoMo/γ-Al_2O_3 and Mo/γ-Al_2O_3 at 340°C and different H_2S partial pressures.

H_2S, kPa	NiMo/γ-Al_2O_3		CoMo/γ-Al_2O_3		Mo/γ-Al_2O_3	
	$k_{tot}^{H_2}/k_{tot}^{H_2S}$	k_{DDS}/k_{DESULF}^{HYD}	$k_{tot}^{H_2}/k_{tot}^{H_2S}$	k_{DDS}/k_{DESULF}^{HYD}	$k_{tot}^{H_2}/k_{tot}^{H_2S}$	k_{DDS}/k_{DESULF}^{HYD}
0	1	0.02	1	0.01	1	0.02
10	1.5	0.02	1.3	0.01	1.1	0.02
35	1.7	0.02	1.3	0.01	1.4	0.02
100	2.5	0.02	1.7	0.01	1.4	0.02

The DDS pathway of the HDS of 4,6-DMDBT was more strongly suppressed by H_2S than the HYD pathway over all three catalysts (Fig. 8.7). However, the ratio of the partially hydrogenated intermediates to the totally desulfurized products in the HYD pathway increased at increasing H_2S partial pressures. Fig. 8.9 presents the rate constants (k_{DESULF}^{HYD}) of the final desulfurization via the HYD pathway for the NiMo, CoMo and Mo catalysts. The activity of the Mo catalyst in the removal of sulfur via HYD is enhanced by the Ni and Co promoters but to a lesser extent than in the HDS of DBT (cf. Figs. 8.6 and 8.9). The ratio k_{DDS}/k_{DESULF}^{HYD} was constant at all partial pressures of H_2S and over all catalysts (Table 8.2). This indicates that the DDS desulfurization of 4,6-DMDBT is inhibited to the same extent as the HYD desulfurization of 4,6-dimethyltetrahydrodibenzothiophene. The k_{DESULF}^{HYD} values for the HDS of DBT and 4,6-DMDBT show that the methyl groups have a strong inhibitory

effect not only on the DDS pathway, but also on the desulfurization via the HYD pathway (Figs. 8.6 and 8.9). The final desulfurization of 4,6-DMDBT via HYD is always faster over the CoMo than over the NiMo catalyst (Fig. 8.9).

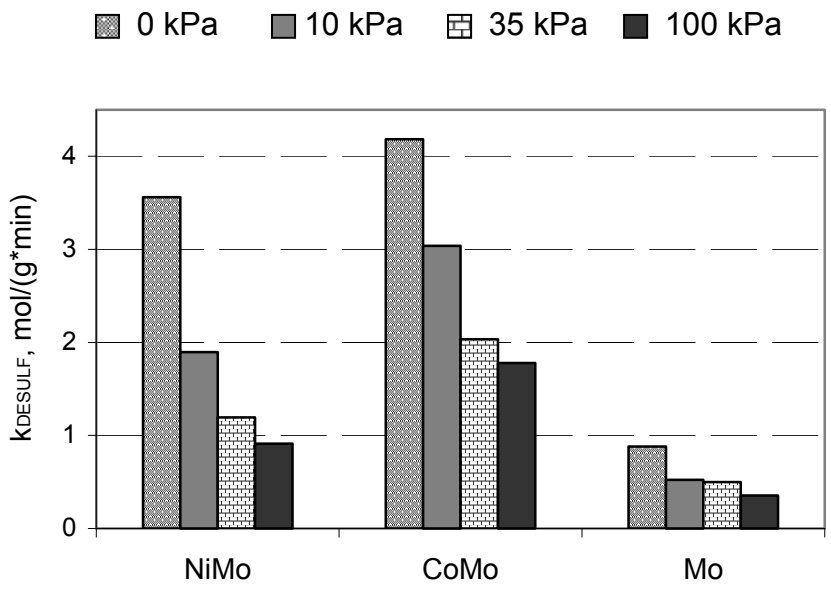

Fig. 8.9. Rate constants k_{DESULF}^{HYD} of the desulfurization of 4,6-dimethyltetrahydrodibenzothiophene over NiMo/γ-Al_2O_3, CoMo/γ-Al_2O_3 and Mo/γ-Al_2O_3 catalysts at different partial pressures of H_2S.

8.4 Discussion

8.4.1 DBT

To enable a comparison of the CoMo and Mo catalysts with the NiMo/γ-Al_2O_3 catalyst in the HDS of DBT and 4,6-DMDBT at 340°C and 35 kPa H_2S, the previous results, obtained for the NiMo catalyst, are presented in Figs. 8.10 and 8.11 [Chapters 5 and 7]. The HDS of DBT was slightly faster over the Ni-promoted catalyst than over the CoMo catalyst (cf. Figs. 8.1a and 8.10a), and both catalysts were much more active than the Mo catalyst (cf. Figs. 8.1a, 8.2a and 8.10a). Tetrahydrodibenzothiophene was the only intermediate and

biphenyl and cyclohexylbenzene were the final products of the HDS over NiMo. The selectivity of biphenyl formation approached 90% at the lowest weight time value and decreased with weight time to 70% (Fig. 8.10b). This indicates that biphenyl is slowly hydrogenated to cyclohexylbenzene, as was also observed over the Mo catalyst but not over the CoMo catalyst.

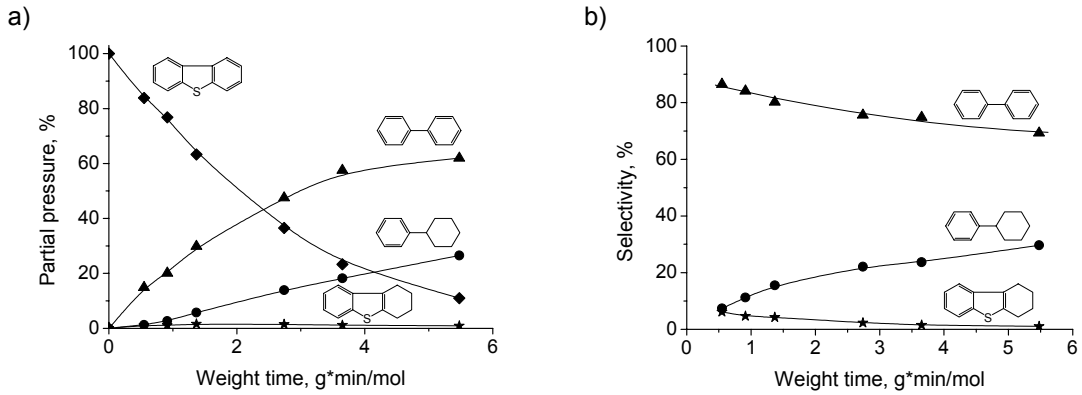

Fig. 8.10. Relative partial pressures (a) and selectivities (b) of the products of the HDS of dibenzothiophene at 340°C and 35 kPa H_2S over NiMo/γ-Al_2O_3 as a function of weight time.

At all partial pressures of H_2S the DDS pathway of the HDS of DBT is about an order of magnitude faster over the CoMo and NiMo catalysts than over the Mo catalyst (Fig. 8.5). The total yield of the HYD products is just slightly higher for the CoMo and NiMo catalysts than for the Mo catalyst but the product distribution is different. In the presence of NiMo and CoMo the main HYD product is cyclohexylbenzene (Figs. 8.1b and 8.10b), whereas over Mo cyclohexylbenzene constitutes only 45% of the HYD products at τ = 5 g·min/mol (Fig. 8.2b). Another 45% comes from the tetrahydro- and hexahydrodibenzothiophenes. Therefore, the promotion of the Mo catalyst by Ni or Co is due not only to the better performance of the DDS pathway, but also to faster desulfurization via the HYD pathway. This was confirmed by the k^{HYD}_{DESULF} values (Fig. 8.6).

The overall network of the HDS of DBT is represented by Scheme 8.1. Over the CoMo and NiMo catalysts the HDS of DBT most probably occurs via reactions 1, 2, 3 and 4. The tetrahydro-intermediate was observed over CoMo and NiMo. Trace amounts of the hexahydro-intermediate were observed over CoMo but not over NiMo. Over the Mo catalyst,

hexahydrodibenzothiophene was detected in higher concentrations; bicyclohexyl was also observed. We assume that bicyclohexyl is formed by hydrogenation of the partially hydrogenated intermediates to perhydrodibenzothiophene and subsequent desulfurization. The hydrogenation of cyclohexylbenzene to bicyclohexyl is unlikely since the hydrogenation of the second phenyl ring of biphenyl ought to be more difficult than that of the first ring. Our results show that the latter does not occur over CoMo and occurs only slowly over NiMo and Mo. Therefore, the HDS of DBT over the Mo catalyst occurs via reactions 1, 2, 3, 4, 5 and 6. Over the NiMo and CoMo catalysts, the hydrogenation of the first phenyl ring is the rate-limiting step in the HYD pathway, and the desulfurization of the partially hydrogenated intermediates is rather fast, since the yields of these intermediates are very low (Figs. 8.1b and 8.10b). Therefore, further hydrogenation of hexahydrodibenzothiophene to perhydrodibenzothiophene does not occur. Over the Mo catalyst, however, the lifetime of the partially hydrogenated molecules is longer. Thus, the hydrogenation to perhydrodibenzothiophene, followed by desulfurization to bicyclohexyl, becomes possible.

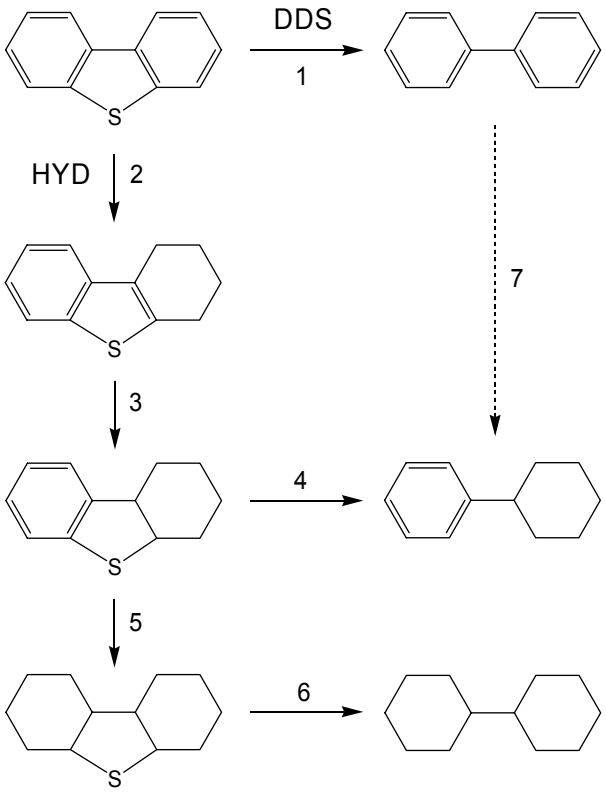

Scheme 8.1. Reaction network of the HDS of dibenzothiophene in the presence of transition metal sulfide catalysts.

Reaction 7, the hydrogenation of biphenyl to cyclohexylbenzene, was observed over the NiMo and Mo catalysts but not over the CoMo catalyst. This suggests that the active sites facilitating HDS over the NiMo and Mo catalysts are different from those over the CoMo catalyst. One reason for this difference may be that, according to DFT theory, the active sites of the NiMo and Mo catalysts are at the molybdenum edge, whereas the Co atoms are at the sulfur edge of the MoS_2 slab [25,26].

8.4.2 4,6-DMDBT

The HDS of 4,6-DMDBT over the NiMo and CoMo catalysts was much slower than the HDS of DBT (cf. Figs. 8.5 and 8.7). At 35 kPa H_2S, the total conversion of 4,6-DMDBT was slightly higher over the CoMo than over the NiMo catalyst due to a somewhat smaller DDS conversion but higher HYD conversion (cf. Figs. 8.3a and 8.11a). Thus, the first reaction, the hydrogenation, was faster over CoMo. Fig. 8.9 shows that the subsequent desulfurization via the HYD pathway is also easier over the CoMo catalyst. Since HYD is the main pathway in the transformation of 4,6-DMDBT, both its overall conversion and its desulfurization are faster over the CoMo catalyst. The rate constants of the total 4,6-DMDBT conversion (k_{tot}) over the three catalysts are plotted as a function of $P(H_2S)$ in Fig. 8.8. The NiMo catalyst was more active than the CoMo catalyst up to 29 kPa H_2S, but at higher partial pressures of H_2S the CoMo catalyst performed better. Therefore, it is assumed that NiMo performs better than CoMo under deep HDS conditions (at low partial pressures of H_2S), without however considering the influence of impurities such as nitrogen-containing compounds.

The activity of the Mo catalyst is somewhat lower in the HDS of 4,6-DMDBT than the activity of the Ni- and Co-promoted catalysts, but for all three catalysts HYD prevails over DDS. However, the amount of hydrogenated, but not desulfurized, products was higher over the Mo catalyst than over the promoted catalysts. The lowest selectivity for 4,6-dimethyltetrahydrodibenzothiophene was observed for the CoMo catalyst. We assume that the mechanism of the HDS of 4,6-DMDBT is similar to that of DBT (Scheme 8.1). Hexahydro- and perhydro-intermediates were not observed for 4,6-DMDBT in our experiments, probably because of their fast desulfurization. The hydrogenation of 3,3'-dimethylbiphenyl to methylcyclohexyl-toluene (reaction 7 in Scheme 8.1) clearly did not occur, as shown by the

fact that the DDS selectivity to 3,3'-dimethylbiphenyl remained constant for all three catalysts. The hydrogenation of methylcyclohexyl-toluene to 3,3'-dimethylbicyclohexyl will probably be even more difficult to achieve. Therefore, we assume that it does not occur either. Thus, 3,3'-dimethylbicyclohexyl can only be the product of further hydrogenation of 4,6-dimethyltetrahydrodibenzothiophene to 4,6-dimethylperhydrodibenzothiophene (reactions 3 and 5 in Scheme 8.1) followed by desulfurization. In the HDS of 4,6-DMDBT the lifetime of the partially hydrogenated intermediate (4,6-dimethyltetrahydrodibenzothiophene) is quite long, as is also the case for tetrahydrodibenzothiophene in the HDS of DBT over the Mo catalyst. Therefore, further hydrogenation to 4,6-dimethylperhydrodibenzothiophene followed by desulfurization can take place. The larger amount of 3,3'-dimethylbicyclohexyl than that of methylcyclohexyl-toluene in the reaction products over the Mo catalyst indicates that hydrogenation of 4,6-dimethylhexahydrodibenzothiophene occurs faster than its desulfurization to methylcyclohexyl-toluene.

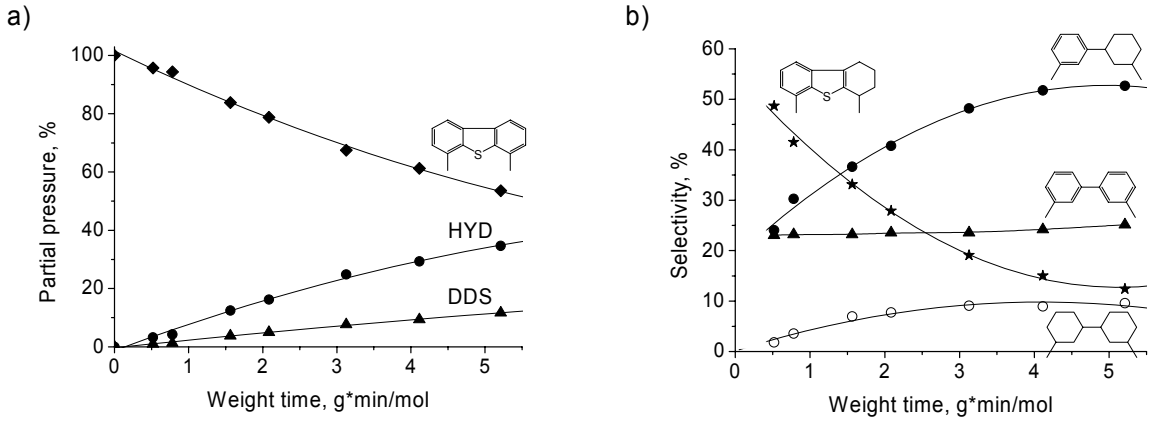

Fig. 8.11. Relative partial pressures (a) and selectivities (b) of the products of the HDS of 4,6-dimethyldibenzothiophene at 340°C and 35 kPa H_2S over NiMo/γ-Al_2O_3 as a function of weight time.

The desulfurization of 4,6-DMDBT in the presence of the NiMo, CoMo and Mo catalysts proceeds mainly via reactions 2, 3, 4, 5 and 6. Over the Mo catalyst the reactions 2, 3, 5 and 6 are the most important, since 3,3'-dimethylbicyclohexyl was observed as the main product. Over the Co- and Ni-promoted catalysts the most important reactions are reactions 2, 3 and 4. The NiMo and CoMo catalysts have a higher activity than the Mo catalyst in the DDS pathway, but the difference is not as large as in the HDS of DBT. This shows the strong steric hindrance of the two methyl groups on the DDS reactivity of the DBT molecule.

8.4.3 Catalytic sites

The cause of the inhibitory effect of the methyl groups on the reactivity of the DBT molecule is still not completely understood. Some researchers attributed the lower reactivity of 4,6-DMDBT to its lower adsorption strength on the catalyst surface [2,8,18], whereas others explained it by steric hindrance of the methyl groups on the C-S bond scission reaction [6,10,12]. Meille et al. reported that the adsorption equilibrium constants of DBT, 4-methyldibenzothiophene, 4,6-DMDBT and 2,8-DMDBT were almost the same on a sulfided NiMo catalyst [10]. Kabe et al. reported that the adsorption equilibrium constants of 4-methyldibenzothiophene and 4,6-DMDBT were even higher than that of DBT on a $CoMo/Al_2O_3$ catalyst [6]. The adsorption constants of the different sulfur-containing molecules were estimated by taking into account the total conversion of the reactant and assuming that the DDS and HYD pathways take place at the same active sites. This approach is the right one when the DDS and HYD reaction routes go through a common intermediate.

The presence of a common intermediate for the DDS and HYD reaction pathways in the HDS of DBT was first suggested by Singhal et al. [27]. They found that such a kinetic model fitted their experimental results the best. As a common intermediate they suggested 1',4'-dihydrodibenzothiophene, in which the hydrogenated bond is between the 6-ring and 5-ring (Scheme 8.2A). This proposal was supported by other researchers, who suggested that elimination is the main reaction, through which sulfur is removed [10,12,28]. They assumed that 4,4'-dihydrodibenzothiophene (Scheme 8.2B) is the common intermediate and that biphenyl is the product of four consecutive reactions, two hydrogenations, each followed by elimination (Scheme 8.3). The HYD pathway also consists of hydrogenation and elimination reactions, but there are two additional hydrogenation steps at the beginning. However, the hydrogenation of a carbon-carbon double bond with three substituents (RXC=CHR') is known to be more difficult than that of a double bond with two substituents (RHC=CHR') [29]. Furthermore, the stability of the 4,4'-dihydro-intermediate (Scheme 8.2B) is extremely low from an energetical point of view. This intermediate B still seems to have a conjugation between the π electrons of the phenyl group and of the partially hydrogenated ring. However, the structure is rather tense because of the presence of the two sp^3-hybridized carbon atoms and, therefore, the phenyl and hexadiene rings are not coplanar. Intermediate A (Scheme 8.2) has the *cis*-conformation and, thus, the plane of the hexadiene ring is oriented at an angle of

54.7° to the plane of the remaining dihydrodibenzothiophene. The conjugation in this molecule is interrupted. Finally, in all the published studies on the HDS of DBTs the only partially hydrogenated intermediate observed was 1,2,3,4-tetrahydrodibenzothiophene, with the double bond in the bridge position (Scheme 8.2C). This suggests that this double bond is the most difficult to hydrogenate and that such an intermediate is the most stable. The proposal for a common intermediate for the DDS and HYD pathways is also based on the assumption that elimination is the only reaction responsible for C-S bond breaking [12]. This assumption is much too restrictive, however, because methanethiol and neopentanethiol can be easily hydrodesulfurized to H_2S and methane and neopentane respectively. This shows that hydrogenolysis is a clear alternative to elimination. Therefore, the assumption of a common dihydro-intermediate for both DDS and HYD reaction pathways seems to be unfounded.

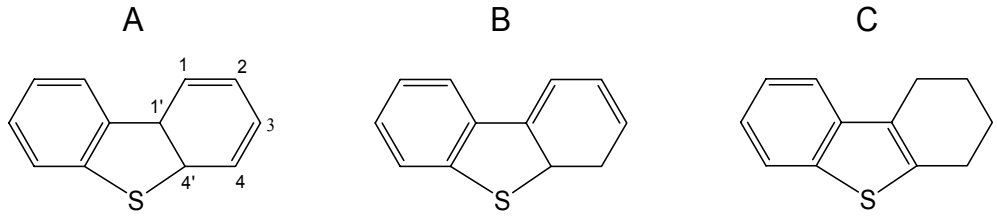

Scheme 8.2. The structures of proposed intermermediates in the HDS of DBT [12,28].

For these reasons and in conformity with other authors [30-32], we assume that the two HDS pathways do not have a common intermediate and are determined by the conformation of the adsorbed DBT molecule. DDS occurs through σ adsorption of the DBT molecule via the sulfur atom, and HYD proceeds through π adsorption of the reactant via the aromatic system. This would require two adsorption constants for the DDS and HYD pathways and these constants may be different. A vibrational study of organometallic complexes with thiophene ligands was used to model the adsorption of thiophene on a hydrodesulfurization catalyst [33]. It was found that in the η^1(S) bonding mode of thiophene (σ adsorption) the C-C bonds in the C_4 hydrocarbon backbone are slightly stronger, while the C-S bonds are substantially weaker relative to free thiophene. Therefore, it was suggested that the cleavage of the C-S bond occurs when thiophene is adsorbed on a coordinatively unsaturated Mo site via the sulfur atom in the σ mode. Vecchi et al. [34] described the effect of the methyl groups on σ coordination in Ru complexes of DBT, 4-methyldibenzothiophene, 4,6-DMDBT and 2,8-DMDBT. They observed that the binding strength increased in the order

4,6-DMDBT < 4-methyldibenzothiophene < DBT < 2,8-DMDBT, in good agreement with catalytic experiments [6,10].

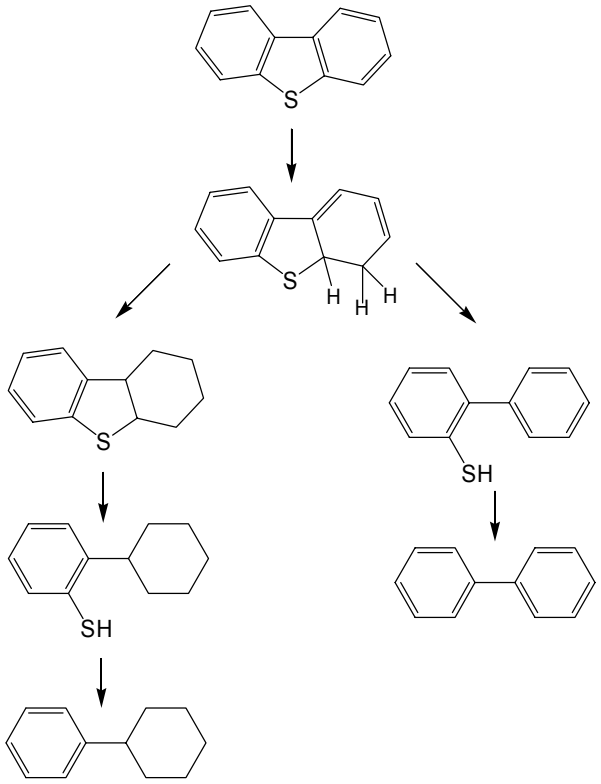

Scheme 8.3. Reaction network of the HDS of dibenzothiophene suggested by Bataille et al. [12].

A study of the C-S bond cleavage in methyl-substituted thiophenes and benzothiophenes in the presence of a binuclear Re complex [35] led to the conclusion that thiophenes and benzothiophenes reacted with $Re_2(CO)_{10}$ to different products. Therefore, it was suggested that the HDS of thiophenes and benzothiophenes may occur via different pathways. DFT calculations of different adsorption conformations of DBT derivatives indicated that the adsorption properties of the refractory DBT and 4,6-DMDBT molecules are very different from those of smaller model compounds such as thiophene and benzothiophene [36,37]. The main reason for this difference is the aromaticity of the DBT structure, making π adsorption more likely than σ adsorption. It was shown that the methyl groups do indeed hinder the perpendicular σ adsorption of DBT but hardly affect the flat adsorption via the aromatic π system.

The inhibitory effect of H_2S on the HDS activity of CoMo-, NiMo- and Mo/Al_2O_3 catalysts was studied before by Kasahara et al. [38]. They found that H_2S decreased the conversions of benzothiophene and DBT on all the catalysts. Moreover, the inhibitory effect of H_2S on NiMo was stronger than on the CoMo and Mo catalysts. In agreement with their observations, our results show that the total activity in the HDS of DBT and 4,6-DMDBT is suppressed to a greater extent by H_2S over the NiMo catalyst. In our work, the Mo catalyst was least affected by H_2S in the HDS of DBT and of 4,6-DMDBT (Tables 8.1 and 8.2). Moreover, the inhibitory factors, $k_{tot}^{H_2}/k_{tot}^{H_2S}$, were larger in the HDS of DBT than of 4,6-DMDBT (Tables 8.1 and 8.2). This is due to the stronger inhibitory effect of H_2S on the DDS pathway than on the HYD pathway. Since the contribution of the DDS is larger in the case of the HDS of DBT, the overall HDS is affected more strongly in the case of DBT. These results are in agreement with those of Bataille et al. [12]. They also observed that the HDS of DBT was affected more strongly by H_2S than that of 4,6-DMDBT over a NiMo catalyst.

In the HDS of DBT the NiMo catalyst is ten times and the CoMo catalyst six times more active than the unpromoted Mo catalyst. In the absence of H_2S, 90% of the DBT reacts via the DDS pathway over NiMo and CoMo and 75% over $Mo/\gamma\text{-}Al_2O_3$. Therefore, the promoters clearly improve the overall activity of the Mo catalyst with a slightly stronger positive influence on the DDS pathway. The amount of the DDS product in the HDS of DBT over the Mo catalyst strongly decreases with increasing partial pressure of H_2S. At 35 and 100 kPa H_2S, the DDS yield is even lower than the total HYD yield (Fig. 8.5c). In agreement with our results, Bataille et al. reported a better performance of the Mo catalyst in the HYD pathway of the HDS of DBT in the presence of 50 kPa H_2S [12]. This performance is better, however, only when one considers the total amount of the HYD products. If one considers the yield of completely desulfurized products via the HYD pathway, then one has to conclude that H_2S has the same inhibitory effect on the desulfurization of DBT via the DDS as via the HYD pathway in the presence of the Mo catalyst. The same behavior was observed for the CoMo and NiMo catalysts (Table 8.1).

In the HDS of 4,6-DMDBT, too, the desulfurization is inhibited to the same extent via both reaction pathways at all partial pressures of H_2S over all three catalysts (Table 8.2). The equal inhibition by H_2S of the DDS pathway and the final sulfur removal via the HYD pathway in the HDS of DBT and 4,6-DMDBT over all three catalysts suggest that the DDS and HYD pathways occur over the same active sites and that a similar mechanism of sulfur

removal is involved in the DDS pathway and in the final step of the HYD pathway. Thus, we suggest that the tetrahydro-intermediate can be desulfurized only via σ adsorption on the active site after having been desorbed from the catalyst surface. Hermann et al. also suggested that common steps are involved in both HDS pathways [39]. They found that the activities of the transition metal sulfides in the HDS of 4,6-DMDBT followed the same trends as in the HDS of DBT, although the DDS pathway was of major importance for DBT, while the HYD pathway was prevalent for 4,6-DMDBT.

The rate constants of the HYD pathway in the HDS of DBT are of the same magnitude as those of 4,6-DMDBT (cf. Figs. 8.5 and 8.7). The final desulfurization of the hindered 4.6-DMDBT via HYD is, however, substantially slower than that of DBT (cf. Figs. 8.6 and 8.9). Therefore, the methyl groups suppress not only the σ adsorption of the reactant, but also the sulfur removal from the partially hydrogenated intermediate. The DDS pathway is retarded to a greater extent by the presence of the methyl groups than is the sulfur removal via the HYD pathway, especially over the CoMo catalyst (cf. the k_{DDS}/k^{HYD}_{DESULF} values in Tables 8.1 and 8.2).

The desulfurization of 4,6-dimethyltetrahydrodibenzothiophene is 4.8 times higher over the CoMo catalyst than over the Mo catalyst at 0 kPa H_2S and 4.9 times higher at 100 kPa H_2S, whereas for the NiMo catalyst these values are 4 and 2.5 respectively (Fig. 8.9). Therefore, the promotion of the Mo catalyst by Co improves the resistance of the catalyst to H_2S with respect to the desulfurization via the HYD pathway in the HDS of hindered DBTs. This again indicates that CoMo is a better catalyst under HDS conditions (at least when only S compounds are present).

The Ni and Co promoters play a crucial role in the DDS activity of the Mo catalyst. The promoter may result in the enhancement of the intrinsic rate of the C-S bond cleavage by increasing the electron density on the active Mo sites as well as in the greater number of sulfur vacancies on the Ni- and Co-promoted catalysts.

8.5 Conclusion

The data obtained in this study indicate that the HDS of DBT and 4,6-DMDBT occurs via the same reaction network over NiMo, CoMo and Mo catalysts. Ni and Co promoters noticeably improve the DDS activity of the Mo catalyst in the HDS of DBT and, to a lesser

extent, in the HDS of 4,6-DMDBT. Since the DDS is the main reaction pathway in the HDS of DBT, the overall activity of the Mo catalyst in the transformation of DBT is remarkably improved by promotion. We suggest that the DDS and HYD pathways of HDS are determined by the adsorption conformation of the reactant molecule on the catalyst surface. The DDS occurs via σ adsorption, and the HYD pathway requires π adsorption. The resilience of 4,6-DMDBT is the result of the hindered removal of sulfur in the DDS pathway as well as in the HYD pathway.

H_2S suppresses the transformation of DBT and 4,6-DMDBT over all three catalysts. The NiMo catalyst is affected most and the Mo catalyst is least affected by the presence of H_2S. The DDS pathway was inhibited more strongly by H_2S than was the HYD pathway in the HDS of DBT and 4,6-DMDBT over all three catalysts. The final desulfurization via the HYD pathway was affected to the same extent as the DDS pathway, as shown by the constant k_{DDS}/k_{DESULF}^{HYD} ratio at all H_2S partial pressures over all catalysts. This suggests that the same mechanism is active in the DDS and in the final HYD step. In the HDS of 4,6-DMDBT the desulfurization via the HYD pathway was inhibited less by H_2S over the CoMo than over the NiMo catalyst. Because the activity of the CoMo catalyst was lower at 0 kPa H_2S, there is a cross-over point, at which the CoMo catalyst becomes better than the NiMo catalyst. As a consequence, at partial pressures of H_2S higher than 29 kPa, the CoMo catalyst performed better in the HDS of 4,6-DMDBT than the NiMo catalyst.

8.6 References

[1] D.R. Kilanowski, H. Teeuwen, V.H.J. de Beer, B.C. Gates, G.C.A. Schuit, H. Kwart, J. Catal. 55 (1978) 129.

[2] M. Houalla, D.H. Broderick, A.V. Sapre, N.K. Nag, V.H.J. de Beer, B.C. Gates, H. Kwart, J. Catal. 61 (1980) 523.

[3] M.J. Girgis, B.C. Gates, Ind. Eng. Chem. Res. 30 (1991) 2021.

[4] A. Ishihara, H. Tajima, T. Kabe, Chem. Lett. 4 (1992) 669.

[5] T. Kabe, A. Ishihara, H. Tajima, Ind. Eng. Chem. Res. 31 (1992) 1577.

[6] T. Kabe, A. Ishihara, Q. Zhang, Appl. Catal. A 97 (1993) L1.

[7] V. Lamure-Meille, E. Schulz, M. Lemaire, M. Vrinat, Appl. Catal. A 131 (1995) 143.

[8] X.L. Ma, K. Sakanishi, I. Mochida, Ind. Eng. Chem. Res. 35 (1996) 2487.

[9] H. Topsøe, B.S. Clausen, F.E. Massoth, in, Catalysis: Science and Technology, 1996.

[10] V. Meille, E. Schulz, M. Lemaire, M. Vrinat, J. Catal. 170 (1997) 29.

[11] T. Kabe, A. Ishihara, W. Qian, Hydrodesulfurization and hydrodenitrogenation, Kodansha Ltd., Tokyo, WILEY-VCH Verlag GmbH, Weinheim, 1999.

[12] F. Bataille, J.L. Lemberton, P. Michaud, G. Perot, M. Vrinat, M. Lemaire, E. Schulz, M. Breysse, S. Kasztelan, J. Catal. 191 (2000) 409.

[13] D.D. Whitehurst, T. Isoda, I. Mochida, Adv. Catal. 42 (1998) 345.

[14] M. Macaud, A. Milenkovic, E. Schulz, M. Lemaire, M. Vrinat, J. Catal. 193 (2000) 255.

[15] B.C. Gates, H. Topsøe, Polyhedron 16 (1997) 3213.

[16] T. Kabe, K. Akamatsu, A. Ishihara, S. Otsuki, M. Godo, Q. Zhang, W.H. Qian, Ind. Eng. Chem. Res. 36 (1997) 5146.

[17] P. Steiner, E.A. Blekkan, Fuel Process Technol. 79 (2002) 1.

[18] X.L. Ma, K. Sakanishi, T. Isoda, I. Mochida, Ind. Eng. Chem. Res. 34 (1995) 748.

[19] I. Mochida, K. Sakanishi, X.L. Ma, S. Nagao, T. Isoda, Catal. Today 29 (1996) 185.

[20] M.V. Landau, D. Berger, M. Herskowitz, J. Catal. 159 (1996) 236.

[21] E. Lecrenay, K. Sakanishi, I. Mochida, Catal. Today 39 (1997) 13.

[22] D.D. Whitehurst, H. Farag, T. Nagamatsu, K. Sakanishi, I. Mochida, Catal. Today 45 (1998) 299.

[23] K.G. Knudsen, B.H. Cooper, H. Topsøe, Appl. Catal. A 189 (1999) 205.

[24] O. Levenspiel, Chemical Reaction Engineering, John Wiley&Sons, New-York, 1999.

[25] L.S. Byskov, J.K. Nørskov, B.S. Clausen, H. Topsøe, J. Catal. 187 (1999) 109.

[26] H. Schweiger, P. Raybaud, H. Toulhoat, J. Catal. 212 (2002) 33.

[27] G.H. Singhal, R.L. Espino, J.E. Sobel, G.A. Huff, J. Catal. 67 (1981) 457.

[28] J. Mijoin, G. Perot, F. Bataille, J.L. Lemberton, M. Breysse, S. Kasztelan, Catal. Lett. 71 (2001) 139.

[29] M.B. Smith, J. March, Advanced Organic Chemistry : Reactions, Mechanisms, and Structure, Wiley-Interscience, New York, 2001.

[30] P. Desikan, C.H. Amberg, Can. J. Chem.-Rev. 42 (1964) 843.

[31] S. Harris, R.R. Chianelli, J. Catal. 86 (1984) 400.

[32] C.N. Satterfield, M. Modell, J.F. Mayer, AIChE J. 21 (1975) 1100.

[33] P. Mills, S. Korlann, M.E. Bussell, M.A. Reynolds, M.V. Ovchinnikov, R.J. Angelici, C. Stinner, T. Weber, R. Prins, J. Phys. Chem. A 105 (2001) 4418.

[34] P.A. Vecchi, A. Ellern, R.J. Angelici, J. Am. Chem. Soc. 125 (2003) 2064.

[35] M.A. Reynolds, I.A. Guzei, R.J. Angelici, J. Am. Chem. Soc. 124 (2002) 1689.

[36] H. Yang, C. Fairbridge, Z. Ring, Energy & Fuels 17 (2003) 387.

[37] S. Cristol, J.F. Paul, E. Payen, D. Bougeard, F. Hutschka, S. Clemendot, submitted to J. Catal. (2003).

[38] S. Kasahara, T. Shimizu, M. Yamada, Catal. Today 35 (1997) 59.

[39] N. Hermann, M. Brorson, H. Topsøe, Catal. Lett. 65 (2000) 169.

Chapter 9

Concluding Remarks

Hydrodesulfurization (HDS) has been used in the refining of crude oil for over 60 years. This process is still a topic of interest due to the need to use new feedstocks and more stringent environmental legislation, for example, to reduce the sulfur level in fuels. Of particular importance in achieving low sulfur content in fuels is the problem how to remove sulfur from hindered dibenzothiophenes, e.g. dibenzothiophene (DBT), 4-methyldibenzothiophene and 4,6-dimethyldibenzothiophene (4,6-DMDBT). Dibenzothiophenes are resilient to HDS when current catalyst formulations are used [1-5]. Moreover, when the level of sulfur compounds has been decreased by means of the classical HDS process, the further removal of sulfur is more difficult due to the presence of nitrogen and aromatic compounds in the refinery streams.

The essential contribution of this thesis is to improve our understanding of the HDS reaction network of DBT and 4,6-DMDBT and of the nature of the active sites that facilitate the different pathways of HDS. This final chapter summarizes the results and presents the perspectives for future research in this field.

9.1 Summary

DBT and 4,6-DMDBT undergo HDS via two reaction pathways: direct desulfurization (DDS) leading to the formation of biphenyls and hydrogenation followed by desulfurization (HYD) yielding first tetrahydro-, hexahydro- and perhydro-intermediates that are further converted to cyclohexylbenzenes and bicyclohexyls. DBT converts predominantly via the DDS pathway, whereas 4,6-DMDBT is converted mainly via the HYD pathway. The reactivity of DBT is one order of magnitude higher than that of 4,6-DMDBT over NiMo and

CoMo catalysts and only three times faster over the Mo catalyst. The resilience of 4,6-DMDBT compared to DBT is due to the hindered removal of sulfur in the DDS as well as in the HYD pathway. It is suggested that the DDS and HYD pathways of HDS are determined by the adsorption conformation of the reactant molecule on the catalyst surface. The DDS occurs via σ (perpendicular) adsorption; π (flat) adsorption is required for the HYD pathway.

Ni and Co promoters clearly improve the DDS activity of the Mo catalyst in the HDS of DBT and, to a lesser extent, in the HDS of 4,6-DMDBT. Sulfur removal via the HYD pathway is also enhanced over the NiMo and CoMo catalysts compared to the Mo catalyst. This enhancement is again more pronounced in the case of DBT than in the case of 4,6-DMDBT. Thus, the methyl groups constitute a strong steric hindrance for the desulfurization via both reaction pathways.

H_2S suppressed the transformation of DBT and 4,6-DMDBT over all the studied catalysts (NiMo/γ-Al_2O_3, CoMo/γ-Al_2O_3 and Mo/γ-Al_2O_3). The NiMo catalyst is most affected and the Mo catalyst least affected by the presence of H_2S. The DDS pathway is inhibited by H_2S to a greater extent than the HYD pathway in the HDS of DBT and 4,6-DMDBT over all three catalysts. However, desulfurization via HYD was affected by H_2S to the same extent as DDS over all the catalysts. This suggests that the active DDS and HYD sites have the same nature and that the mechanisms of sulfur removal in the DDS pathway and the final step in the HYD pathway may be the same.

To better understand competitive HDS and hydrodenitrogenation (HDN), the HDN of 2-methylpyridine and its intermediate products, 2-methylpiperidine, 1-aminohexane, and 2-aminohexane, were studied over sulfided NiMo catalyst. The presence of most intermediates is explained by a combination of pyridine ring hydrogenation, piperidine ring opening by elimination or S_N2 nucleophilic substitution and nitrogen removal by elimination as well as by nucleophilic substitution of the amino group by a sulfhydryl group, followed by elimination of H_2S or hydrogenolysis of the C-S bond. Amino-alkenes and amino-thiols, which are assumed to be the primary products of the ring opening of alkylpiperidine, were not observed, probably because of the fast transformation to the corresponding amines. The ring opening of 2-methylpiperidine occurred preferentially between the nitrogen atom and the methylene group rather than between the nitrogen atom and the carbon atom bearing the methyl group. This was confirmed by comparative HDN experiments of piperidine, 2-methylpiperidine and 2,6-dimethylpiperidine. Although the methyl groups have extra β hydrogen atoms, these primary hydrogen atoms are not used for elimination. Instead, the methyl groups hinder the

adsorption, which leads to the elimination of the β hydrogen atoms on the side of the molecule bearing the methyl group. H_2S promoted the hydrogenation of 2-methylpyridine up to 10 kPa and inhibited it at higher partial pressures. The hydrodenitrogenation conversions of 2-methylpiperidine and 2-methylpyridine were positively influenced by H_2S.

The influence of 2-methylpyridine and 2-methylpiperidine on the HDS of DBT and 4,6-DMDBT and the effect of sulfur-containing molecules on the HDN of 2-methylpyridine and 2-methylpiperidine were studied over a sulfided $NiMo/Al_2O_3$ catalyst at 5 MPa, 35 kPa H_2S and 300 and 340 °C. Both N-containing molecules strongly poisoned the HYD pathway of the HDS of DBT and 4,6-DMDBT, but the inhibitory effect of 2-methylpiperidine was somewhat stronger than that of 2-methylpyridine. The DDS pathway of the HDS of 4,6-DMDBT was also suppressed more in the presence of 2-methylpiperidine than in the presence of 2-methylpyridine. The DDS route of the HDS of DBT, however, was suppressed in the presence of 2-methylpyridine and promoted at low partial pressures of 2-methylpiperidine. The enhancement of the DDS pathway in the HDS of DBT at low partial pressures of 2-methylpiperidine is explained in three ways: a) transformation of HYD sites into DDS sites, because the HYD site consists of several metal centers and is not completely covered after adsorption of 2-methylpiperidine in the one-point mode; b) electronic modification of the catalyst surface, resulting in an increase in the electron density on the metal centers due to interaction with the 2-methylpiperidine molecules, leading to a greater number of sulfur vacancies or to higher intrinsic activity of the active site; c) interaction between 2-MPiper and DBT (acid – base interaction) when both are adsorbed perpendicular to the catalyst surface. DBT and 4,6-DMDBT had a negative effect on the hydrogenation of 2-methylpyridine but did not influence the C-N bond cleavage of 2-methylpiperidine. Therefore, we assume that the adsorption of 2-MPiper on both DDS and HYD sites is much stronger than that of 4,6-DMDBT or DBT.

Toluene and naphthalene were chosen to study the effect of aromatics on the HDS of DBT and 4,6-DMDBT. Toluene was a commonly used solvent in our studies. In the presence of toluene neither the rates of the HDS of DBT and 4,6-DMDBT, nor the product distributions are affected. Toluene itself does not undergo hydrogenation in the presence of sulfur or nitrogen compounds. Thus, the solvent molecules do not compete with the reactant for the active sites. Naphthalene inhibited the DDS and HYD pathways in the HDS of DBT and 4,6-DMDBT to the same extent. Thus, the hydrogenation of naphthalene takes place at the DDS as well as at the HYD sites. This again suggests that the nature of the DDS and HYD

active sites is similar. DBT and 4,6-DMDBT suppressed the hydrogenation of naphthalene to the same extent. It is assumed that the adsorption of naphthalene is much weaker than that of S-containing molecules.

In the HDS of 4,6-DMDBT the desulfurization via the HYD pathway was inhibited much less by H_2S and was initially higher over the CoMo than over the NiMo catalyst. As a consequence, at H_2S partial pressures higher than 29 kPa the CoMo catalyst performed better than the NiMo catalyst.

9.2 Outlook

DBT and 4,6-DMDBT are often used as model sulfur-containing molecules in HDS studies [6-20]. Although the HDS network of DBT and 4,6-DMDBT is well understood, this study is the first to suggest the presence of perhydrodibenzothiophenes as reaction intermediates. HDS experiments with tetrahydro- and hexahydrodibenzothiophene as a substrate may clarify the reaction network of the HDS of dibenzothiophenes. The kinetic data presented in Chapter 8 suggest that the desulfurization of tetrahydrodibenzothiophenes is two orders of magnitude faster than the direct desulfurization of dibenzothiophenes. Therefore, the HDS of tetrahydrodibenzothiophenes can be carried out under more moderate reaction conditions.

Nitrogen-containing molecules strongly inhibit HDS reactions [21-33] because of their high adsorption constants on the catalyst surface. Nagai reported the promotion of the DDS of DBT over $NiMo/Al_2O_3$ and NiW/Al_2O_3 catalysts, i.e. an enhancement of the overall conversion of DBT in the presence of acridine, but gave no explanation [34,35]. We observed that 2-methylpiperidine promotes the DDS of DBT. This phenomenon, however, has not been observed in the HDS of 4,6-DMDBT. Further research on the competitive HDS of DBT and HDN of basic nitrogen compounds is called for. The DDS of DBT was promoted over the NiMo catalyst. The same experiments over CoMo and Mo catalysts may clarify the nature of the promoting influence of 2-methylpiperidine.

9.3 References

[1] B.C. Gates, J.R. Katzer, G.C.A. Schuit, in, Chemistry of Catalytic Processes, McGraw-Hill, New-York, 1979,

[2] M.L. Vrinat, Appl. Catal. 6 (1983) 137.

[3] M.J. Girgis, B.C. Gates, Ind. Eng. Chem. Res. 30 (1991) 2021.

[4] H. Topsøe, B.S. Clausen, F.E. Massoth, in, Catalysis: Science and Technology, 1996,

[5] T. Kabe, A. Ishihara, W. Qian, Hydrodesulfurization and hydrodenitrogenation, Kodansha Ltd., Tokyo,WILEY-VCH Verlag GmbH, Weinheim, 1999.

[6] M. Houalla, N.K. Nag, A.V. Sapre, D.H. Broderick, B.C. Gates, AIChE J. 24 (1978) 1015.

[7] D.R. Kilanowski, H. Teeuwen, V.H.J. de Beer, B.C. Gates, G.C.A. Schuit, H. Kwart, J. Catal. 55 (1978) 129.

[8] G.H. Singhal, R.L. Espino, J.E. Sobel, J. Catal. 67 (1981) 446.

[9] I.A. van Parijs, L.H. Hosten, G.F. Froment, Ind. Eng. Chem. Prod. Res. Dev. 25 (1986) 437.

[10] T.C. Ho, J.E. Sobel, J. Catal. 128 (1991) 581.

[11] V. Lamure-Meille, E. Schulz, M. Lemaire, M. Vrinat, Appl. Catal. A 131 (1995) 143.

[12] X.L. Ma, K. Sakanishi, T. Isoda, I. Mochida, Ind. Eng. Chem. Res. 34 (1995) 748.

[13] T. Isoda, S. Nagao, X.L. Ma, Y. Korai, I. Mochida, Energy & Fuels 10 (1996) 482.

[14] T. Kabe, K. Akamatsu, A. Ishihara, S. Otsuki, M. Godo, Q. Zhang, W.H. Qian, Ind. Eng. Chem. Res. 36 (1997) 5146.

[15] V. Meille, E. Schulz, M. Lemaire, M. Vrinat, J. Catal. 170 (1997) 29.

[16] K. Sakanishi, T. Nagamatsu, I. Mochida, D.D. Whitehurst, Abstr. Pap. Am. Chem. Soc. 216 (1998) 015.

[17] V. Vanrysselberghe, R. Le Gall, G.F. Froment, Ind. Eng. Chem. Res. 37 (1998) 1235.

[18] H. Topsøe, K.G. Knudsen, L.S. Byskov, J.K. Nørskov, B.S. Clausen, in Science and Technology in Catalysis 1998, ELSEVIER, Amsterdam, 1999, p. 13.

[19] F. Bataille, J.L. Lemberton, P. Michaud, G. Perot, M. Vrinat, M. Lemaire, E. Schulz, M. Breysse, S. Kasztelan, J. Catal. 191 (2000) 409.

[20] C. Kwak, J.J. Lee, J.S. Bae, K. Choi, S.H. Moon, Appl. Catal. A 200 (2000) 233.

[21] F.W. Kirsch, H. Shalit, H. Heinemann, Ind. Eng. Chem. 51 (1959) 1379.

[22] C.N. Satterfield, M. Modell, J.F. Mayer, AIChE J. 21 (1975) 1100.

[23] C.N. Satterfield, M. Modell, J.A. Wilkens, Ind. Eng. Chem. Proc. Des. Dev. 19 (1980) 154.

[24] M. Nagai, T. Sato, A. Aiba, J. Catal. 97 (1986) 52.

[25] J. Yang, F.E. Massoth, Appl. Catal. 34 (1987) 215.

[26] V. La Vopa, C.N. Satterfield, J. Catal. 110 (1988) 375.

[27] F. Gioia, F. Murena, J. Hazard. Mater. 57 (1998) 177.

[28] G.C. Laredo, J.A. De los Reyes, J.L. Cano, J.J. Castillo, Appl. Catal. A 207 (2001) 103.

[29] C. Kwak, J.J. Lee, J.S. Bae, S.H. Moon, Appl. Catal. B 35 (2001) 59.

[30] P. Zeuthen, K.G. Knudsen, D.D. Whitehurst, Catal. Today 65 (2001) 307.

[31] T. Koltai, M. Macaud, A. Guevara, E. Schulz, M. Lemaire, R. Bacaud, M. Vrinat, Appl. Catal. A 231 (2002) 253.

[32] G.C. Laredo, E. Altamirano, J.A. De los Reyes, Appl. Catal. A 243 (2003) 207.

[33] P. Afanasiev, M. Cattenot, C. Geantet, N. Matsubayashi, K. Sato, S. Shimada, Appl. Catal. A 237 (2002) 227.

[34] M. Nagai, Ind. Eng. Chem. Prod. Res. Dev. 24 (1985) 489.

[35] M. Nagai, Chem. Lett. 6 (1987) 1023.

Acknowledgements

This work would not have been possible without the help of many people. I would like to sincerely thank:

Prof. Dr. Roel Prins (who made this all happen), for giving me the opportunity to join his group and to perform this PhD work, for his supervision, brilliant remarks and advice, fruitful discussions and great patience in correcting my manuscripts.

Prof. Dr. Alexander Wokaun, for agreeing to be co-examiner and for reviewing my thesis.

Marcia Schoenberg, for being exceptionally kind, for her help in many ways and for her concern.

Dr. Fabio Rota, for his invaluable help in building my unit, sharing his experiences and for the nice evenings dancing in “Palavrion”.

The late Mr. Fortunat Luck, for his assistance in solving technical problems and for always being helpful.

Dr. Mingyong Sun, for his understanding and friendship, for fruitful discussions on catalysis and for being such a good student of Russian. (Your “pozhalujsta” (“please”) always sounded so lamentable.)

Yonggang Zhao, for being a real gentlemen, for his help and fruitful collaboration. (I know you did your best to pronounce my first name.)

Samantha, for her guidance and help in adapting to life in Switzerland, for her friendship and for the lectures on basic Italian. (You were the most successful learner of Russian in our group!)

My “high pressure” colleges, Lianglong, Daniele and Adeline, for their help and cooperation.

Jan Kovacovic, for his technical assistance in the new high pressure lab.

Luciana, for valuable advice on preparing catalysts and for accompanying me to various sport activities and sauna-tours.

Dr. Thomas Weber, for valuable criticism of my posters, which helped in the development of a poster template, much used by the Prins group and for fruitful discussions on the “flowerization” process.

Teodora, for her help in the computer-support business and Norbert for taking over these responsibilities.

My “sulfide-phosphide” mates, André, Christoph and Virginie, for being so special and making life in the group so colorful.

My “zeolite” colleagues, Anna, Jeroen, Marco, Lukas, Pijus, Gerhard, Martin, Anuji and Eveline, “homogeneous” colleagues, Achim, Pavel, Barbara, Tom and Antonella, as well as all the former members of our group, for making the time spent in the Prins-group unforgettable.

I would like to thank my husband, Valeri, for being with me through all the years of my PhD work, for his assistance with complicated calculations and his interest in the chemical kinetics, as well as for his love, concern and support for the last ten years.

I am grateful to my parents for everything I have. Я благодарна своим родителям за все что имею сегодня, за их поддержку, заботу и любовь.

Publications

M. Egorova, Y. Zhao, P. Kukula, and R. Prins
„On the role of beta hydrogen atoms in the hydrodenitrogenation of 2-methylpyridine and 2-methylpiperidine“, ***Journal of Catalysis***, 206 (2002) 263.

Marina Egorova and Roel Prins
„Effect of N-containing molecules on the HDS of dibenzothiophene“, ***Abstracts of Papers of the American Chemical Society***, 224 (2002) 010.

Marina Egorova and Roel Prins
„Poisoning of the HDS of dibenzothiophene and 4,6-dimethyldibenzothiophene by N-containing molecules“, ***Chemical Engineering Transactions***, 1 (2003) 545.

Marina Egorova and Roel Prins
„Mutual influence of the HDS of dibenzothiophene and HDN of 2-methylpyridine“, ***Journal of Catalysis***, 221 (2004) 11.

Marina Egorova and Roel Prins
“Promotion effect of 2-methylpiperidine on the direct desulfurization of dibenzothiophene over NiMo/γ-Al_2O_3”, ***Catalysis Letters***, 92 (2004) 87.

Marina Egorova and Roel Prins
“Competitive hydrodesulfurization of 4,6-dimethyldibenzothiophene, hydrodenitrogenation of 2-methylpyridine and hydrogenation of naphthalene over sulfided NiMo/γ-Al_2O_3”, ***Journal of Catalysis***, to be published (2004).

Marina Egorova and Roel Prins
“Hydrodesulfurization of dibenzothiophene and4,6-dimethyldibenzothiophene over sulfided NiMo/γ-Al2O3, CoMo/γ-Al2O3 and Mo/γ-Al2O3 catalysts“, ***Journal of Catalysis***, to be published (2004).

Curriculum Vitae

Name:	Marina Borisovna Egorova
Date of birth:	05.05.1976
Place of birth:	Samarkand, Uzbekistan
Nationality:	Russian

Education

1999 – 2003 Doctoral study at the Institute for Chemical and Bioengineering in the group of Prof. Dr. Roel Prins
Swiss Federal Institute of Technology (ETH), Zurich

1997 – 1999 Master of Science in Chemistry
Novosibirsk State University, Russia

1993 – 1997 Bachelor of Science in Chemistry, Biology and Nature Management
Novosibirsk State University, Russia

1992 – 1993 Study at the Specialized Scientific Study Center for Physics, Mathematics, Chemistry and Biology Education (High School)
Novosibirsk State University, Russia

1991 – 1992 Gymnasium № 51, Samarkand, Uzbekistan

1983 – 1991 Primary and Secondary School № 29, Samarkand, Uzbekistan